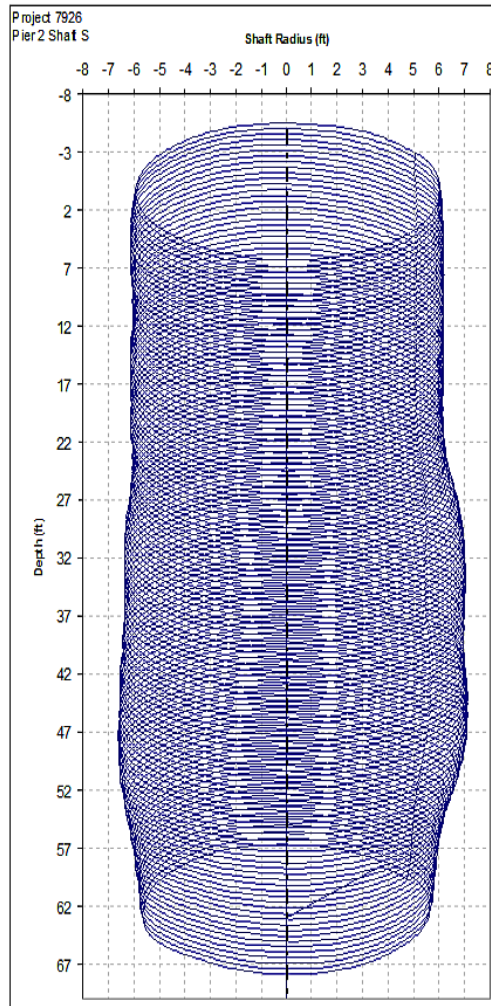
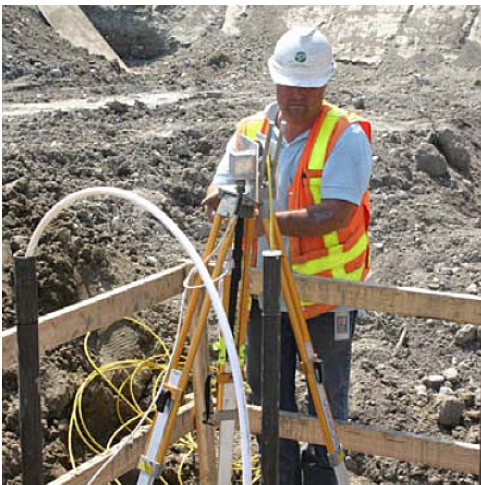


# Infrared Thermal Integrity Testing Quality Assurance Test Method to Detect Drilled Shaft Defects

WA-RD 770.1

Gray Mullins  
Danny Winters

June 2011



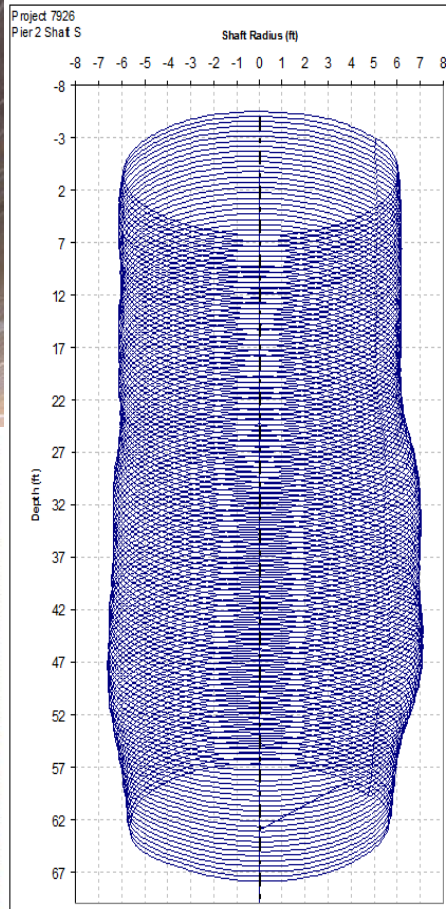


**INFRARED THERMAL INTEGRITY TESTING  
QUALITY ASSURANCE TEST METHOD TO DETECT DRILLED SHAFT DEFECTS**

**FINAL REPORT**

*Principal Investigator:  
Gray Mullins, Ph.D., P.E.*

*Research Associate:  
Danny Winters*



Prepared for

**Washington State Department of Transportation**  
Paula J. Hammond, Secretary  
Olympia, WA 98504-7372

**June 2011**

1. REPORT NO. <b>WA-RD 770.1</b>	2. GOVERNMENT ACCESSION NO.	3. RECIPIENTS CATALOG NO.	
4. TITLE AND SUBTITLE <b>Infrared Thermal Integrity Testing Quality Assurance Test Method To Detect Drilled Shaft Defects</b>		5. REPORT DATE <i>June 2011</i>	
		6. PERFORMING ORGANIZATION CODE	
7. AUTHOR(S) <b>G. Mullins and D. Winters</b>		8. PERFORMING ORGANIZATION REPORT NO.	
9. PERFORMING ORGANIZATION NAME AND ADDRESS <b>University of South Florida 4202 E. Fowler Avenue Tampa, FL 33620</b>		10. WORK UNIT NO.	
		11. CONTRACT OR GRANT NO. <b>GCA5855</b>	
12. CO-SPONSORING AGENCY NAME AND ADDRESS <b>Washington State Department of Transportation Transportation Building, MS 47372 Olympia, Washington 98504-7372 Research Manager: Kim Willoughby 360.705.7978</b>		13. TYPE OF REPORT AND PERIOD COVERED <i>Final Report</i>	
		14. SPONSORING AGENCY CODE	
15. SUPPLEMENTARY NOTES <i>This study was conducted in cooperation with the U.S. Department of Transportation, Federal Highway Administration.</i>			
16. ABSTRACT <p>Thermal integrity profiling uses the measured temperature generated in curing concrete to assess the quality of cast in place concrete foundations (i.e. drilled shafts or ACIP piles) which can include effective shaft size (diameter and length), anomaly detection inside and outside reinforcement cage, cage alignment, and proper hydration of the concrete. The ability to detect concrete volumes outside the reinforcing cage is perhaps its strongest feature. For this study, no anomalies within the reinforcing cage were encountered but various forms of external section changes were identified as well as several cases of off-center cages. Cage alignments generally varied with depth. Notably, only two cases of reduced concrete cover were detected; bulges were most common.</p>			
17. KEY WORDS <i>Thermal, Integrity Testing, Drilled Shafts, Anomaly, Conductivity, Detection</i>		18. DISTRIBUTION STATEMENT	
19. SECURITY CLASSIF. (of this report) <i>None</i>	20. SECURITY CLASSIF. (of this page) <i>None</i>	21. NO. OF PAGES <i>163</i>	22. PRICE



## **Disclaimer**

The contents of this report reflect the views of the authors, who are responsible for the facts and the accuracy of the data presented herein. The contents do not necessarily reflect the official views or policies of the Washington State Department of Transportation (WSDOT) or the Federal Highway Administration (FHWA). This report does not constitute a standard, specification, or regulation.

SI\* (MODERN METRIC) CONVERSION FACTORS

**APPROXIMATE CONVERSIONS TO SI UNITS**

SYMBOL	WHEN YOU KNOW	MULTIPLY BY	TO FIND	SYMBOL
<b>LENGTH</b>				
<b>in</b>	inches	25.4	millimeters	mm
<b>ft</b>	feet	0.305	meters	m
<b>yd</b>	yards	0.914	meters	m
<b>mi</b>	miles	1.61	kilometers	km

SYMBOL	WHEN YOU KNOW	MULTIPLY BY	TO FIND	SYMBOL
<b>VOLUME</b>				
<b>fl oz</b>	fluid ounces	29.57	milliliters	mL
<b>gal</b>	gallons	3.785	liters	L
<b>ft<sup>3</sup></b>	cubic feet	0.028	cubic meters	m <sup>3</sup>
<b>yd<sup>3</sup></b>	cubic yards	0.765	cubic meters	m <sup>3</sup>

NOTE: volumes greater than 1000 L shall be shown in m<sup>3</sup>

SYMBOL	WHEN YOU KNOW	MULTIPLY BY	TO FIND	SYMBOL
<b>MASS</b>				
<b>oz</b>	ounces	28.35	grams	g
<b>lb</b>	pounds	0.454	kilograms	kg
<b>T</b>	short tons (2000 lb)	0.907	megagrams (or "metric ton")	Mg (or "t")

SYMBOL	WHEN YOU KNOW	MULTIPLY BY	TO FIND	SYMBOL
<b>TEMPERATURE (exact degrees)</b>				
<b>°F</b>	Fahrenheit	5 (F-32)/9 or (F-32)/1.8	Celsius	°C

SYMBOL	WHEN YOU KNOW	MULTIPLY BY	TO FIND	SYMBOL
<b>FORCE and PRESSURE or STRESS</b>				
<b>lbf</b>	poundforce	4.45	newtons	N
<b>lbf/in<sup>2</sup></b>	poundforce per square inch	6.89	kilopascals	kPa

\*SI is the symbol for the International System of Units. Appropriate rounding should be made to comply with Section 4 of ASTM E380.

### *Acknowledgments*

The authors would like to acknowledge the Washington State Department of Transportation for funding this project with specific thanks to the review team for their insightful contributions. Therein, both Mohammad Sheikhzadeh, P.E. and Kim Willoughby, P.E. are gratefully recognized. Further, congratulations to Mo for his long years of service and best wishes for his post retirement era. It was a pleasure to have had this opportunity.

Additional thanks are extended to Rick Cameron for his dedication in performing the thermal integrity profiles and attention to detail. Although no names are cited, the cooperation of the contractors that participated in these projects are duly noted.

Finally, the authors would like to express how impressed they were with cooperation between the WSDOT and the drilling contractors as well as the drilling industry.

## *Executive Summary*

Over the past 3 decades, a trend toward higher quality assurance in constructed drilled shafts has moved from monitoring only concrete quantities to refined slurry properties and post-construction, non-destructive testing. Although not always practical, the use of multiple test methods can provide more information and better assessment of shaft acceptability. These methods vary in the types of information obtained as well as the regions of the shaft that can be tested. However, recognizing the limitations of these state-of-the-art quality assurance methods to inspect these subsurface concrete columns, the Washington State Department of Transportation opted to entertain other technologies for their assessment. As a result, a relatively new testing method that uses the energy expended from hydrating concrete (and the associated temperature signature) was selected for this study. This thermal integrity approach provides an overall perspective of the shaft based on the presence or absence of intact heat producing concrete. The shaft shape, cage placement, cover and concrete health can all be addressed.

Thermal integrity profiling uses the measured temperature generated in curing concrete to assess the quality of cast in place concrete foundations (i.e. drilled shafts or ACIP piles). In concept, the absence of intact / competent concrete is registered by cool regions (necks or inclusions) relative to the shaft norm; the presence of additional / extra concrete is registered by warm regions (over-pour bulging into soft soil strata or voids). Anomalies both inside and outside the reinforcing cage not only disrupt the normal temperature signature for the nearest access tube, but also the entire shaft; anomalies (inclusions, necks, bulges, etc.) are detected by more distant tubes but with progressively less effect.

Over the duration of the 18 month study, eleven drilled shafts were tested at eight sites throughout the state of Washington. Testing was mostly performed by WSDOT personnel using equipment provided. Various shaft sizes and geology were encountered. Shaft sizes included: 4, 6.5, 7, 8, 9, 10, and 12 ft diameters. Time of thermal testing (after concreting) ranged from 1 to 16 days after casting. The concrete mix designs, from which the usable heat energy stems, also varied including slag and both Type F and C flyash mixes. These materials were catalogued while providing mechanisms for future tests to build on a database of mixes. This information is used to establish thermal testing times and aid in scheduling.

Thermal testing provides various details of shaft integrity which include effective shaft size (diameter and length), anomaly detection inside and outside reinforcement cage, cage alignment, and proper hydration of the concrete. The ability to detect concrete volumes outside the reinforcing cage is perhaps its strongest feature. For this study, no anomalies within the reinforcing cage were encountered but various forms of external section changes were identified as well as several cases of off-center cages. Cage alignments generally varied with depth. Notably, only two cases of reduced concrete cover were detected; bulges were most common.



## Table of Contents

List of Tables .....	ix
List of Figures .....	x
<i>Chapter One: Introduction</i> .....	1
1.1 Background .....	1
1.2 Problem Statement .....	5
1.3 Approach .....	5
1.4 Report Organization .....	6
<i>Chapter Two: Thermal Integrity Profiling</i> .....	7
2.1 Integrity Testing of Drilled Shafts .....	7
2.1.1 CSL Analysis .....	7
2.1.2 GGL Analysis .....	8
2.2 Thermal Integrity Profiling .....	11
2.2.1 Historical Development .....	12
2.2.2 Hydration Energy and Heat Dissipation .....	13
2.2.3 Field Testing Considerations .....	17
2.3 Chapter Summary .....	17
<i>Chapter Three: Field Testing and Analysis</i> .....	19
3.1 Field Testing Procedures .....	19
3.1.1 Establishing Testing Times .....	19
3.1.2 Access Tube Preparation .....	20
3.2 Thermal Test Equipment .....	23
3.3 TIP Data Collection .....	26
3.3.1 TIP Field Testing Software .....	26
3.3.2 Field Testing Operations .....	32
3.4 TIP Analysis Concepts .....	33
3.4.1 Level 1 Analysis .....	33
3.4.2 Level 2 Analysis .....	35
3.5 Visual Basic, Microsoft Excel and TIP View .....	43
3.5.1 Field Notes Worksheet .....	43
3.5.2 Field Worksheet .....	46
3.5.3 Concrete Worksheet .....	50
3.5.4 Radius Calcs Worksheet .....	51
3.5.5 Graphs Worksheet .....	52
3.5.6 ZTSDData Worksheet .....	53
3.6 Modeling User Guide .....	55
3.6.1 Editors .....	55
3.6.2 Visual Post Processor .....	62

<i>Chapter Four: Field Testing and Results</i> .....	63
4.1 Project 7594: Nalley Valley .....	64
4.1.1 Thermal Modeling .....	64
4.1.2 Thermal Testing Pier 6 Shaft A .....	69
4.1.3 Thermal Testing Pier 6 Shaft B .....	75
4.1.4 Thermal Testing Pier 6 Shaft C .....	81
4.1.5 Project 7594 Conclusions .....	81
4.2 Project 7465: Scatter Creek .....	87
4.2.1 Thermal Modeling .....	87
4.2.2 Thermal Testing Pier 1 Shaft A .....	87
4.2.3 Thermal Testing Pier 1 Shaft B .....	87
4.2.4 Project 7465 Conclusions .....	88
4.3 Project 7743: Tieton River.....	97
4.3.1 Thermal Modeling .....	97
4.3.2 Thermal Testing Pier 1 Shaft 1 .....	97
4.3.3 Project 7743 Conclusions .....	97
4.4 Project 7777L: US 395 Wandermere Vicinity.....	104
4.4.1 Thermal Modeling .....	104
4.4.2 Thermal Testing Pier 4 Shaft Left .....	104
4.4.3 Project 7777L Conclusions .....	104
4.5 Project 7681: Vancouver Rail.....	114
4.5.1 Thermal Modeling .....	114
4.5.2 Thermal Testing Pier 2 Shaft North.....	114
4.5.3 Project 7681 Conclusions .....	114
4.6 Project 7911: Gallup Creek.....	121
4.6.1 Thermal Modeling .....	121
4.6.2 Thermal Testing Pier 1 Shaft South.....	121
4.6.3 Project 7911 Conclusions .....	121
4.7 Project 7852: Hyak to Snowshed.....	132
4.7.1 Thermal Modeling .....	132
4.7.2 Thermal Testing Pier 4 Shaft B .....	132
4.7.3 Project 7852 Conclusions .....	132
4.8 Project 7926: Manette Bridge .....	131
4.8.1 Thermal Modeling .....	131
4.8.2 Thermal Testing Pier 2 Shaft South.....	131
4.8.3 Project 7926 Conclusions .....	131
 <i>Chapter Five: Conclusions and Recommendations.</i> .....	 153
5.1 Overview.....	153
5.2 Thermal Testing Sites .....	154
5.3 Field Testing and Equipment .....	155
5.4 Significant Features .....	156
5.5 New Developments .....	157
5.6 Limitations .....	158
5.7 Thermal Testing Checklist.....	158
 <i>References</i> .....	 161

## List of Tables

Table 2-1. WSDOT Rating of Drilled Shaft based on CSL results (WSDOT, 2009)...	8
Table 2-2. Effect of slag and flyash in shaft mixes on energy and duration (Eqns 1-7)....	14
Table 4-1. Thermal Testing Project Log.....	63
Table 5-1 Summary of shaft mix, model parameters, and testing information....	142

## List of Figures

Figure 1-1. Drilled shaft failed during load testing at 1100 psi concrete stress.....	1
Figure 1-2. Bridge pier plunging failure from insufficient geotechnical capacity..	3
Figure 1-3a. Exhumed shaft with compromised durability as well as structural and geotechnical capacity..	4
Figure 1-3b. Close-up after washing.....	4
Figure 1-4. CSL results identifying only end defect.....	4
Figure 2-1 Significance of standard deviation on sample GGL data set... ..	8
Figure 2-2. Typical effect of Cs137 probe life on the gamma count for 150 pcf concrete..	9
Figure 2-3. Tested area of shaft cross section from GGL and CSL.....	10
Figure 2-4 TIP probe equipped with four infrared thermocouples..	11
Figure 2-5 Thermal integrity profiling (left) data collection computer (right).....	12
Figure 3-1. Heat Source Calculator used to define the testing time window..	20
Figure 3-2 De-watering equipment (a) air cap, (b) compressor, (c) storage containers, and (d) heat resistant discharge tubing... ..	21
Figure 3-3 Simultaneous de-watering and thermal profiling.....	23
Figure 3-4 Thermal probe (left) encased infrared sensor (right)..	23
Figure 3-5 Tripod-mounted depth wheel (left) tube-mounted depth wheel (right)..	24
Figure 3-6 Laptop based data collection system shaded in field vehicle.....	25
Figure 3-6 Ruggedized data collection system with waterproof keyboard and screen.....	25
Figure 3-7 Opening TIP software screen to confirm equipment settings..	26
Figure 3-8 Initial input used to define software operation and output file names..	27
Figure 3-9 Status waiting mode..	28
Figure 3-10 The Running status state activated by clicking Start Collection.....	28
Figure 3-11 The estimated tube length (in feet) Accepted to start data collection. ....	29
Figure 3-12 Running status shows estimated tube depth but is similar to waiting screen.	29
Figure 3-13 Resetting the software and probe for the next run of the same tube.....	30
Figure 3-14 Display runs screen asking operator to review the previous scans..	31
Figure 3-15 Sample data showing importance of redundant scans.....	31
Figure 3-16 Good shaft based on level 1 analysis only..	34
Figure 3-17 Modeled temperature distribution across a 10ft diameter shaft at a given depth.....	35
Figure 3-18 Thermal integrity profile of 10ft diameter shaft..	36
Figure 3-19 Radial plot of Figure 3-18 shaft at 40ft.....	37
Figure 3-20 Average TIP measurements from all tubes and diameter from yield plots....	39
Figure 3-21 Linear relationship between measured tube temperature and shaft radius..	40
Figure 3-22 TIP data converted to radius for each tube (left) revolved into 3-D shape (right)..	41
Figure 3-23 Thermal integrity profiles from 4ft shaft cast with known anomalies..	42
Figure 3-24 Field Notes worksheet.....	44
Figure 3-25 Field Notes worksheet (continued)..	45
Figure 3-26 Field worksheet. ....	46
Figure 3-27 Tube Selection user form. ....	47



Figure 3-28 Individual tube data worksheet..	48
Figure 3-29 Example data of wheel run-on..	49
Figure 3-30 Example data of water at the bottom of tubes.....	50
Figure 3-31 Concrete worksheet.....	51
Figure 3-32 Radius Calc sheet.....	52
Figure 3-33 Graphs worksheet.....	53
Figure 3-34 ZTSDData worksheet.....	54
Figure 3-35 T3DModel opening / main menu screen.....	55
Figure 3-36 Materials editor screen.....	56
Figure 3-37 Section geometry editor screen.....	57
Figure 3-38 Saturated granular soil section fill example .....	58
Figure 3-39 4 ft diameter concrete cylindrical fill in 2m x 2m space.....	58
Figure 3-40 A different color is selected for each section as it is imported..	59
Figure 3-41 Sub-Model editor screen.....	60
Figure 3-42 Integrated model screen showing stacked sub-models..	61
Figure 3-43 Execute model screen with 5 defined steps.....	62
Figure 4-1 Nalley Valley concrete mix design page 1.....	65
Figure 4-2 Nalley Valley concrete mix design page 2.....	66
Figure 4-3 Nalley Valley Portland cement mill certificate.....	67
Figure 4-4 Nalley Valley fly ash mill certificate.....	68
Figure 4-5 Thermal predictions for a 10' diameter shaft showing the differences in old and current mix design parameters. ....	69
Figure 4-6 Measured tube temperatures versus depth (Nalley Valley Pier 6 Shaft A).....	70
Figure 4-7 Measured and modeled temperature versus depth (Nalley Valley Pier 6 Shaft A).....	71
Figure 4-8 Concrete Placement Log versus average measured temperature (Nalley Valley Pier 6 Shaft A).....	72
Figure 4-9 Effective shaft radius showing cage alignment uncorrected for axial heat dissipation (Nalley Valley Pier 6 Shaft A).....	73
Figure 4-10 3-D rendering from tube spacings and effective radius calculations (Nalley Valley Pier 6 Shaft A).....	74
Figure 4-11 Measured tube temperatures versus depth (Nalley Valley Pier 6 Shaft B).....	75
Figure 4-12 Thermocouple data for Pier 6 Shaft B compared with model response (top); elevated temperatures in shaft over 3 wk sampling period (bottom).....	76
Figure 4-13 Measured and modeled temperature versus depth (Nalley Valley Pier 6 Shaft B).....	77
Figure 4-14 Concrete Placement Log versus average measured temperature (Nalley Valley Pier 6 Shaft B).....	78
Figure 4-15 Effective shaft radius showing cage alignment uncorrected for axial heat dissipation (Nalley Valley Pier 6 Shaft B).....	79
Figure 4-16 3-D rendering from tube spacings and effective radius calculations (Nalley Valley Pier 6 Shaft B).....	80
Figure 4-17 Measured tube temperatures versus depth (Nalley Valley Pier 6 Shaft C).....	82
Figure 4-18 Measured and modeled temperature versus depth (Nalley Valley Pier 6 Shaft C).....	83

Figure 4-19 Concrete Placement Log versus average measured temperature (Nalley Valley Pier 6 Shaft C).....	84
Figure 4-20 Effective shaft radius showing cage alignment uncorrected for axial heat dissipation (Nalley Valley Pier 6 Shaft C).....	85
Figure 4-21 3-D rendering from tube spacings and effective radius calculations (Nalley Valley Pier 6 Shaft C).....	86
Figure 4-22 Scatter Creek concrete mix design page 1. ....	89
Figure 4-23 Scatter Creek concrete mix design page 2. ....	90
Figure 4-24 Scatter Creek Portland cement mill certificate.....	91
Figure 4-25 Scatter Creek fly ash mill certificate. ....	92
Figure 4-26 Measured tube temperatures versus depth (Scatter Creek Pier 1 Shaft A). ..	93
Figure 4-27 Measured and modeled temperature versus depth (Scatter Creek Pier 1 Shaft A).....	94
Figure 4-28 Measured tube temperatures versus depth (Scatter Creek Pier 1 Shaft B)..	95
Figure 4-29 Measured and modeled temperature versus depth (Scatter Creek Pier 1 Shaft B).....	96
Figure 4-30 Tieton River concrete mix design page 1.....	98
Figure 4-31 Tieton River concrete mix design page 2.....	99
Figure 4-32 Tieton River Portland cement mill certificate.....	100
Figure 4-33 Tieton River fly ash mill certificate.. ....	101
Figure 4-34 Measured tube temperatures versus depth (Tieton River Pier 1 Shaft 1)..	102
Figure 4-35 Measured and modeled temperature versus depth (Tieton River Pier 1 Shaft 1).....	103
Figure 4-36 US 395 Wandermere concrete mix design page 1. ....	106
Figure 4-37 US 395 Wandermere concrete mix design page 2.. ....	107
Figure 4-38 US 395 Wandermere Portland cement mill certificate. ....	108
Figure 4-39 US 395 Wandermere fly ash mill certificate.....	109
Figure 4-40 Measured tube temperatures versus depth (US 395 Wandermere Pier 4 Shaft L).....	110
Figure 4-41 Measured and modeled temperature versus depth (US 395 Wandermere Pier 4 Shaft L).....	111
Figure 4-42 Concrete Placement Log versus average measured temperature (US 395 Wandermere Pier 4 Shaft L).....	112
Figure 4-43 Effective shaft radius showing cage alignment uncorrected for axial heat dissipation (US 395 Wandermere Pier 4 Shaft L).. ....	113
Figure 4-44 3-D rendering from tube spacings and effective radius calculations (US 395 Wandermere Pier 4 Shaft L).....	114
Figure 4-45 Vancouver Rail concrete mix design page 1.....	116
Figure 4-46 Vancouver Rail concrete mix design page 2.....	117
Figure 4-47 Vancouver Rail Portland cement mill certificate.....	118
Figure 4-48 Vancouver Rail fly ash mill certificate. ....	119
Figure 4-49 Measured tube temperatures versus depth (Vancouver Rail Pier 2 Shaft N).....	120
Figure 4-50 Measured and modeled temperature versus depth (Vancouver Rail Pier 2 Shaft N).....	121
Figure 4-51 Gallup Creek concrete mix design page 1.....	124
Figure 4-52 Gallup Creek concrete mix design page 2.....	125

Figure 4-53 Gallup Creek Portland cement mill certificate.....	126
Figure 4-54 Measured tube temperatures versus depth (Gallup River Pier 1 Shaft S)...	127
Figure 4-55 Measured and modeled temperature versus depth (Gallup Creek Pier 1 Shaft S).....	128
Figure 4-56 Concrete Placement Log versus average measured temperature (Gallup River Pier 1 Shaft S)..	129
Figure 4-57 Effective shaft radius showing cage alignment uncorrected for axial heat dissipation (Gallup River Pier 1 Shaft S).....	130
Figure 4-58 3-D rendering from tube spacings and effective radius calculations (Gallup River Pier 1 Shaft S)..	131
Figure 4-59 Hyak concrete mix design page 1. ....	134
Figure 4-60 Hyak concrete mix design page 2. ....	135
Figure 4-61 Hyak cement mill certificate. ....	136
Figure 4-62 Hyak slag mill certificate. ....	137
Figure 4-63 Measured tube temperatures versus depth (Hyak Pier 4 Shaft B)..	138
Figure 4-64 Measured and modeled temperature versus depth (Hyak Pier 4 Shaft B). .	139
Figure 4-65 Concrete Placement Log versus average measured temperature (Hyak Pier 4 Shaft B)..	140
Figure 4-66 Effective shaft radius showing cage alignment uncorrected for axial heat dissipation (Hyak Pier 4 Shaft B)..	141
Figure 4-67 3-D rendering from tube spacings and effective radius calculations (Hyak Pier 4 Shaft B).....	142
Figure 4-68 Manette concrete mix design..	145
Figure 4-69 Manette Portlant cement mill cert. ....	146
Figure 4-70 Manette fly ash mill cert..	147
Figure 4-71 Measured tube temperatures versus depth (Manette Pier 2 Shaft S). ....	148
Figure 4-72 Measured and modeled temperature versus depth (Manette Pier 2 Shaft S).....	149
Figure 4-73 Concrete Placement Log versus average measured temperature (Manette Pier 2 Shaft S). ....	150
Figure 4-74 Effective shaft radius showing cage alignment uncorrected for axial heat dissipation (Manette Pier 2 Shaft S)..	151
Figure 4-75 3-D rendering from tube spacings and effective radius calculations (Manette Pier 2 Shaft S).....	152
Figure 5-1 Predicted tube temperature for various sizes of shafts (Nalley Valley mix)..	143
Figure 5-2 Effective radius from increases or decreases in cover around 3 ft cage..	144
Figure 5-3 Modeled step shaft and resultant temperature from a fixed radius from shaft center.....	145

## Chapter One: Introduction

### 1.1 Background

Drilled shafts are large diameter, cast-in-place, deep foundation concrete elements that as a result of their construction processes are vulnerable to anomaly formation. Therein, blind concrete placement beneath the water table (wet construction) makes it difficult to inspect and/or verify a contiguous and intact concrete element. Until recently, no method could assure that a shaft was truly constructed as expected. Three primary issues arise pertaining to the effects of shaft defects: (1) reduced structural capacity, (2) reduced geotechnical capacity, and (3) compromised long-term durability. Each of these is discussed in depth with a quick overview of the applicability of a new shaft integrity verification method.

*Structural Effects.* The AASHTO code specified capacities for concrete elements in flexure and compression are identical for structures both above and below ground regardless of construction methodology. The presumption is that sufficient quality assurance and inspection is exercised. The most commonly accepted form of Q/A is concrete break strength, slump, and above ground cage dimensions/verification (e.g. clear spacing, splice lengths, cage diameter, auger/tool diameter, etc.). In reality, concrete cylinders prepared straight from the truck are an optimistic look into the strength of the shaft throughout. Further, the actual shape of the shaft and quality of the concrete goes unknown. Figure 1-1 shows the result of a shaft load tested and that failed at 30% of the laboratory strength value,  $f'_c$ .



Figure 1-1 Drilled shaft failed during load testing at 1100 psi concrete stress.



Insufficient concrete over-pour (over-topping) was suspected to be the source of the poor concrete quality; in such instances the upper most portion of the shaft results in a weakly cemented mix of slurry, soil debris, and concrete.

When considering structural design, the resistance factors for above ground concrete columns are routinely assigned to drilled shafts in spite the disparity between the post construction inspections available. Assurance that a shaft has the full anticipated section is just as important as an above ground column but separate resistance factors due to the difference in confidence are not assigned. To that end, methods of inspection prior to this study were incapable of fully defining the as-constructed shaft concrete shape.

*Geotechnical Effects.* In addition to the inspection/test methods cited above (e.g. slump,  $f'c$ , etc.) fresh concrete properties such as slump loss and mix design parameters like maximum aggregate size play heavily into the geotechnical capacity that can be developed. For instance, studies have shown that construction that makes use of full length temporary casing may inadvertently *slip-form* a shaft in place when the slump falls below 5 inches prior to casing extraction (Mullins and Ashmawy, 2005). The net effect is near-zero side shear. If it falls below 3 inches, the casing may not be removable without damaging the shaft. Other adverse effects have been noted when the clear spacing to maximum aggregate size ratio is designed below 5 (8 minimum preferred). This causes stacking of the concrete inside the cage that can then *roll* over debris and increase the likelihood of soil/debris encapsulation. The latter is usually the result of structural performance criteria being superimposed on to shaft length requirements to obtain sufficient geotechnical capacity. It looks good on paper where AASHTO clear spacing requirement is 1.5 the maximum aggregate diameter (AASHTO, 2010), but for wet shaft construction, it simply does not work. A slightly larger shaft that reduces cage congestion eliminates the problem.

When designing for geotechnical capacity of shafts, the most common uncertainties are associated with soil type, soil strength, and to a lesser degree, shaft construction. This uncertainty is reflected in reduced AASHTO resistance factors based on whether or not load testing is used, results of past load test programs, and the desire to maintain an acceptable level of confidence. As all the shafts tested and used to statistically develop these resistance factors were constructed with an assortment of various construction methods, the resistance factors can be loosely thought to account for these variations. Regardless, geotechnical failures still occur; the source of failure is sometimes identified as being either soil strata/strength variability or construction effects, but it is not always clear. Figure 1-2 shows the result of a catastrophic shaft failure in Tampa, Florida. The cause is thought to have been the variations between the actual soil strata and the design boring log assumed to have been representative.



Figure 1-2 Bridge pier plunging failure from insufficient geotechnical capacity.

*Durability Effects.* Many of the same parameters mentioned above affect the long-term performance of the shaft. The most widely recognized durability issue lies with exposed rebar. This can be the result of low concrete slump, tight rebar spacing (relative to maximum aggregate size), high slurry sand content (encapsulation), and/or excavation instability. In each of these cases, the rebar is exposed to groundwater, seawater, or soil acidity. The time-dependent loss in steel coupled with the as-built concrete section loss can/will ultimately leave the supported structure unsafe. However, in many cases the structure is vulnerable to structural or geotechnical failure at the onset. Figures 1-3a and 1-3b show an exhumed shaft for a high mast highway light that suffered from all three issues discussed. Although the entire shaft is flawed with little to no concrete cover throughout, only the most-extreme condition at the toe of the shaft was discernible from cross-hole sonic logging, CSL (one of the most common shaft integrity methods used today). Figure 1-4 shows the results of the CSL testing which was incapable of detecting flaws outside the reinforcing cage.

Finally, the durability of a drilled shaft can be adversely affected by the heat generated during the cement hydration. This has two mechanisms of interest with respect to shaft integrity both dealing with mass concrete conditions: the peak temperature developed and the differential temperature between the core and edge. These conditions have been shown to occur in shaft diameters smaller than once considered problematic (Mullins and Kranc, 2007). Shafts as small as 3 or 4 ft in diameter can exhibit peak and differential temperatures above safe limits due to the insulating properties of soils and rock (both dry and submerged).



Figure 1-3a Exhumed shaft with compromised durability as well as structural and geotechnical capacity.



Figure 1-3b Close-up after washing.

Means of controlling the temperature in drilled shafts without cooling systems have been devised. The enormous energy created by hydrating cement provides the means by which the system proposed for this study is capable of identifying the presence of as well as the magnitude of shaft anomalies. As the test is conducted relatively quickly after initial set, information regarding shaft intactness can be made readily available prior to full strength development.

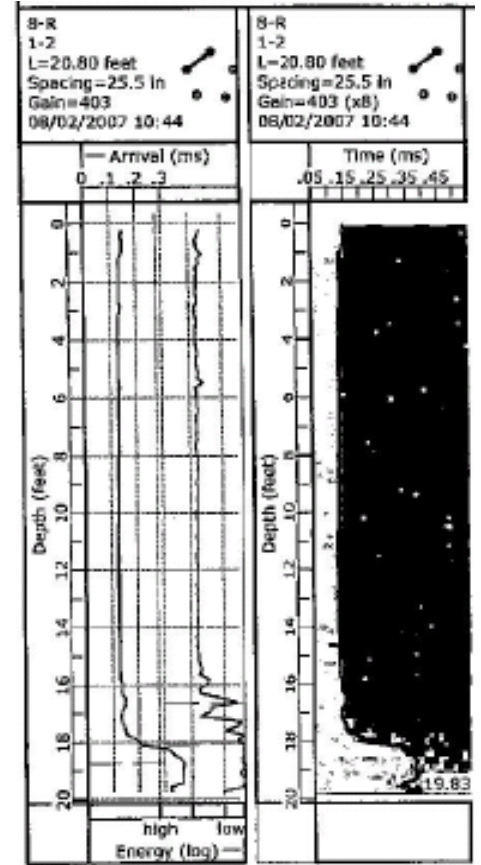


Figure 1-4 CSL results identifying only end defect.

## 1.2 Problem Statement

This report summarizes the findings of a research project funded by the Washington State Department of Transportation (WSDOT) based on the following request for research proposal.

*WSDOT constructs drilled shafts using the wet method and typically accepts them based on the successful results of the Cross Sonic Log (CSL) testing. This method of Quality Assurance (QA) testing can only verify the quality of concrete inside the shaft core and does not provide for verification of the quality or adequacy of the concrete cover on the outside of the shaft rebar cage. The lack of quality of the concrete cover can occur when (1) the tremie concrete has low slump and does not penetrate through the closely spaced rebar cage and results in unprotected rebar, which is then subject to corrosion, or (2) the tremie concrete mixes with the slurry and is contaminated, which leads to lower quality concrete.*

*There is a lack of reliable test methods among the States utilizing drilled shafts to verify the quality of concrete throughout the entire drilled shaft (including the concrete on the outside of the rebar cage), so WSDOT is interested in a new test method to determine the quality and adequacy of the concrete. Some of the methods that are/have been used, but WSDOT is not interested in are:*

- *Impact/Sonic Echo;*
- *Gamma-Gamma Logging;*
- *Transient Dynamic Response/Impulse Response; and*
- *Cross Sonic Logging.*

*The objective of this research is to develop a reliable, practical, innovative, safe, and cost-effective testing method that can verify shaft core concrete quality as well as presence of adequate concrete cover outside the shaft rebar cage.*

## 1.3 Approach

Based on the above problem statement, a scope of services was outlined to address the deficiencies in drilled shaft QA methods. The chosen approach was based on a newly developed method to assess drilled shaft concrete presence/intactness using temperature profiles of the shaft obtained from temperature scans of the inner walls of access/logging tubes. The test methodology is referenced to herein as Thermal Integrity Profiling or TIP. In order to accomplish the project objectives, the proposed research was envisioned to undertake four primary supporting tasks:

- Field Temperature Measurements of WSDOT Constructed Shafts
- Develop Libraries of Soil Properties and WSDOT-Concrete Mix Designs
- Thermal Software Upgrade to include library values

- Recommendations and Conclusions / Reporting

These tasks were completed and in some cases modified in keeping with the findings and progression of the study.

#### **1.4 Report Organization**

This report is broken out into four subsequent chapters that address the outlined tasks of the project. Chapter 2 provides an overview and historical development of Thermal Integrity Profiling. Chapter 3 addresses the field testing procedures, analysis methods that can be applied to TIP data, and the resulting output. Chapter 4 introduces the WSDOT tests sites used for this study, the data collected, and results. Chapter 5 concludes with a summary of the project findings and includes on-going and possible future efforts to further TIP capabilities and features.

## *Chapter Two: Thermal Integrity Profiling*

This chapter presents an overview of drilled shaft integrity testing while providing the historical development and capabilities of thermal integrity profiling.

### **2.1 Integrity Testing of Drilled Shafts**

The Federal Highway Administration provides guidelines for the inclusion of access tubes in the reinforcing cages of drilled shafts for the purposes of performing post construction integrity testing (O'Neill and Reese, 1999). The recommended tube materials, diameters, and plurality are assigned to provide sufficient access to the shaft cross-section for non-destructive evaluation. Therein, both cross-hole sonic logging, CSL, and gamma-gamma logging, GGL, can be performed but with a limited detection zone within the shaft cross-section: CSL most commonly assesses the concrete quality directly between the tubes (inside the reinforcing cage) based on the compression wave velocity between tubes; GGL makes a determination of concrete density within 3 - 4.5in radius from the centerline of the access tube using gamma radiation measurement (Caltrans 2005 and 2010). Although sonic echo test methods are available, they are less frequently used for DOT structures and tend to be less quantitative; these methods are not discussed herein.

#### **2.1.1 CSL Analysis**

In general, to analyze CSL results, the recorded arrival time required for sound waves to travel between two tubes is divided by the measured tube spacing to compute the compression wave velocity as a function of depth. The local velocity is then compared to the average velocity for that tube pair to calculate the percent reduction in velocity. Acceptance or rejection of a shaft tested with CSL varies from state to state. For example where the Florida Department of Transportation (FDOT) defines a threshold level for acceptance of anything less than 30 percent reduction in wave speed, WSDOT assigns a lower threshold to indicate a defect or poor concrete (Table 2-1).

At one point in time, FDOT had a similar threshold but due to recurring false positive results, a decrease in the stringency of the acceptance standard resulted (higher allowable percent reduction). A false positive is when anomalous results (higher arrival times) are caused by something other than faulty concrete. Primary causes of false positives include, but are limited to, debonded access tubes, early age concrete or segregation of coarse aggregate which may or may not be problematic when cored and tested.

Although always included in CSL results (in one form or another), the computed wave speed should also be checked against an acceptable range for competent concrete. Simple comparison to average wave speeds for a given tube pair may be misleading if the entire length of the tube pair tested is affected.



Table 2-1. WSDOT Rating of Drilled Shaft based on CSL results (WSDOT, 2009).

Good (G)	No signal distortion and decrease in signal velocity of 10% or less is indicative of good quality concrete.
Questionable (Q)	Minor signal distortion and a lower signal amplitude with a decrease in signal velocity between 10% and 20%. Results indicative of minor contamination or intrusion and/or questionable quality concrete. Investigation of anomalies with 10% to 15% reductions in velocity have identified sound concrete at some sites and flawed concrete at others.
Poor/Defect (P/D)	Severe signal distortion and much lower signal amplitude with a decrease in signal velocity of 20% or more. Results indicative of water slurry contamination or soil intrusion and/or poor quality concrete.
No Signal (NS)	No signal was received. Highly probable that a soil intrusion or other severe defect has absorbed the signal (assumes good bonding of the tube-concrete interface). If PVC tubes are used or if measurement is from near the shaft top the tube-concrete bonding is more suspect.
Water (W)	A measured signal velocity of nominally $V = 4,800$ to $5,000$ fps. This is indicative of a water intrusion or of a water filled gravel intrusion with few or no fines present.

### 2.1.2 GGL Analysis

Similarly, GGL test results are most often compared to an average tube response and an acceptable number of standard deviations from the average. Therein, data that falls within two standard deviations from the average represents 95% of a normally distributed population of data points (Figure 2-1). Data that falls within three standard deviations encompasses 99.9% of a similar data set. If outside three standard deviations, such data is statistically unrepresentative and for gamma count rates indicates anomalous concrete. This can be misleading if gamma rate counts are used without physical correlations. When analyzed properly, GGL test results should be converted from gamma count rate to bulk density to be assured that the average and standard deviation are meaningful.

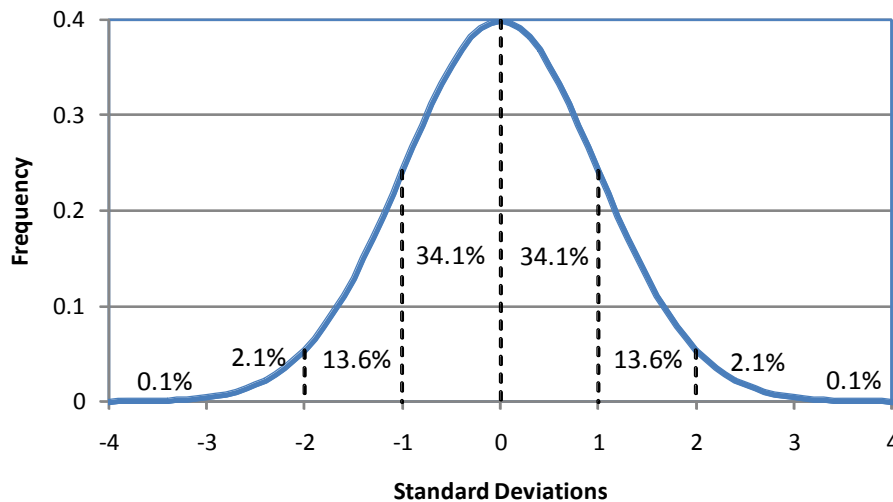


Figure 2-1 Significance of standard deviation on sample GGL data set.

Typical bulk densities of concrete are well defined depending on mix design. Likewise, a reasonable standard deviation for concrete can also be adopted. California Transportation (Caltrans) Department specifies that the standard deviation be no more than 2.5 pcf and no less than 3.75 pcf (Caltrans, 2010). This keeps drastically varying data sets from assigning seemingly normal or acceptable values when large amounts of variation statistically skew the results. It also prevents atypically consistent concrete (e.g. varies only several pcf throughout) from being mislabeled as bad when it statistically varies outside three standard deviations. Caltrans appears to have the most comprehensive state GGL program which has identified these issues and provided the remedies cited above. Using the permissible range for standard deviation (above), concrete that is 7.5 to 11.25 pcf less than the average (based on the 3 STDEV criteria) is deemed deficient and that zone is considered anomalous if it persists for a length of 0.5ft or more around a single tube. Further specifications defining the extent of the affected region are also provided (Caltrans, 2005).

GGL probes function based on the amount of gamma photons that are either shielded by the surrounding material or not. The predicted bulk density is inversely proportional to the logarithm of the unshielded/detected gamma count rate. Higher count rates indicate lower density and vice versa. The material and diameter of the logging tubes affect the measured response. Steel tubes provide more shielding and a lower gamma count rates than plastic; smaller diameter logging tubes likewise reduce the measured gamma count rate by reducing the non-shielding void volume. As the radioactive material is constantly decaying, the intensity of the emitter source is also decreasing. This means that like most sensors, it should be recalibrated periodically; the emitter intensity is cut in half every twenty years based on the half-life of the radioactive material. Figure 2-2 shows an example change in measurements due to life of probe for a 150 pcf concrete.

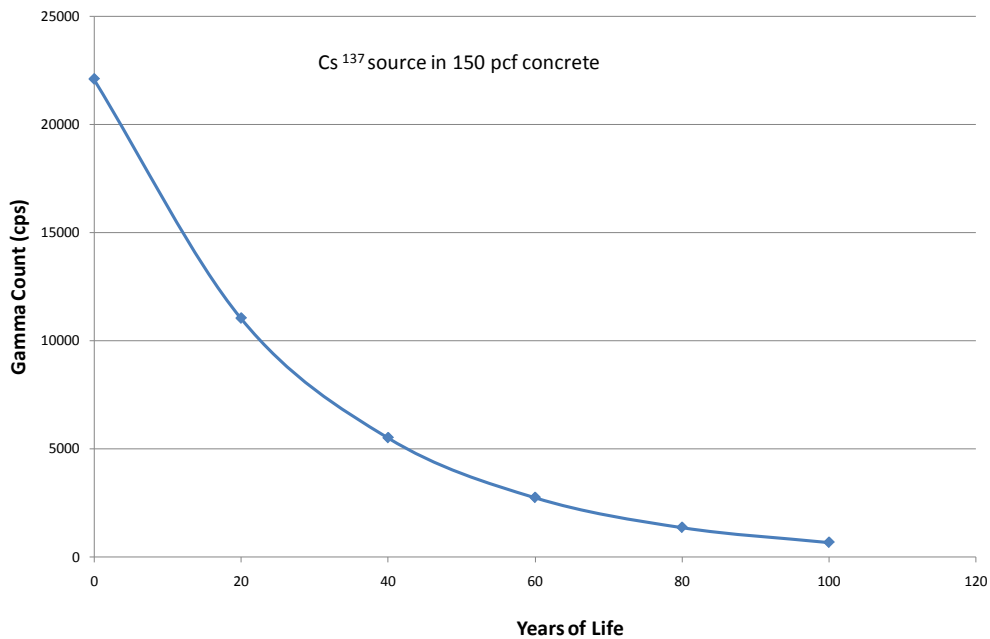


Figure 2-2 Typical effect of  $Cs^{137}$  probe life on the gamma count for 150 pcf concrete.



The Caltrans program clearly specifies probe calibration procedures that include periodic gamma count rate to density correlations and detection zone determinations. The detection zone should not be so large that it detects and is affected by soil outside a shaft with a normal cover. However, within the detection zone the closest material to the access tube (including access tube material and diameter of tube) has the most effect on the measured gamma count rate. The material on the outer fringes of the detection zone has a far less effect.

Whether using CSL or GGL, areas of the shaft are untested. Figure 2-3 shows the percentage of the cross sectional area tested by GGL and CSL for a wide range of shaft diameters assuming 6in of cover used (FDOT, 2010). Two images have been superimposed that represent graphically the coverage (shaded) when applied to a 3ft diameter shaft with four tubes. WSDOT allows 4 inches of cover for smaller diameter shafts which provides a larger fraction of the core concrete coverage when using CSL testing.

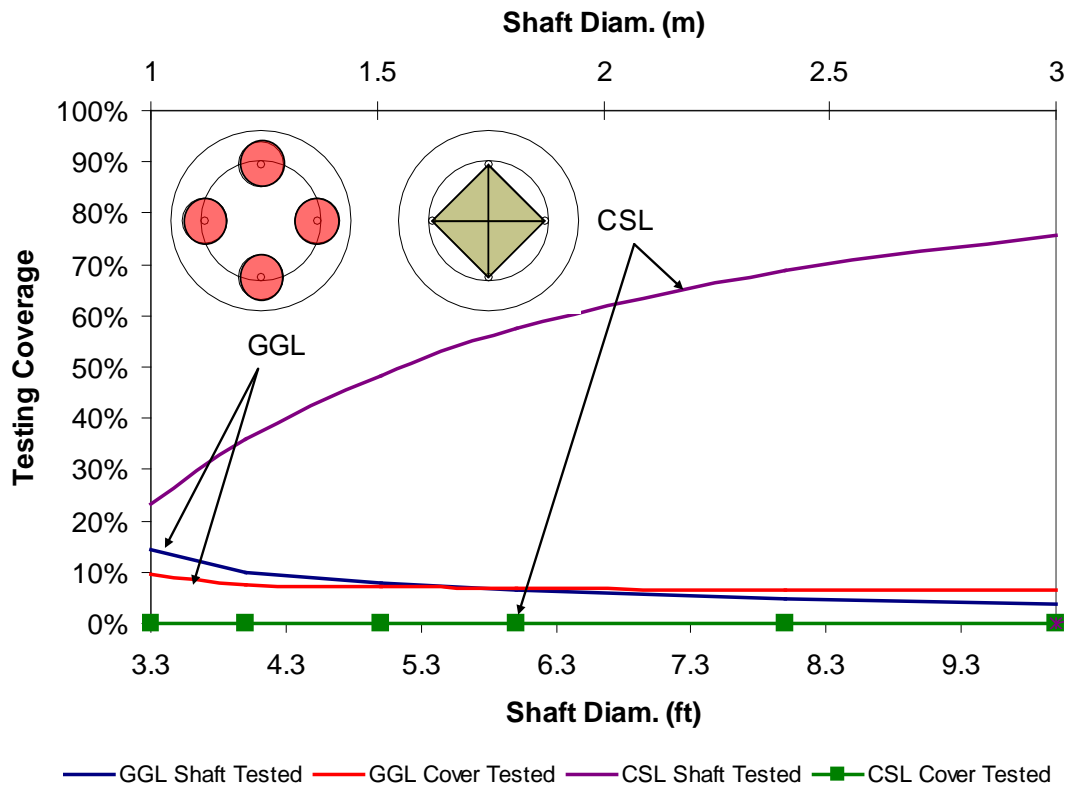


Figure 2-3 Tested area of shaft cross section from GGL and CSL.

The outermost concrete of the shaft provides the most benefit to the shaft. Geotechnically, it provides the bond to the bearing strata. Structurally, the contribution to the bending capacity from the core concrete is negligible when compared to that of the outer regions where the moment of inertia is proportional to the square of the distance from the centroid to the contributing concrete area ( $I = \sum A_i x_i^2$ ). Recent studies assessed

the feasibility of casting shafts with a full length central void to remove the unneeded core concrete (Johnson and Mullins, 2007; Mullins et al., 2009). Little reduction in bending capacity was noted but reductions in axial capacity (structural) roughly proportional to the fraction of the removed concrete cross section were recognized. The focus there was to reduce the peak internal temperature and the associated mass concrete conditions.

Consequently, the concrete cover that forms the bond between the shaft reinforcement and the bearing strata and can be considered the most important concrete in the shaft. Unfortunately, this concrete is only partially tested by GGL and not routinely tested by CSL without single tube methods. Single tube sonic tests (not discussed) are far less quantitative than tube pair testing. These shortcomings were identified by WSDOT and formed the impetus for this study. The thermal method of assessing shaft integrity, presented herein, is equally sensitive to anomalies both inside and outside the reinforcing cage.

## 2.2 Thermal Integrity Profiling

Thermal integrity profiling uses the measured temperature generated in curing concrete to assess the quality of cast in place concrete foundations (i.e. drilled shafts or ACIP piles). The necessary information is obtained by lowering a thermal probe into access tubes and measuring the tube wall temperature in all directions over the entire length of shaft. The probe is equipped with four horizontally-directed, infrared thermocouples oriented at 0, 90, 180 and 270 degrees about the longitudinal axis of the probe. Throw-away embedded devices can also perform the same function given adequate quantities are used to provide sufficient coverage (Mullins, 2010).



Figure 2-4 TIP probe equipped with four infrared thermocouples.

In general, the absence of intact / competent concrete is registered by cool regions (necks or inclusions) relative to the shaft norm; the presence of additional / extra concrete is registered by warm regions (over-pour bulging into soft soil strata or voids). Anomalies both inside and outside the reinforcing cage not only disrupt the normal temperature signature for the nearest access tube, but also the entire shaft; anomalies (inclusions, necks, bulges, etc.) are detected by more distant tubes but with progressively less effect.

Figure 2-5 shows a thermal integrity profile being performed whereby the depth of the probe is tracked by a digital encoder wheel over which the lead wire is passed.



Figure 2-5 Thermal integrity profiling (left) data collection computer (right).

### 2.2.1 Historical Development

In the wake of cone penetrometer development in the late 1970's and early 1980's, cone penetrometers were being outfitted with various sensors (e.g. pore pressure, resistivity, cameras, etc). At that time, faculty researchers at the University of South Florida gave serious consideration to taking soil temperature measurements around freshly cast shafts using the cone as the means to gain access to these regions. Two hurdles seemed insurmountable: (1) the time to achieve thermal equilibrium between a cone-based temperature sensor and the soil (without creating thermal disturbances) was too long to be practical and (2) the inability to penetrate rock or stiff soil commonly the target bearing strata. Additionally, the cost of throw-away embedded instrumentation (e.g. thermocouples or similar) in the reinforcing cage or in small boreholes surrounding the excavation was exorbitant. However, as instrumented load tests came into favor of many designers, so did embedded inclinometer casings which opened the door to measurements from reusable down-hole devices capable of monitoring inclination, lateral acceleration, axial strain, density, wave speed, and temperature.

The first full scale versions of thermal integrity profilers used inclinometer wheel bodies with much larger infrared sensors than those used today. By the turn of the 21<sup>st</sup> century, several versions of the equipment had evolved progressively smaller to provide access in smaller diameter tubes staying abreast with the trend toward smaller CSL devices. Smaller access tubes reduce cage congestion and aid in providing better concrete flow through the cage openings. The probe used in this study was 1.25in diameter and 6 in long for use in tubes as small as 1.5in inner diameter (Figure 2-4).

## 2.2.2 Hydration Energy and Heat Dissipation

Various physical, chemical, and molecular principles are combined in the concept of thermal integrity profiling of drilled shafts that address heat production in the concrete, diffusion of the heat into the soil, and the resulting temperature signature produced by a properly shaped drilled shaft (Mullins, 2010, Mullins et al., 2004, 2005, 2007, and 2009; Kranc and Mullins, 2007). At various stages of the curing process these principles have more prominent effects; heat production tends to dominate the resulting temperature in the early stages whereas the surrounding dissipation process controls later on.

*Heat Production.* The quantity of heat and rate of heat production are directly linked to the concrete mix design and the chemical constituents of the cementitious materials. These materials are generally comprised of cement and flyash or slag. Each material produces heat when hydrating, the total magnitude of which is dependent on the cementitious fraction  $p$  (by weight) with respect to total cementitious material. The total heat,  $H_u$ , and the rate of production can be determined from equations (1) – (5) where  $H$  is in units of kJ/kg (Schindler, 2005).

$$H_u = H_{cem}p_{cem} + 461p_{slag} + h_{FA}p_{FA} \quad (1)$$

Where the energy per kilogram of slag is directly given to be 461 kJ/kg, the cement and flyash energy production can be determined using equations (2) and (3), respectively.

$$H_{cem} = 500p_{C_3S} + 260p_{C_2S} + 866p_{C_3A} + 420p_{C_4AF} + 624p_{SO_3} + 1186p_{FreeCaO} + 850p_{MgO} \quad (2)$$

$$h_{FA} = 1800p_{FACaO} \quad (3)$$

Both equations (2) and (3) require precise knowledge of the chemical composition of the cement and flyash in the form of the weight fraction of the various chemical compounds,  $p_i$ . These are usually available from the concrete supplier and flyash source (municipal power plant).

Schindler (2005) provided means to compute rate of heat production whereby curve fitting algorithms were applied to extensive laboratory studies again based on the weight fraction of the various cementitious constituents. The degree of hydration at time,  $t_e$ , can be determined using equation (4).

$$\alpha(t_e) = \alpha_u \exp\left(-\left[\frac{\tau}{t_e}\right]^\beta\right) \quad (4)$$

When  $\mathbf{a}$  equals 1.0 all hydration energy has been developed from equation (1). The parameters  $\mathbf{a}_u$ ,  $\mathbf{b}$ , and  $\mathbf{t}$  are determined again by cementitious constituent fractions,  $p_i$ , shown in equations (5) – (7), respectively, as well as the water cement ratio,  $w/cm$ .

$$\alpha_u = \frac{1.031w/cm}{0.194 + w/cm} + 0.5p_{FA} + 0.3p_{SLAG} \leq 1.0 \quad (5)$$

$$\beta = p_{C_3S}^{0.227} \cdot 181.4 p_{C_3A}^{0.146} \cdot Blaine^{-0.535} \cdot p_{SO_3}^{0.558} \cdot \exp(-0.647 p_{SLAG}) \quad (6)$$

$$\tau = p_{C_3S}^{-0.401} \cdot 66.78 p_{C_3A}^{-0.154} \cdot Blaine^{-0.804} \cdot p_{SO_3}^{-0.758} \cdot \exp(2.187 \cdot p_{SLAG} + 9.5 \cdot p_{FA} \cdot p_{FA-CaO}) \quad (7)$$

For typical shaft mixes with moderate flyash percentages (15%)  $\tau$  usually is around 18-24 meaning that all energy has been expended in roughly 18 - 24 hours. High slag content mixes (e.g. 60% replacement) usually take upwards of 50 hours. Mixes with no flyash or slag are usually expended in about 15 hours. Table 2-2 shows the effect of using flyash or slag on approved shaft mixes from both Washington and Florida DOTs.

Table 2-2. Effect of slag and flyash in shaft mixes on energy and duration (Eqns 1-7).

Concrete Constituents	WSDOT 4000P (Flyash)	WSDOT 4000P (Slag)	FDOT Class IV 4000 (Flyash)	FDOT Class IV 4000 (Slag)
Cement, kg (%)	276.7 (85%)	272.2 (77%)	226.8 (66%)	122.5 (39.7%)
MgO, %	0.83	1	0.7	0.9
C <sub>2</sub> S, %	13	14	10	9
C <sub>3</sub> A, %	7.1	5	7	7
C <sub>3</sub> S, %	58	60	62	63
SO <sub>3</sub> , %	2.8	2.7	2.9	2.9
C <sub>4</sub> AF, %	11.2	10	12	11.3
Blaine, m <sup>2</sup> /kg	387	411	391	386
Flyash, kg (%)	49.9 (15%)	-	114.8 (34%)	-
SO <sub>3</sub> , %	1	-	1.8	-
CaO, %	15.1	-	5.2	-
Slag, kg (%)	-	81.3 (23)	-	186.0 (60.3%)
w/cm	0.37	0.41	0.52	0.41
Energy (kJ/kg)	76.2	87.7	57.5	53.8
<b>a</b>	0.753	0.769	0.921	0.881
<b>b</b>	0.630	0.699	0.699	0.435
<b>τ</b> (hrs)	19.4	26.3	17.4	54.5

*Heat Diffusion.* Just as important as the energy production is the mechanism by which the heat is dissipated into the surrounding environment. Although the thermal integrity approach can be applied to all concrete structural elements, it is most commonly used for drilled shafts wherein the surrounding environment is largely dominated by a soil structure or geo-material.

Heat flow in soils involves simultaneous mechanisms of conduction, convection, and radiation of which conduction overwhelmingly dominates the heat transport. Conductive heat flow in soils is analogous to fluid or electrical systems. The *thermal conductivity*,  $\lambda$ , is defined as the heat flow passing through a unit area,  $A$ , given a unit temperature gradient,  $\Delta T / L$ , equation (8).

$$\lambda = \frac{q}{A \cdot \Delta T / L} \quad (8)$$

This value can be estimated by the geometric mean of the thermal conductivity of the individual matrix components: solids, water, and air. Thermal conductivity of soil minerals range from 2 to 8 W/m-C for clay to quartz, respectively. Although dependent on temperature and relative humidity, water is roughly 0.5 W/m-C and air, 0.03 W/m-C. For a saturated soil, the thermal conductivity can be determined using equation (9) where  $n$  represents the volumetric fraction of water (Johansen, 1975; Duarte, 2006).

$$\lambda_{sat} = \lambda_s^{(1-n)} \lambda_w^n \quad (9)$$

Likewise, the thermal conductivity of the solids,  $\lambda_s$ , is related to the fraction of quartz or sand,  $q$ , in the soil and is determined using equation (10). The subscript “o” denotes other soil minerals.

$$\lambda_s = \lambda_q^q \lambda_o^{(1-q)} \quad (10)$$

Not surprisingly, there is a strong correlation between thermal conductivity and mechanical properties as close contact / dense packing of the soil particles aides in transmitting heat by means of thermo-elastic waves. Farouki (1966) provided translation of this concept from Debye (1914) wherein heat flow through non-metallic crystalline solids occurs when warmer atoms vibrate more intensely than adjacent cooler atoms which in turn propagate waves by way of atom to atom contact at a characteristic speed. As a result, the thermal conductivity can be related to the compression wave velocity for a given material. The strength of the bonds between atoms affects this speed which is also dependent on the heat capacity of the material.

The *heat capacity* of the soil can be determined based on the volumetric fraction of solids, water, and air wherein the heat capacity of each component is defined as the heat required to raise the temperature of a unit volume of material one degree C. The heat capacity is actually the product of the mass specific heat,  $c$ , and the dry density of the soil,  $\rho$ . Farouki (1981) and Duarte (2006) define the specific heat of a volume of soil by introducing  $X_i$  as the volumetric fraction of each component, equation (11) can be use to determine the effective specific heat of the soil matrix where  $C_S$ ,  $C_W$ , and  $C_A$  represent the heat capacity of the solids, water, and air, respectively.

$$C = X_S C_S + X_W C_W + X_A C_A \quad (11)$$

In essence, two almost conflicting parameters affect heat dissipation into the surrounding soils: the ability to conduct heat (**L**) and the reluctance of the soil to be heated (**C**). The more dense the material the better it conducts while also requiring more energy to warm. This combines into an additional parameter, the *diffusivity* ( $k$ ) which is defined as the ratio of the thermal conductivity to the heat capacity, equation (12).

$$k = \frac{\lambda}{\rho \cdot c} \quad (12)$$

For the prediction of normal internal shaft temperature, the thermal conductivity, heat capacity, and the resultant diffusivity can be determined from boring logs whereby the soil type and blow count are used to estimate mineral content and density (Pauly, 2010).

Finally, the temperature diffusion is characterized by the partial differential equation (13) where the change in temperature,  $T$ , with respect to time,  $t$ , is proportional to the product of the diffusivity,  $k$ , and the second derivative of temperature with respect to distance in three spatial directions  $x$ ,  $y$ , and  $z$  [6].

$$\frac{\partial T}{\partial t} = k \left( \frac{\partial^2 u}{\partial x^2} + \frac{\partial^2 u}{\partial y^2} + \frac{\partial^2 u}{\partial z^2} \right) \quad (13)$$

When a heat source,  $Q$ , is added (like concrete hydration energy) the following equation (14) governs wherein the product of the heat capacity,  $\rho C$ , and the change in temperature,  $T$ , with respect to time,  $t$ , are proportional to the sum of the heat added,  $Q$ , and the divergence of the product of the conductivity,  $\mathbf{L}$ , and temperature gradient.

$$\rho C \frac{\partial T}{\partial t} = Q + \nabla \cdot (\lambda \nabla T) \quad (14)$$

This overview of heat production and dissipation provides an insight into the workings of three-dimensional finite difference algorithms that can be used to predict the temperature within the shaft at various thermal integrity testing times (Johnson, 2007; Mullins, 2009). This is then coupled with shaft geometry to provide the most beneficial timeframe for performing thermal integrity profiles of the curing shaft concrete. To that end, it is important to note that these mechanics are theoretically sound and provide the reproducibility for reliable thermal integrity assessment.

### **2.2.3 Field Testing Considerations**

Thermal integrity profiles are collected as the probe descends and displayed real-time to the operator (Figure 2-5). The descent rate is kept between 0.3 to 0.5 ft/s to both assure that sufficient depth resolution is obtained and that the infrared sensor has successfully captured the internal wall temperature. Typically, two scans of each tube are performed to assure reproducible data. At 0.5 ft/s testing a 100ft tube takes about 3 minutes; running twice while resetting the computer between runs takes about 8 minutes overall (per 100ft of tube).

Standard construction practices require that access tubes installed for the purposes of CSL testing must be filled with clean water prior to concreting. This minimizes the potential of tube de-bonding and extends the viable timeframe for sonic testing. Thermal integrity profiling does not require the tubes to be filled for three reasons: (1) thermal measurements are insensitive to de-bonding, (2) testing is performed early enough that de-bonding has not yet occurred, and (3) the infrared sensor performance. However, unless the client or contractor is certain that only thermal profiles are needed, the tubes are generally filled. Water filled tubes must be dewatered prior to thermal profiling to eliminate infrared distortion. A recommended procedure has been adopted (discussed in Chapter 3) that allows for the capture and return of the already warmed tube contents. The discharge tube used to perform this procedure is shown in Figure 2-5 (white) where the contents of one tube is moved to a tube that has already been tested. This reduces the volume of warmed water that is stored outside of the shaft.

### **2.3 Chapter Summary**

This study stemmed from the need to better assess the as-built quality of drilled shafts. Although a combination of multiple state-of-the-art test methods does provide a more thorough perspective, this is often not cost-effective. It is therefore desirable to explore other technologies that could be extended to integrity testing that may provide a more comprehensive assessment. The use of concrete hydration energy has been successfully employed in other states to make these determinations and was proposed for this study.



This page is intentionally left blank.

## *Chapter Three: Field Testing and Analysis*

This chapter provides an overview of thermal testing equipment, standard testing practices, and general evaluation of thermal data. Multiple levels of analysis that can be undertaken depending on need.

### **3.1 Field Testing Procedures**

Thermal integrity profiling should be performed in accordance with the procedures defined by this chapter. At present, there is no ASTM standard specification for thermal integrity profiling.

#### **3.1.1 Establishing Testing Times**

Thermal integrity profiling requires temperature generation from hydrating materials to provide distinction between cementitious and non-cementitious materials. Testing should be performed while these materials are warm enough to establish a usable temperature gradient which ranges from 2 to 10 days depending on shaft diameter which is roughly proportional to shaft diameter in feet, respectively. However, this timeframe is dependent on the concrete mix design, cement constituent composition, use of alternative cementitious materials, and retardation. It is therefore preferable to define an estimated time frame using as much of this information as possible.

When available the cement constituent composition and mix design can be inputted into a simple Heat Source Calculator (HSC) which has been provided (Figure 3-1). This software computes the time required to complete the hydration process which serves as a lower bound for the time of testing (earliest test time). This can range from approximately 15 to 50 hours. Mixes with high slag content take longer to complete the hydration. Testing too early presents the possibility of having variations in maturation between trucks. By waiting to this minimum time the peak energy has been deployed, the highest anomaly sensitivity exists, and truck variations fade away.

It is often not practical to test precisely at this time, so an upper limit on the time frame can be estimated based on diameter shaft. Larger shafts are unable to dissipate heat quickly and therefore retain a usable temperature gradient with the surround environment for a longer time. The HSC defines the latest time of testing to be numerically equal to the feet of shaft diameter but in the units of days. The HSC does not account for retarder dosages or water reducers that might cause delayed hydration onset. This should be estimated either by the requested slump loss window or by the concrete supplier and added to delay the entire testing time window.



Figure 3-1. Heat Source Calculator used to define the testing time window.

Many parameters are input into and output by the HSC all of which can be stored in a mix design library / database for future use. Input values are shown in white cells and come from mix design, cement and flyash certifications. Output values are shown in grey cells and are used for modeling parameters or to set test times. At present several WSDOT mix designs have been input that correspond to the various sites tested over the duration of the project.

### 3.1.2 Access Tube Preparation

Thermal integrity profiling can be performed in both PVC and steel access tubes. These tubes should be installed by the contractor during cage fabrication in keeping with local state practices. Preferably, both the top and bottom of the access tubes should be threaded with water-tight end caps. If tubes are filled with water during construction, the water must be expelled prior to testing, stored, and returned after testing if CSL tests are be conducted. If CSL tests are not planned, water is not necessary during construction as TIP results are not sensitive to debonding and the water is not used.

Tube Measurements. The depth of each access tube should be measured with a weighted measuring tape and recorded referencing the tube number where the northerly most tube is denoted as Tube No. 1. Tube numbering should increase clockwise looking down on

the top of the shaft. Although thermal testing requires the water to be removed from the tubes, tube depths should be measured prior to de-watering to both note the condition of the tubes with regards to debris or blockages and also take advantage of the buoyancy and lubrication on the tape that is afforded by the water. The center to center spacing between tubes should be measured such that the coordinates of each tube can be calculated relative to Tube No. 1. This requires varying amounts of measurements depending on the number of tubes. The height of tubes above the top of shaft concrete should also be recorded for each tube.

**Water Removal.** The procedure for water removal and storage has been established to minimize structural and thermal disturbances to the tubes and the surrounding concrete both for thermal profiling and any subsequent integrity testing. The water expelled is captured, stored and returned after testing to assure the tubes do not become thermally shocked by the introduction of cooler water (if not captured). Again, if thermal profiling is the only test performed then the water does not need to be stored and returned nor does it need to be used at all.

A simple low volume portable air compressor can be used to expell the tube contents using a long length of heat resistant pipe or tubing and a pass-through pipe cap or tee fitting. Figure 3-2 shows de-watering equipment similar to that used for this project.

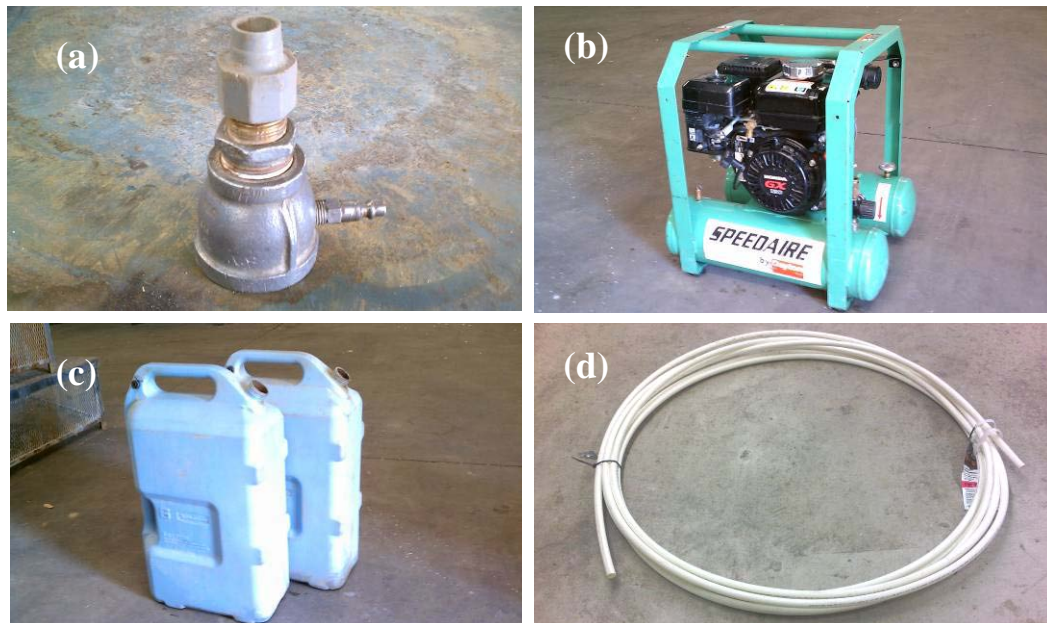


Figure 3-2 De-watering equipment (a) air cap, (b) compressor, (c) storage containers, and (d) heat resistant discharge tubing.

The top of access tubes, when threaded, can directly be coupled to the air head shown in Figure 3-2 through which the heat resistant discharge tubing is passed until it reaches the bottom of the tube. The top of the air cap is fitted with a ferrel type compression fitting that is tightened to form an air-tight seal around the tubing. A standard air hose is then used to connect the compressor to the side of the air cap. Once connected, the

compressed air will pressurize the air over the water in the tube and push the water down the access tube to escape via the full length discharge tubing. The pressure at the compressor should be set to overcome the hydrostatic head in the access tube (1 psi air pressure for every two feet of access tube). The end of the discharge tube must be secured (manually or otherwise) while filling the storage containers to prevent whipping upon completion. Allow the build up of pressure within the access tube to fully dissipate which helps to expell the most amount of moisture.

*NOTE 1: If the top of the access tube is not threaded an appropriately sized compression fitting must be used to make the connection. This is not the preferred method, but if necessary be certain to restrain the air cap to the reinforcing cage with rope or similar to prevent inadvertent slippage from the compression fitting. Typically these fittings are not intended for high pressures (above 50 psi) which may be necessary when dewatering long access tubes.*

*NOTE 2: If the access tubes are very near the main reinforcing bars, it may be necessary to remove the air fitting from the side of the air cap to provide additional clearance and then reinstall when the air cap is secured.*

*NOTE 3: In some cases drill slurry, sand, or other contaminants may have fallen into the access tubes during construction if not properly capped. This may cause the discharge tube to become plugged at the bottom. This can be cleared by raising the discharge tube several inches. If steady flow does not resume then disconnect air hose and back flush the discharge tube with a standard blow tip/nozzle to dislodge this material. This debris can be removed while de-watering by starting the discharge tube slightly higher and progressively pushing the discharge tube deeper with the ferrel fitting partially loosened. In cases of excessive debris volume, the tube can be refilled with the liquid portion of the expelled contents and repeat the de-watering process until clear.*

Adaptations from the above recommendations are expected as site conditions vary. For large diameter shafts it is common practice to empty only the first two or three of the tubes (starting with Tube 1) and then move subsequent tube contents back to the first tubes after those tubes are tested. Figure 3-3 shows the simultaneous de-watering and thermal profiling in progress. Only five containers were used for the ten foot diameter shaft (10 tubes). As shown, the operator is thermal profiling Tube 7 while water is being transferred from Tube 10 back to Tube 5.

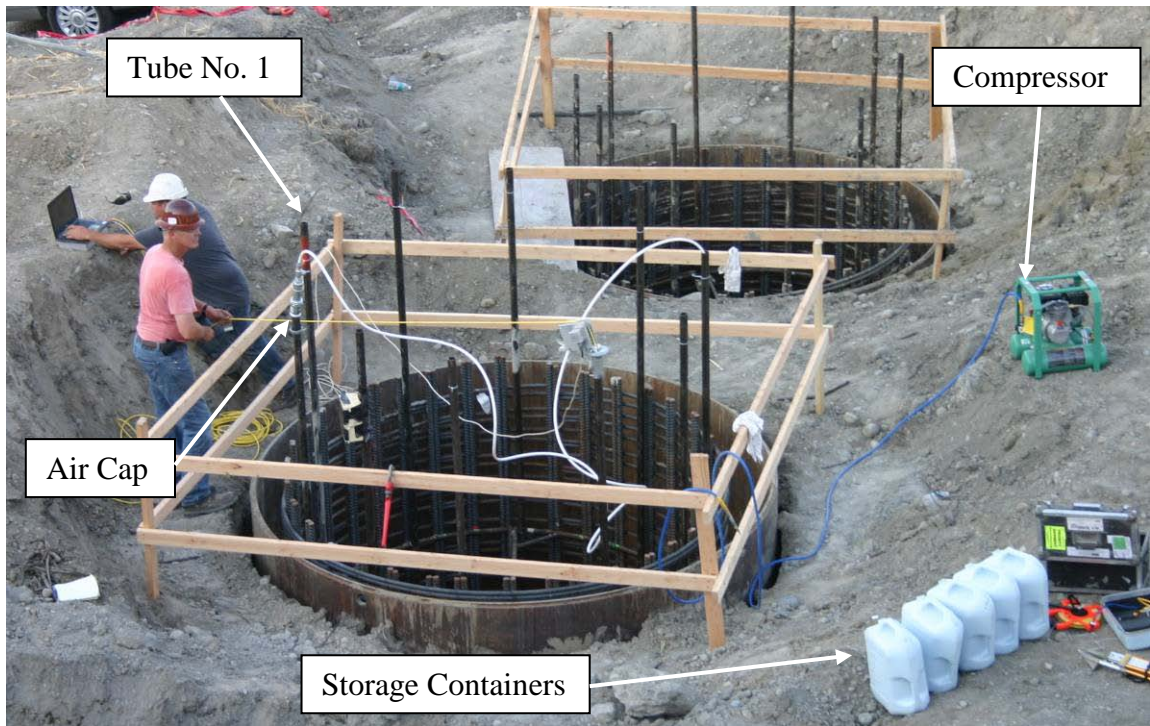


Figure 3-3 Simultaneous de-watering and thermal profiling.

### 3.2 Thermal Test Equipment

*Thermal Probe.* The Thermal Integrity Profile (TIP) system uses four focused, windowed infrared sensors within a single thermal probe (Figure 3-4) to measure the inside wall temperature of standard 1.5 or 2.0 inch access tubes (plastic or steel). The four sensors are encased in a 1.25 inch O.D. x 6 inch long stainless steel body with a waterproof lead wire that connects the probe to the data collection computer. The temperature measurements from the four orthogonally oriented sensors are used to provide both redundancy and the capability of detecting thermal gradients.



Figure 3-4 Thermal probe (left) encased infrared sensor (right).



*Depth Wheel.* A depth-encoded wheel attached directly to the top of the access tube (or tripod) tracks the depth of the probe position while both the internal temperature and the associated depth are recorded via a computerized data acquisition system. Figure 3-5 shows both a tripod-mounted and tube-mounted depth-encoder wheel.



Figure 3-5 Tripod-mounted depth wheel (left) tube-mounted depth wheel (right).

*Data Collection System.* The computerized data acquisition system has evolved throughout the duration of the project. The initial system incorporated a standard laptop and data acquisition box with military-type connectors. Figure 3-6 shows the initial data collection system assigned to the project. One of the disadvantages of this system was the battery life of the laptop in remote testing areas with insufficient access to external power. The second downfall to this system was the visibility of the computer screen in full daylight. As point of reference, standard laptops have a 200-250 NIT rating. Sunlight viewable screens have a NIT rating of 1000 or more. The last disadvantage of the system was the software which was not tailored for field use; it required to the user to assign a data file name after every test and keep track of which tube number and run number they were conducting.



Figure 3-6 Laptop based data collection system shaded in field vehicle.

A custom built data collection system was developed for the project with a larger capacity battery (8-12 hrs), sunlight-viewable screen (1200 NIT rating) and touch screen capability. These components along with the data acquisition system were housed in a ruggedized case (Figure 3-6). Data collection software was developed to aid the field engineer while testing. This software is discussed below.



Figure 3-6 Ruggedized data collection system with waterproof keyboard and screen.



### 3.3 TIP Data Collection

This section first discusses the data collection software and how it is used and then outlines the field collection process overall.

#### 3.3.1 TIP Field Testing Software

The original data collection software utilized the “off-the-shelf” software which was included with the data acquisition hardware. This software was a generic data acquisition software which allowed the user far more flexibility in configuration than necessary for TIP scans. However, the software did not allow for quick and easy review of TIP data. A task-specific data collection software was designed for TIP testing using LabVIEW programming.

The opening screen of the TIP field testing software requires the user to verify settings which include calibration constants for thermal probe and depth encoder wheel. Figure 3-7 shows the opening screen of the TIP software.

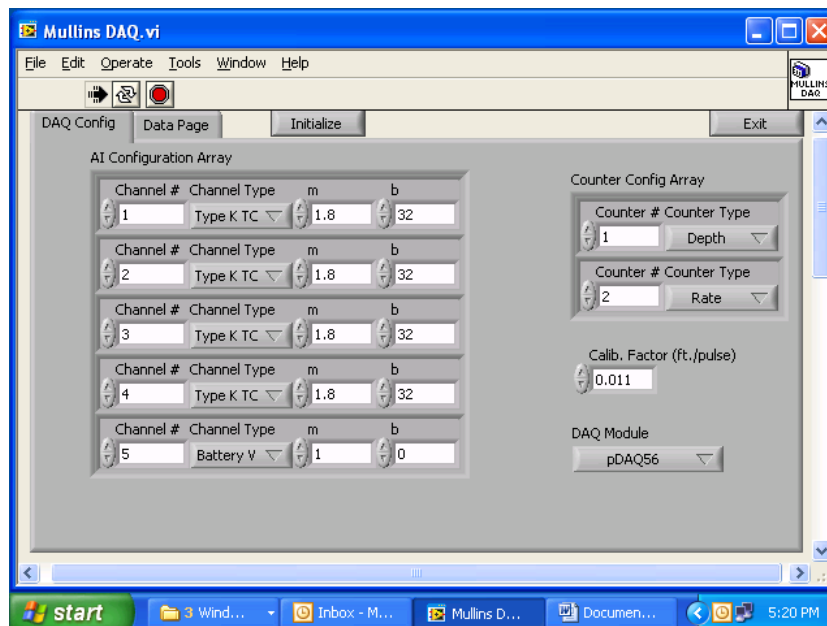


Figure 3-7 Opening TIP software screen to confirm equipment settings.

Once all equipment settings are confirmed, the user initializes the software by clicking on the *Initialize* tab. The user is then prompted for the *Project Name*, *Shaft Number*, and *Number of Tubes* (Figure 3-8). These inputs are used to set the data file names. The software is designed to be 100% touch screen usable which also requires that no external keyboard entries are accepted (only mouse clicks on the on-screen keyboard provided).



Figure 3-8 Initial input used to define software operation and output file names.

After *accepting* the last input field as entered, the data monitoring page is shown with the input fields filled in and the *Status* window indicating *Waiting* (Figure 3-9). At this point all four infrared sensors are active, the depth wheel can be checked for proper operation, and the battery voltage is displayed. When the system is fully operational, the battery voltage should be above 12V and displayed in black. When the battery voltage falls below 12V the display changes to red to warn the user of possible system shut down.

All electronic devices should be operated in a steady state condition / fully warmed up. The status waiting mode should be engaged while de-watering the access tubes. This window also identifies to the operator the next tube that should be tested and which run number is impending. Recall that two runs per tube are customary to assure reproducible data.

Once the operator is ready to begin testing, the *Start Collection* tab is clicked which activates the *Running* status state. The software reminds the operator of the tube and run number (Figure 3-10) and asks for an estimated length of tube (Figure 3-11). *Accepting* (entering) the inputted tube length activates data collection.

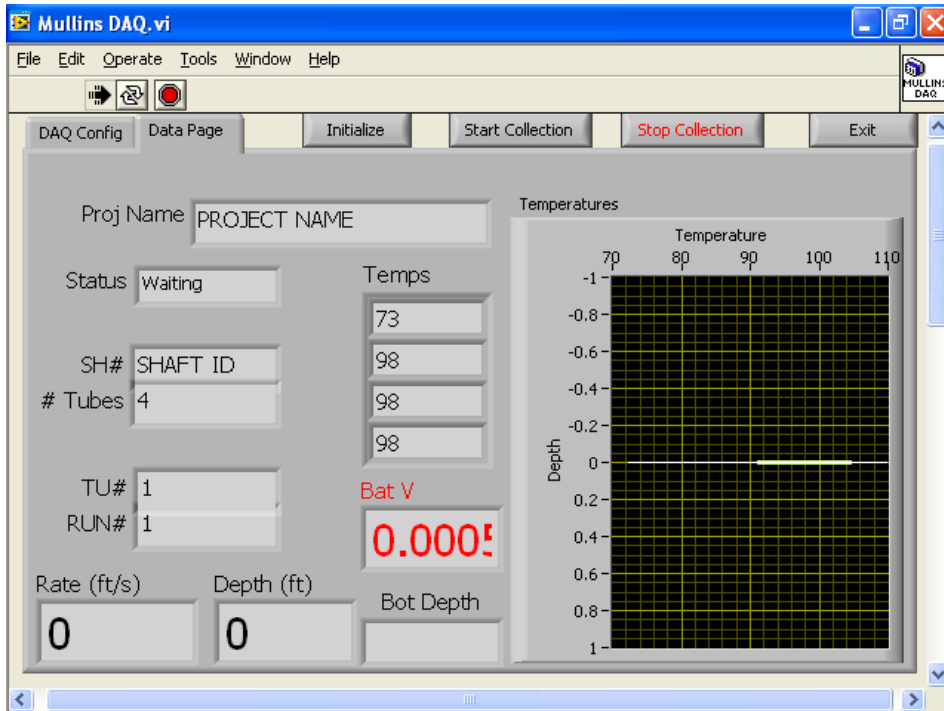


Figure 3-9 Status waiting mode.

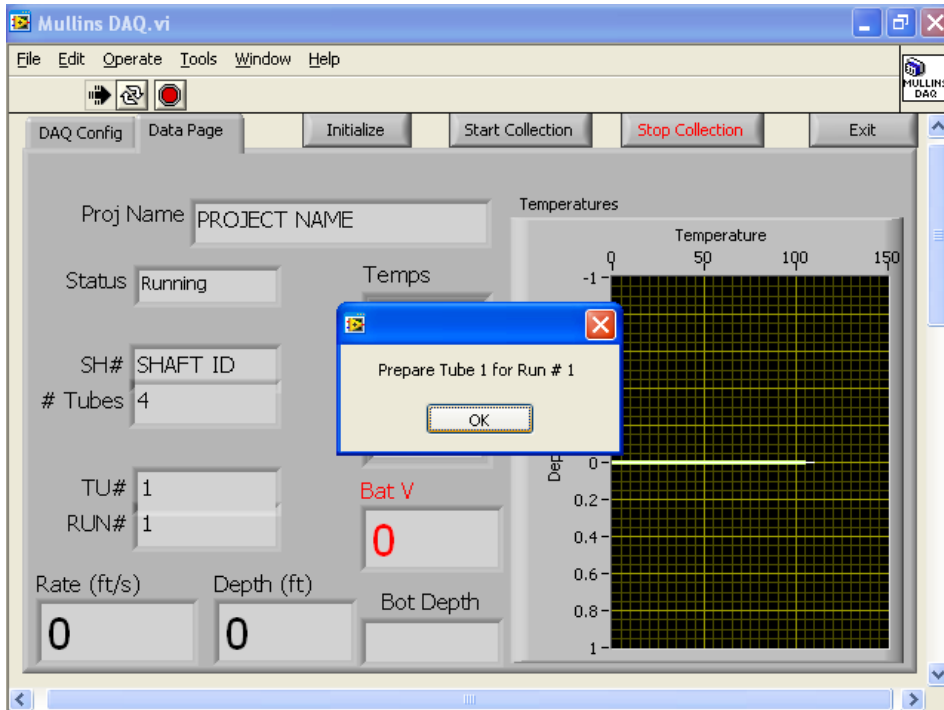


Figure 3-10 The *Running* status state activated by clicking *Start Collection*.

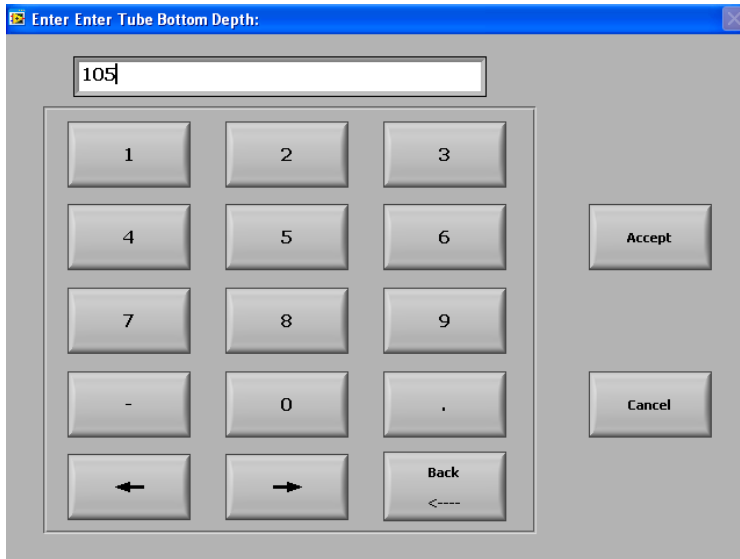


Figure 3-11 The estimated tube length (in feet) *Accepted* to start data collection.

Aside from the inputted tube length and the removal of the battery voltage window, the *Running* (data collection) window looks the same as the *Waiting* window. The depth in feet and rate of descent in ft/s are displayed on the bottom left corner. The rate window is displayed in black unless it exceeds 0.5 ft/s. This helps the operator to keep the proper descent rate even if his view of the screen is not clear. The battery voltage is not displayed during data collection.

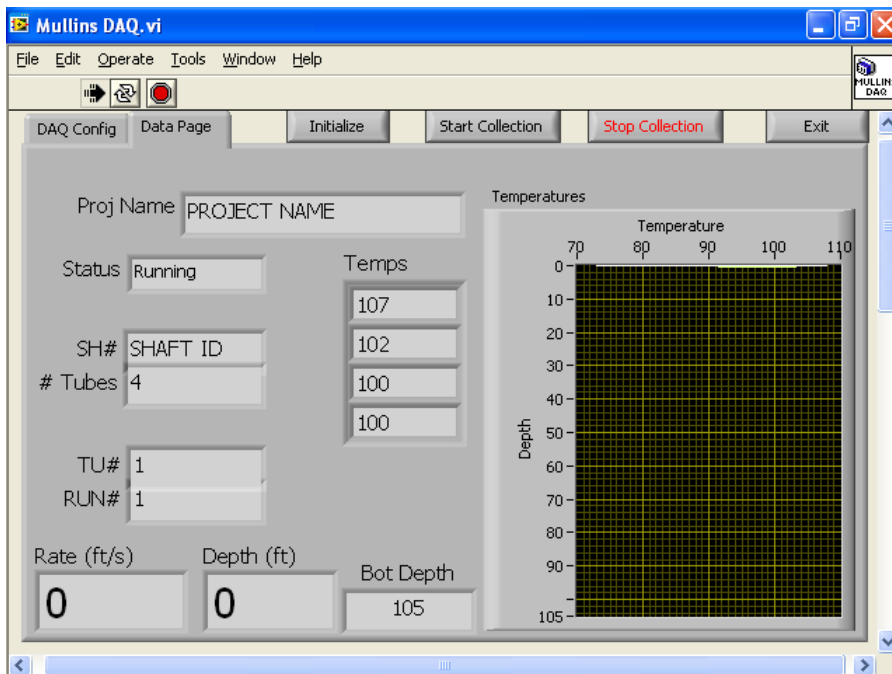


Figure 3-12 *Running* status shows estimated tube depth but is similar to waiting screen.

When the bottom of the tube is reached the *Stop Collection* tab is clicked which returns the screen to the *Waiting* status. The probe is generally pulled to the surface during this time, the probe is checked for debris on the infrared sensor windows and the *Start Collection* tab is again clicked. The operator is reminded of the impending tube and run number and is again asked to input the estimated tube length and the data collection process is repeated.

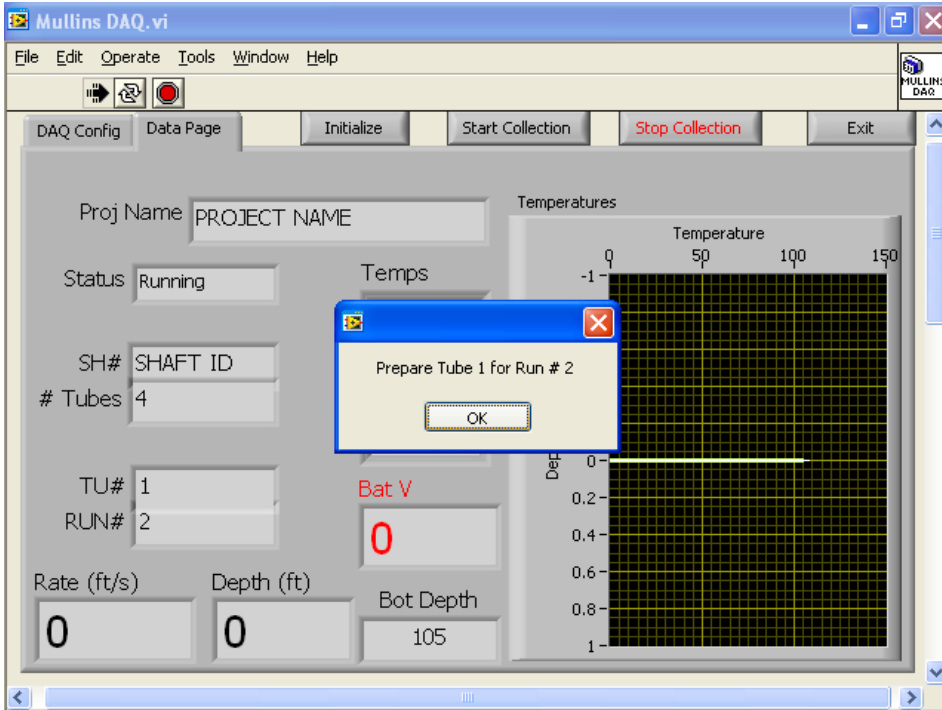


Figure 3-13 Resetting the software and probe for the next run of the same tube.

Ideally, the two scans of the tube will be very similar and therefore representative of the internal temperature. The user is asked to review the two scans and either proceed to the next tube or re-run the same tube based on the operators decision. Figure 3-14 shows the review screen (although no data is shown). If satisfied, the operator clicks the *Selected Runs OK* tab and the process continues for the subsequent tubes. Figure 3-15 shows sample data from two sequential tubes wherein Tube 1 was run with the thermal probe or data collection system before it had come into steady state. Therein, the first and second scans of tube 1 are dissimilar but the second and third are the same. It also shows the results from the next tube tested wherein the data has become reproducible with only two runs.

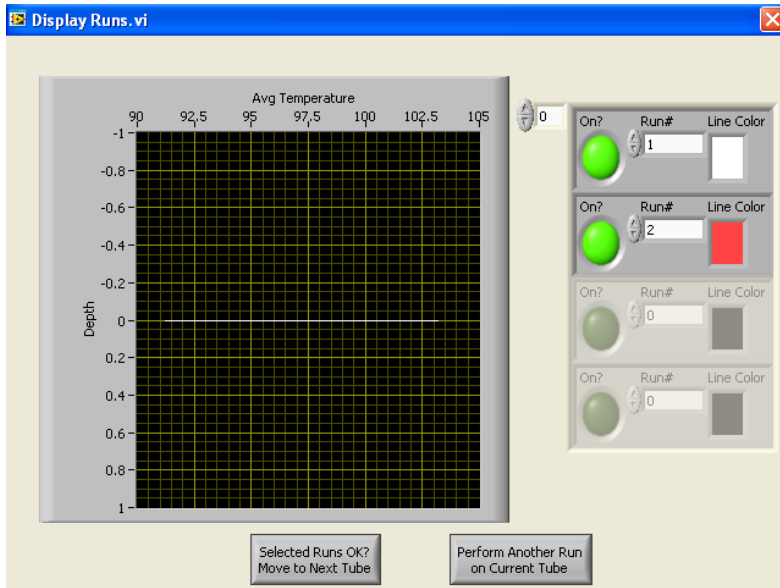


Figure 3-14 Display runs screen asking operator to review the previous scans.

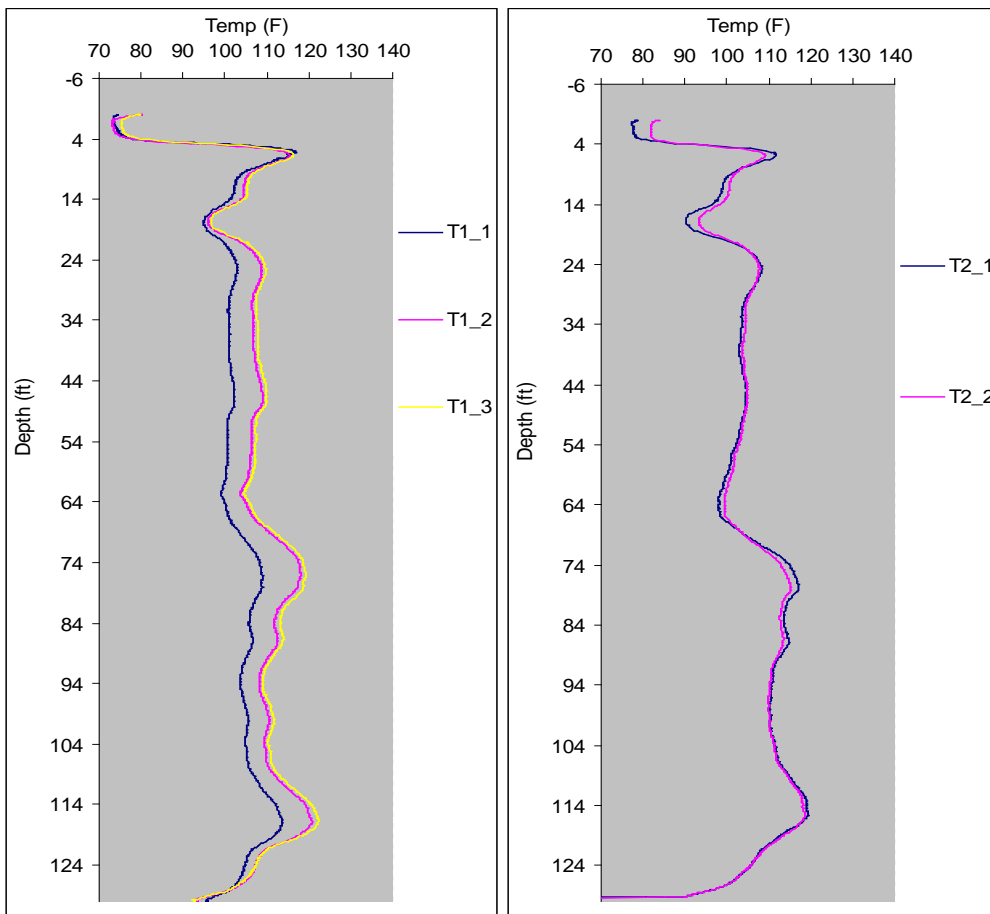


Figure 3-15 Sample data showing importance of redundant scans.

### 3.3.2 Field Testing Operations

Only a single probe is used and no tube pairs or combinations are necessary to complete the integrity profile. Further, the data is collected from the top down instead of from bottom up. This section provides an overview of recommended field testing procedures to obtain this data.

1. Upon arrival to the site locate a suitable position for the data collection computer and layout the equipment to optimize efficiency while also minimizing tripping hazards. The thermal probe should be connected to the computer and fully initialized (Figures 3-7 through 3-9).
2. Measure the depth, the stickup height, and the necessary CTC spacing of the access tubes.
3. Setup the de-watering system on Tube 1 and fill the storage containers as discussed in Section 3.1.1. If no water was used during construction skip to Step 6 and see note below.\*
4. Submerge thermal probe in the heated water in one of the storage containers to allow the internal components to acclimate to the down-hole temperature conditions. At this point, both the data collection system and thermal probe should be warming up.
5. Continue to de-water subsequent tubes in order to provide adequate time for each tube to return to its steady state temperature disrupted by the introduction of the cooler compressed air. This should take about 20 minutes which is typically the time required to de-water the remaining tubes. At least 4 tubes should be prepared in this fashion with all water captured and stored. When large shafts are tested with 5 or more tubes, the operator can optionally discontinue the use of containers and systematically move water from the 5<sup>th</sup> tube back to the 1<sup>st</sup> after tube 1 has been tested, 6<sup>th</sup> tube to the 2<sup>nd</sup> tube and so on.
6. Place wheel body assembly either on the top of tube 1 or on tripod with clear access to tube 1 and connect to data collection system. Spin wheel to assure proper operation (one rotation is approximately equivalent to 1.5ft of probe descent).
7. Remove thermal probe from hot water (or dry tube\*), dry or clean IR sensor windows as necessary and confirm basic operation by focusing each sensor on your hand one at a time. The sensor will typically read around 85-90F on your palm depending on the air temperature / season.
8. A marker band is recommended to be permanently placed on the lead wire 1 ft above the IR sensor windows. Place the thermal probe in the first access tube and align the marker band at the top of tube. The data collected will start at a tube depth of 1ft.
9. Route the thermal probe lead wire over the grooved depth wheel and restrain movement while you click the *Start Collection* tab. Once the tube depth has been inputted, the data collection will begin.
10. Slowly lower the thermal probe at a descent rate (shown on display screen) between 0.3 and 0.5 ft/s. Rates slower than 0.3 ft/s have no benefit; faster rates

- tend to give less reproducible results.
11. Once the thermal probe reaches the tube bottom, verify the depth displayed is reasonable (from taped measurements) and click the *Stop Collection* tab and pull the thermal probe to the surface for inspection. Clean and dry as necessary.
  12. Reposition the thermal probe at the starting depth using the marker band and click the *Start Collection* tab.
  13. Repeat Steps 10 and 11.
  14. Review the data from each run (Figures 3-14 and 3-15) and either select *OK* or *Perform Another Run*.
  15. Repeat Steps 8 through 13 for each tube.
  16. Upon completion of all tubes the TIP software will ask you to either *EXIT* or *Test Another Shaft*. It is recommended that you exit and review the data in TIPVIEW discussed in Section 3.5.
  17. If satisfied with the TIPVIEW data quality check, refill all tubes with the stored water.
  18. Clean and repackage equipment.
  19. If available obtain elevation of access tubes.

\*If no water was placed in the access tubes during construction place the thermal probe in one of the dry tubes for 10-15 minutes to accelerate the temperature acclimation rate.

### 3.4 TIP Analysis Concepts

Thermal integrity profiles can be analyzed at various levels ranging from direct observations to detailed signal matching field measurements with numerical models. Depending on the results of the profiles a more or less intense analysis may be needed. In some instances, especially when multiple shafts are tested on a site, direct evaluation of the temperature profiles for temperature magnitude and basic profile shape is all that is needed. These analyses have been broken into four levels:

Level 1	Direct observation of the temperature profiles
Level 2	Superimposed construction logs and concrete yield data
Level 3	Three dimensional thermal modeling
Level 4	Signal matching numerical models to field data

In most cases, a Level 2 analysis is all that is necessary. However, more detailed Level 3 and 4 analyses can be employed when highly unusual thermal integrity profiles arise.

#### 3.4.1 Level 1 Analysis

A Level 1 analysis identifies the top and bottom of shaft based on normal / anticipated profile shapes. This can verify the overall shaft length, confirm proper cage alignment, locate changes in shaft diameter and identify immediate areas of concern. Figure 3-16 shows a thermal integrity profile for shaft that would likely require no further evaluation. The top and bottom of shaft (and length) are clearly seen, the top and bottom roll-off



zone appears normal (approximately 1 diameter deep for this 4 ft shaft), the bottom of temporary casing was likely near 12-13 ft and the water table was likely near 17-18 ft.

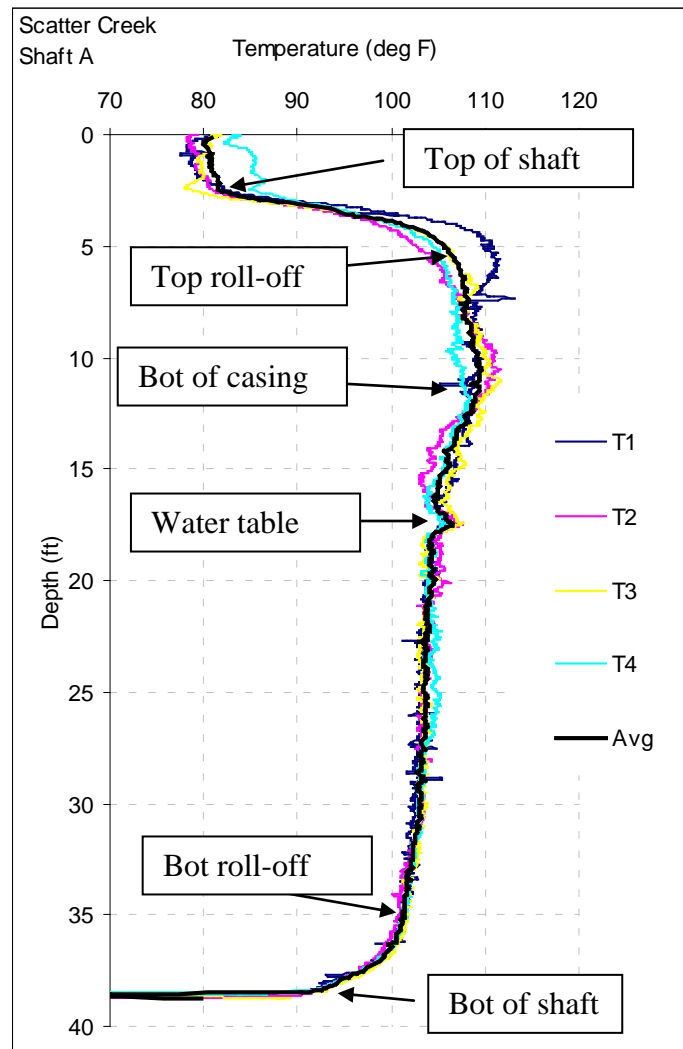


Figure 3-16 Good shaft based on level 1 analysis only.

The cased region of the shaft is usually oversized (relative to the tool size) causing slightly warmer temperatures. The water table when encountered causes sloughing until the slurry is fully in place. The cage is very well centered throughout where all tube profiles have virtually identical shapes staying very near the average (shown in black). Near the surface only tube 1 varies significantly from the average which is most likely caused by casing extraction where the casing was pulled to the north (direction of tube 1). This depressed the soil laterally near the surface allowing more concrete to fill the zone outside that tube and oversize or make the circular cross-section oblong. If the opposite side of the cage (tube 3) had exhibited an equal and opposite decrease in temperature, then it would have indicated cage eccentricity and not shape change.

Although this shaft appears fine with a Level 1 analysis, the information required to perform a Level 2 analysis is usually available and adds value without significant effort.

### 3.4.2 Level 2 Analysis

Level 2 analyses make use of additional site / construction information to better evaluate the results and define the significance of various thermal profile features. This approach confirms the Level 1 direct observations by superimposing known construction information such as top and bottom of shaft elevation, depth or length of temporary and permanent casing, water table, etc. The concrete yield information (concreting logs) can also be used to define a temperature – radius correlation that defines the shape of the as-built shaft. The Level 2 analysis also better defines the extent of cage eccentricity that can be recognized by Level 1 analysis but not quantified. Finally, boring logs can be used to delineate changes in soil strata that may impact the diffusivity of thermal energy into the surrounding environment.

The internal temperature distribution across a normal cylindrical shaft is roughly bell-shaped with the effect of temperature reaching into the surrounding soil (Figure 3-17). The magnitude of the peak temperature is dependent on the concrete mix design, shaft diameter, thermal properties of the soil, and the time of hydration. A distinct, usable temperature profile exists dependent on mix design and site conditions. Although the magnitude of the temperature varies with time, the features of the profile do not.

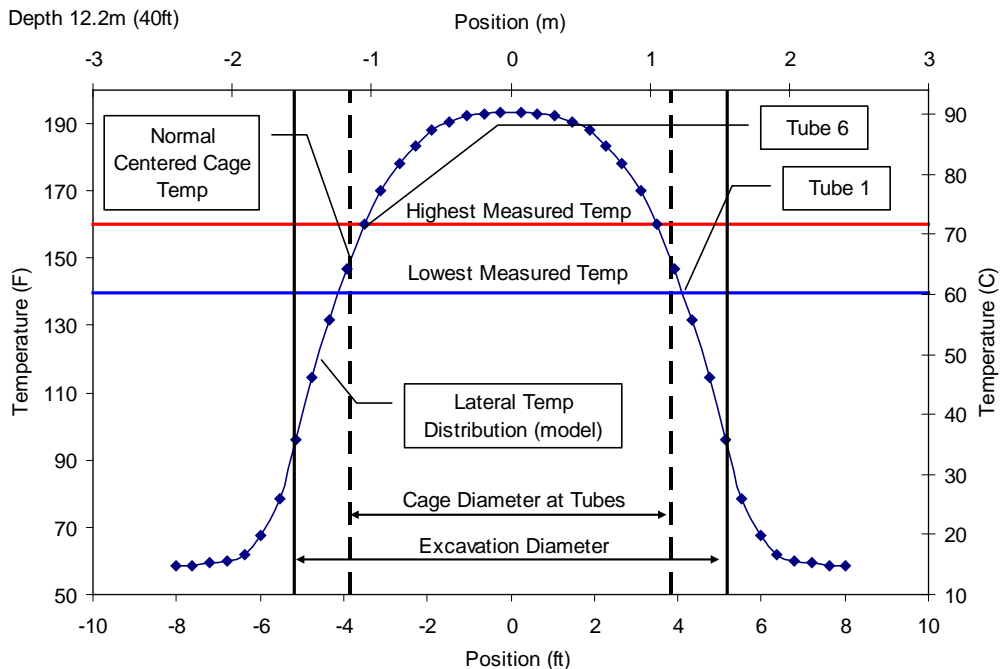


Figure 3-17 Modeled temperature distribution across a 10ft diameter shaft at a given depth.

*Cage Alignment.* The temperature measurements from each tube are sensitive to cage eccentricity as well as the surrounding cover and time of testing. As shown in Figure 3-17, the temperature in all tubes should be the same when the cage (dashed black lines) is centered. A cage slightly closer to one side of the excavation will exhibit cooler temperatures from tubes closest the soil wall and warmer temperatures from tubes closer to the center of the shaft. Cages are often slightly off center for various reasons including: oversized excavation or casing, missing or broken spacers, bent cage, etc. Therefore, a perfectly formed cylindrical shaft can exhibit higher and lower temperatures from tubes on opposite sides of the cage when the cage is not centered. By comparing both the highest tube temperature measurement and the lowest from the opposite side of the cage to the average at a given depth, cage offset can be differentiated from unwanted changes in cross section. Further, by dividing the change in temperature (from the average) by the slope of the linear portion of the modeled temperature / radius curve (Figure 3-17), the magnitude of cage offset can be determined as well as the remaining concrete cover. Figure 3-18 shows the results of TIP scans, for which the Figure 3-17 results were modeled, showing opposite side tubes warmer or cooler than the average dependent on the amount of cage eccentricity.

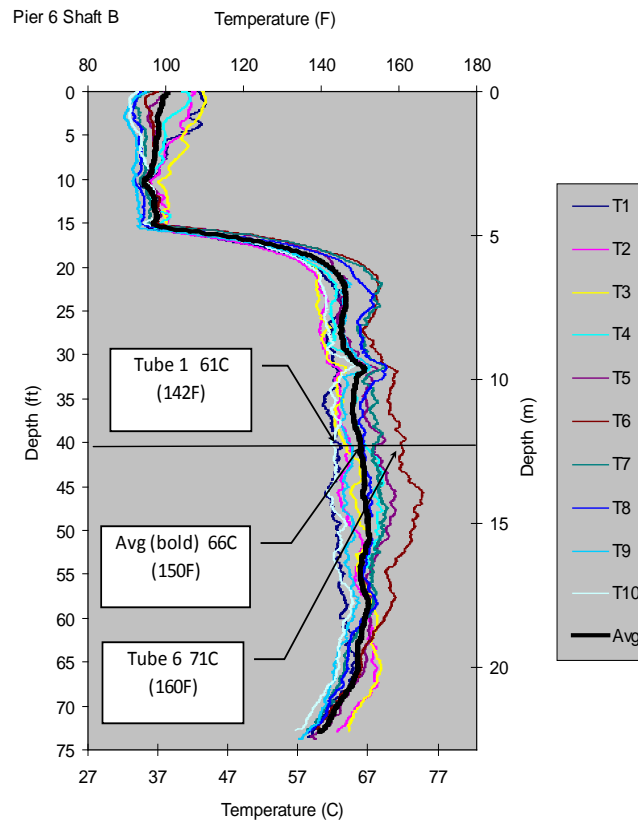


Figure 3-18 Thermal integrity profile of 10ft diameter shaft.

The data shown in Figure 3-18 was collected from the 10ft diameter shaft (with 10 access tubes) constructed in Tacoma, Washington as part of the I-5 / SR16, Nalley Valley Project discussed later in Chapter 4. Using a Level 1 approach, features of the as-built shaft geometry become recognizable. For instance, the water table was at 32ft and caused some sloughing before slurry was fully introduced which is seen in all tubes as being slightly warmer (bulge). The upper 15ft of measurements represent the access tube stick up above the top of shaft which does not affect the analysis but verifies field observations. The top and bottom of shaft show the normal effect of both radial and longitudinal temperature dissipation which extends a distance roughly 1 diameter down and up from the respective boundaries. At mid shaft elevations, dissipation is purely radial so a uniform shaft in uniform soil should register as straight line (vertical) profiles. Additionally, the cage alignment over the length of the shaft is obtained by comparing opposite side tubes and the change in temperature relative to the average. The amount of cage offset can be determined using the Figure 3-17 information.

The data for all tubes of the same shaft shown in Figure 3-18 can be displayed for a single elevation on a radial temperature scale where warmer tubes are plotted closest to the graph center (Figure 3-19). The local temperature axes for each tube are oriented on an azimuth line away from the center based on tube spacing and the corresponding angles (Tube 1 axis; north; azimuth 0 degrees). This shows that the cage is slightly north to northwest of the excavation center at that depth; a cooler measurement indicates closer proximity to the shaft edge.

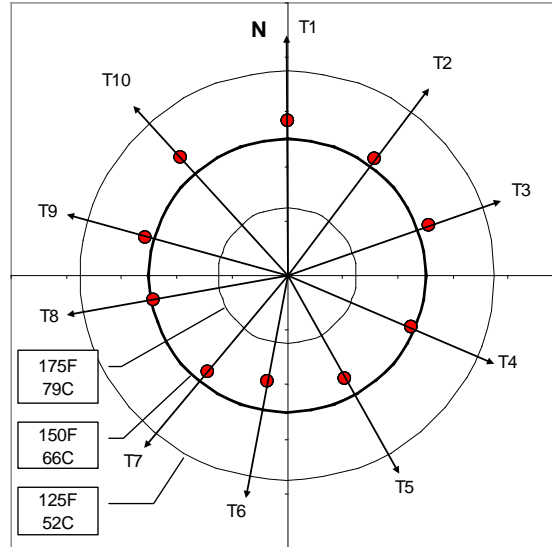


Figure 3-19 Radial plot of Figure 3-18 shaft at 40ft.

Shaft Shape. Concreting logs (i.e. yield plots) are a key mechanism for identifying unusual shaft volume or shape. This information is collected by measuring the rise in the fluid concrete level between trucks using a weighted measuring tape. The volume of concrete from each truck and the associated rise in concrete level are compared to the

theoretical volumes as a first level of post construction review / inspection and are often used to decide whether or not to perform integrity testing. When converted to the effective diameter from each truck a basic shape of the shaft can be estimated. For smaller, one or two-truck pours, no definition or shape can be defined. However, as the temperature distribution near the cage is strongly linear, the average tube temperature plotted versus depth reflects the as-built shape of the shaft. As a result, a refined rendering of the shaft can be prepared regardless of the number of trucks.

The data shown in Figure 3-20 was collected from a 7ft diameter shaft (7 access tubes) constructed in Lake Worth, Florida. This shows the average temperature from all seven tubes and the concrete yield information converted to diameter as well as the planned / theoretical diameter. The first and last trucks have not been corrected for the estimated volume required to fill the tremie and to over pour the shaft, respectively. Regardless, the diameter calculated for the other seventeen trucks closely correlates to the measured average temperature at those depths. In this case, a large amount of additional concrete was used due to flowing sands above the top of rock (TOR). Level 2 information has also been superimposed for additional understanding of these effects on measured temperature profile. This includes the bottom of the temporary 7.5ft diameter surface casing (BOC), top and bottom of shaft (TOS and BOS), water table (WT), top of loose sand layer which continued down to TOR and the ground surface elevation.

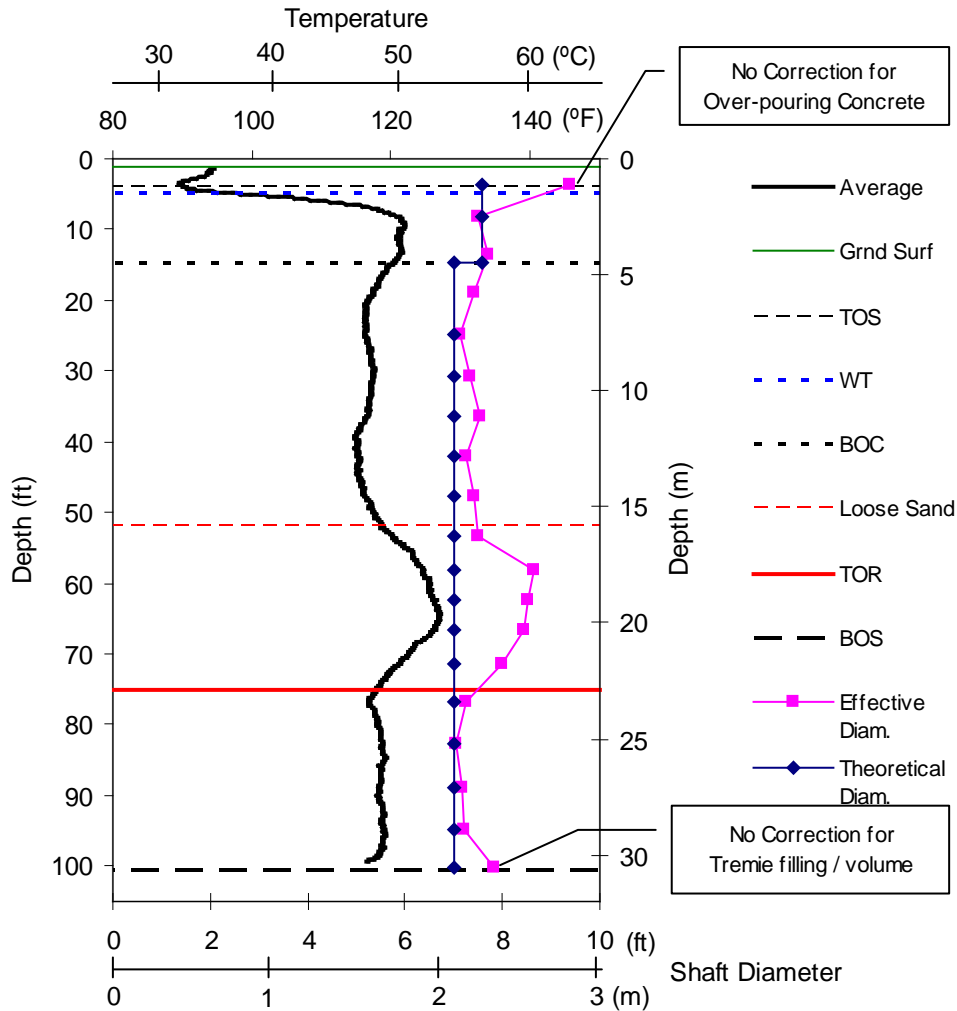


Figure 3-20 Average TIP measurements from all tubes and diameter from yield plots.

This similarity in shape is reflected in a linear relationship between the concrete yield predicted radius (or diameter) and the average tube temperature for that depth. Figure 3-21 shows this trend and provides for the computations needed to convert from temperature to radius without modeling. Recall from Figure 3-17 that this relationship is only valid for the region near the edge of shaft ( $\pm 1 - 1.5\text{ft}$ ). Therefore, the negative intercept value implies that the shaft would have a negative radius when tube temperature is zero. As the domain of the equation is limited to  $\pm 18\text{in}$  from the average diameter, the range only has meaning for temperatures approximately between 90 and 140F. Outside this temperature range, both necking and bulging are under-predicted (necks actually smaller and bulges actually larger). Section 3.5 addresses this with respect to the number of trucks and data points used to develop this relationship.

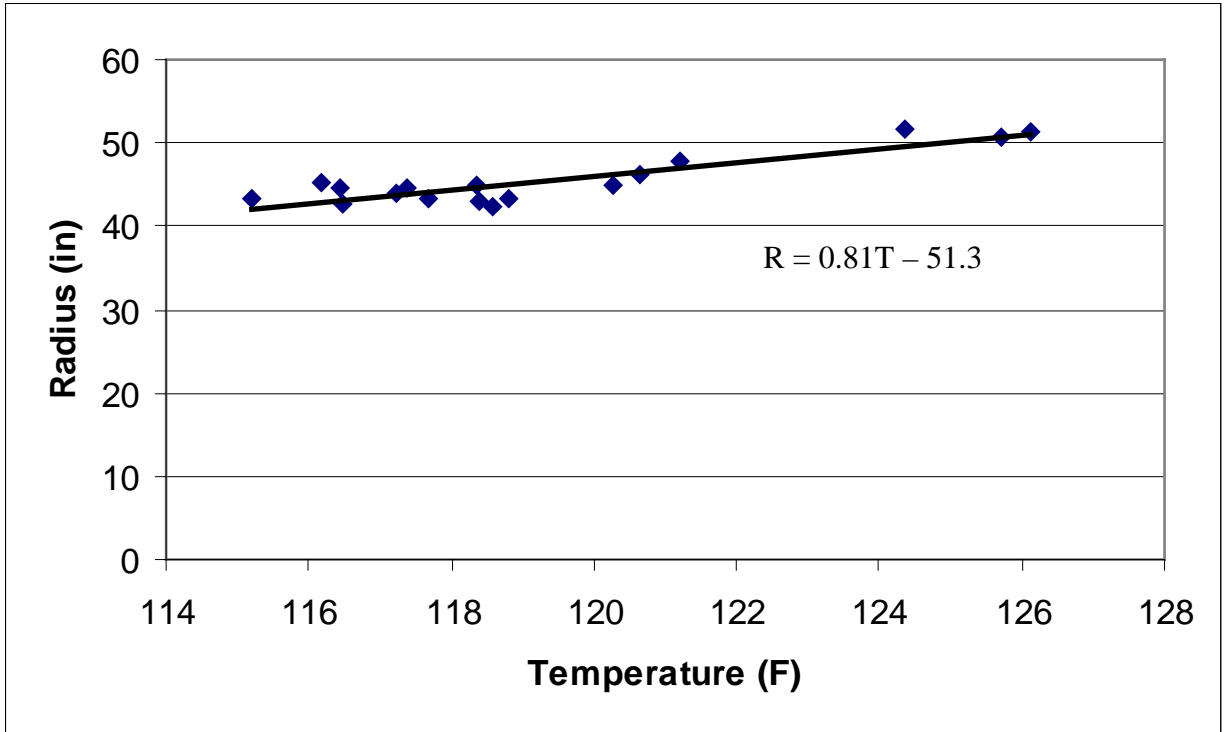


Figure 3-21 Linear relationship between measured tube temperature and shaft radius.

Each tube temperature profile when converted to radius can be plotted radially similar to Figure 3-19 but for all depths and used to produce a 3-D rendering of the as-built shaft as shown in Figure 3-22. Also shown is all Level 2 information including individual concrete truck radii. This type of graph identifies the tubes with or without sufficient cover. The dashed black line represents the target 6in cover. Many of the tubes have reduced cover; some are touching the excavation wall.

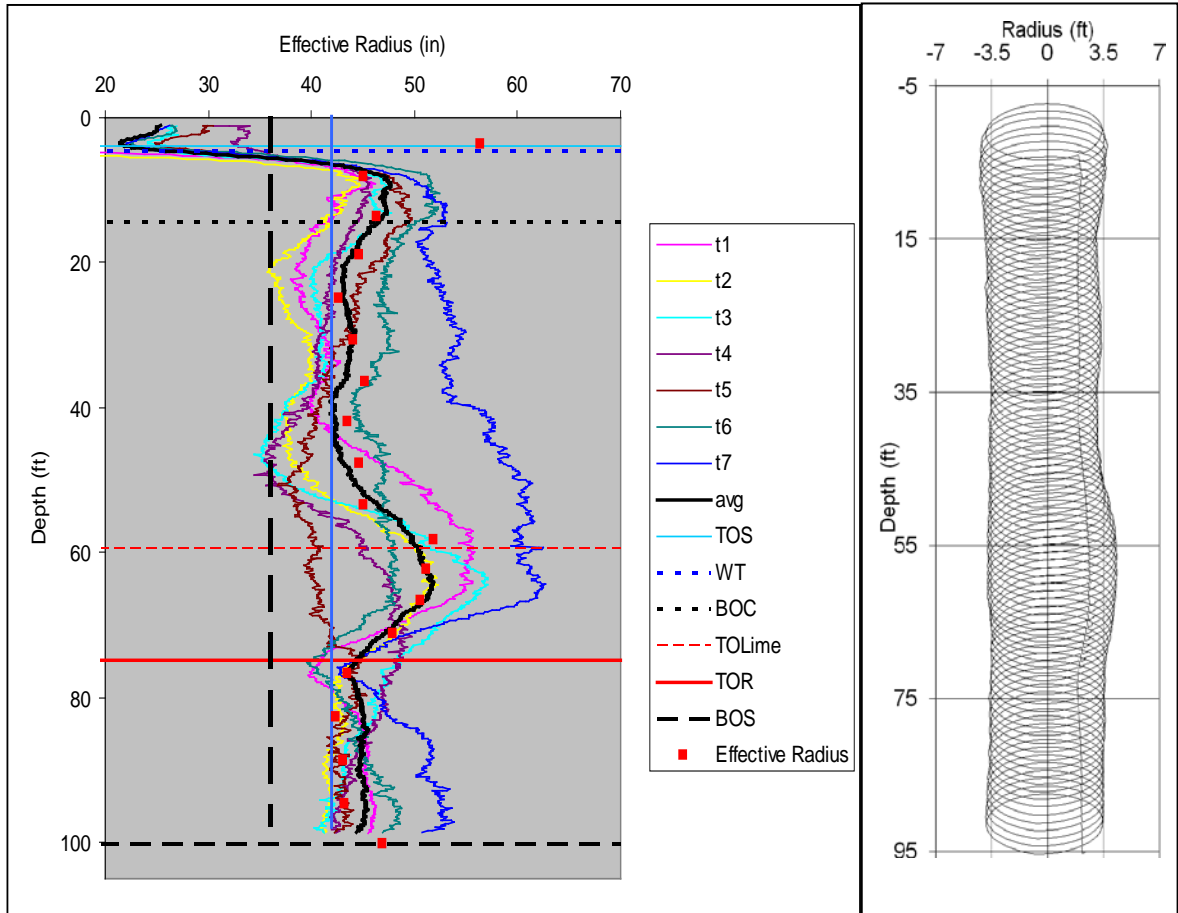


Figure 3-22 TIP data converted to radius for each tube (left) revolved into 3-D shape (right).

Just as the presence of excess concrete (higher temperatures) and proximity of the access tubes to the excavation wall (closer is cooler) affect the measured temperature, the absence of concrete is similarly telling. Interestingly, most shafts tested exhibit over-pour features rather than necks or inclusions; however, when encountered, the lack of an intact concrete volume is also detected.

A study conducted for the Florida Department of Transportation in 2005 demonstrated the effects of cave-ins or necks on the measured temperature. A 4ft diameter, 25ft long shaft was cast with two levels of bagged natural cuttings tied to the outside of the 3ft diameter reinforcing cage at depths approximate 1/3 from the top and bottom. The cross sectional loss at both levels was roughly 10 percent of the total area and was about 1.5ft long. At the upper level the bags were split and lumped at two locations across the shaft from each other (5% loss each); at the lower level all the bags were grouped together. Figure 3-23 shows the results of the thermal integrity profiles taken 15 hrs after concreting and the cross section of the two anomaly levels.



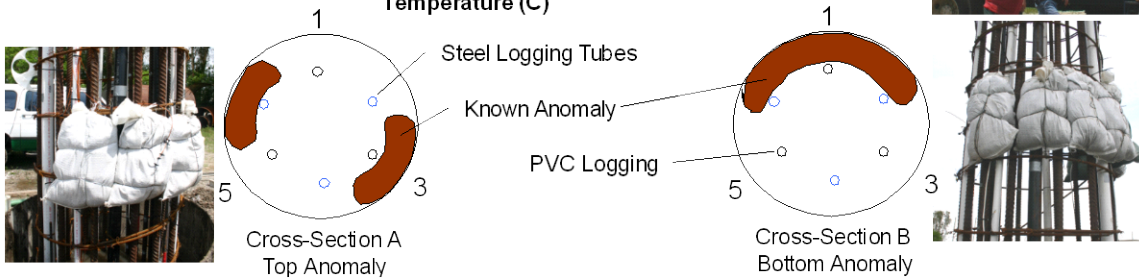
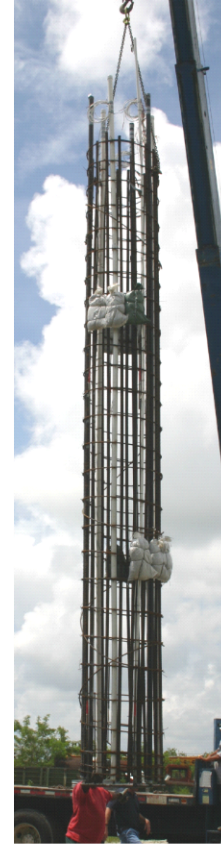
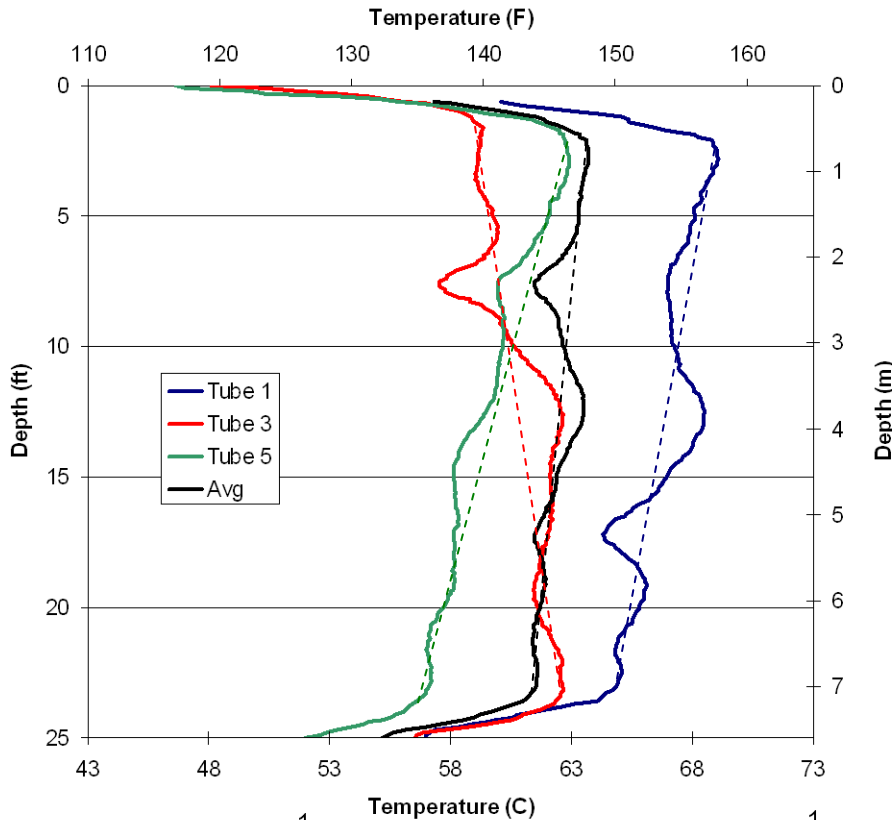


Figure 3-23 Thermal integrity profiles from 4ft shaft cast with known anomalies.

The reinforcing cage was equipped with both steel and PVC access tubes (3 each). For convenience, tubes 1, 3, and 5 (PVC) were left dry dedicated for thermal scans while tubes 2, 4, and 6 (steel) remained flooded for CSL. Regrettably, this did not provide for the normal plurality of tubes but was intended to facilitate a series of thermal scans run on 3 hr intervals.

At the upper level one group of bags was directly beside tube 3, the other was close to tube 5, and neither was adjacent tube 1. Qualitatively, the proximity of the anomaly to the tubes is shown both by the sharpness of the change in temperature with respect to depth as well as the magnitude of change in temperature. Tube 1 shows the least temperature change but the broadest disturbance. At the lower level, only tube 1 was in close proximity which showed both the sharp change in profile as well as a change in temperature with magnitude similar to tube 3 above.

Variation in temperatures between tubes again indicates poor cage alignment where at the top of shaft tube 1 starts farthest from the edge (warmest), tube 3 closest (coolest) and tube 5 very near the average (normal cover). Moving down the shaft the cover increases or decreases proportional to the measured temperature where the average represents a centered cage. The dashed lines provide a reference for a straight cage that is slightly sloped; deviations from the lines show necks or bulges. From this simplified review, when a neck in one tube corresponds to bulge on the other side, it implies the cage is deviating from straight and the cross section is not varying. For this shaft, the CSL results showed no indication of flaws but those tests were only performed using 3 and not 4 tubes.

Results of the study were used to establish thermal probe requirements, testing procedures, and preliminary analysis methods. These recommendations have been incorporated into the devices and software now used to perform these tests. Full details of the study can be found elsewhere (Mullins and Kranc, 2007).

Level 3 and 4 analysis methods require use of thermal modeling software discussed in Section 3.6.

### **3.5 Visual Basic, Microsoft Excel and TIP View**


Visual Basic is a user-friendly programming package which uses graphical user interfaces (GUIs) to develop programs (Schneider, 1999). Visual Basic is a programming language for creating and controlling elements in a Windows program through the use of dialog boxes, drop-down lists, command buttons, menu bars, etc. Microsoft incorporated programming language into their products and further developed a new version of Visual Basic called Visual Basic for Applications, VBA (Harris, 1999). Microsoft Excel is one of the products which utilizes VBA. A convenient difference, VBA code for Microsoft Excel is stored in the workbook whereas original Visual Basic code is stored in text files.

The development of VBA has further advanced the ability to quickly analyze drilled shaft thermal test data using the software discussed herein, *TIP View*. *TIP View* is a macro-driven Excel spreadsheet which utilizes VBA programming for analyzing thermal data. The organization of thermal data is broken into six main worksheets: (1) *Field Notes*, (2) *Field*, (3) *Concrete*, (4) *Radius Calcs*, (5) *Graphs*, and (6) *ZTSDData*. The following section discusses the analysis procedure for *TIP View*.

#### **3.5.1 Field Notes Worksheet**

The *Field Notes* worksheet (Figure 3-24) is the platform for the user to define the job specifications and shaft information. The job specifications include project name, bridge number, pier number, and shaft number. The bridge, pier, and shaft number will be transferred to the finished graphs/plots for ease of identification of the shaft being tested.




**Washington State  
Department of Transportation**

Project: Scatter Creek      Concrete Batch Time: 8/3/2009 12:00  
 Bridge No.: 5-305      Time of Testing: 8/4/09 15:00  
 Pier No.: 1      Concrete Temp: #DIV/0! deg F  
 Shaft No.: A      Starting Probe Depth: 0 ft

Shaft Diameter: 4 ft      Number of Tubes: 4     

Concrete Cover: 6 in  
 Concrete Age: 27 hr

Casing I.D.:      in  
 Casing O.D.:      in  
 Top Casing EL:      ft  
 Bottom Casing EL:      ft  
 Casing Type:

Bottom of Shaft EL: 190.00 ft  
 Ground EL: 225.00 ft  
 Water Table EL: 0.00 ft  
 Top of Shaft is 5.00 ft ABOVE Ground Surface  
 Access Tubes are 40.00 ft BELOW Shaft Bottom

Tube Information						
#	S.U. (in)	S.U. (ft)	L (ft)	S (in)	Top EL (ft)	Bot EL (ft)
1		0.00			230.00	230.00
2		0.00			230.00	230.00
3		0.00			230.00	230.00
4		0.00			230.00	230.00
1 to 2						
2 to 3						
3 to 4						
4 to 1						
AVERAGE	#DIV/0!	0.00	#DIV/0!	#DIV/0!	230.00	230.00

**Click Tube Info Table Button**

**Fill in all White areas**

Figure 3-25 Field Notes worksheet tube table information.

### 3.5.2 Field Worksheet

The *Field* worksheet (Figure 3-26) is the platform for the user to import thermal data for review and further analysis. Thermal data is imported into the spreadsheet by defining the *Data Directory*, *Job I.D.*, and *Shaft Number*. These parameters define the location of the data files and the file name. Due to the evolution of data collection, the user is required to select the data acquisition software used during testing (Omega DAQ or LabView DAQ).

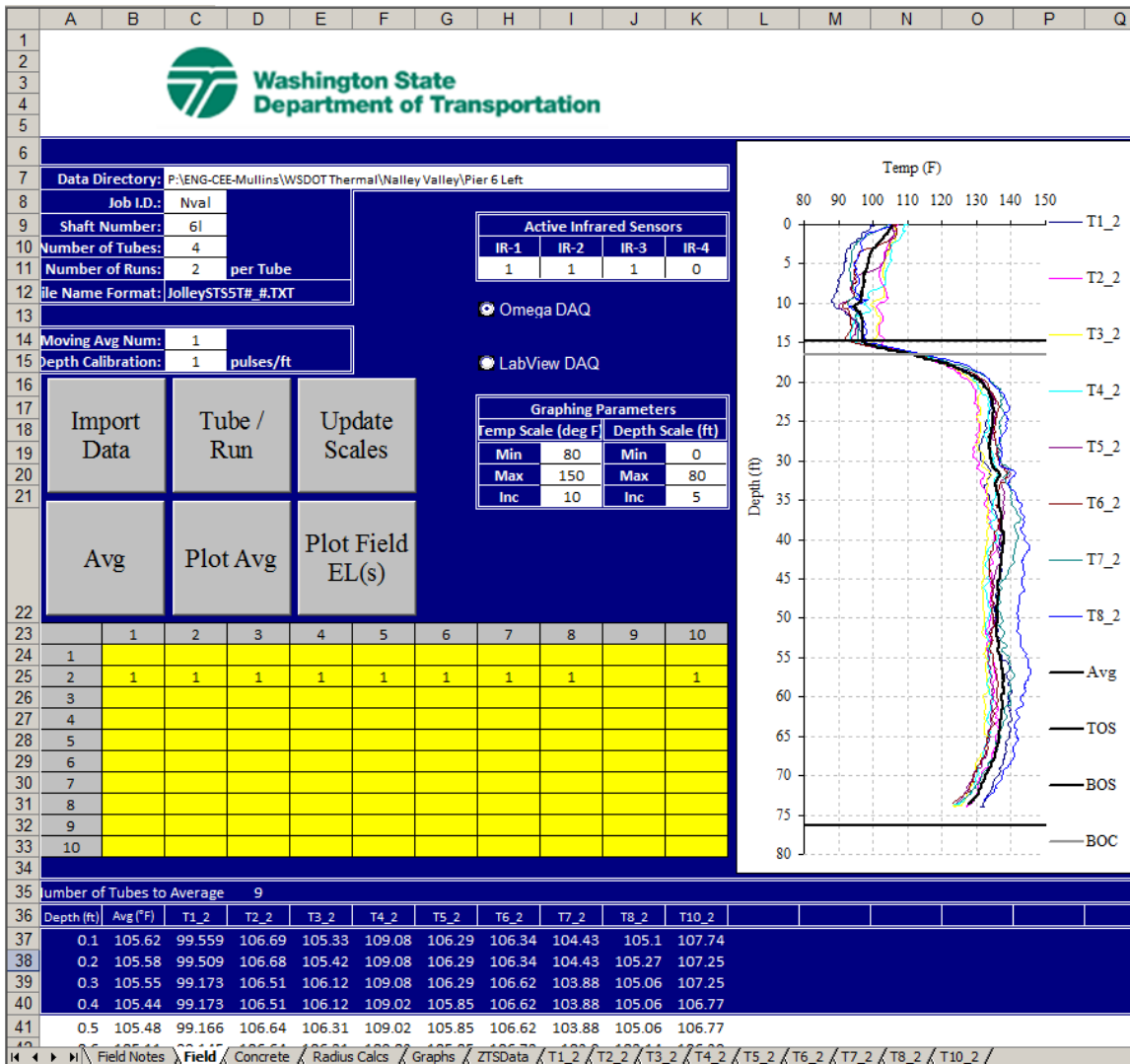


Figure 3-26 Field worksheet.

Tube numbers and runs are selected for import by clicking the *Tube/Run* button. The desired tube and run number are selected from the user form shown in Figure 3-27. The user selects a run by double clicking the white box under the run number. A “1” will show which indicates the selected run will be imported for the current tube number. Double clicking the white box a second time will unselect the run from being imported.

Press the *Exit* button when all tube runs have been selected for import. The data matrix (yellow area) should be filled in for the selected runs which will be imported.

TUBE #	Run 1	Run 2	Run 3	Run 4
↑		1		
1	Run 5	Run 6	Run 7	Run 8
↓	Reset Current Tube		Reset All Tubes	
Exit				

Figure 3-27 Tube Selection user form.

Import the selected runs by clicking the *Import Data* button. The workbook will automatically open each data file and import the data into a tube-run specific worksheet (i.e. T1\_2) for review. It is important to review each tube run and compare them to the average of the shaft. A plot of the imported tube runs is shown. To plot the average of the imported tube runs, click the *Avg* button. The program will average the select tube runs based on tenth of a foot depth readings for the full length of tube tested. The average is plotted with the selected tube runs by clicking the *Plot Avg* button. Before any further analysis is performed, the user needs to confirm the quality of the imported data.

Each tube run imported for analysis can be reviewed individually with the tube-run specific worksheet (Figure 3-28). Within each worksheet, the user can verify the tested length versus measured length and the quality of signal from each sensor. If the lengths are not the same or close to expected, error could have come from wire/wheel slip, incorrect depth calibration, wheel roll-off at end of test, or water at the bottom of access tubes. The user also can plot field elevations to verify measurements and construction elevations. This is done by clicking the *Plot Field EL(s)* button. Typical field elevations include top of shaft (TOS), bottom of shaft (BOS), and bottom of casing (BOC).



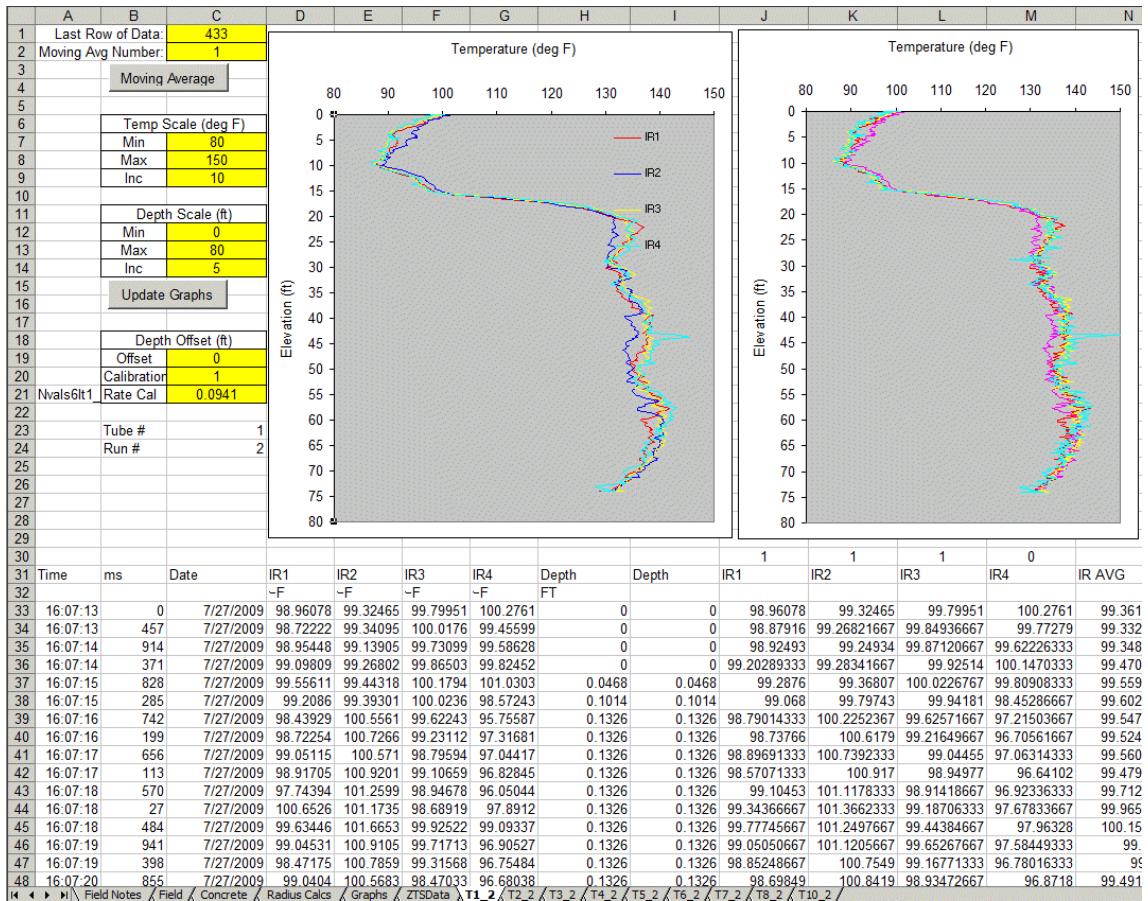


Figure 3-28 Individual tube data worksheet

*Wire-Wheel Slip.* A wire/wheel slippage is difficult to determine after testing is complete without cross checking taped tube length with computer recorded length (bottom left corner of screen) at time of testing. It is necessary for the user to make a note of any slippage during testing. For wire/wheel slippage, the user should re-run the test or select another run for analysis.

*Incorrect Depth Calibration.* During field testing, the user measures the depth of each tube and must verify the depth wheel is producing similar results at the end of each test run. If the user determines the depth calibration was entering incorrectly, the depth calibration can be post-processed by adjusting the *Calibration* cell (C20) to provide an accurate depth reading per tube. A note of the incorrect depth reading should be made at the time of testing. The corrected calibration should be a ratio of the correct depth wheel calibration to the incorrect value.

*Wheel Run-On.* Wheel roll-on occurs at the end of a test as the probe reaches the bottom of the access tube and the user does not stop the test at that moment. It is difficult for the user to “feel” when the probe reaches the bottom of the access tube and the weight of the wire continues rotate the depth wheel. Typically, temperatures near the bottom of the

shaft will decrease with depth; however with wheel run-on the temperature will stay constant with depth. Figure 3-29 shows a typical wheel run-on. The user corrects this error by deleting the extra data occurred from wheel run-on.

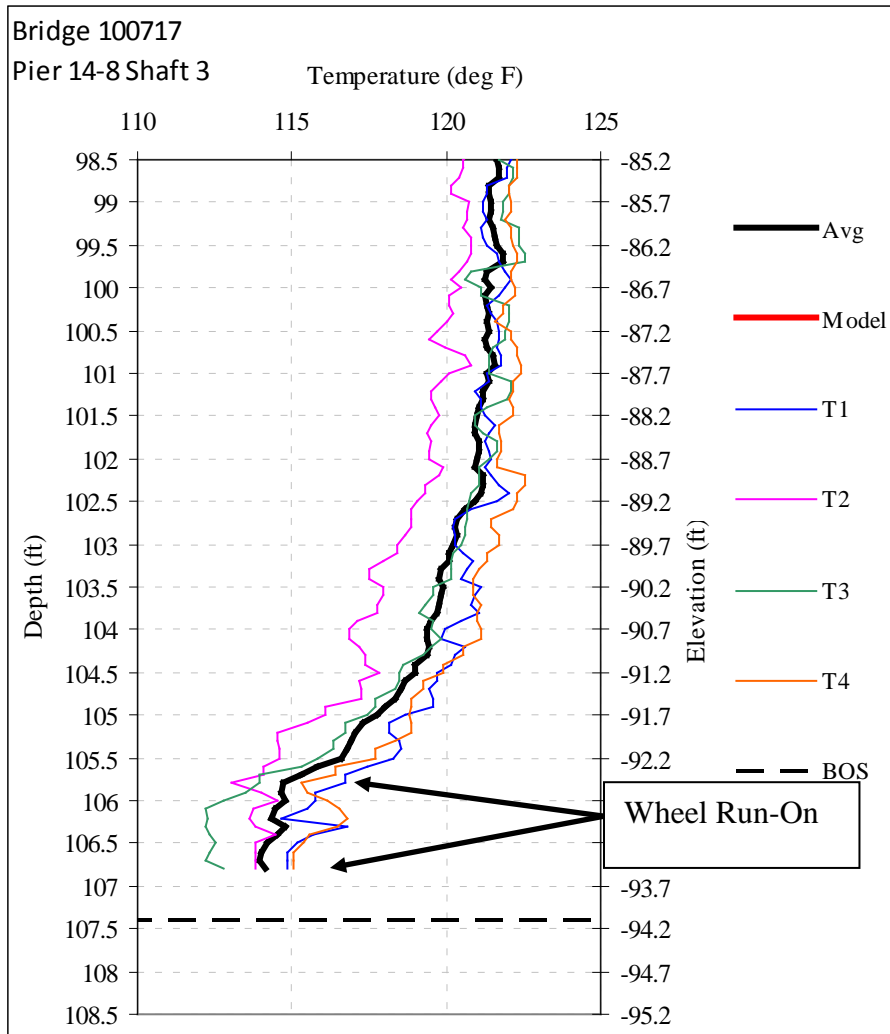


Figure 3-29 Example data of wheel run-on.

*Water at Bottom of Access Tubes.* Dewatering of the access tubes is typically performed to provide the best quality of data. However, in some instances it is impossible to provide a dry access tube due to improper construction of reinforcement cages. If tubes are not sealed properly, water may enter the access tubes during testing. Attempts should be made to seal the tubes during testing. However, if the user is unable to seal and fully dewater the access tubes, post-processing of the data can be performed. The user addresses this error by deleting the data occurred from water at the bottom of the access tubes; this means the last several inches deleted are not reported. Figure 3-30 shows an example of water at the bottom of the access tube(s).



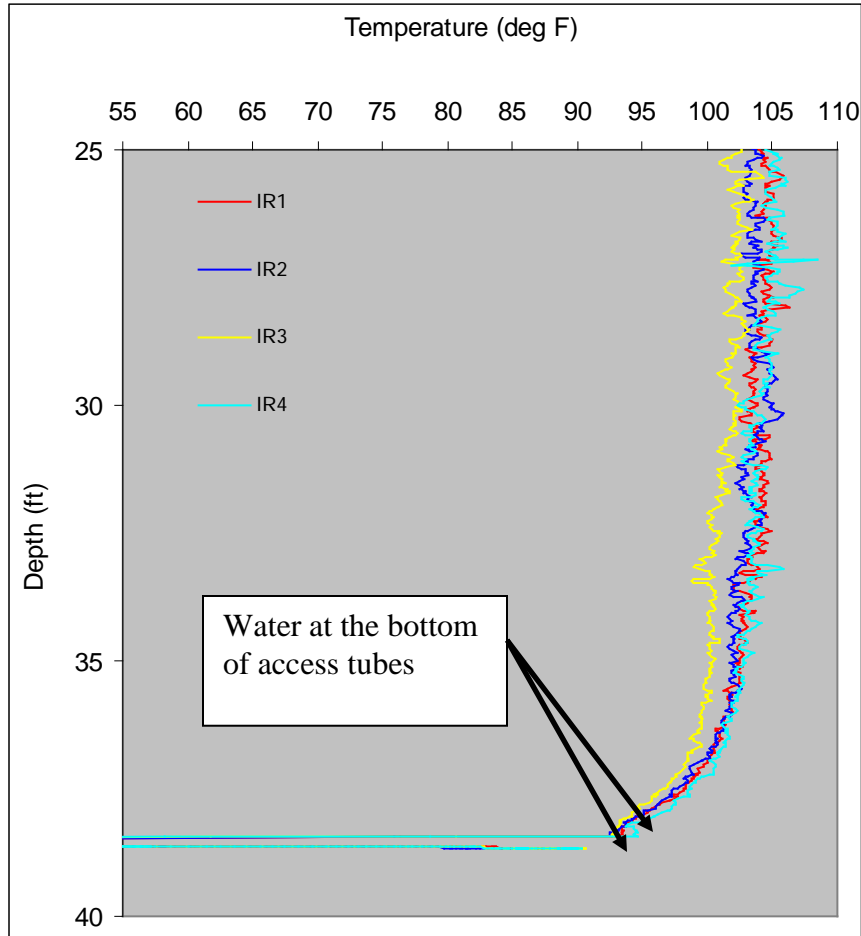


Figure 3-30 Example data of water at the bottom of tubes

### 3.5.3 Concrete Worksheet

The *Concrete* worksheet (Figure 3-31) is the platform for the user to enter concrete placement information for the test shaft, if available. Again, all white cells need to be filled in with the appropriate information. The *Reference Elevation* (cell C12) is the elevation used during concrete placement to measure the depth to concrete level. *Volume in Lines* (cell G13) is the concrete waste from the first truck. This value will be automatically subtracted from the first trucks concrete volume. The *Concrete Wastage* (cell G14) is the volume of concrete not used from the last truck and will be automatically subtracted from that truck. *Rebar Cage EL* (cell G15) is used to verify the field measurements. The *Number of Trucks* (cell G16) is needed for performing the calculations.

The concrete placement log information is entered in cells B19 to D19 plus the number of trucks. This information includes the volume of each truck and the concrete level rise after placement of each truck. Also, the concrete placement temperature is needed if a

model will be used for analysis. The model is usually run without knowledge of concrete placement temperature and can be adjusted accordingly during analysis.

Once all information is entered, the user clicks on the *Calculate* button. Calculations include total concrete volume, theoretical concrete volume, change in concrete level, plot depth, calculated radius from the volume of the truck, and the average temperature for the given depth of concrete fill. This information is used to produce correlations between measured temperatures and effective shaft radii. Two methods can be used for converting temperature to radius: (1) Single-Point and (2) Multi-Truck.

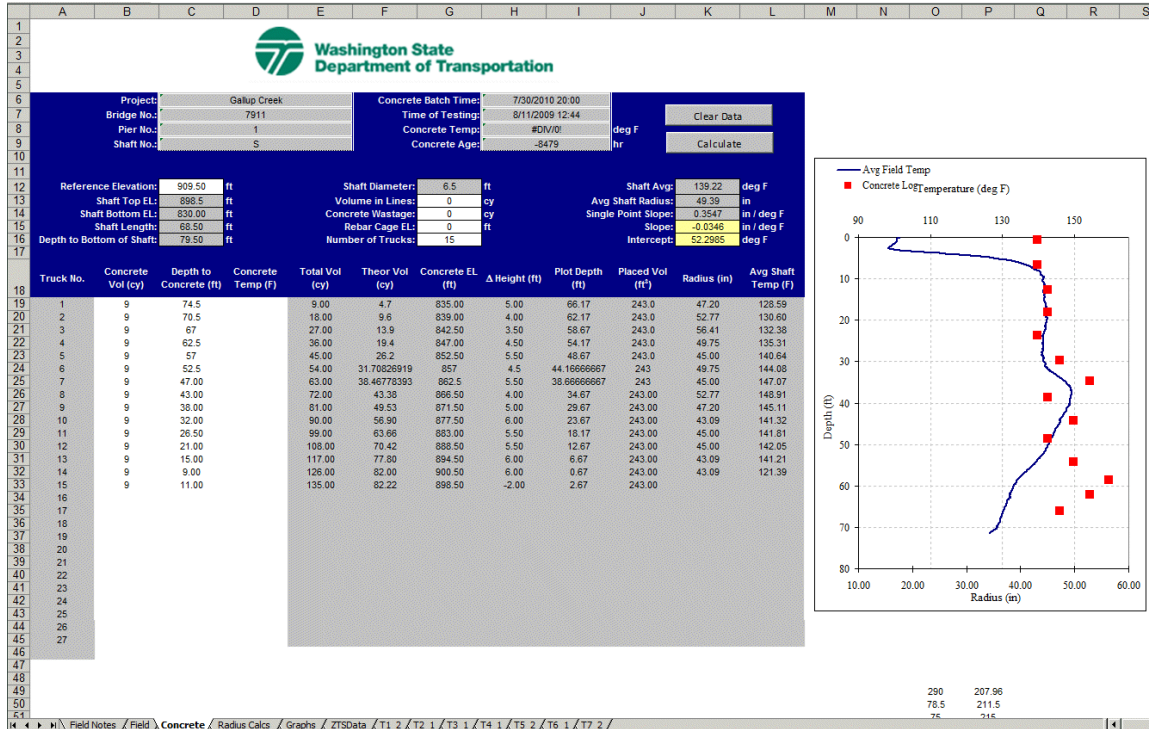


Figure 3-31 Concrete worksheet

The Single-Point method uses the average temperature and radius of the entire shaft length tested to convert field measurements. This method is valid for uniform shafts. The Multi-Truck method uses a linear trend from individual truck measurements and temperatures. This method is more accurate for varying shaft size.

### 3.5.4 Radius Calcs Worksheet

The *Radius Calcs* worksheet (Figure 3-32) is the platform for the user to convert temperature measurements into effective shaft radius, if applicable. The user selects the appropriate conversion method from the drop-down box in cells N7 and O7. If a time series model is available, the user selects the *Model Time* and *Model Radius*. The *Model Time* should be the nearest hydration time relative to time of testing. The *Model Radius* is the planned shaft radius or the “known” as-built radius. Adjustments in the models top and bottom elevations, as well as the placement temperature can be made by clicking the

arrow buttons on the right. Incorporation of end-effect corrections (heat dissipations one-diameter from ends) are currently not available for use in the analysis.

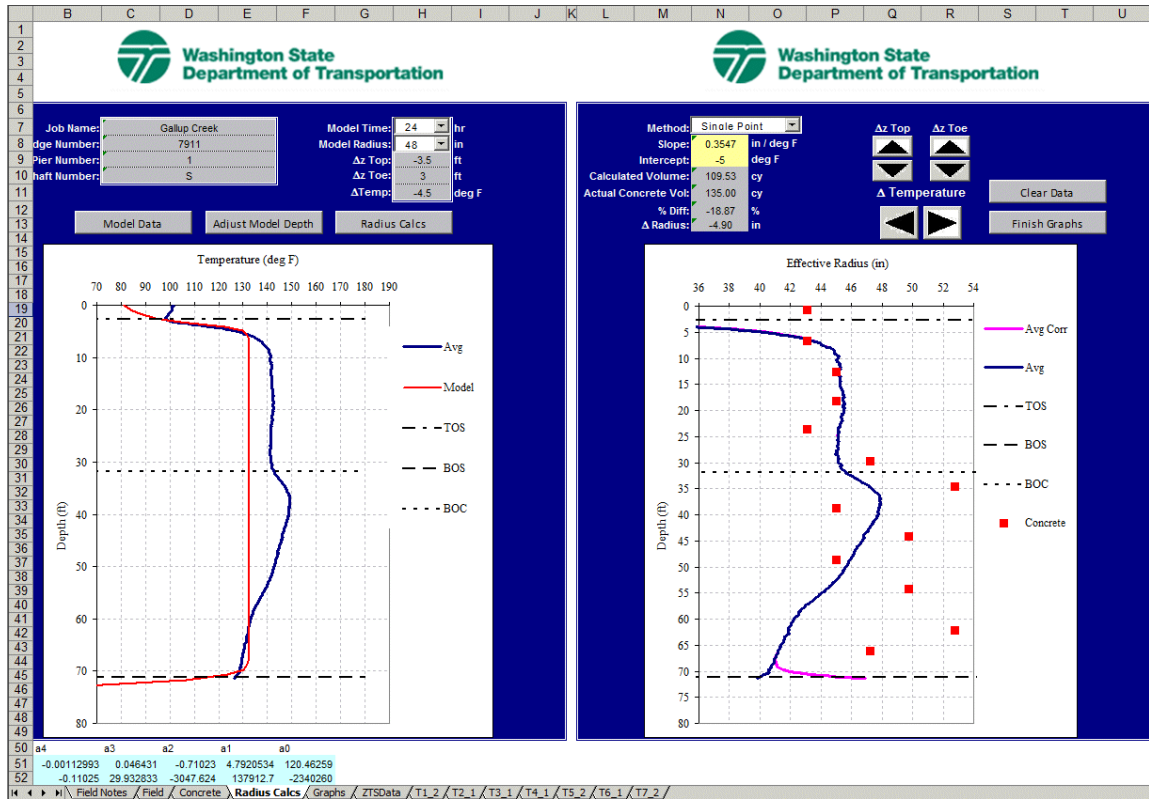


Figure 3-32 Radius Calc sheet

The plot on the right (Figure 3.##) is the effective radius temperature conversion and the concrete placement log. This is a check of the effective radius compared to concrete placement calculations. Small adjustments can be made to the conversion formula by changing the *Slope* (cell N8) and *Intercept* (cell N9). These changes should only be made in fine increments. If the user is unable to produce a reliable/reasonable radius, the quality of all the data should be revisited. Once all calculations are analyzed and reviewed, the user clicks the *Finish Graphs* button. This will finish conversion calculations from each tube and plot all data in the *Graphs* worksheet.

### 3.5.5 Graphs Worksheet

The *Graphs* worksheet (Figure 3-33) is the platform for the user to obtain the necessary plots for a final report. Plots include the thermal data from each tube (selected single run) with average and field elevations, the average shaft temperature versus model predictions (if applicable), zoomed in view of the top and bottom of shaft, and the effective radius.

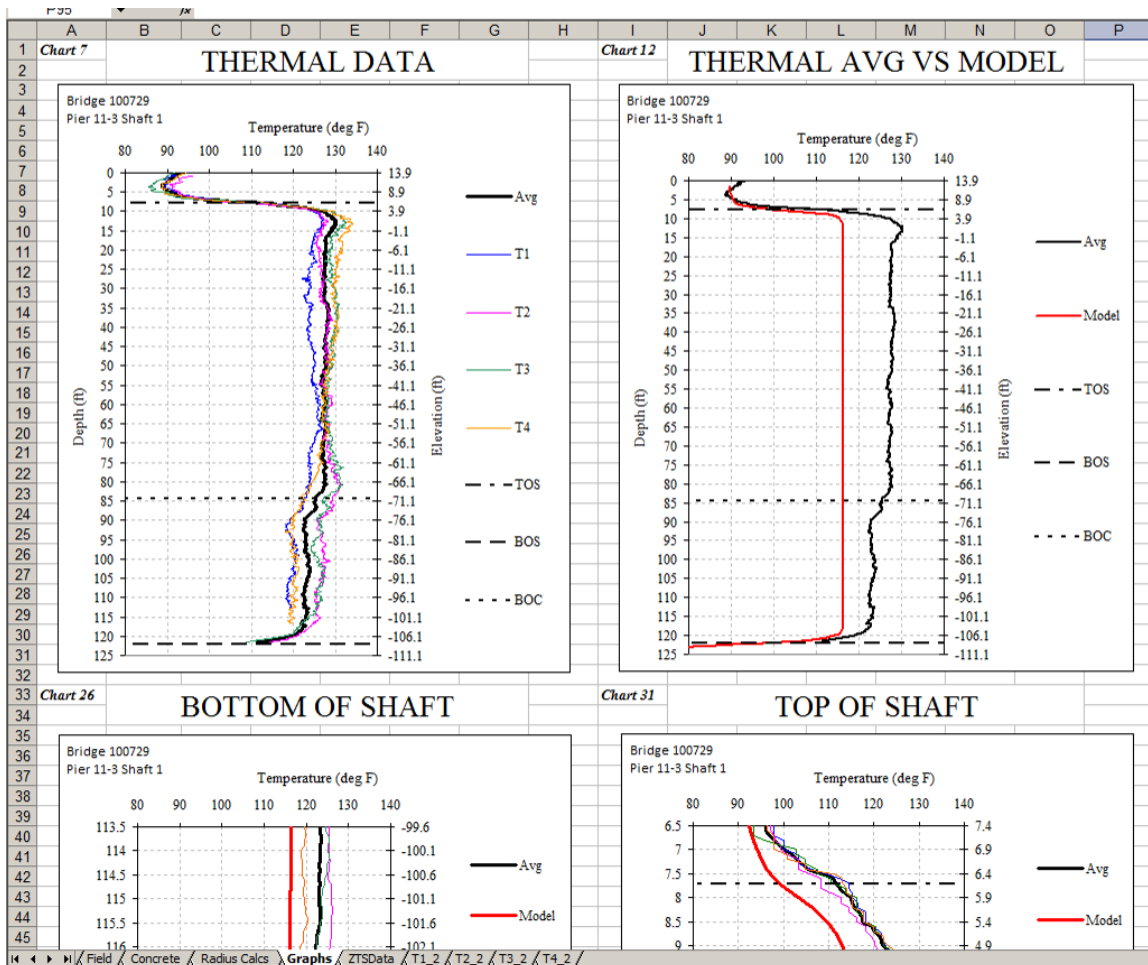


Figure 3-33 Graphs worksheet

### 3.5.6 ZTSDData Worksheet

The *ZTSDData* worksheet (Figure 3-34) is the model database for a given shaft, job, etc. Information about the model is entered as well as the model data. Model data is imported from T3DModel discussed in Section 3.6.

	A	B	C	D	E	F	G	H	I	J	K	L
1												
2		Start Radius:	48			Number of Slices Above Shaft Top		10			Start Time:	6
3		End Radius:	48			Number of Slices Below Shaft Bottom		15			End Time:	48
4		Radius Inc.:	1			Number Total Slices		80			Time Inc.:	6
5		Num of Radius:	1			Model Length		20.00			Num of Time Steps:	8
6		Last Row:	94			Nz		0.25				
7												
8												
9												
10						Import Z-TS Data						
11												
12												
13												
14		Depth (ft)	6 hr	12 hr	18 hr	24 hr	30 hr	36 hr	42 hr	48 hr		
15		0.8202	82.04	82.04	82.04	82.04	82.04	82.04	82.04	82.04		
16		1.6404	80.474	82.166	83.138	83.606	83.822	83.894	83.894	83.876		
17		2.4606	79.178	82.616	84.596	85.532	85.946	86.072	86.072	85.982		
18		3.2808	78.422	83.804	86.828	88.232	88.808	88.97	88.916	88.754		
19		4.101	78.71	86.342	90.446	92.264	92.948	93.056	92.894	92.57		
20		4.9212	80.87	91.202	96.422	98.564	99.194	99.122	98.69	98.114		
21		5.7414	86.738	100.526	106.736	108.842	109.058	108.428	107.474	106.376		
22		6.5616	100.994	119.534	126.086	127.04	125.708	123.656	121.442	119.264		
23		7.3818	102.956	123.926	132.224	134.15	133.268	131.324	129.074	126.752		
24		8.202	103.154	124.682	133.7	136.31	135.986	134.492	132.548	130.46		
25		9.0222	103.172	124.79	133.988	136.85	136.796	135.572	133.88	132.026		
26		9.8424	103.172	124.79	134.042	136.958	137.012	135.896	134.33	132.602		
27		10.6626	103.172	124.808	134.042	136.994	137.048	135.986	134.474	132.782		
28		11.4828	103.172	124.808	134.042	136.994	137.066	136.004	134.492	132.836		
29		12.303	103.172	124.808	134.042	136.994	137.066	136.004	134.51	132.854		
30		13.1232	103.172	124.808	134.042	136.994	137.066	136.004	134.51	132.854		
31		13.9434	103.172	124.808	134.042	136.994	137.066	136.004	134.51	132.854		
32		14.7636	103.172	124.808	134.042	136.994	137.066	136.004	134.51	132.854		
33		15.5838	103.172	124.808	134.042	136.994	137.066	136.004	134.51	132.854		
34		16.404	103.172	124.808	134.042	136.994	137.066	136.004	134.51	132.854		
35		17.2242	103.172	124.808	134.042	136.994	137.066	136.004	134.51	132.854		
36		18.0444	103.172	124.808	134.042	136.994	137.066	136.004	134.51	132.854		
37		18.8646	103.172	124.808	134.042	136.994	137.066	136.004	134.51	132.854		
38		19.6848	103.172	124.808	134.042	136.994	137.066	136.004	134.51	132.854		
39		20.505	103.172	124.808	134.042	136.994	137.066	136.004	134.51	132.854		
40		21.3252	103.172	124.808	134.042	136.994	137.066	136.004	134.51	132.854		
41		22.1454	103.172	124.808	134.042	136.994	137.066	136.004	134.51	132.854		
42		22.9656	103.172	124.808	134.042	136.994	137.066	136.004	134.51	132.854		
43		23.7858	103.172	124.808	134.042	136.994	137.066	136.004	134.51	132.854		
44		24.606	103.172	124.808	134.042	136.994	137.066	136.004	134.51	132.854		
45		25.4262	103.172	124.808	134.042	136.994	137.066	136.004	134.51	132.854		
46		26.2464	103.172	124.808	134.042	136.994	137.066	136.004	134.51	132.854		
47		27.0666	103.172	124.808	134.042	136.994	137.066	136.004	134.51	132.854		
48		27.8868	103.172	124.808	134.042	136.994	137.066	136.004	134.51	132.854		

Figure 3-34 ZTSDData worksheet

When thermal modeling is used as the comparative basis for shaft acceptance, verification of mill certifications from the concrete supplier (constituent fractions) may be necessary as the most common method used by industry to establish constituent percentages are not exact tests. As a result, field validation of model predicted time versus temperature relationships can be performed by simple shaft temperature monitoring using small inexpensive thermocouple data collectors. Thermal integrity profiling using multiple embedded can provide data for both purposes.



### 3.6 Modeling User Guide

This section presents only the user instruction for the use of T3DModel, software developed for predicting mass concrete in large diameter shafts as well as normal internal temperature for the purposes of thermal integrity analysis. A more in depth discussion of the numerical operation can be found elsewhere (Mullins and Kranc, 2007).

In general, the software uses four editors to create the model: (1) the *materials editor*; this allows the user to either use or create thermal properties for various materials, (2) the *section editor*; this makes 2-D horizontal slices through the model space, (3) the *sub-model editor*; this stacks different slice types into vertically aligned sub-parts making up a portion of the entire 3-D model, and (4) the *model editor*; this editor stacks sub-models and makes up the entire model. In addition to the editors, libraries of boundary conditions and concrete energy source files are pre-prepared which can be selected as necessary to meet the desired model needs. Finally, when executing the run, several variables such as time of run, amount of cementitious material/energy and selected output locations can be adjusted to meet the needs of the user.

The main menu of the software screen (Figure 3-35) is relatively simple with three important pull-down menus: *File* (file management), *Editors* (access the four editors), and *Model* (to finalize a model assembly).

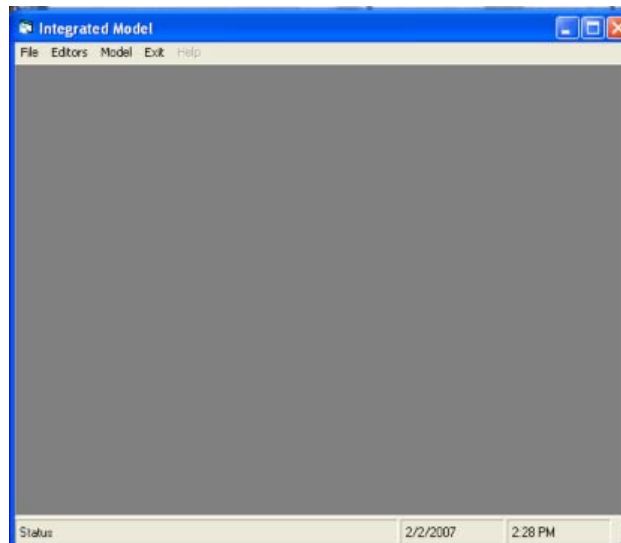


Figure 3-35 T3DModel opening / main menu screen.

#### 3.6.1 Editors

*Materials editor.* The materials editor provides an overview of the material library which contains parameters such as the conductivity, specific heat, density, and heat production potential for 26 materials that might be encountered. The editor gives the user the option of defining a representative material color (for easy identification in the section editor) as well as new materials not yet encountered by the software. In this way the software can

be tailored to the user's needs and experiences. Figure 3-36 shows the standard materials editor screen. Upon editing, the user can save the collection of materials in the library under a new name for future use.

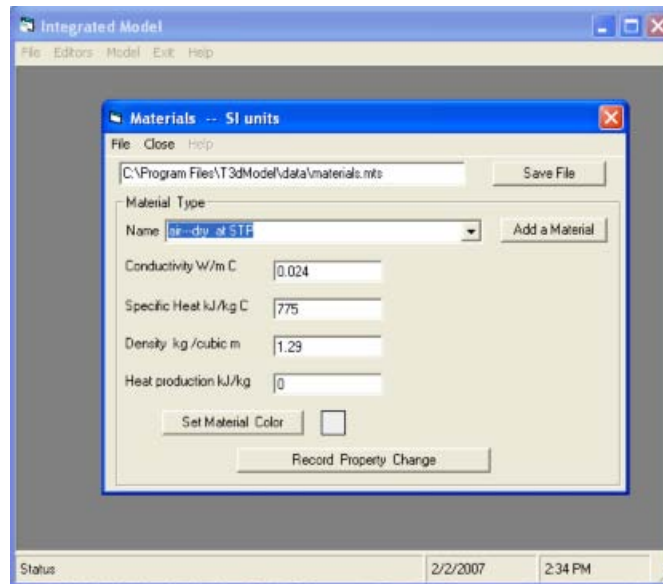


Figure 3-36 Materials editor screen.

*Section editor.* The section editor creates slices that define the typically encountered cross sections for a given model. In general, one section should be created for every cross sectional geometry intended for modeling.

When the section editor is opened it asks for the DX, DY, and model space X and Y dimensions. DX and DY refer to the number of elements in that slice and is limited to 80 x 80 elements. The X and Y dimensions refer to the overall dimensions of that section (slice of the overall model) in the units of meters. These values can be edited using the geometry menu at the top of the window Figure 3-37.



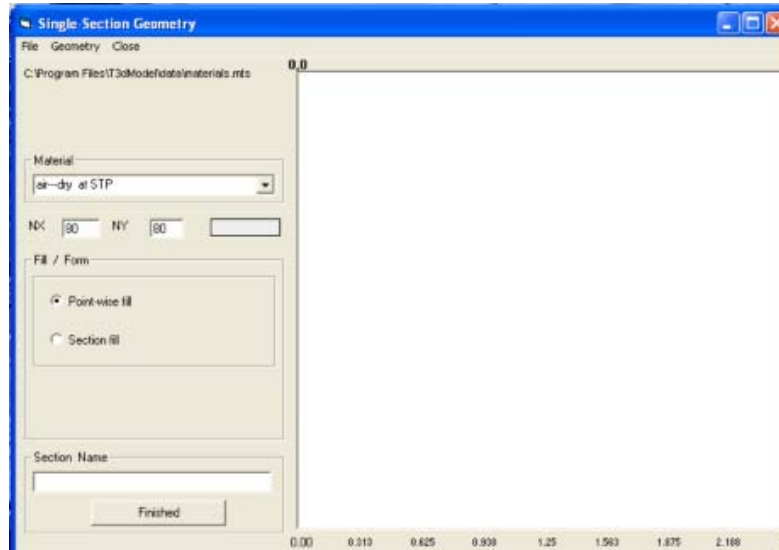


Figure 3-37 Section geometry editor screen.

A material file should be opened in the section editor from which the user selects the type of materials for their model. Usually, the user's selection of material file is based on their past use and updates to the library. It is not uncommon for a given user to use the same material file over and over updating it as new material information becomes needed/available. If editing an existing section file, it is not necessary to establish the material file one will have been appended to the section file for direct access.

Section geometries can be as complex as deemed necessary by the user. However, it is recommended to start with less complex section geometries and add complexity only if the results do not reflect observed features. Generally, small details have little affect on the overall temperature distribution. Starting from the largest features to the smallest fill the 2-D model space with the desired materials. For example, to create a slice through a 4ft (1.2m) drilled shaft in saturated sand, select *soil-saturated granular*. . . from the material pull down and click on *section fill* (Figure 3-38). To insert the shaft in the sand, select the desired concrete type from the materials pull down list and click on *cylindrical fill*. The default location for cylindrical or rectangular fills in the center of the model space ( $X/2, Y/2$ ). Enter the desired center location for the shaft or simply push ENTER twice for the default. The fill body radius should be input in meters (or 0.6 for a 4ft diameter shaft). Figure 3-39 shows the 1.2m (4ft) diameter shaft in a 2.5m x 2.5m 2-D model space (section). Because the program is designed to accommodate both rectilinear as well as cylindrical model spaces, regions around the shaft that are incompletely covered by the rectangular grid are assigned partial properties of the two adjoining materials proportional to their area ratio. This is shown by the ring around the shaft of a third color.

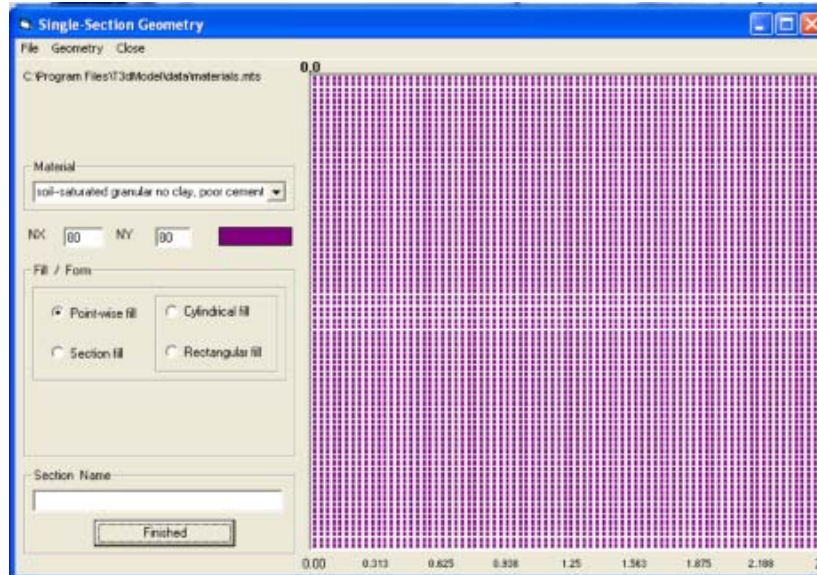


Figure 3-38 Saturated granular soil section fill example.

A detailed section name should be inputted into the lower left most window and then the section should be saved. Modifications to this section can be made using replacement over-lays to the existing cross section file and renamed as another section name. For instance, upon completing the section fill with saturated sand (above) the user could have saved that section as just sand and then subsequently added the shaft and resaved to have two sections with the same space dimensions.

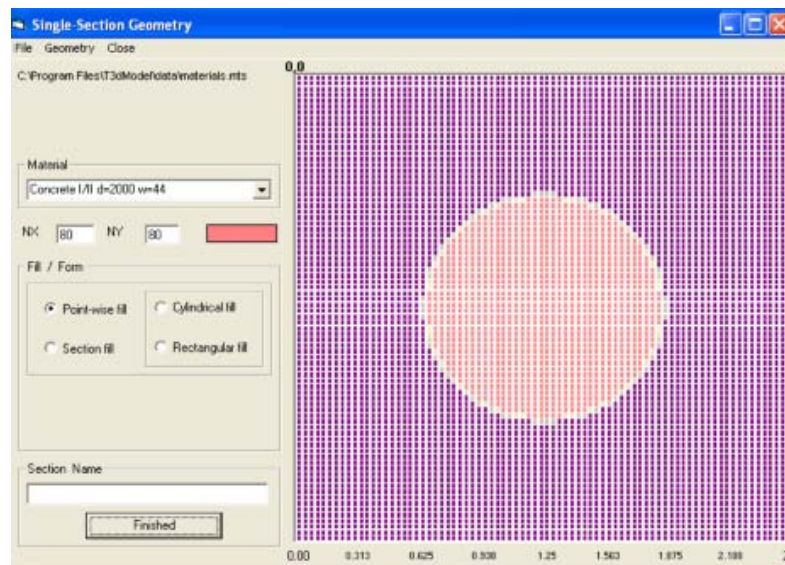


Figure 3-39 4 ft diameter concrete cylindrical fill in 2m x 2m space.

*Sub-Model editor.* The sub-model editor opens by instructing the user to identify the number of vertical slices/sections that will be stacked or assembled and how long/deep the overall sub-model will be. Alternately, the user may open a previously created sub-

model with that information already saved. Click into the number of Z zones window and then the sub-model length for Z and enter these values. The number of Z zones is limited to 80 slices/sections. Next click on the *Add a Section* button and select each of the sections that were created for that model. The user should select a different color for each of the sections added to the sub-model so that they can be easily identified in the stacked view on the right of the sub-model window (Figure 3-40).

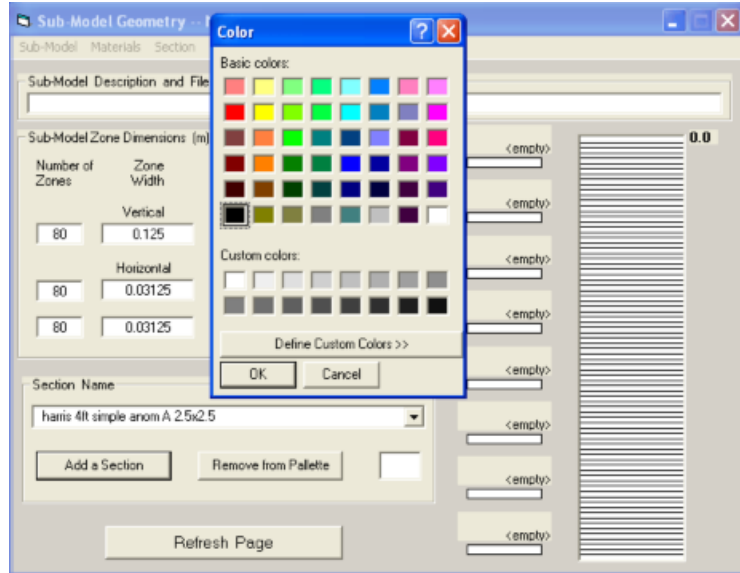


Figure 3-40 A different color is selected for each section as it is imported.

*NOTE: Each of the sections added to the sub-model should have the same X-Y space dimensions and DX and DY values. Sub-models of different dimensions can be assembled in the Model Editor to reduce the computations with less complex regions of the overall model.*

To assemble the sub-model, select the section from the *Section Name* pull down menu and paint the individual slices/sections on the right with the corresponding section color for that position in the vertical model. After painting in each section click the *Refresh Page* button to assure proper section position assignment. Figure 3-41 shows from top to bottom a modeled shaft with five different section types starting with air on top, the 4 ft shaft in sand, a void in the same shaft in sand, back to the shaft only in sand, a different anomaly, and then just sand at the bottom of the sub-model.

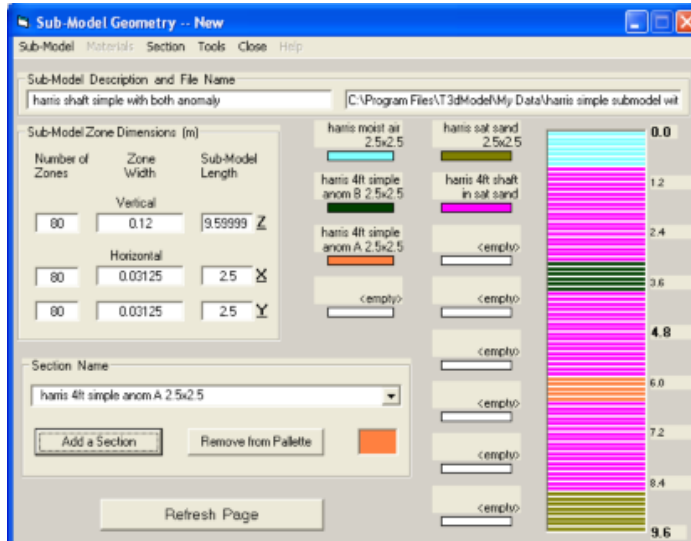


Figure 3-41 Sub-Model editor screen.

Both the sub-model description (top left window) and the file name (top right window) should be filled in before saving and exiting.

*Model editor.* The last step before running the model is to assemble the sub-models in the *Integrated Model* editor which is found on the main menu under *Model*. Select *new* or *open* to begin creating or editing, respectively. Sub-models of different X and Y dimensions can be assembled in the *Integrated Model* which allows complex models with large dimensions (e.g. pile cap or footing) to be joined with smaller model spaces (e.g. pier column). This reduces the computation overhead and provides detailed results where necessary. A given model must have at least one sub-model; in reality most models can be run with a single sub-model. One disadvantage, is that sub-models are restricted to 80 slices which may provide too coarse a mesh for long shafts. Multiple sub-models provides for finer vertical meshing.

To assemble the model, add sub-models by clicking the *Append a Sub-Model* button, input the rough overall model length, and assigning a unique color to each sub-model (similar to assembling sections in the sub-model editor). Click to the right in the vertically aligned model window once for each sub-model you want to add. After painting in each of the sub-models click on the *Adjust Model Length* button and assure the *total unmodeled length* is zero and the *total model length* is as intended. Input the model name in the top-most input window and save the model. Figure 3-10 shows the *Integrated Model* screen with two sub-models and an overall model length of 58.8m.

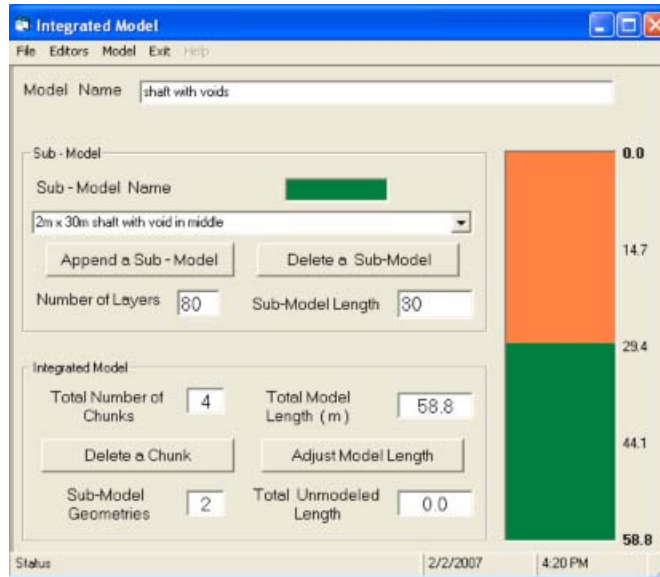


Figure 3-42 Integrated model screen showing stacked sub-models.

*Model Execution/output.* To run a generated model, select the *Editors* menu from the main menu and select *model execution/output*. This will open the *Program control and output viewer* window. Within this window select the *Open Model File* tab and open the desired model. Next select the *Concrete Source* tab. Several options are available for the user: *Time Series*, manual inputting **a**, **b**, and **t** or the *Concrete Database*. The latter is recommended which uses the same HSC discussed in Section 3.1. This choice automatically calculates the time release and energy parameters. Details of the other two options can be found elsewhere but are not needed (Mullins and Kranc, 2007).

The *Model Specifications* option in the *Model* pull down menu will be greyed out until the concrete source information is completed. After which it can be selected to set the boundary conditions along the edges of each section. The *No-flux boundary* is the default, but each of the materials identified at the edges of the sections must be at least clicked/highlighted to establish the default boundary condition. The *specified temperature* option allows the user to input user defined or more sophisticated boundary conditions (e.g. diurnal temperature variations, bay water temperature, etc.). When specifying a boundary condition temperature, \*.ts files must be selected by clicking in the *Time Series Filename* text box from which a file menu will appear. Two model formats (Cylindrical or Rectangular) can be selected which may or may not be more appropriate for a given application; cylindrical is the default. For primarily circular features (e.g. shafts), cylindrical is perhaps better; for pier columns try turning the default off by clicking on that check box. Both model formats produce realistic results unless the model space is too small and/or approaching the edge of the heat source. Within the *Program control and output viewer* window there are several option text boxes that can be altered by the user. In general the default values can be used successfully. However, one output file is created which contains the temperature values at the end of the simulation time which can be selected in the *Global Completion Time (h)* text box. By selecting a given time of interest every point in the model can be queried from the output

file named *modelname.1.out* where the *modelname* come from the name of the model run. Figure 3-43 shows the *Program control and output viewer* window in which certain execution controls can be exercised by the user.

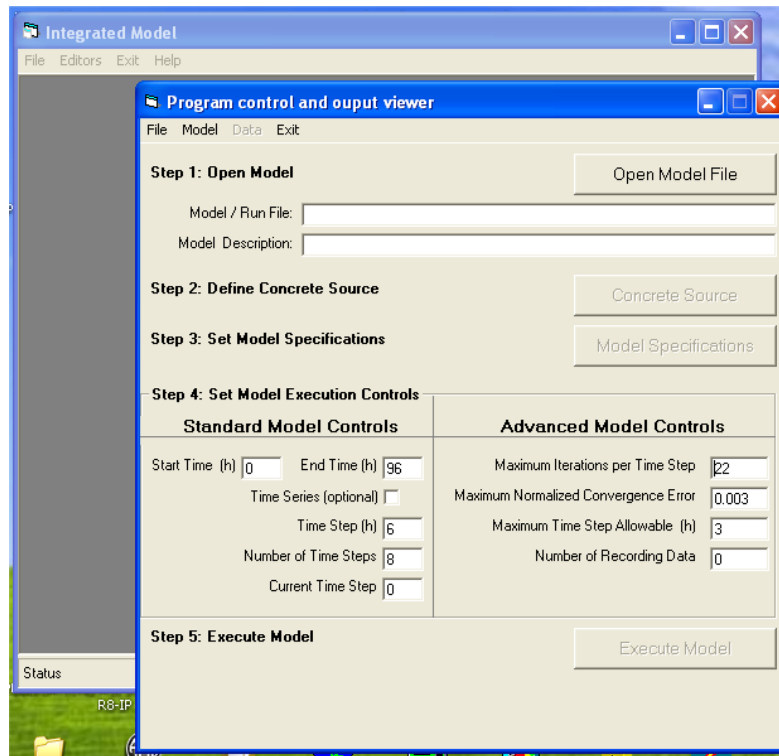


Figure 3-43 Execute model screen with 5 defined steps.

If the user is uncertain of how the time-temperature will evolve, then the default run time of 96 hours can be used and the output reviewed from another output file. The maximum, minimum, and center line modeled temperature developed in the 3-D model space are outputted in an ASCII file named *Tmax.out* along with the times at which those temperatures occurred. With this information, the user may opt to re-run the model with a specific simulation time. Alternately, time steps can be run by checking the optional time series box. This increases the run time, but provides the final temperatures over the full model space at the end of each time step. Without the stepping option only one output file is created based only on the ending conditions for the entire model space.

### 3.6.2 Visual Post Processor

The *modelname.1.out* file contains the output temperature for each element of each section in sub-model 1. The *modelname.2.out* file would contain the same information for the second sub-model and so on. Due to the potentially enormous amount of data stored in these files (e.g. 80 x 80 x 80), a simple macro-run post processing EXCEL spread sheet has been provided to review each of the data visually.



**Chapter Four: Field Testing and Results**

The primary focus of this research project was to conduct large-scale thermal integrity tests on drilled shafts and evaluate the test data to develop the thermal integrity testing procedures. In conjunction with the tasks of this project, thermal testing was conducted on a total of 11 shafts. Table 4-1 shows the project log for all shafts which were thermally profiled. The following sections discuss the thermal program for each project.

Table 4-1. Thermal Testing Project Log

<i>Test Date</i>	<i>Project Name</i>	<i>Pier</i>	<i>Shaft</i>	<i>Diameter (ft)</i>
07/27/09	Nalley Valley	6	A	10
07/29/09	Nalley Valley	6	C	10
07/30/09	Nalley Valley	6	B	10
08/04/09	Scatter Creek	1	A	4
08/04/09	Scatter Creek	1	B	4
08/11/09	Tieton River Bridge	1	1	8
01/13/10	US 395 Wandermere Vicinity	4	L	10
02/24/10	Vancouver Rail Project	2	N	6.5
08/01/10	Gallup Creek	2	South	7
08/20/10	Hyak to Snowshed	4	B	9
9/13/10	Manette Bridge	2	B	12

*Data Analysis.* Field measurements were taken from each tube. The average of these measurements at any given depth provides an indication of the overall shaft integrity and in many cases is a reflection of the shaft shape. However, when compared to model predictions, the integrity of the shaft can be even better assessed. A model was run based on theoretical shaft dimensions and compared to the field measurements.

It is normal for the temperature to decrease near the ends of the shaft (over a length approximately 1 diameter) forming a somewhat circular shape which accounts for both axial and radial dissipation of heat. Farther from the ends (beyond 1D), dissipation is purely radial and allows for a direct correlation between measured temperature and the as-built radius. The effective radius is predicted based on the temperature that would have resulted in the presence of uncompromised intact concrete with that dimension. Irregularities in the effective radius near the very ends of the shaft are due to uncorrected heat dissipation. An effective radius value less than theoretical can be caused by a complete section loss or a slightly larger radius (than predicted) with a poorly cemented mixture of concrete and debris. In either case, the absence of heat producing cementitious material can have a deleterious effect on strength and/or durability.

*Cage Alignment.* The cage alignment can be assessed based on tube temperatures higher and lower than average temperatures. As a result tubes on opposite sides of the cage will respond with roughly equal and opposite temperature variations when misaligned. Higher temperatures correspond to tubes closer to the center of shaft while lower temperatures



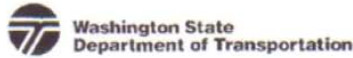
corresponds to tubes closer to wall excavation. Cage alignment within the excavation and concrete cover can be determined by comparing the individual tube temperatures to the average temperature at any depth.

#### **4.1 Project 7594: Nalley Valley**

Thermal testing was conducted on the shafts at Pier 6 for I-5 / SR16 West Bound Nalley Valley Project in Tacoma, WA. This pier is comprised of three - 10 foot diameter drilled shafts approximately 70 feet long. The shafts were equipped with ten - 1.5" I.D. steel access tubes in general accordance with standard practice for tube plurality in State specifications. The tube identification / numbering used for this project assumed the northerly most tube to be No. 1 and increased in value in a clockwise fashion looking down on to the shaft top. Standard infrared thermal testing was conducted on the shafts within Pier 6. Testing protocols requires a minimum of 2 tests per tube and verifying the reproducibility of each scan.

##### **4.1.1 Thermal Modeling**

Prior to the testing, a sample mix design for the area was provided to the researchers. The mix design is used within the thermal model (T3DModel) to predict the heat generated in the shaft for optimal testing time, defects / anomalies within the shaft, cage alignment, etc. An up-to-date mix design (Figures 4-1 through 4-4) was provided upon arrival to the test site. Slight differences were noticed in the mix design and the model responses from both mixes are compared in Figure 4-5. Figure 4-5 shows the temperature in a 10 foot diameter shaft using the current parameters falling faster than with the original parameters. This would result in a shorter timeframe for testing these shafts.



CMD-0005  
Concrete Mix Design

Contractor Atkinson Construction		Submitted By Greg Smith	Date 12/17/2008
Concrete Supplier Holroyd Co., Inc.		Plant Location 1002 E. 26th St., Tacoma, WA 98421	
Contract Number 150093-204	Contract Name I-5 / SR16 Westbound Nalley Valley I/C		

This mix is to be used in the following Bid Item No(s): 89.01

Concrete Class: (check one only)

3000  
  4000  
  4000D  
  4000P<sup>a</sup>  
  4000W  
  Concrete Overlay  
  Cement Concrete Pavement<sup>d</sup>  
  Other

Remarks: \_\_\_\_\_

Mix Design No. 7631FRD

Cementitious Materials	Source	Type or Class	Sp. Gr.	Lbs/cy
Cement	Lehigh Cement Co., Seattle, WA	Type I-II	3.15	610
Fly Ash <sup>a</sup>	Lafarge, Seattle, WA	Type F	2.54	110
Microsilica				
Latex				
Slag				

Concrete Admixtures	Manufacturer	Product	Type	Est. Range (oz/cy)
Air Entrainment				
Water Reducer	BASF Admixtures, Inc.	Polyheed 997	Type A	30.0-45.0
High-Range Water Reducer				
Set Retarder	BASF Admixtures, Inc.	Pozzilith 100 XR	Type B	20.0-30.0
Other				

Water (Maximum) 290 (lbs/cy)      Reclaimed/Recycled Water<sup>e</sup> (Maximum) \_\_\_\_\_ (lbs/cy)

Water Cementitious Ratio (Maximum) 0.40

Design Performance	1	2	3	4	5	Average
28 Day Compressive Strength (cylinders) psi	5,730	5,860	5,720	5,820	5,370	5,700
14 Day Flexural <sup>d</sup> Strength (beams) psi						

Reviewed By:  PE Signature      2/18/09 Date

Distribution: Original - Contractor  
Copies To - State Materials Lab-General Materials Eng. ; Regional Materials Lab; Project Inspector

DOT Form 350-040 EF  
Revised 5/2003

Figure 4-1 Nalley Valley concrete mix design page 1.

**Combined Gradation Chart**

Concrete Aggregates	Component 1	Component 2	Component 3	Component 4	Component 5	Combined Gradation
WSDOT Pit No.	J-9	J-9				
ASR Mitigation Required? <sup>b</sup>	<input checked="" type="checkbox"/> Yes <input type="checkbox"/> No	<input checked="" type="checkbox"/> Yes <input type="checkbox"/> No	<input type="checkbox"/> Yes <input type="checkbox"/> No	<input type="checkbox"/> Yes <input type="checkbox"/> No	<input type="checkbox"/> Yes <input type="checkbox"/> No	
Grading <sup>c</sup>	Class 2	#8				
Percent of Total Aggregate	38.6	61.4				100%
Specific Gravity	2.65	2.69				
Lbs/cy (ssd)	1175	1870				

Percent Passing						
2 inch						
1-1/2 inch						
1 inch						
3/4 inch						
1/2 inch		100.00				
3/8 inch	100.00	93.20				
No. 4	97.10	10.20				
No. 8	77.60	0.80				
No. 16	58.30	0.30				
No. 30	37.20					
No. 50	13.90	0.10				
No. 100	4.10					
No. 200	2.20	0.10				

Aggregate Correction Factor: 0.20      Fineness Modulus: 3.12 (Required for Class 2 Sand)

**Notes:**

- <sup>a</sup> Required for Class 4000D and 4000P mixes.
- <sup>b</sup> If Alkali Silica Reactivity Mitigation is required per WSDOT ASA Database - Attach evidence that mitigating measure controls expansion in the form of ASTM C 1260 / AASHTO T303, ASTM C 1293, or ASTM C 295 test results
- <sup>c</sup> AASHTO No. 467, 57, 67, 7, 8; WSDOT Class 1, Class 2; or combined gradation. See Standard Specification 9-03.1
- <sup>d</sup> Required for Cement Concrete Pavements
- <sup>e</sup> Attach test results indicating conformance to Standard Specification 9-25.1

DOT Form 350-040 EF  
Revised 5/2003

Figure 4-2 Nalley Valley concrete mix design page 2.

**MILL TEST REPORT**

Cement Type: **ASTM Type I/II, AASHTO Type I  
Low Alkali Portland Cement**

Plant: **Delta, BC**

**Certificate #: D2-374**

Production Period:	Jun 01 2009 Jun 30 2009	Test Result	ASTM C150-07 Specification	AASHTO M 85-07 Specification
SiO <sub>2</sub> (%)	ASTM C114	20.0	-	-
Al <sub>2</sub> O <sub>3</sub> (%)	ASTM C114	5.03	max. 6.0	-
Fe <sub>2</sub> O <sub>3</sub> (%)	ASTM C114	3.69	max. 6.0	-
CaO (%)	ASTM C114	65.0	-	-
MgO (%)	ASTM C114	0.83	max. 6.0	max. 6.0
SO <sub>3</sub> (%)	ASTM C114	2.80	max. 3.0	max. 3.0
Na <sub>2</sub> O (%)	ASTM C114	0.30	-	-
K <sub>2</sub> O (%)	ASTM C114	0.36	-	-
TiO <sub>2</sub> (%)	ASTM C114	0.25	-	-
C <sub>3</sub> S (%)	ASTM C150	58	-	-
C <sub>2</sub> S (%)	ASTM C150	13	-	-
C <sub>3</sub> A (%)	ASTM C150	7.1	max. 8	max. 8
C <sub>4</sub> AF (%)	ASTM C150	11.2	-	-
Equivalent Alkalies (%)	ASTM C150	0.54	max. 0.60	max. 0.60
C <sub>4</sub> AF + 2(C <sub>3</sub> A) (%)	ASTM C150	25.4	-	-
C <sub>3</sub> S + 4.75(C <sub>3</sub> A) (%)	ASTM C150	92.0	max. 100	-
Loss on Ignition (%)	ASTM C114	2.5	max. 3.0	max. 3.0
Insoluble Residue (%)	ASTM C114	0.30	max. 0.75	max. 0.75
Free Calcium Oxide (%)	ASTM C114	0.41	-	-
CO <sub>2</sub> in Cement (%)	ASTM C114	1.42	-	-
CaCO <sub>3</sub> in Limestone (%)	ASTM C114	96	min. 70	min. 70
Limestone in Cement (%)	ASTM C150	3.4	max. 5.0	max. 5.0
Vicat Setting Time				
Initial (minutes)	ASTM C191	108	min. 45 max. 375	min. 45 max. 375
Final (minutes)	ASTM C191	214	-	-
Blaine Fineness (m <sup>2</sup> /kg)	ASTM C204	387	min. 280	min. 280
+325 mesh	ASTM C430	1.5	-	-
Air Content (%)	ASTM C185	6.60	max. 12	max. 12
Autoclave Expansion (%)	ASTM C151	0.00	max. 0.80	max. 0.80
Compressive Strength		MPa / psi		
3 Day	ASTM C109/109M	28.3 / 4098	min. 12.0	min. 12.0
7 Day	ASTM C109/109M	35.3 / 5115	min. 19.0	min. 19.0
28 Day (previous month)	ASTM C109/109M	42.4 / 6148	-	-

This will certify that the above described cement meets the standard chemical and physical requirements of ASTM Specification C-150-07 for Type I and Type II Low Alkali Portland Cements and AASHTO Specification M-85-07 for Type I Low Alkali Portland Cement.

Eileen M. Jang  
Quality Control Manager/Mill Engineer



July 17, 2009

Figure 4-3 Nalley Valley Portland cement mill certificate.



Cement

FLY ASH TEST REPORT

Analysis by: Lafarge Seattle Concrete Lab  
Sample from : Centralia Power Plant  
Average Analysis: June 1<sup>st</sup> - June 30th 2009

Chemical Analysis

Silicon Dioxide (SiO <sub>2</sub> )	48.0 %
Aluminum Oxide (Al <sub>2</sub> O <sub>3</sub> )	17.2 %
Iron Oxide (Fe <sub>2</sub> O <sub>3</sub> )	5.8 %
Total (SiO <sub>2</sub> ) + (Al <sub>2</sub> O <sub>3</sub> ) + (Fe <sub>2</sub> O <sub>3</sub> )	70.9 %
Sulphur Trioxide (SO <sub>3</sub> )	1.0 %
Calcium Oxide (CaO)	15.1 %
Magnesium Oxide	4.6 %
Moisture Content	0.40 %
Loss on Ignition	0.25 %
Available Alkali as Equiv. Na <sub>2</sub> O (previous month's result)	2.6 %
Total Alkalies as Equivalent Na <sub>2</sub> O	4.34 %

Physical Analysis

Fineness Retained on 45 um (No. 325 Sieve)	16.6 %
Strength Activity Index with Portland Cement	
% of Control at 7 Days	87 %
% of Control at 28 Days (previous month's result)	94 %
Water Requirement, Percent of Control	97 %
Autoclave Expansion	0.03 %
Density	2.67 Mg/m <sup>3</sup>

We hereby certify the fly ash represented by the above chemical and physical analysis meets the requirements of ASTM C618-05 for Fly Ash.

Certified: Robert S. Shogren

Figure 4-4 Nalley Valley fly ash mill certificate.

The mix design information was used to create the input hydration energy parameters using the **a**, **b**, and **t** method outlined by Schindler (2005). The model parameters

used in the T3DModel software were 0.751, 0.629, and 19.338, respectively with an overall energy production of 76.28 kJ per kg of total concrete mass (current parameters).

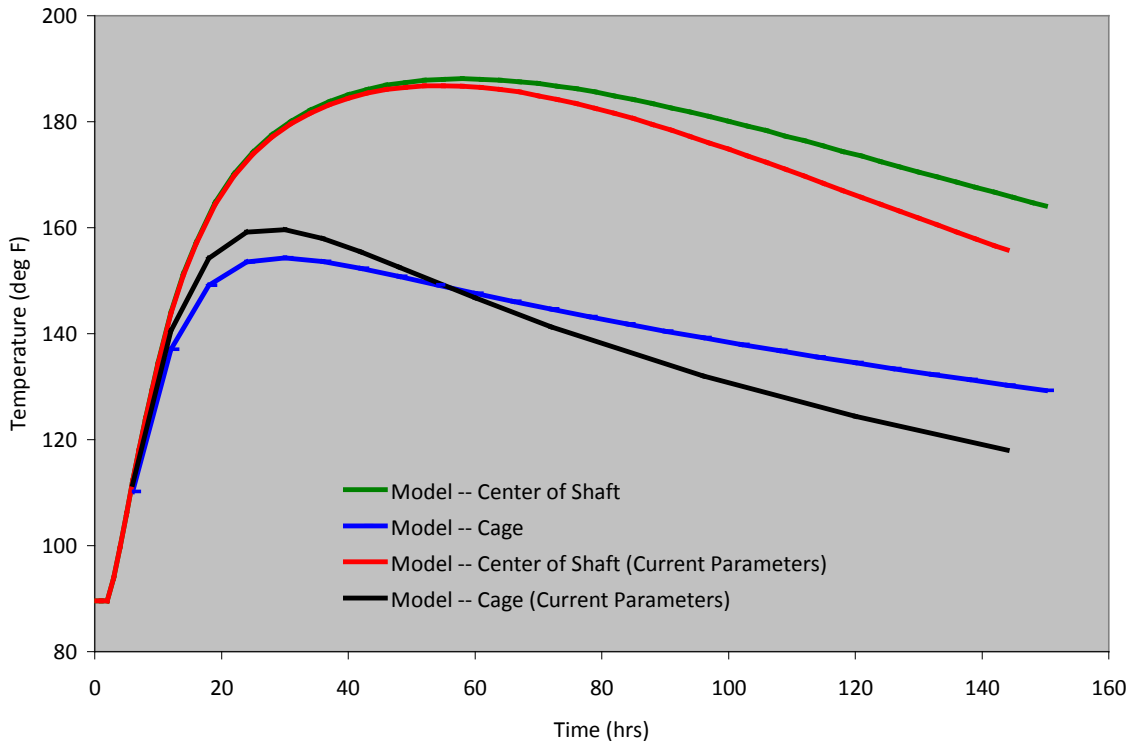


Figure 4-5 Thermal predictions for a 10' diameter shaft showing the differences in old and current mix design parameters.

#### 4.1.2 Thermal Testing Pier 6 Shaft A

The testing was performed on July 27, 2009 approximately 73 hours after concreting Shaft A. Field measurements were taken from each of the nine tubes (tube 9 was blocked and not tested) and are presented in Figure 4-6. A model was run based on theoretical shaft dimensions (10 ft diameter) and compared to the field measurements (Figure 4-7). The average field temperature from an elevation of 213ft to the bottom of shaft is less than the predicted model response. This indicates a smaller diameter shaft in this region, which is reasonable when compared to the construction logs. The construction log shows the use of a 9ft diameter cleanout bucket for approximately the last 4ft of excavation. This would cause a lower temperature as seen in the field data.

Project 7594  
Pier 6 Shaft A

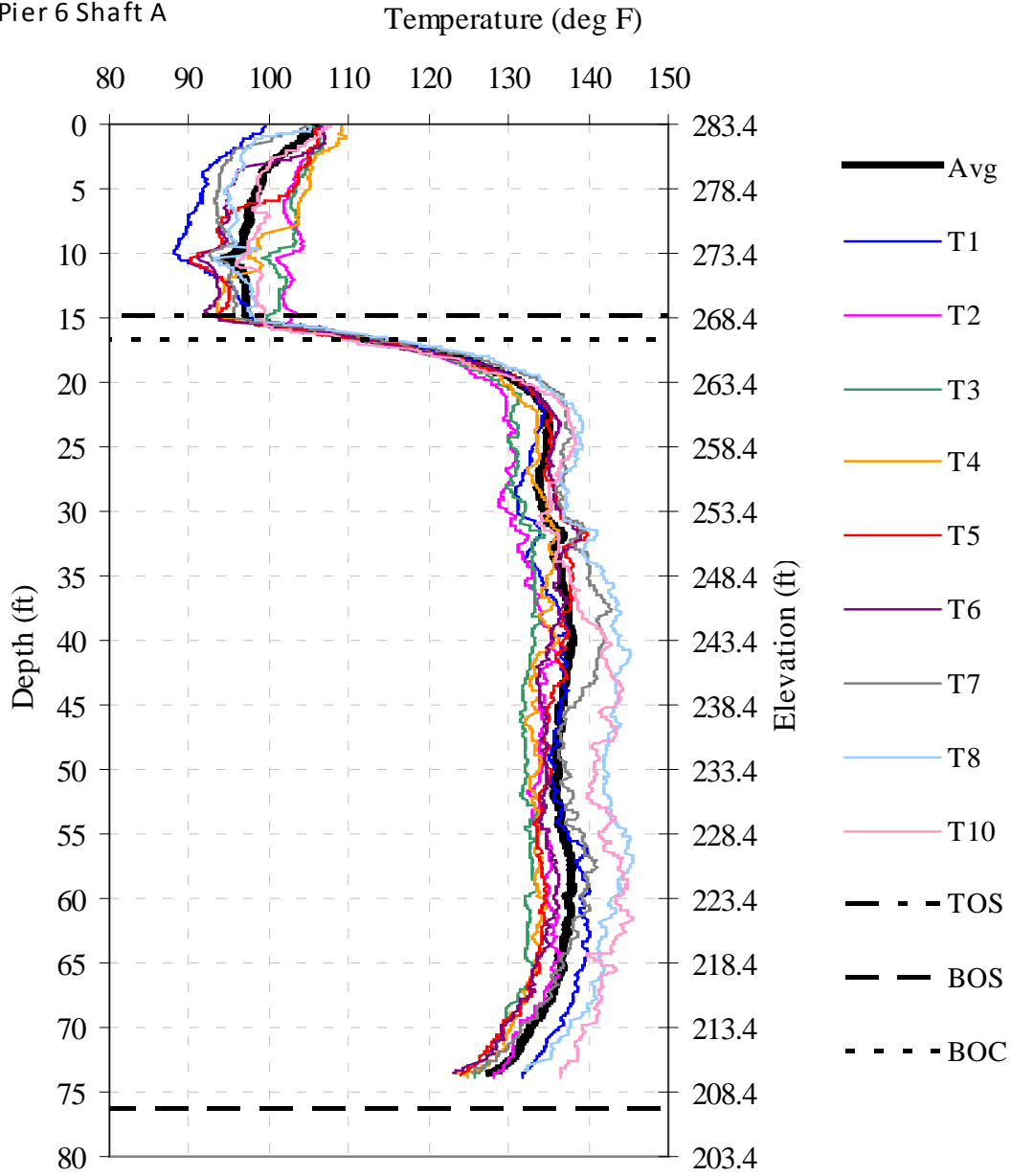


Figure 4-6 Measured tube temperatures versus depth (Nalley Valley Pier 6 Shaft A).



Project 7594  
 Pier 6 Shaft A

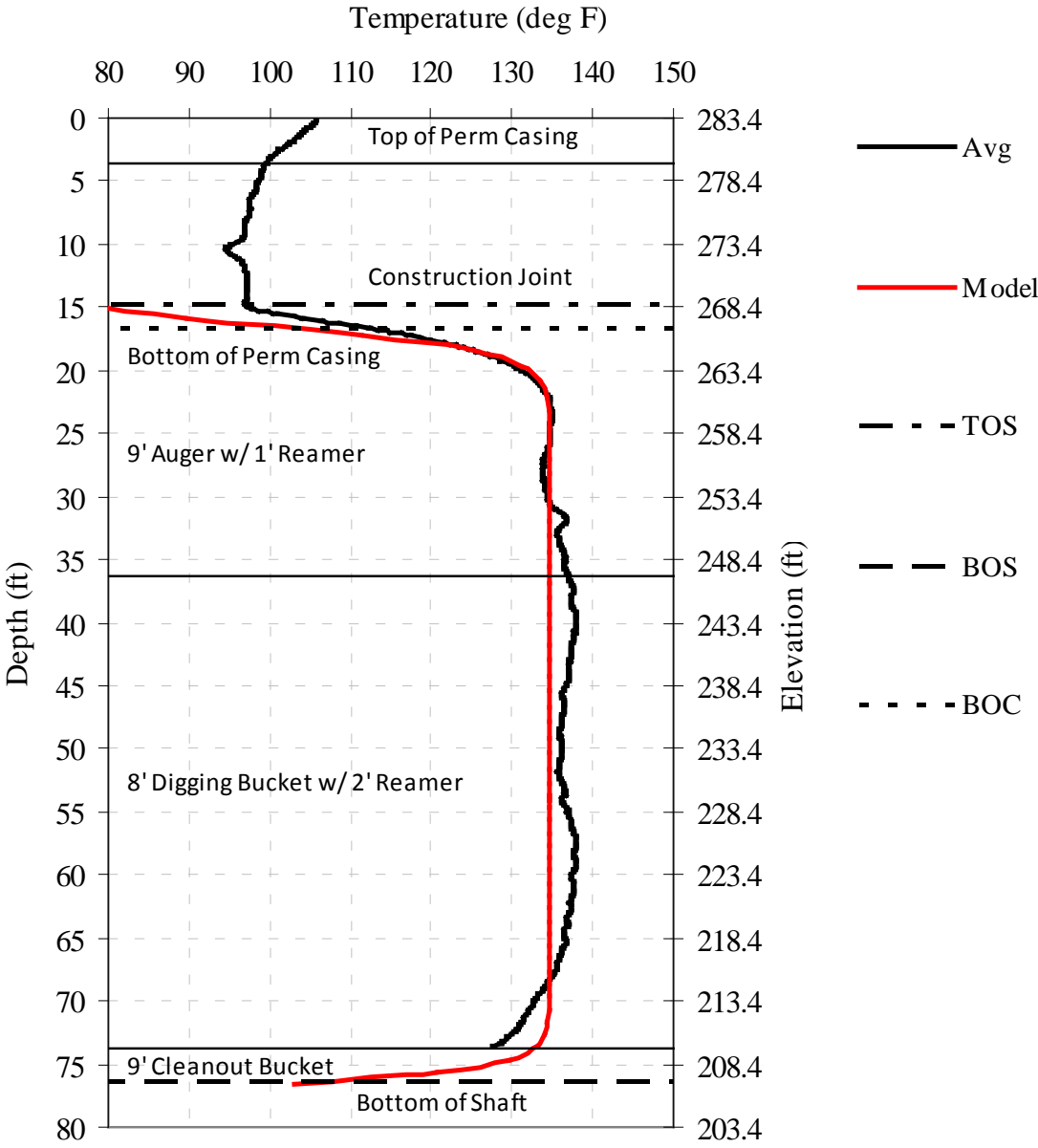


Figure 4-7 Measured and modeled temperature versus depth (Nalley Valley Pier 6 Shaft A).

Figure 4-8 shows the average measured temperatures versus the concrete placement log. The effective radius (Figure 4-9) is predicted based on the temperatures that would result in the presence of uncompromised intact concrete with that dimension. The shaded area in Figure 4-9 is not corrected for the axial heat dissipation. However, based on the

general roll-off, the shaft appears to be of reasonable diameter within those areas. Finally, a 3-D rendering can be developed providing an image of the as-built shaft (Figure 4-10).

Project 7594  
 Pier 6 Shaft A

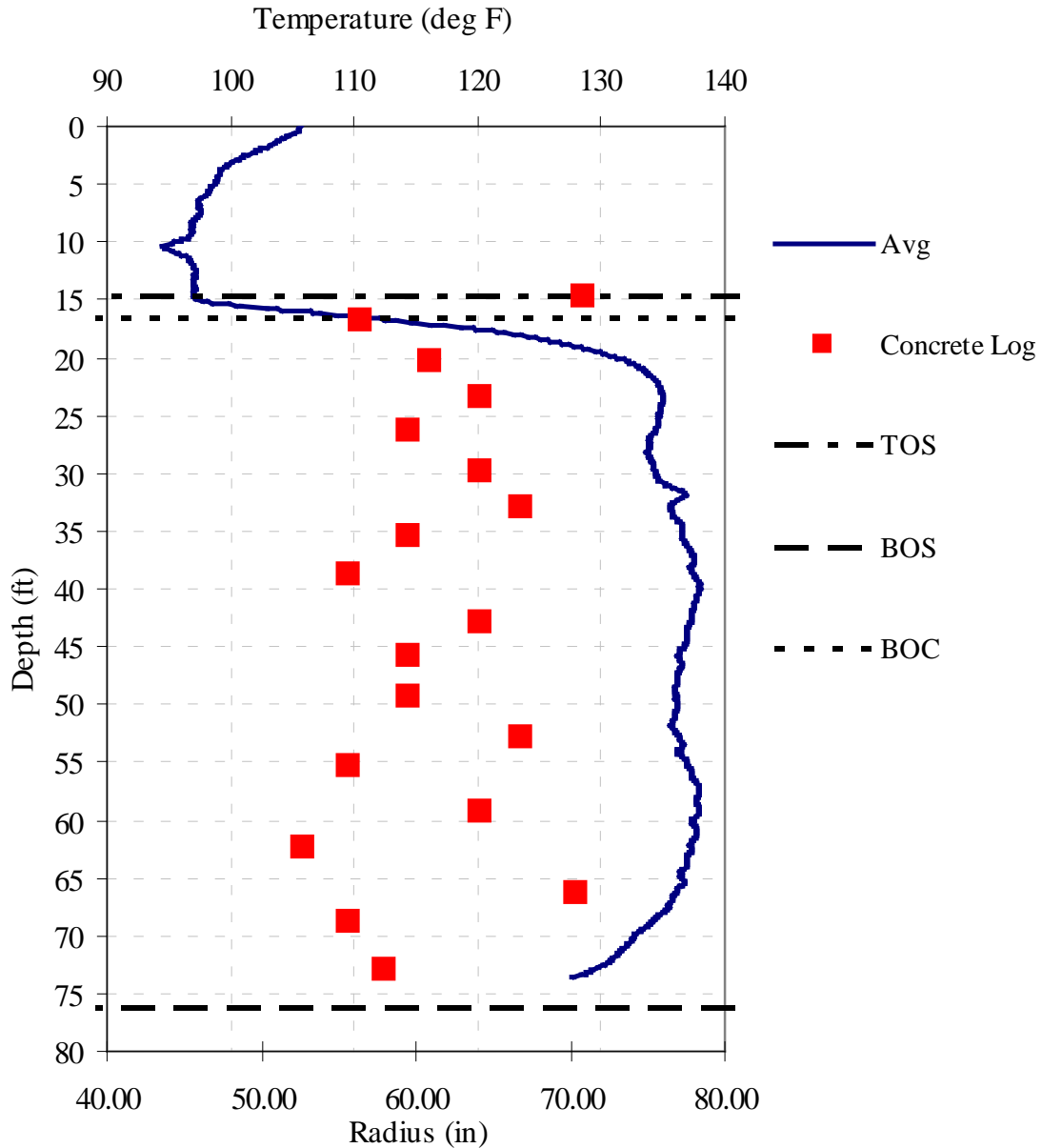


Figure 4-8 Concrete Placement Log versus average measured temperature (Nalley Valley Pier 6 Shaft A).

Project 7594  
 Pier 6 Shaft A

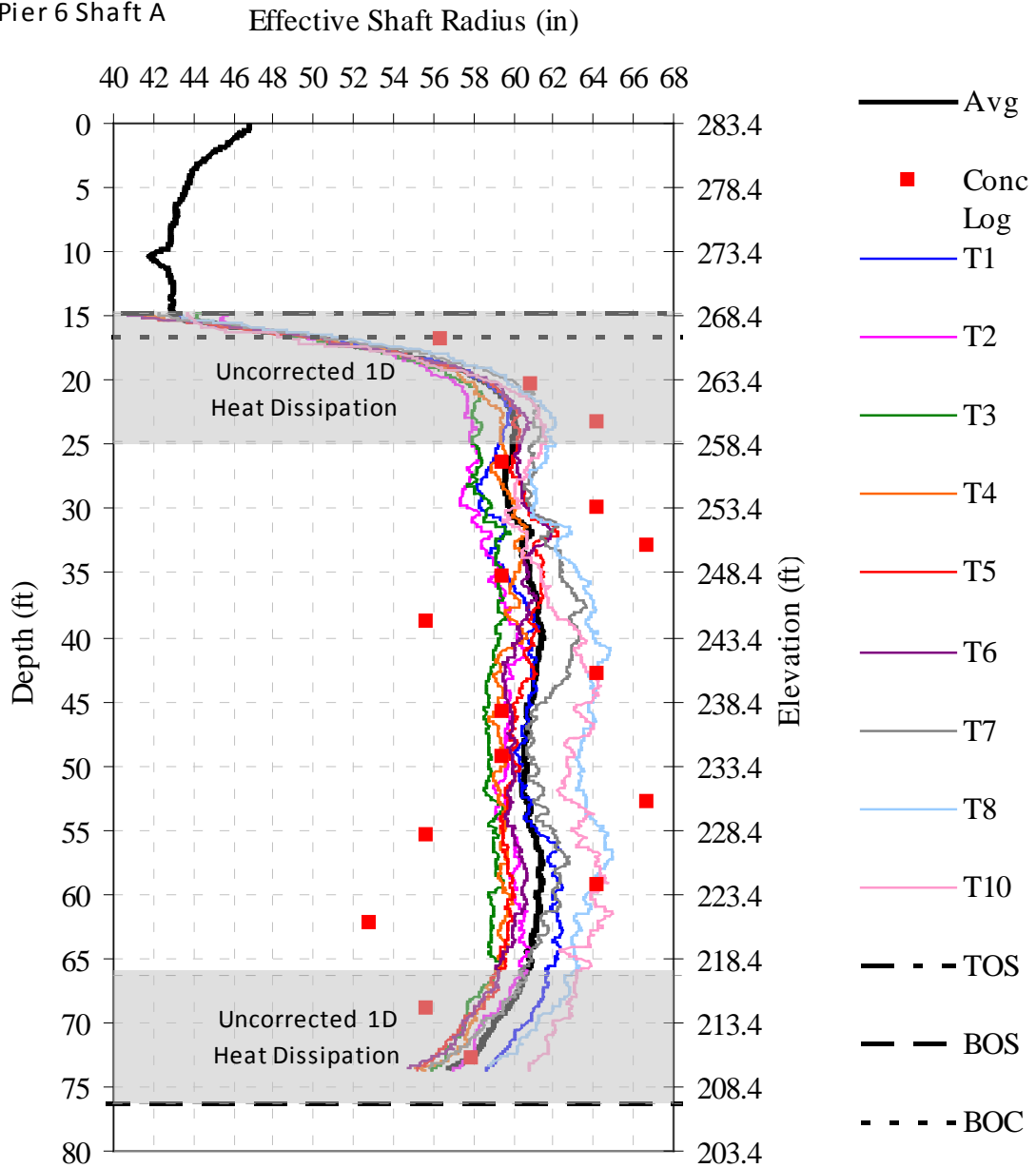


Figure 4-9 Effective shaft radius showing cage alignment uncorrected for axial heat dissipation (Nalley Valley Pier 6 Shaft A).

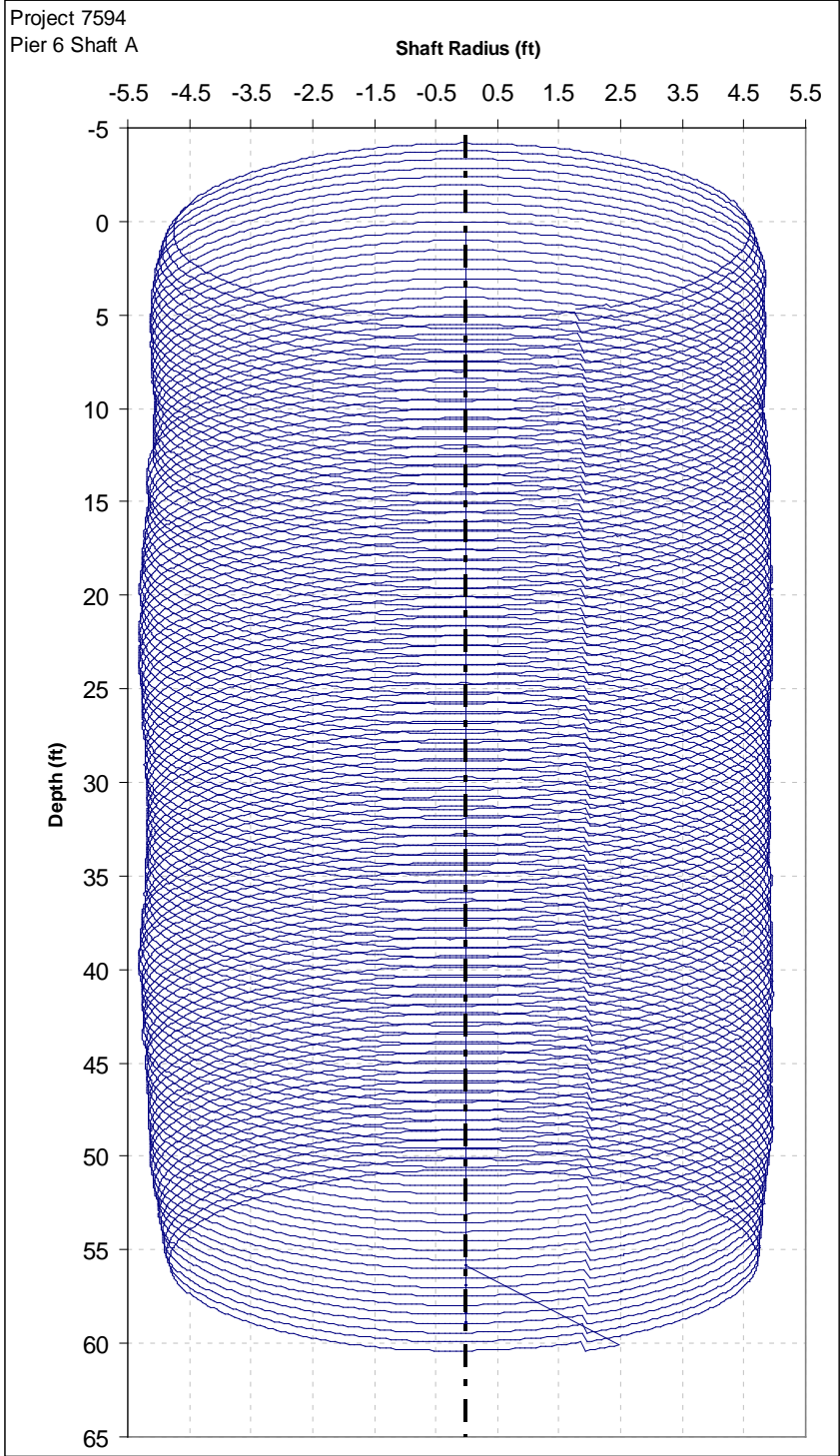


Figure 4-10 3-D rendering from tube spacings and effective radius calculations (Nalley Valley Pier 6 Shaft A).

### 4.1.3 Thermal Testing Pier 6 Shaft B

The testing was performed on July 30, 2009 approximately 52 hours after concreting Shaft B. Field measurements were taken from each of the ten tubes and are presented in Figure 4-11. To verify the thermal model predictions, thermocouples, T/C, were installed and monitored in Pier 6 Shaft B. A total of 6 T/C were installed on the reinforcement cage 6ft, 16ft, 26ft, 36ft, 46ft, and 56ft from the toe with a 7<sup>th</sup> T/C monitoring the air temperature. Figure 4-12 (top) shows the thermocouple data compared to the model temperature prediction.

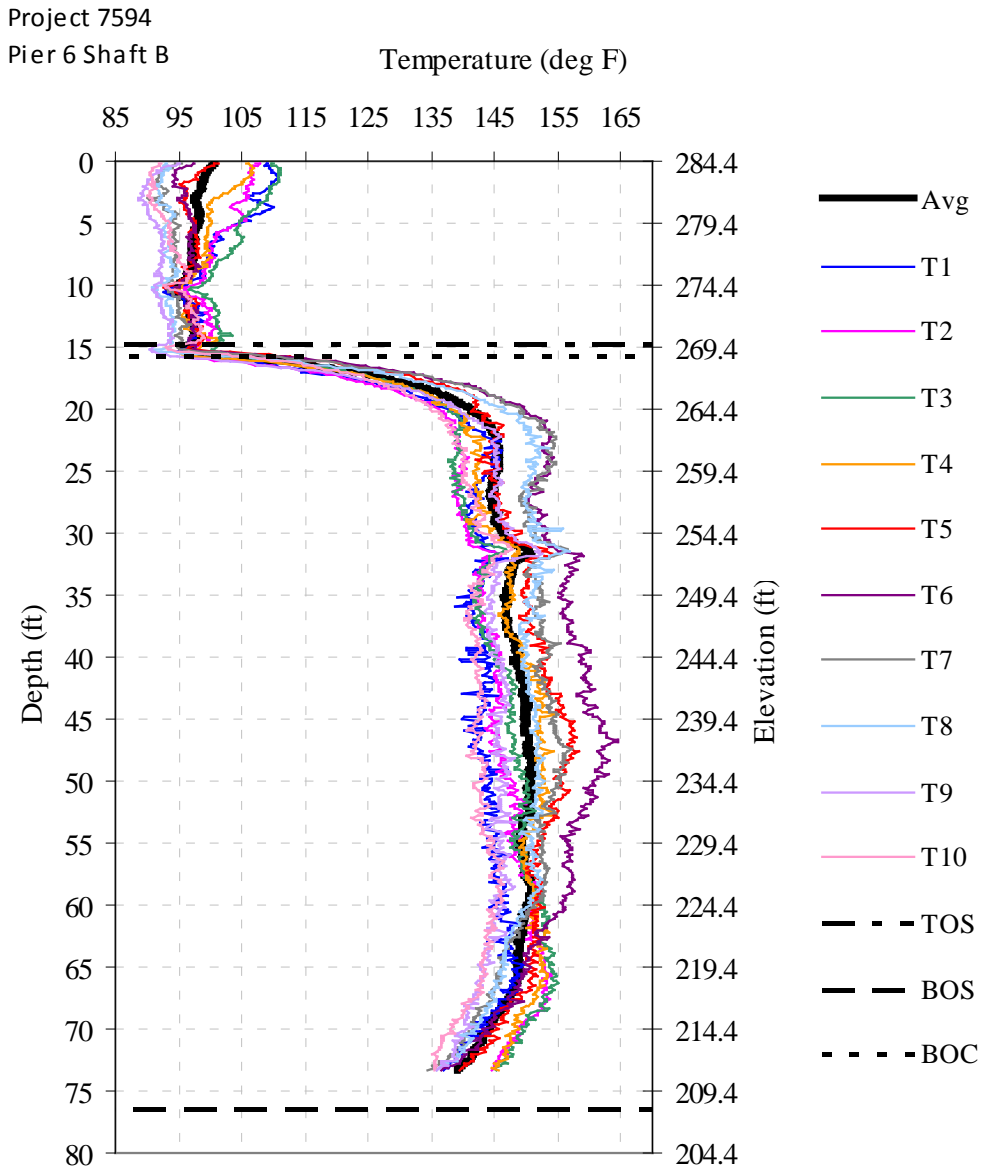


Figure 4-11 Measured tube temperatures versus depth (Nalley Valley Pier 6 Shaft B).

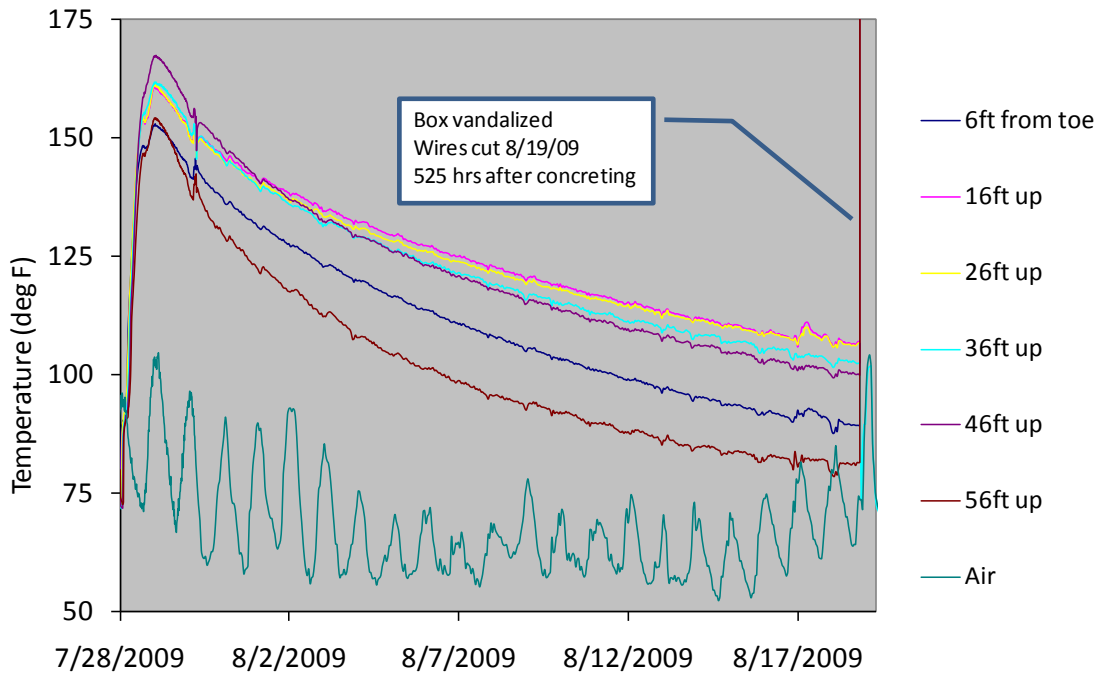
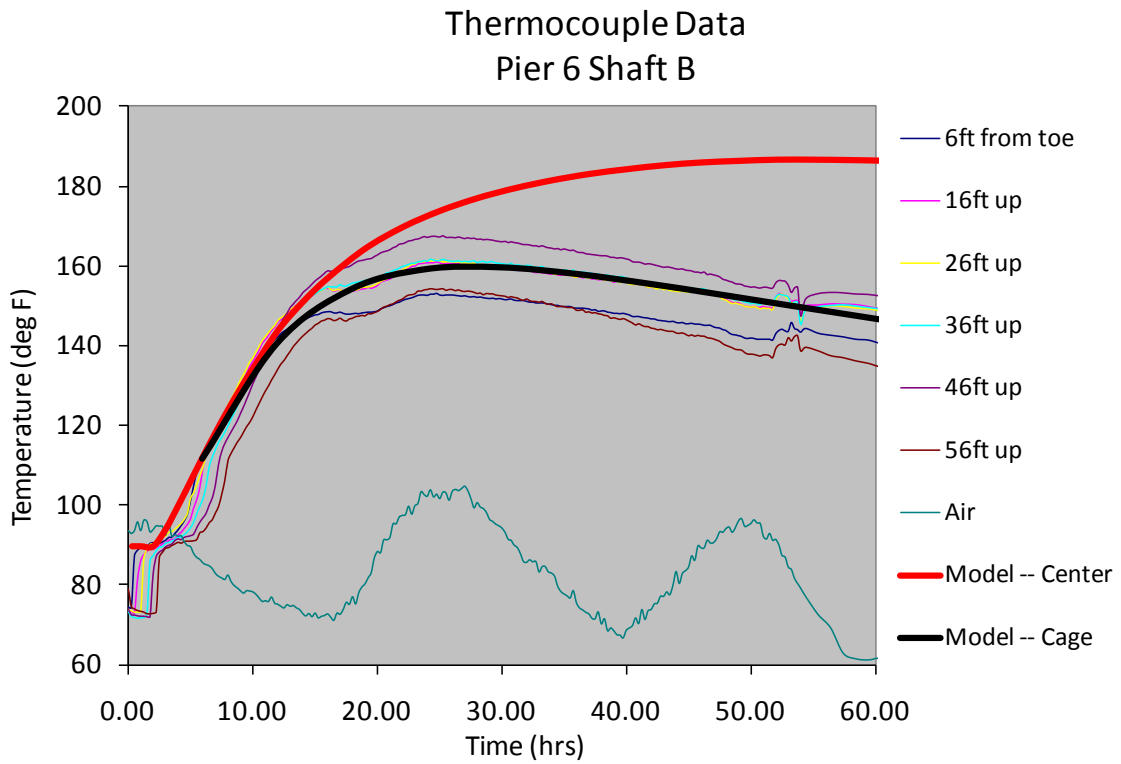


Figure 4-12 Thermocouple data for Pier 6 Shaft B compared with model response (top); elevated temperatures in shaft over 3 wk sampling period (bottom).

Thermocouple data collection was continued which showed elevated temperatures existed for at least 3 weeks (525 hrs) after concreting. A model was run based on theoretical shaft dimensions (10 ft diameter) and compared to the field measurements (Figure 4-13). The average field temperature is either in line with or greater than the model indicating an effective shaft diameter of 10ft or greater. Figure 4-14 shows the average measured temperature versus the concrete placement log. The effective radius (Figure 4-15) is predicted without axial heat dissipation corrections. Figure 4-16 shows a 3-D rendered image of the as-built shaft.

Project 7594  
Pier 6 Shaft B

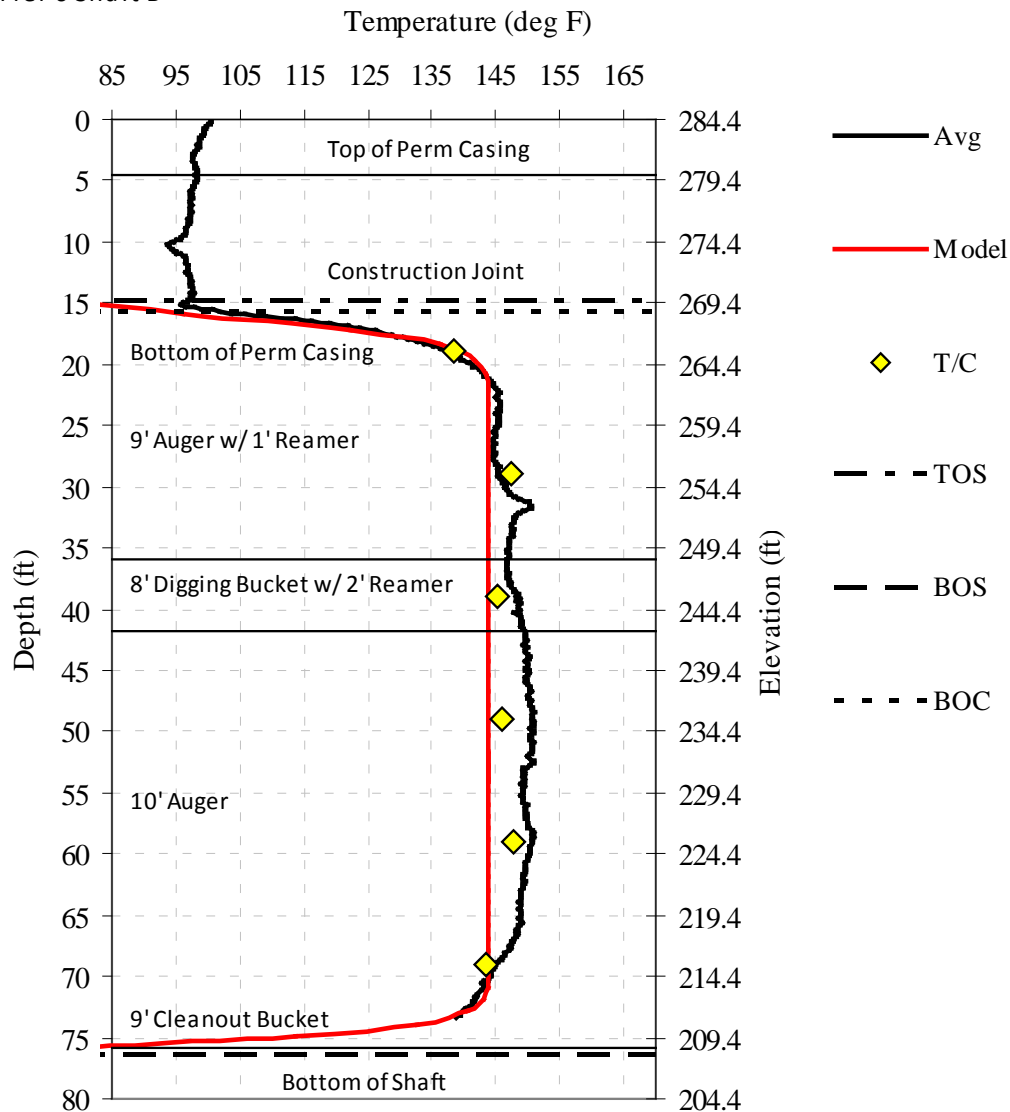


Figure 4-13 Measured and modeled temperature vs depth (Nalley Valley Pier 6 Shaft B).



Project 7594  
 Pier 6 Shaft B

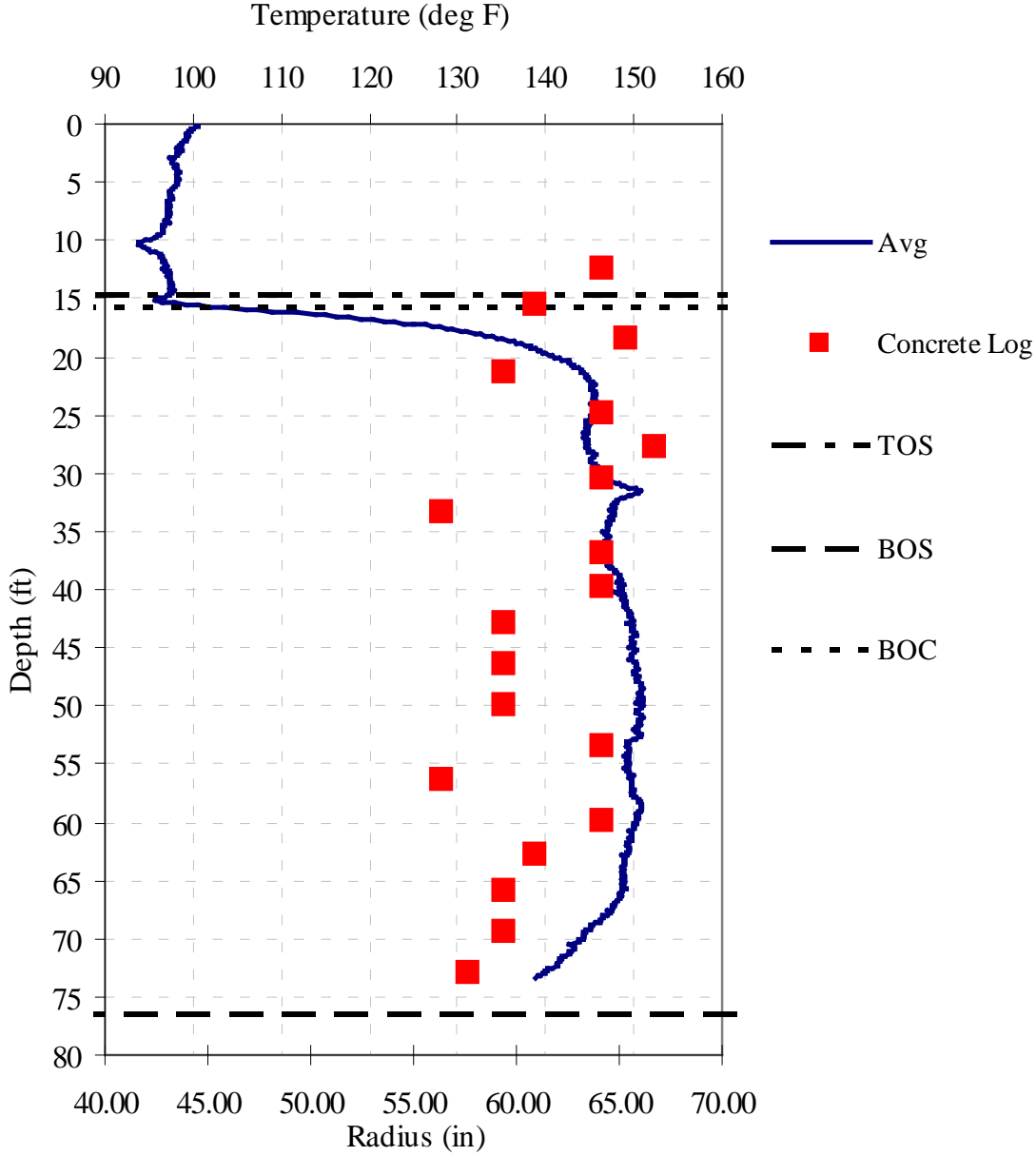


Figure 4-14 Concrete Placement Log versus average measured temperature (Nalley Valley Pier 6 Shaft B).

Project 7594

Pier 6 Shaft B

Effective Shaft Radius (in)

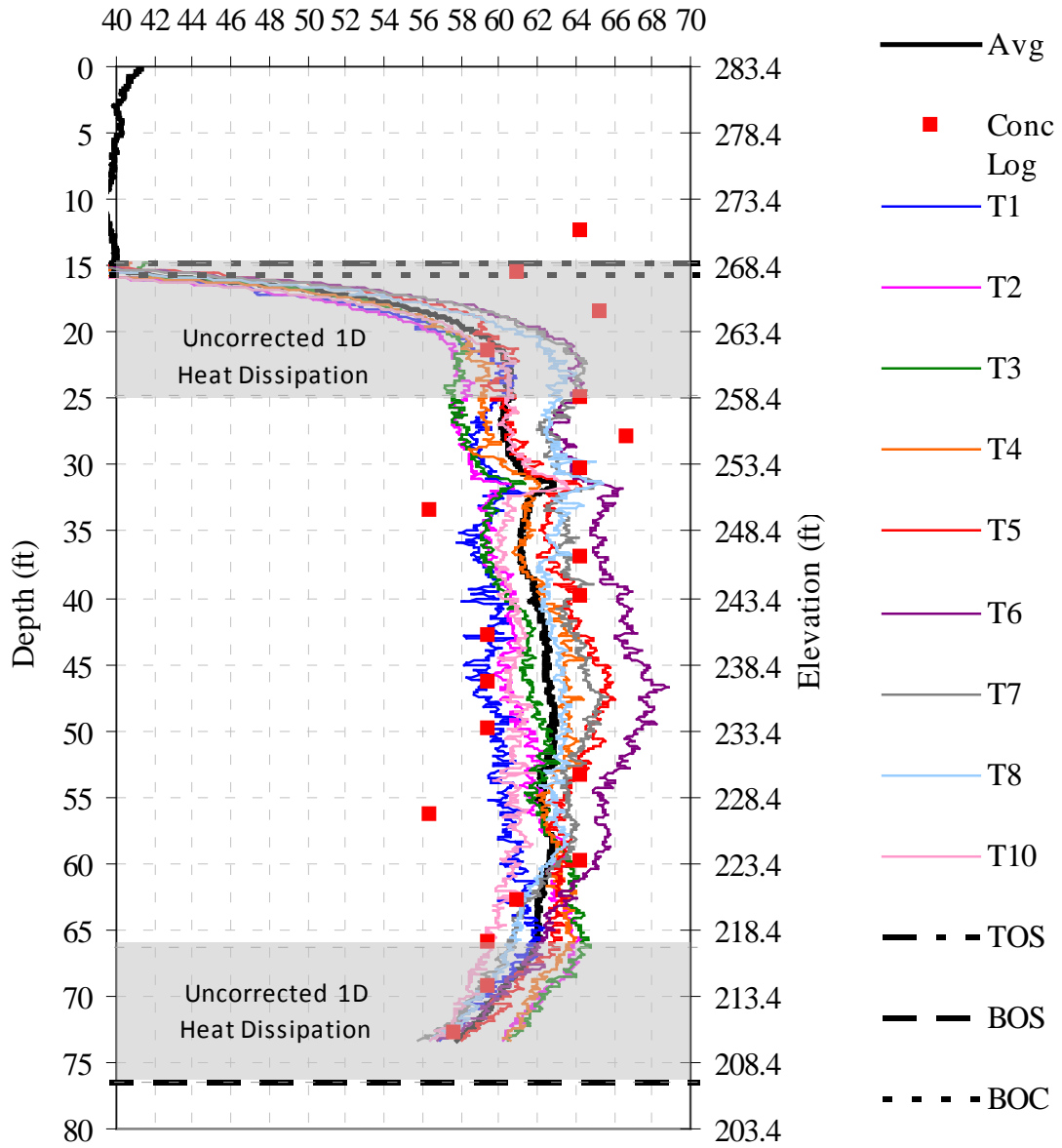


Figure 4-15 Effective shaft radius showing cage alignment uncorrected for axial heat dissipation (Nalley Valley Pier 6 Shaft B).

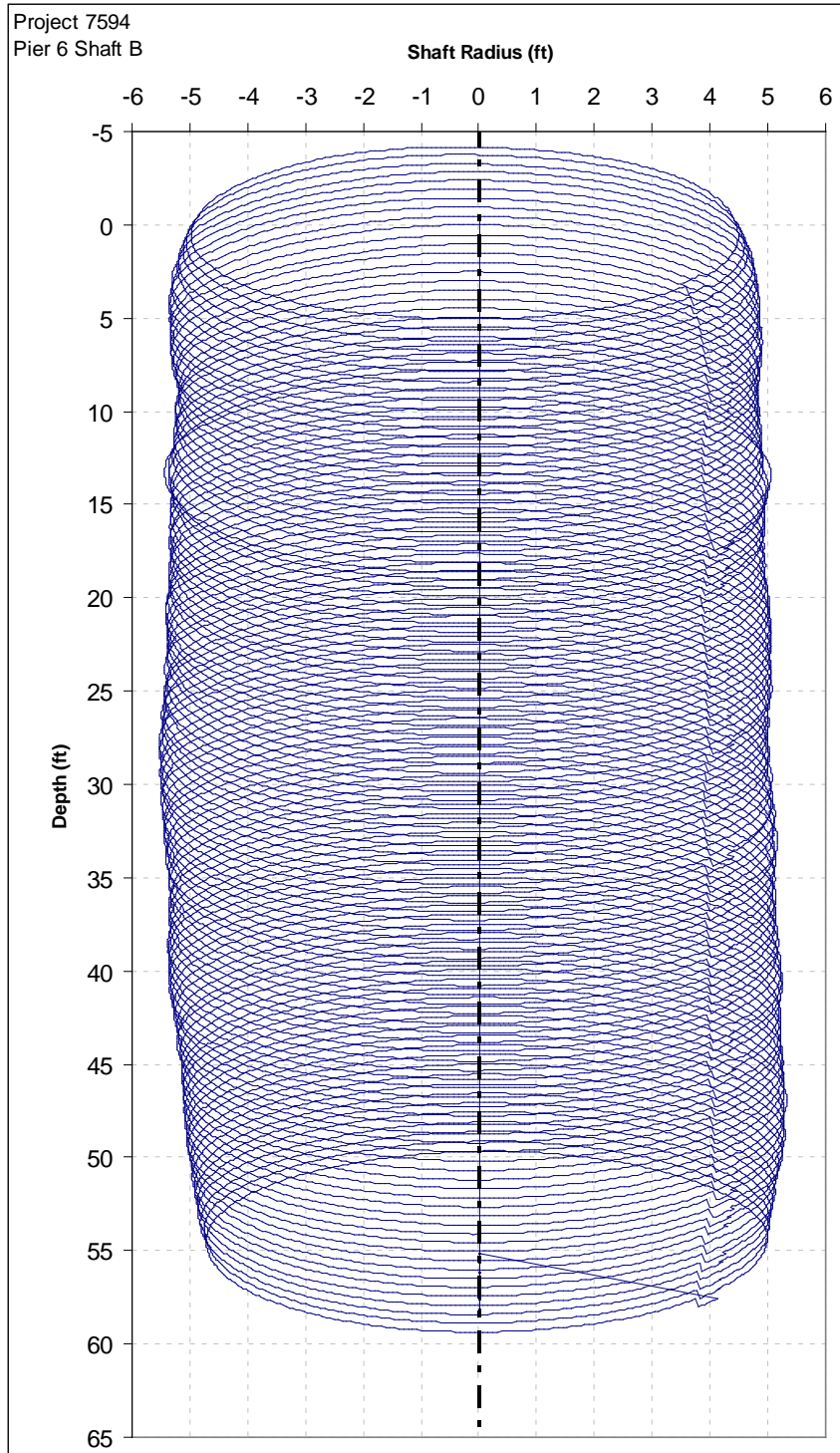


Figure 4-16 3-D rendering from tube spacings and effective radius calculations (Nalley Valley Pier 6 Shaft B).

#### **4.1.4 Thermal Testing Pier 6 Shaft C**

The testing was performed on July 29, 2009 approximately 141 hours after concreting Shaft C. Field measurements were taken from each of the ten tubes and are presented in Figure 4-17. A model was run based on theoretical shaft dimensions (10 ft diameter) and compared to the field measurements (Figure 4-18). The average field temperature is either in line with or greater than the model indicating an effective shaft diameter of 10ft or greater. Figure 4-19 shows the average measured temperature versus the concrete placement log. The effective radius (Figure 4-20) is predicted without axial heat dissipation corrections. Figure 4-21 shows a 3-D rendered image of the as-built shaft.

#### **4.1.5 Project 7594 Conclusions**

Based on the thermal integrity test results presented herein, the following conclusions can be drawn concerning Project 7594, Pier 6:

##### *Shaft A*

- The average field temperature is either in line with or greater than the model indicating an effective shaft diameter of 10ft or greater to an approximate elevation of 213ft.
- From an approximate elevation of 213ft to the bottom of shaft, a reduce effective diameter was measured. This is likely from the use of a smaller diameter (9ft) cleanout bucket within the last 4ft of shaft excavation.
- The reinforcement cage alignment varies (up to approximately 2 inches) throughout the length of the shaft.

##### *Shaft B*

- The average field temperature is either in line with or greater than the model indicating an effective shaft diameter of 10ft or greater throughout.
- The reinforcement cage alignment varies (up to approximately 2 inches) throughout the length of the shaft.

##### *Shaft C*

- The average field temperature is either in line with or greater than the model indicating an effective shaft diameter of 10ft or greater throughout.
- The reinforcement cage alignment varies (up to approximately 2 inches) throughout the length of the shaft.

Project 7594  
Pier 6 Shaft C

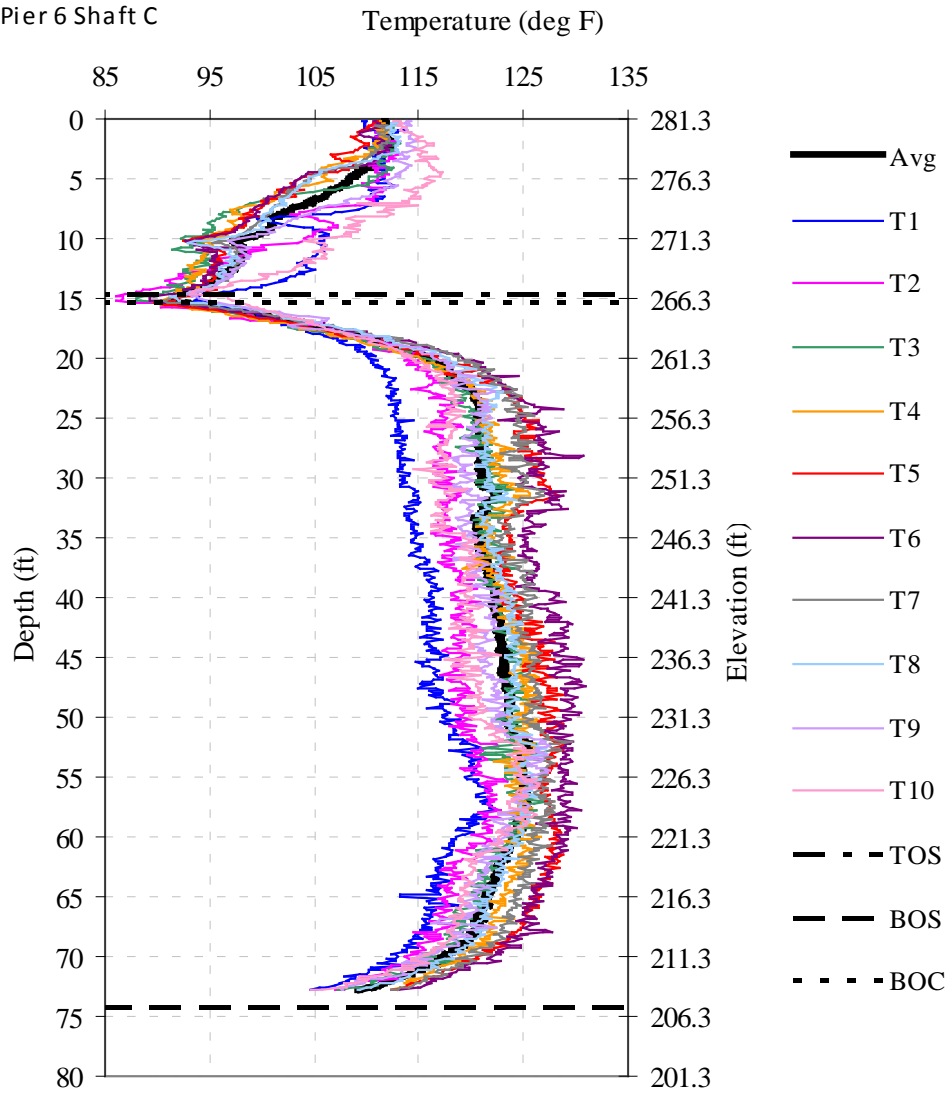


Figure 4-17 Measured tube temperatures versus depth (Nalley Valley Pier 6 Shaft C).

Project 7594  
 Pier 6 Shaft C

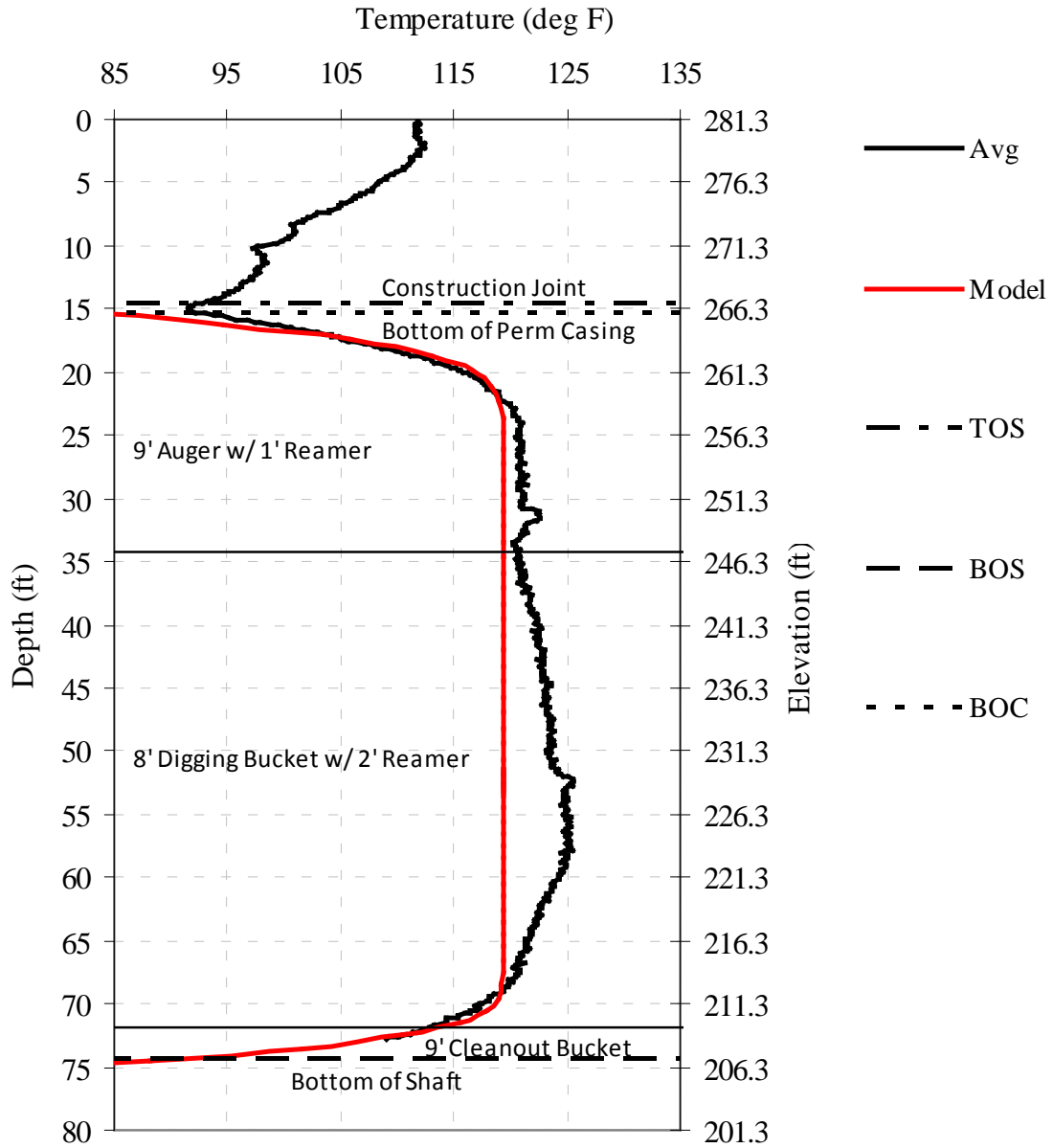


Figure 4-18 Measured and modeled temperature versus depth (Nalley Valley Pier 6 Shaft C).

Project 7594  
 Pier 6 Shaft C

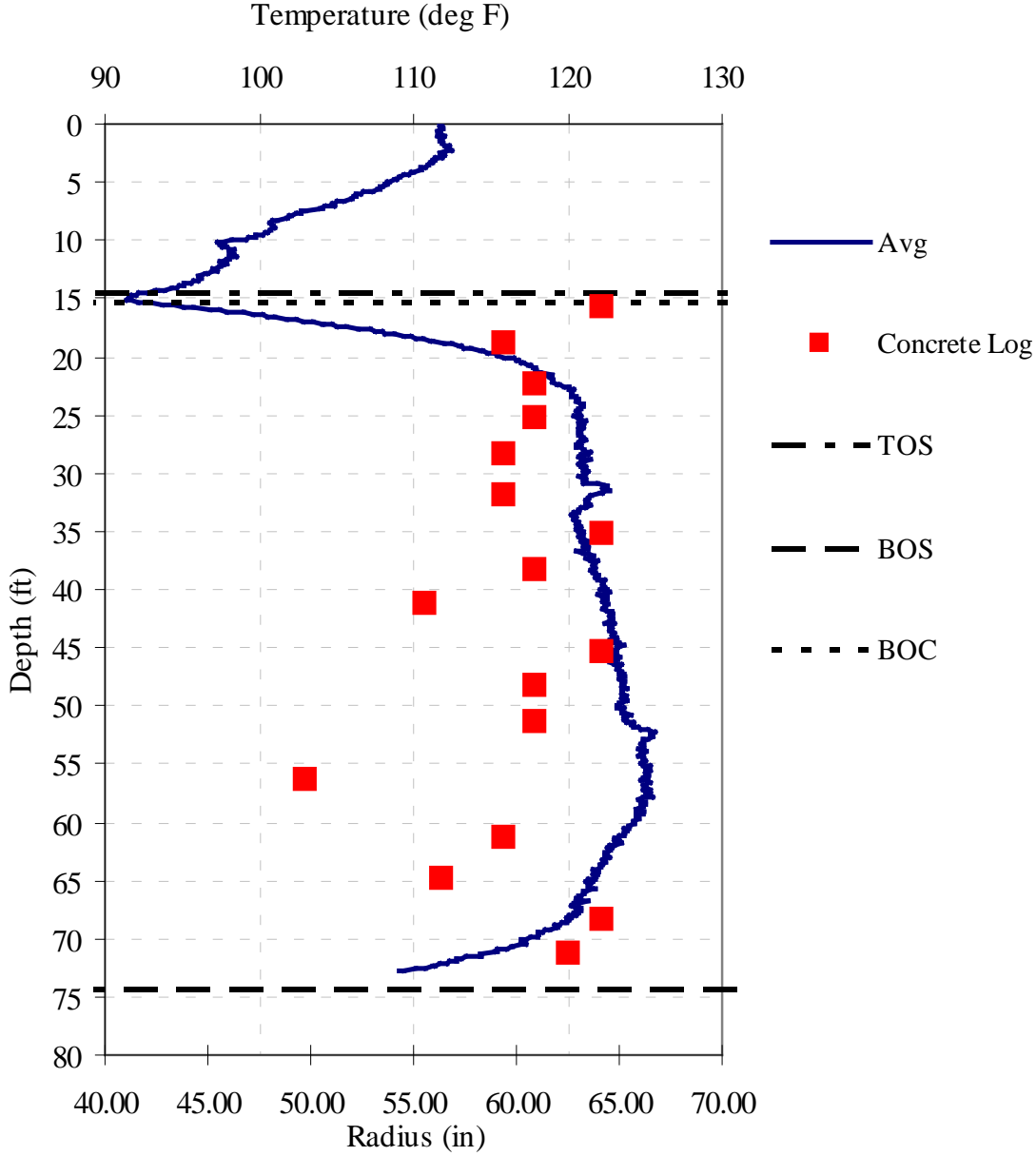


Figure 4-19 Concrete Placement Log versus average measured temperature (Nalley Valley Pier 6 Shaft C).



Project 7594  
 Pier 6 Shaft C

Effective Shaft Radius (in)

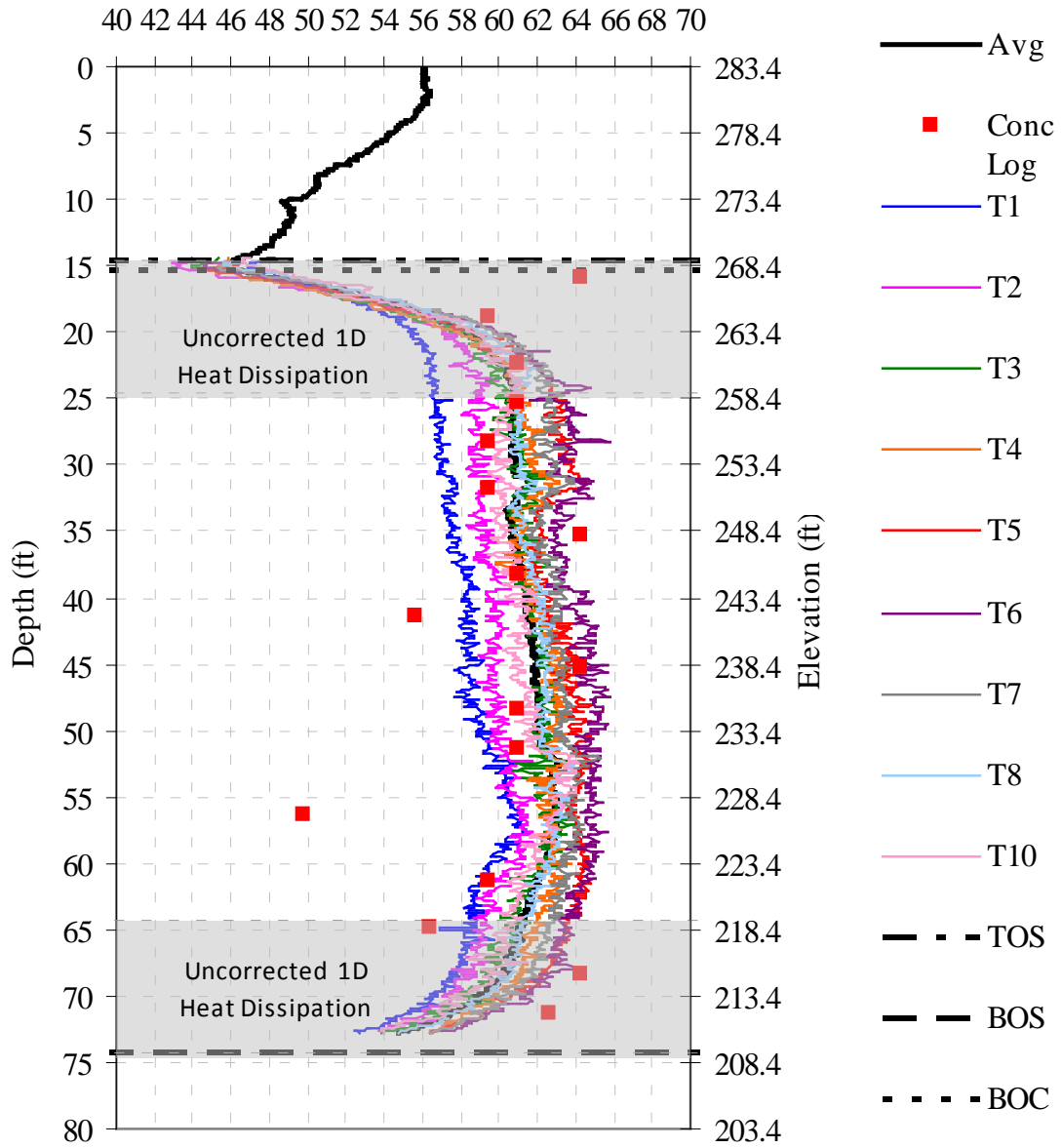


Figure 4-20 Effective shaft radius showing cage alignment uncorrected for axial heat dissipation (Nalley Valley Pier 6 Shaft C).

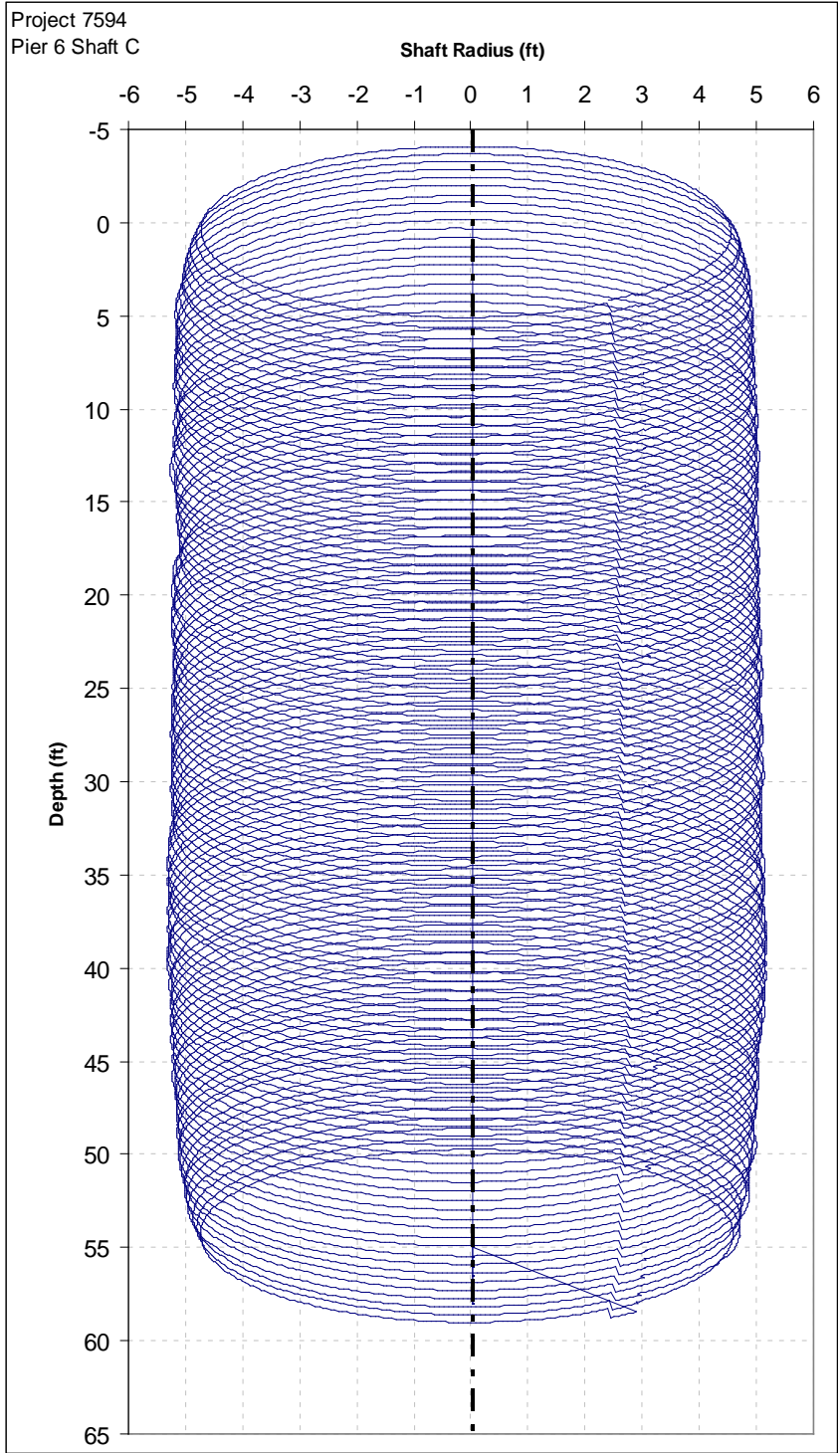


Figure 4-21 3-D rendering from tube spacings and effective radius calculations (Nalley Valley Pier 6 Shaft C).

## **4.2 Project 7465: Scatter Creek**

Thermal testing was conducted on the shafts at Bridge 5-305 Pier 1 for the Scatter Creek bridge replacement project. This pier is comprised of six - 4 foot diameter drilled shafts approximately 40 feet long. The shafts were equipped with 4 access tubes in general accordance with standard practice for tube plurality in State specifications. The tube identification / numbering used for this project assumed the northerly most tube to be No. 1 and increased in value in a clockwise fashion looking down on to the shaft top. Standard infrared thermal testing was conducted on the shafts A and B within Pier 1. Standard testing protocols were followed to verify reproducibility of each scan.

### **4.2.1 Thermal Modeling**

Thermal modeling was conducted based on the concrete mix design (Figures 4-22 through 4-25). The mix design information was used to create the input hydration energy parameters using the **a**, **b**, and **t** method outlined by Schindler (2005). The model parameters used in the T3DModel software were 0.751, 0.611, and 17.194, respectively with an overall energy production of 76.42 kJ per kg of total concrete.

### **4.2.2 Thermal Testing Pier 1 Shaft A**

The testing was performed on August 4, 2009 approximately 50 hours after concreting Shaft A. Field measurements were taken from each of the four tubes and are presented in Figure 4-26. A model was run based on theoretical shaft dimensions (4 ft diameter) and compared to the field measurements (Figure 4-27). The average field temperature is either in line with or greater than the model indicating an effective shaft diameter of 4ft or greater.

Construction logs were not received. As a result, no further analysis could be performed on the thermal data.

### **4.2.3 Thermal Testing Pier 1 Shaft B**

The testing was performed on August 4, 2009 approximately 52 hours after concreting Shaft B. Field measurements were taken from each of the four tubes and are presented in Figure 4-28. A model was run based on theoretical shaft dimensions (4 ft diameter) and compared to the field measurements (Figure 4-29). The average field temperature is either in line with or greater than the model indicating an effective shaft diameter of 4ft or greater.

Construction logs were not received. As a result, no further analysis could be performed on the thermal data.

#### **4.2.4 Project 7465 Conclusions**

Based on the thermal integrity test results presented herein, the following conclusions can be drawn concerning Project 7465, Pier 1:

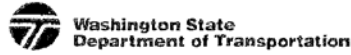
##### *Shaft A*

- The average field temperature is either in line with or greater than the model indicating an effective shaft diameter of 4ft or greater throughout.
- The reinforcement cage alignment is well centered throughout the length of the shaft.

##### *Shaft B*

- The average field temperature is either in line with or greater than the model indicating an effective shaft diameter of 4ft or greater throughout.
- The reinforcement cage alignment varies slightly throughout the length of the shaft.

CMD 17  
BI 85



Concrete Mix Design

Contractor <b>INLAND Structures FOUNDATION &amp; SPECIALTIES</b>	Submitted By <b>KEVIN SLATER</b>	Date <b>7/21/2008</b>
Concrete Supplier <b>Glacier Northwest, Inc.</b>	Plant Location <b>Chehalis</b>	
Contract Number <b>7465</b>	Contract Name <b>Grand Mound to Maytown</b>	

This mix is to be used in the following Bid Item No(s): 85.01, 85.02, 85.03, 85.04, 85.05, 85.06 & 85.07

Concrete Class: (check one only)

3000     4000     4000D<sup>a</sup>     4000P<sup>a</sup>     4000W     Concrete Overlay     Cement Concrete Pavement<sup>d</sup>

Other \_\_\_\_\_

Remarks: MAX SLUMP = 9"  
Mix may be retarded more than 8 hours. Please allow cylinder 48 hours prior to transportation.

Mix Design No. 1882 Plant No. 277

Cementitious Materials	Source	Type, Class, or Grade	Sp. Gr.	Lbs/cy
Cement	Lafarge Seattle	Type I-II	3.15	610
Fly Ash <sup>a</sup>	HEADWATERS	SEE PLANT CERT	2.20	110
GGBFS				
Latex				
Microsilica	---			

Concrete Admixtures	Manufacturer	Product	Type	Est. Range (oz/cy)
Air Entrainment	---	---		
Water Reducer	W.R. Grace	WRDA 64	D-WRA & RET	5 - 50
High-Range Water Reducer	W.R. Grace	ADVA 190	F-HRWR (min 12%)	5 - 150
Set Retarder	W.R. Grace	Recover	S-Retarder	0 - 50
Other	---			

Water (Maximum) 267 (lbs/cy) Is any of the water Recycled or Reclaimed? Yes<sup>a</sup>  No

Water/Cementitious Ratio (Maximum) 0.37 Mix Design Density: 150 lbs/cf<sup>d</sup>

Design Performance	1	2	3	4	5	Average <sup>f</sup>
28 Day Compressive Strength (cylinders) psi	8125	9485	9325	8245	8800	8,796
14 Day Flexural <sup>d</sup> Strength (beams) psi						

Agency use only: Check appropriate box

This mix design Meets Contract Specifications and may be used on the bid items noted above

This mix design Does Not Meet Contract Specifications and is being returned for corrections

Reviewed By: [Signature] (PE Signature) 8/18/08 (Date)

Distribution: Original - Contractor  
Copies To - State Materials Lab-General Materials Eng ; Regional Materials Lab; Project Inspector

DOT Form 350-040 EF  
Revised 5/2003

⇒ MILL CERT/ANALYSIS REPORT # S-1-08-05

Figure 4-22 Scatter Creek concrete mix design page 1.

**Combined Gradation Chart**

Concrete Aggregates	Component 1	Component 2	Component 3	Component 4	Component 5	Combined Gradation
WSDOT Pit No.	L-231	B-335	-	-	-	
WSDOT ASR 14-Day Results (%) <sup>b</sup>						
Grading <sup>c</sup>	WSDOT Class 2 BLD SAND	AASHTO #8 .AGG 3/8	-	-	-	
Percent of Total Aggregate	40	60	-	-	-	100%
Specific Gravity	2.62	2.68	-	-	-	
Lbs/cy (ssd)	1225	1850				

**Percent Passing**

	Component 1	Component 2	Component 3	Component 4	Component 5	Combined
2 inch	100.0	100.0	-	-	-	100.0
1-1/2 inch	100.0	100.0	-	-	-	100.0
1 inch	100.0	100.0	-	-	-	100.0
3/4 inch	100.0	100.0	-	-	-	100.0
1/2 inch	100.0	100.0	-	-	-	100.0
3/8 inch	100.0	92.0	-	-	-	95.2
No. 4	98.0	19.8	-	-	-	51.0
No. 8	90.0	0.9	-	-	-	36.4
No. 16	75.0	0.7	-	-	-	30.3
No. 30	47.0	0.5	-	-	-	19.0
No. 50	13.0	0.5	-	-	-	5.5
No. 100	3.0	0.5	-	-	-	1.5
No. 200	1.0	0.5	-	-	-	0.7

Fineness Modulus: 2.74 (Required for Class 2 Sand)

ASR Mitigation Method Proposed<sup>d</sup> Minimum 15% Headwaters Centralia Production Flyash - See C1567 Report

**Notes:**

- <sup>a</sup> Required for Class 4000D and 4000P mixes
- <sup>b</sup> If Alkali Silica Reactivity Mitigation is required per WSDOT ASA Database - Attach evidence that mitigating measure controls expansion in the form of ASTM C 1260 / AASHTO T303, ASTM C 1293 or ASTM C 295 test results
- <sup>c</sup> AASHTO No. 487, 57, 87, 7 & 8; WSDOT Class 1, Class 2, or combined gradation. See Standard Specification 9-03.1
- <sup>d</sup> Required for Cement Concrete Pavements
- <sup>e</sup> Attach test results indicating conformance to Standard Specification 9-25.1

DOT Form 350-040 EF  
Revised 5/2003

Figure 4-23 Scatter Creek concrete mix design page 2.

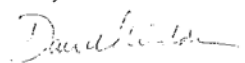


# Cement Test Report

Cement

Mill Test Report Number:	S-I-09-3
YEAR:	2009
MONTH:	March
PLANT:	Seattle
CEMENT TYPE:	ASTM I and II

PHYSICAL DATA		CHEMICAL ANALYSIS		Percent
Fineness by Air Permeability (m <sup>2</sup> /kg; ASTM C204)	402	Silica Dioxide (SiO <sub>2</sub> ; ASTM C114)		20.9
Fineness by 45 µm (No. 325) Sieve (% passing; ASTM C430)	94.4	Ferric Oxide (Fe <sub>2</sub> O <sub>3</sub> ; ASTM C114)		3.2
Compressive Strength (ASTM C109/C109 M)		Aluminum Oxide (Al <sub>2</sub> O <sub>3</sub> ; ASTM C114)		4.6
		Calcium Oxide (CaO; ASTM C114)		64.3
		Sulfur Trioxide (SO <sub>3</sub> ; ASTM C114)		2.8
		Magnesium Oxide (MgO; ASTM C114)		1.3
Time of set, Vicat (Initial minutes; ASTM C191)	107	Loss on Ignition (L.O.I.; ASTM C114)		1.47
Air Content of Mortar (%, ASTM C185)	9	Insoluble Residue (ASTM C114)		0.42
Autoclave Expansion (%, ASTM C151)	-0.001	Alkali Equivalent (NaEQ; ASTM C114)		0.66
Processing Addition: LGA-1 (Percent)	1.7	Free Calcium Oxide, (% f-CaO)		0.5
		C3S (ASTM C150)		60
		C3A (ASTM C150)		7
		C4AF (ASTM C150)		10

Certified by:  
  
 Daniel Waldron  
 Quality Control Laboratory Supervisor

The cement represented by the above analysis is certified to comply with ASTM C150 Type I and II specifications.

Figure 4-24 Scatter Creek Portland cement mill certificate.



MILZ | LA  
~~3028988~~



### Chemical and Physical Analysis of Fly Ash

Developed For: *Headwaters Resources*  
16817 - 155th PI SE  
Renton, WA 98058

Ticket: 8510 Job: 14420 Report Date: 02/05/2009	Plant of Origin: <i>Centralia US</i> Sample ID: <i>Ce-086-08</i> Docket: 3028988 - 3029080	Sample Date Range: 11/25/2008 to: 11/29/2008 Date Received: 12/04/2008
<b>Chemical Composition (%)</b> <small>(by Wyoming Analytical Laboratories, Inc.)</small>		ASTM C 618-08 Specifications
		<b>Class F</b> <b>Class C</b>
Total Silica, Aluminum, Iron:	77.6	70.0 Min      50.0 Min
Silicon Dioxide:	54.6	
Aluminum Oxide:	16.9	
Iron Oxide:	6.0	
Sulfur Trioxide:	0.5	5.0 Max      5.0 Max
Calcium Oxide:	9.8	
Moisture Content:	0.0	3.0 Max      3.0 Max
Loss on Ignition:	0.1	6.0 Max      6.0 Max
		AASHTO M295-06 Specifications
Available Alkalies (as Na <sub>2</sub> O):	1.4	1.5 Max      1.5 Max
Sodium Oxide:	1.06	
Potassium Oxide:	0.56	
<b>Physical Test Results</b>		ASTM C 618-08 Specifications
		<b>Class F</b> <b>Class C</b>
Fineness, Retained on #325 Sieve (%):	18.4	34 Max      34 Max
<b>Strength Activity Index (%)</b>		
Ratio to Control @ 7 Days:	84.5	
Ratio to Control @ 28 Days:	91.3	75 Min      75 Min
Water Requirement, % of Control:	93.4	105 Max      105 Max
Soundness, Autoclave Expansion (%):	0.02	0.8 Max      0.8 Max
Drying Shrinkage, Increase @ 28 Days (%):	0.00	0.03 Max      0.03 Max
Density Mg/m <sup>3</sup> :	2.51	

Comments:

CTL | Thompson Materials Engineers, Inc.

Orville R. Werner II, P.E.



22 Lipan Street | Denver, Colorado 80223 | Telephone: 303-825-0777 Fax: 303-893-1568

This test report relates only to the items tested and shall not be reproduced, except in full, without written approval of CTL Thompson, Inc.

Figure 4-25 Scatter Creek fly ash mill certificate.

Project 7465  
Bridge 5-305  
Pier 1 Shaft A

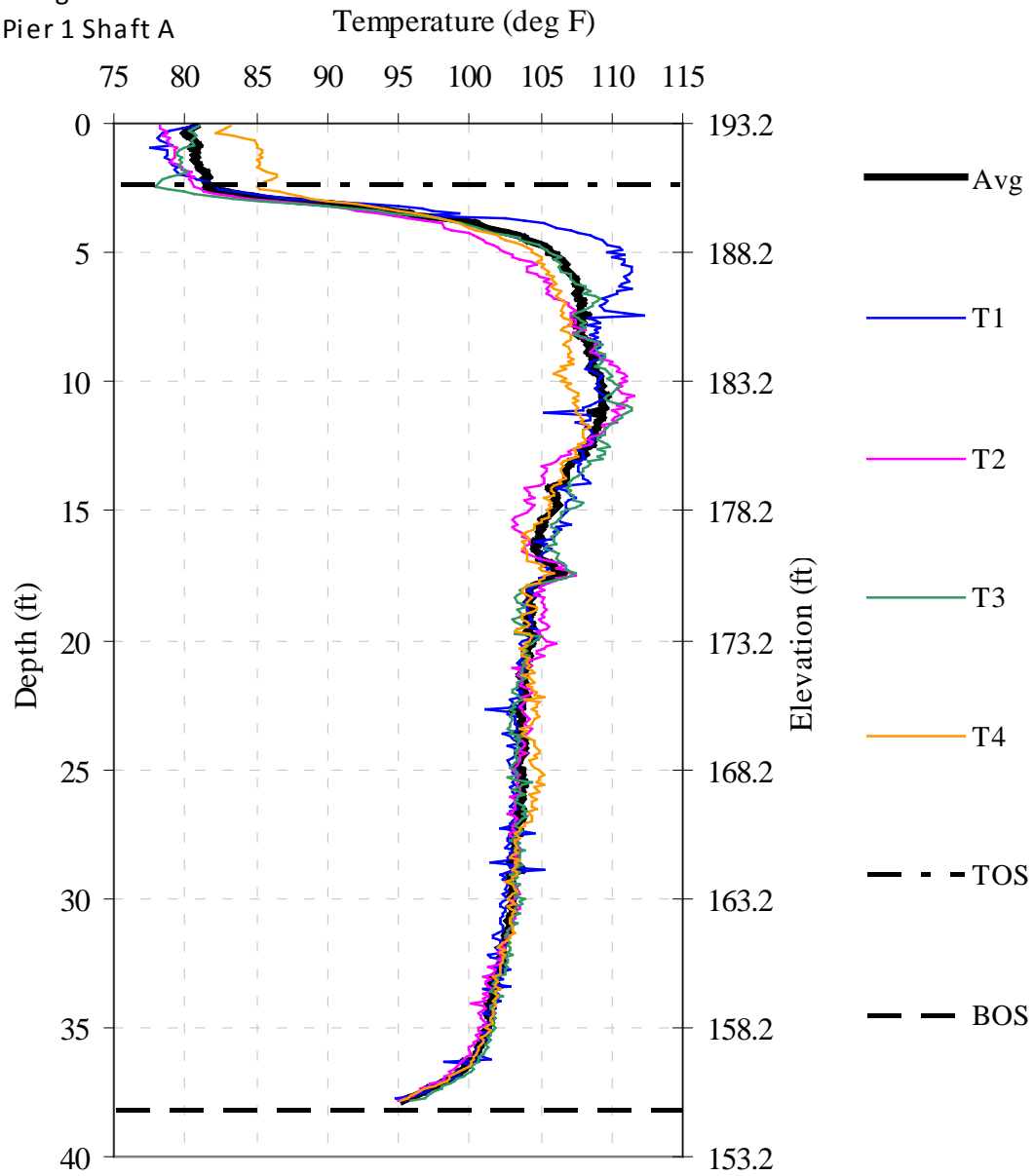


Figure 4-26 Measured tube temperatures versus depth (Scatter Creek Pier 1 Shaft A).

Project 7465  
Bridge 5-305  
Pier 1 Shaft A

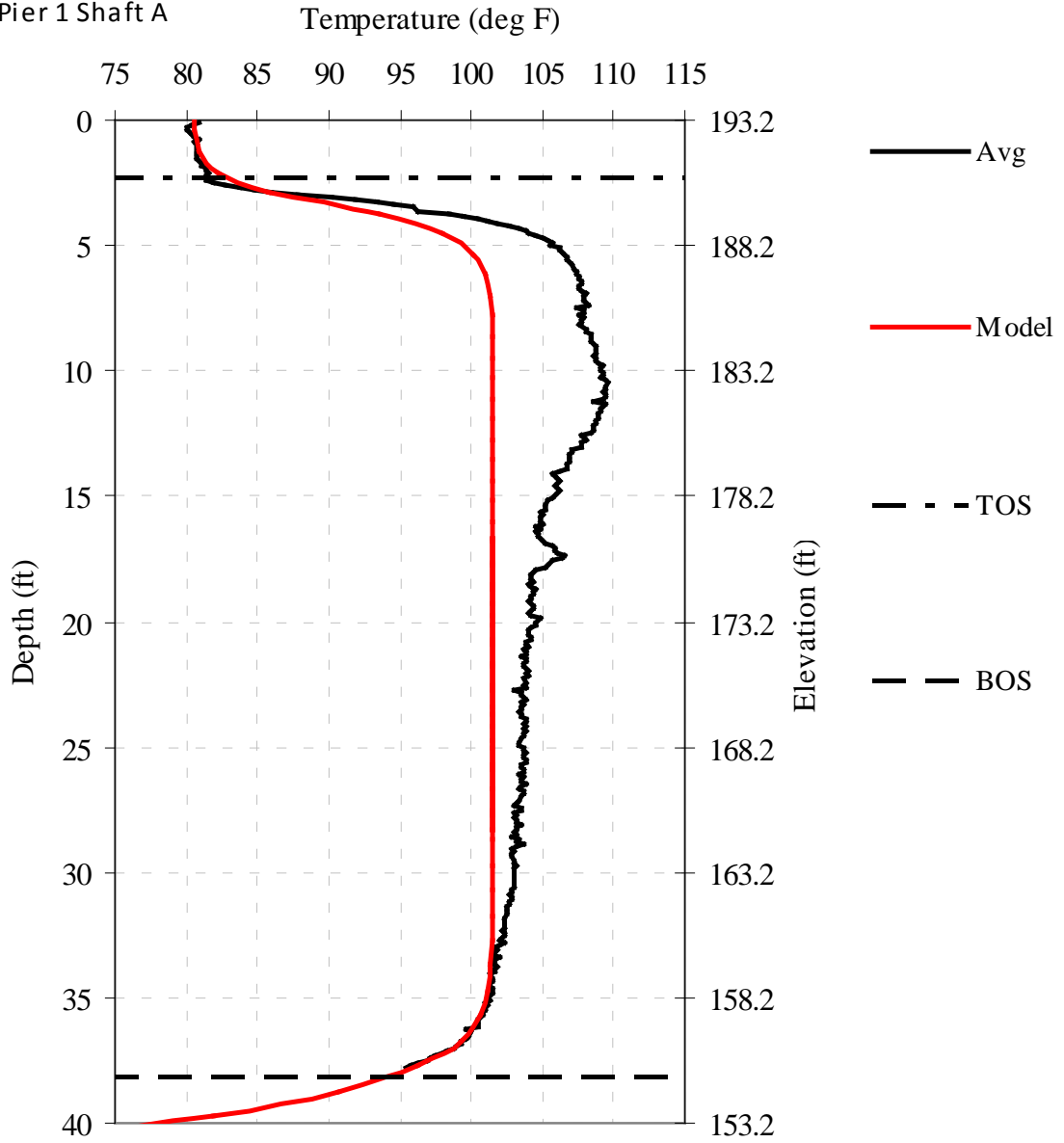


Figure 4-27 Measured and modeled temperature versus depth (Scatter Creek Pier 1 Shaft A).

Project 7465  
Bridge 5-305  
Pier 1 Shaft B

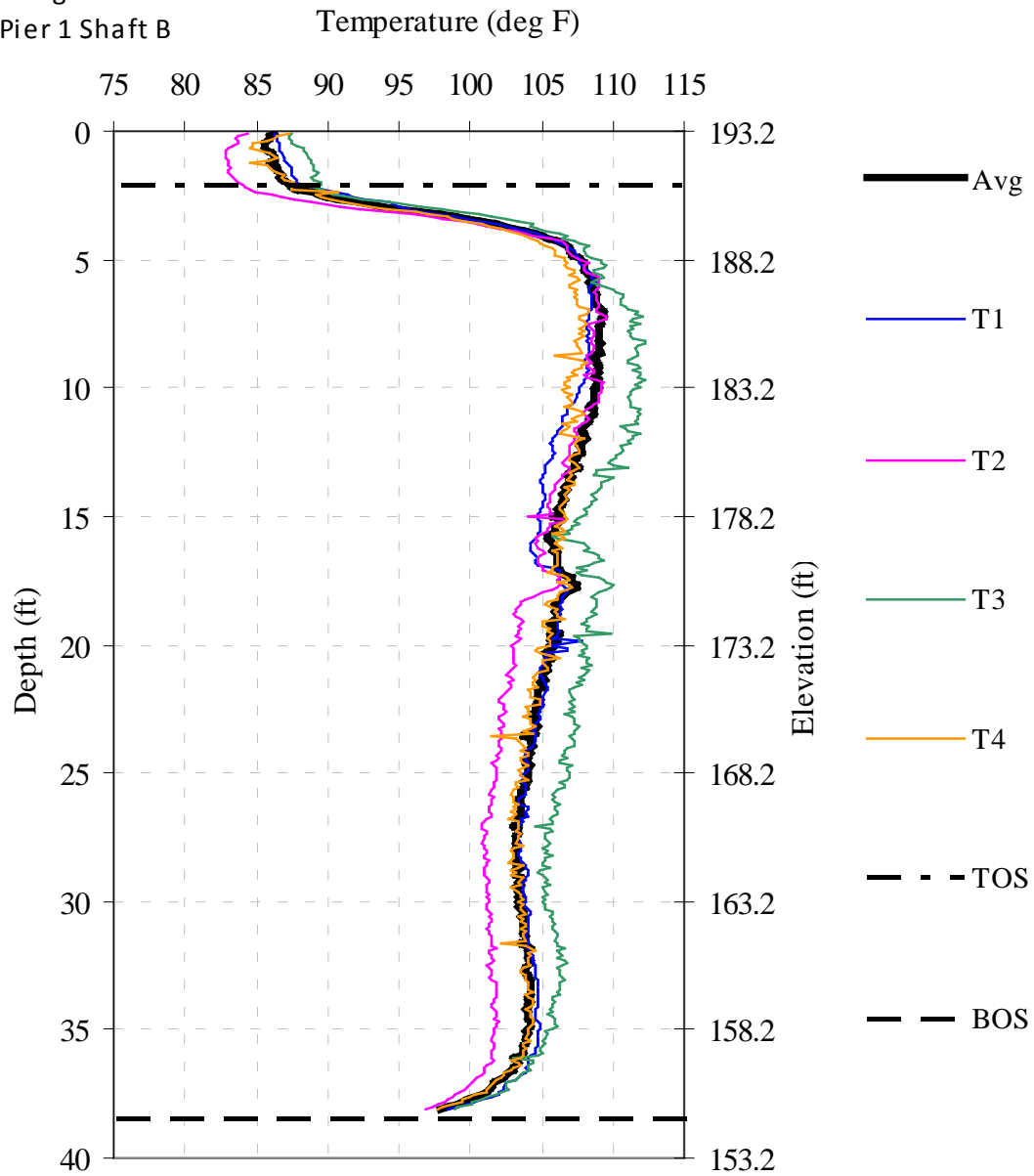


Figure 4-28 Measured tube temperatures versus depth (Scatter Creek Pier 1 Shaft B).

Project 7465  
 Bridge 5-305  
 Pier 1 Shaft B

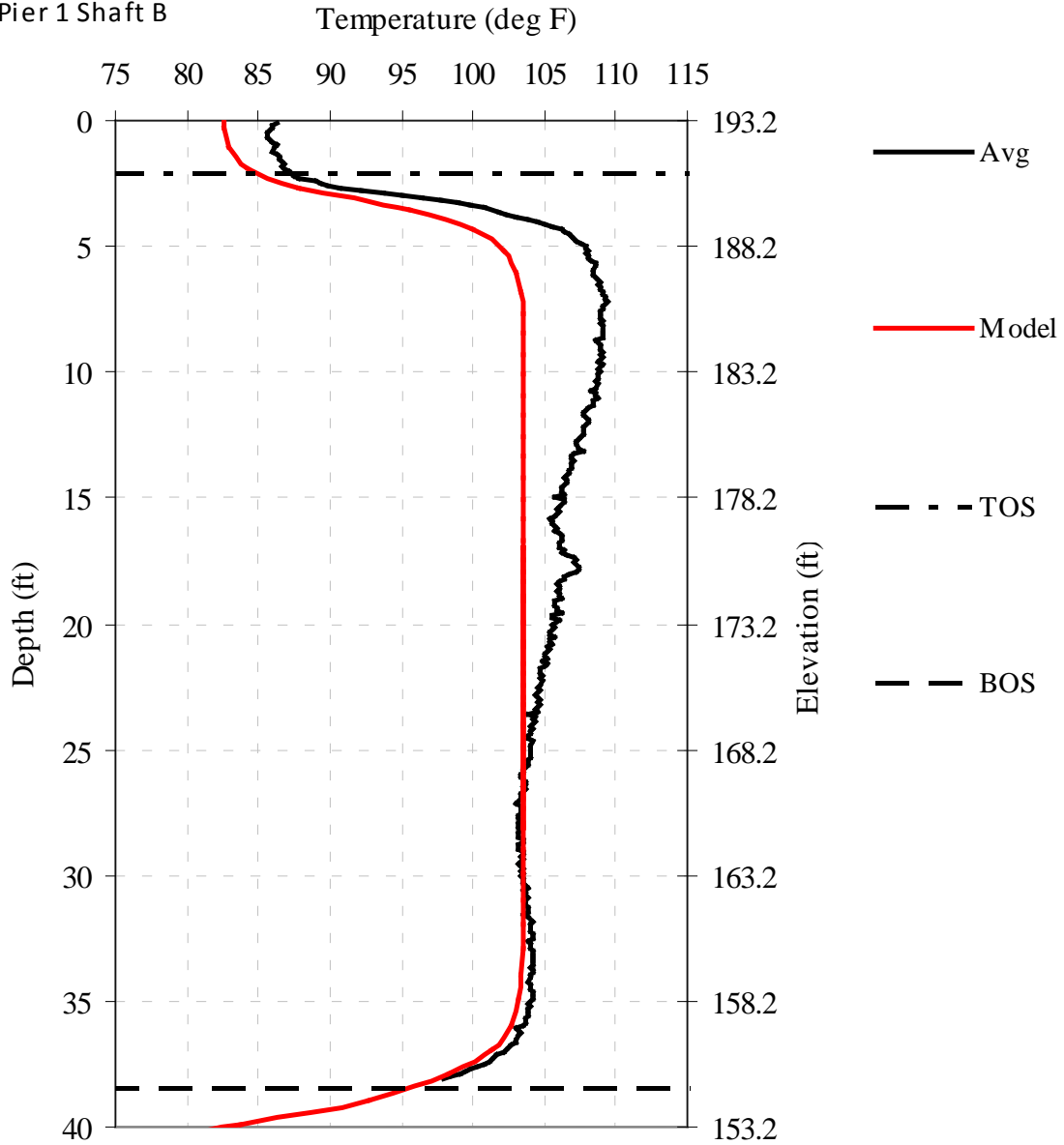


Figure 4-29 Measured and modeled temperature versus depth (Scatter Creek Pier 1 Shaft B).

### **4.3 Project 7743: Tieton River**

Thermal testing was conducted on a shaft at Bridge 12-317 Pier 1 for the Tieton River bridge replacement project. This pier is comprised of a single 8 foot diameter drilled shafts approximately 40 feet long. The shaft was equipped with 8 access tubes in general accordance with standard practice for tube plurality in State specifications. The tube identification / numbering used for this project assumed the northerly most tube to be No. 1 and increased in value in a clockwise fashion looking down on to the shaft top. Standard infrared thermal testing was conducted on Shaft 1 within Pier 1. Standard testing protocols were followed to verify reproducibility of each scan.

#### **4.3.1 Thermal Modeling**

Thermal modeling was conducted based on the concrete mix design (Figures 4-30 through 4-33). The mix design information was used to create the input hydration energy parameters using the **a**, **b**, and **t** method outlined by Schindler (2005). The model parameters used in the T3DModel software were 0.795, 0.605, and 17.519, respectively with an overall energy production of 76.02 kJ per kg of total concrete.

#### **4.3.2 Thermal Testing Pier 1 Shaft 1**

The testing was performed on August 11, 2009 approximately 25 hours after concreting Shaft 1. Field measurements were taken from each of the eight tubes and are presented in Figure 4-34. A model was run based on theoretical shaft dimensions (8 ft diameter) and compared to the field measurements (Figure 4-35). The average field temperature is either in line with or greater than the model suggesting a shaft with a diameter 8ft or greater.

Construction logs were not received. As a result, no further analysis could be performed on the thermal data.

#### **4.3.3 Project 7743 Conclusions**

Based on the thermal integrity test results presented herein, the following conclusions can be drawn concerning Project 7743, Pier 1 Shaft 1:

- The average field temperature is either in line with or greater than the model indicating an effective shaft diameter of 8ft or greater throughout.
- The reinforcement cage alignment varies slightly throughout the length of the shaft.



### Concrete Mix Design

Contractor <u>MALCOLM DRILLING SB Structures CO., INC.</u>		Submitted By Nick Martinez	Date 6/19/2009
Concrete Supplier Central PreMix		Plant Location Yakima Wa.	
Contract Number <u>7743</u>	Contract Name WSDOT US 12 - Tieton River Crossings		

This mix is to be used in the following Bid Item No(s): 38

Concrete Class: (check one only)

- 3000  
  4000  
  4000D<sup>a</sup>  
  4000P<sup>a</sup>  
  4000W  
  Concrete Overlay  
  Cement Concrete Pavement<sup>d</sup>  
 Other

Remarks: 4000 Psi Concrete "P" Shafts

Mix Design No. 320233 Plant No. 24-25

Cementitious Materials	Source	Type, Class or Grade	Sp. Gr.	Lbs/cy
Cement	Lafarge Cement	Type I-II	3.15	600
Fly Ash <sup>a</sup>	Lafarge Cement Co.	Type F	2.2	110
GGBFS (Slag)				
Latex				
Microsilica				

Concrete Admixtures	Manufacturer	Product	Type	Est. Range (oz/cy)
Air Entrainment				
Water Reducer	Grace	Zyla 630	A	20-30
High-Range Water Reducer				
Set Retarder	Basf	100XR	B & D	14-30
Other				

Water (Maximum) 318 lbs/cy Is any of the water Recycled or Reclaimed?  Yes  No<sup>e</sup>

Water Cementitious Ratio (Maximum) .45 Mix Design Density 147.44 lbs/cf<sup>d</sup>

Design Performance	1	2	3	4	5	Average <sup>f</sup>
28 Day Compressive Strength (cylinders) psi	6,580	6,210	5,890	6,300	5,500	6,100
14 Day Flexural <sup>d</sup> Strength (beams) psi						

Agency Use Only (Check appropriate Box)

- This Mix Design MEETS CONTRACT SPECIFICATIONS and may be used on the bid items noted above  
 This Mix Design DOES NOT MEET CONTRACT SPECIFICATIONS and is being returned for corrections

Reviewed By: [Signature]

PE Signature

7/22/09  
Date

DOT Form 359-040 EF  
Revised 6/06

Distribution: Original - Contractor  
Copies To - State Materials Lab-Structural Materials Eng.; Regional Materials Lab; Project Inspector

7/23/09  
Robert, Kurt, Andy

ROM ENTRY DATE 7/23/09  
ENTERED BY HB

010-005

Figure 4-30 Tieton River concrete mix design page 1.

Mix Design No. 320233 Plant No. 24-25

**Aggregate Information**

Concrete Aggregates	Component 1	Component 2	Component 3	Component 4	Component 5	Combined Gradation
WSDOT Pit No.	E-158	E-158				
WSDOT ASR 14-day Results (%) <sup>b</sup>	<input checked="" type="checkbox"/> Yes <input type="checkbox"/> No	<input checked="" type="checkbox"/> Yes <input type="checkbox"/> No	<input type="checkbox"/> Yes <input type="checkbox"/> No	<input type="checkbox"/> Yes <input type="checkbox"/> No	<input type="checkbox"/> Yes <input type="checkbox"/> No	
Grading <sup>c</sup>	Class 2 Sand	No. 8 Pea Gravel				
Percent of Total Aggregate	47%	53%				100%
Specific Gravity	2.65	2.69				
Lbs/cy (ssd)	1392	1571				

**Percent Passing**

Size	Component 1	Component 2	Component 3	Component 4	Component 5	Combined
2 inch						
1-1/2 inch						
1 inch						
3/4 inch						
1/2 inch	100	99.8				100 <sup>f</sup>
3/8 inch	100	87.5				93
No. 4	99.8	5.2				50
No. 8	83.8	.3				40
No. 16	65.2	.2				31
No. 30	50.7					24
No. 50	20.8					10
No. 100	3.6					2
No. 200	.7	.2				.4

Fineness Modulus: 2.76 (Required for Class 2 Sand)

ASR Mitigation Method Proposed <sup>b</sup>: 15% Type F ash

**Notes:**

- a Required for Class 4000D and 4000P mixes.
- b Alkali Silica Reactivity Mitigation is required for sources with expansions over 0.20% - Incidate method for ASR mitigation. For expansion of 0.21% - 0.45%, acceptable mitigation can be the use of low alkali cement or 25% type F fly ash. Any other proposed mitigation method or for pits with greater than 0.45% expansion, proof of mitigating measure, either ASTM C1260 / AASHTO T303 test results must be attached. If ASTM C 1293 testing has been submitted indicating 1-year expansion of 0.04% or less, mitigation is not required.
- c AASHTO No. 467, 57, 67, 7, 8; WSDOT Class 1, Class 2; or combined gradation. See Standard Specification 9-03.1.
- d Required for Cement Concrete Pavements.
- e Attach test results indicating conformance to Standard Specification 9-25.1.
- f Actual Average Strength as determined from testing or estimated from ACI 211.

*Meets Sec. 9-03.1(c) 3/8" Nominal*

WSDOT  
JUL 14 2009  
454301

DOT Form 350-040 EF  
Revised 6/06

Figure 4-31 Tieton River concrete mix design page 2.



C7743  
 B1 38  
 8/10/09  
 82 CY DELIVERED  
 80 CY USED



## Cement Test Report

Cement

Mill Test Report Number:	S-I-09-4
YEAR:	2009
MONTH:	April
PLANT:	Seattle
CEMENT TYPE:	ASTM I and II

PHYSICAL DATA		CHEMICAL ANALYSIS		Percent	
Fineness by Air Permeability (m <sup>2</sup> /kg; ASTM C204)	401	Silica Dioxide (SiO <sub>2</sub> ; ASTM C114)		21.5	
Fineness by 45 μm (No. 325) Sieve (% passing; ASTM C430)	95	Ferric Oxide (Fe <sub>2</sub> O <sub>3</sub> ; ASTM C114)		3.2	
Compressive Strength (ASTM C109/C109 M)		Aluminum Oxide (Al <sub>2</sub> O <sub>3</sub> ; ASTM C114)		4.5	
		Calcium Oxide (CaO; ASTM C114)		65.1	
	3-day	Mpa	psi	Sulfur Trioxide (SO <sub>3</sub> ; ASTM C114)	2.8
	7-day	27.3	3,959	Magnesium Oxide (MgO; ASTM C114)	1.1
28-day (previous month)	34.8	5,046	Loss on Ignition (L.O.I.; ASTM C114)	1.4	
Time of set, Vicat (Initial minutes; ASTM C191)	111	Insoluble Residue (ASTM C114)		0.42	
Air Content of Mortar (%, ASTM C185)	9.4	Alkali Equivalent (NaEQ; ASTM C114)		0.62	
Autoclave Expansion (%, ASTM C151)	-0.0002	Free Calcium Oxide, (% f-CaO)		0.5	
Processing Addition: LGA-1 (Percent)	1.8	C3S (ASTM C150)		59	
		C3A (ASTM C150)		7	
		C4AF (ASTM C150)		10	

Certified by:

Daniel Waldron  
 Quality Control Laboratory Supervisor

The cement represented by the above analysis is certified to comply with ASTM C150 Type I and II specifications.

Figure 4-32 Tieton River Portland cement mill certificate.



**Cement**

**FLY ASH TEST REPORT**

Analysis by: Lafarge Edmonton Lab  
 Sample from : Sundance Power Plant, **Classified**  
 Average Analysis: 01-Apr-09 to 30-Apr-09

**Chemical Analysis**

Silicon Dioxide (SiO <sub>2</sub> )	56.5 %
Aluminum Oxide (Al <sub>2</sub> O <sub>3</sub> )	22.9 %
Iron Oxide (Fe <sub>2</sub> O <sub>3</sub> )	3.5 %
Total (SiO <sub>2</sub> ) + (Al <sub>2</sub> O <sub>3</sub> ) + (Fe <sub>2</sub> O <sub>3</sub> )	82.8 %
Sulphur Trioxide (SO <sub>3</sub> )	0.2 %
Calcium Oxide (CaO)	10.5 %
Magnesium Oxide	1.1 %
Moisture Content	0.05 %
Loss on Ignition	0.31 %
Available Alkali as Equiv. Na <sub>2</sub> O (previous month's result)	0.9 % ✓ x4

**Physical Analysis**

Fineness Retained on No. 325 Sieve (45 µm)	12.4 %
Strength Activity Index with Portland Cement	
% of Control at 7 Days	87 %
% of Control at 28 Days (previous month's result)	98 %
Water Requirement, Percent of Control	94.8 %
Autoclave Expansion	0.07 %
Density	2.02 Mg/m <sup>3</sup>

**Uniformity Requirements**

Density, Variation from Average	0.40 %
Fineness No. 325 Sieve, Variation from Average	-4.40 %

We hereby certify the fly ash represented by the above chemical and physical analysis meets the requirements of ASTM C618-04 for Class F Fly Ash.

Certified : 

Israel Ginez  
 Laboratory Manager - Edmonton

**WSDOT**  
**JUL 10 2009**  
**454301**

CEMENT GROUP / ALBERTA SALES  
 12420 17th St. N. E., Edmonton, AB T6S 1A8  
 Telephone: (780) 472-5933 Fax: (780) 472-6648 Toll Free: 1-800-661-1522

Figure 4-33 Tieton River fly ash mill certificate.

Project 7743  
 Bridge 12-317  
 Pier 1 Shaft 1

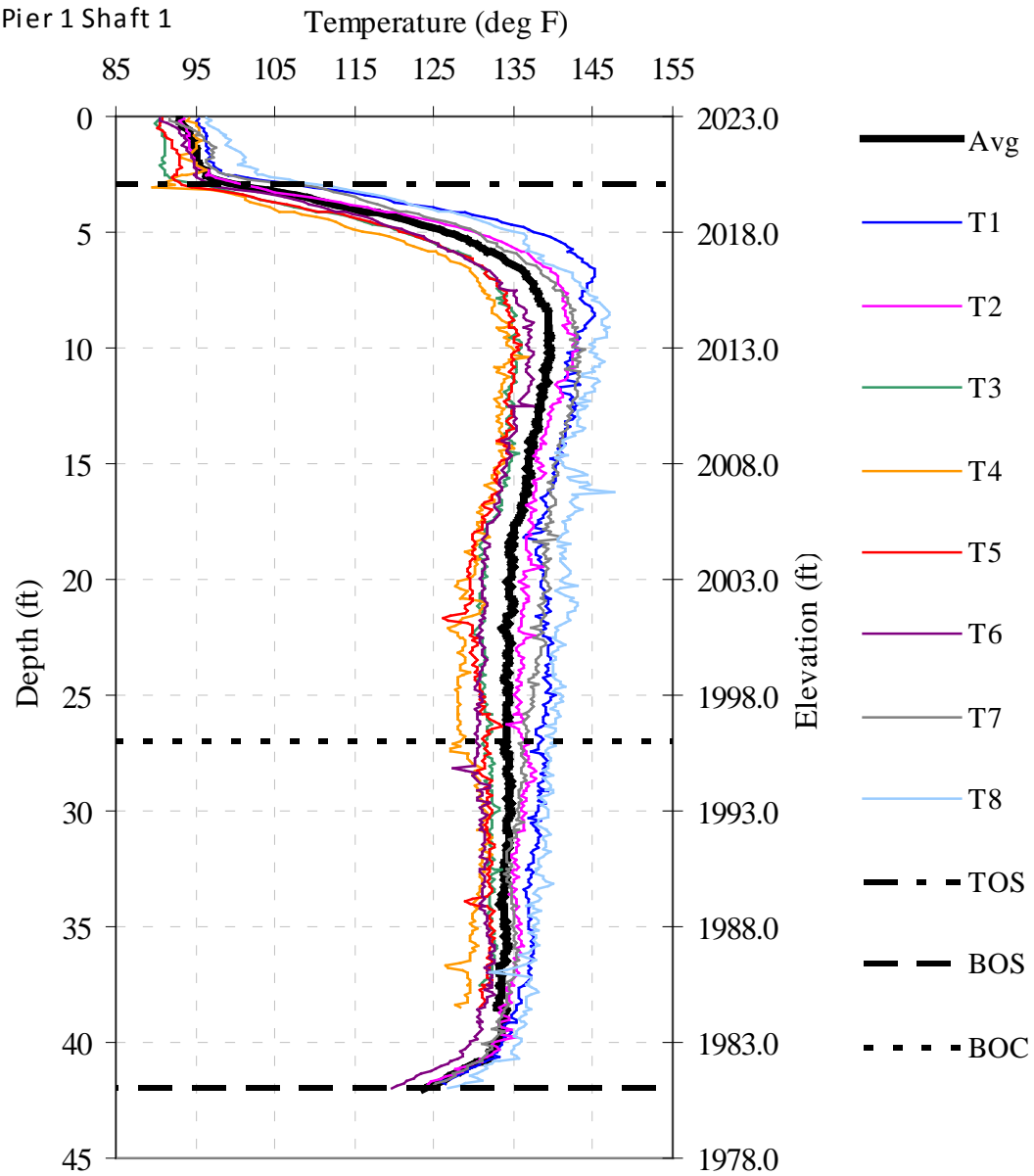


Figure 4-34 Measured tube temperatures versus depth (Tieton River Pier 1 Shaft 1).

Project 7743  
 Bridge 12-317  
 Pier 1 Shaft 1

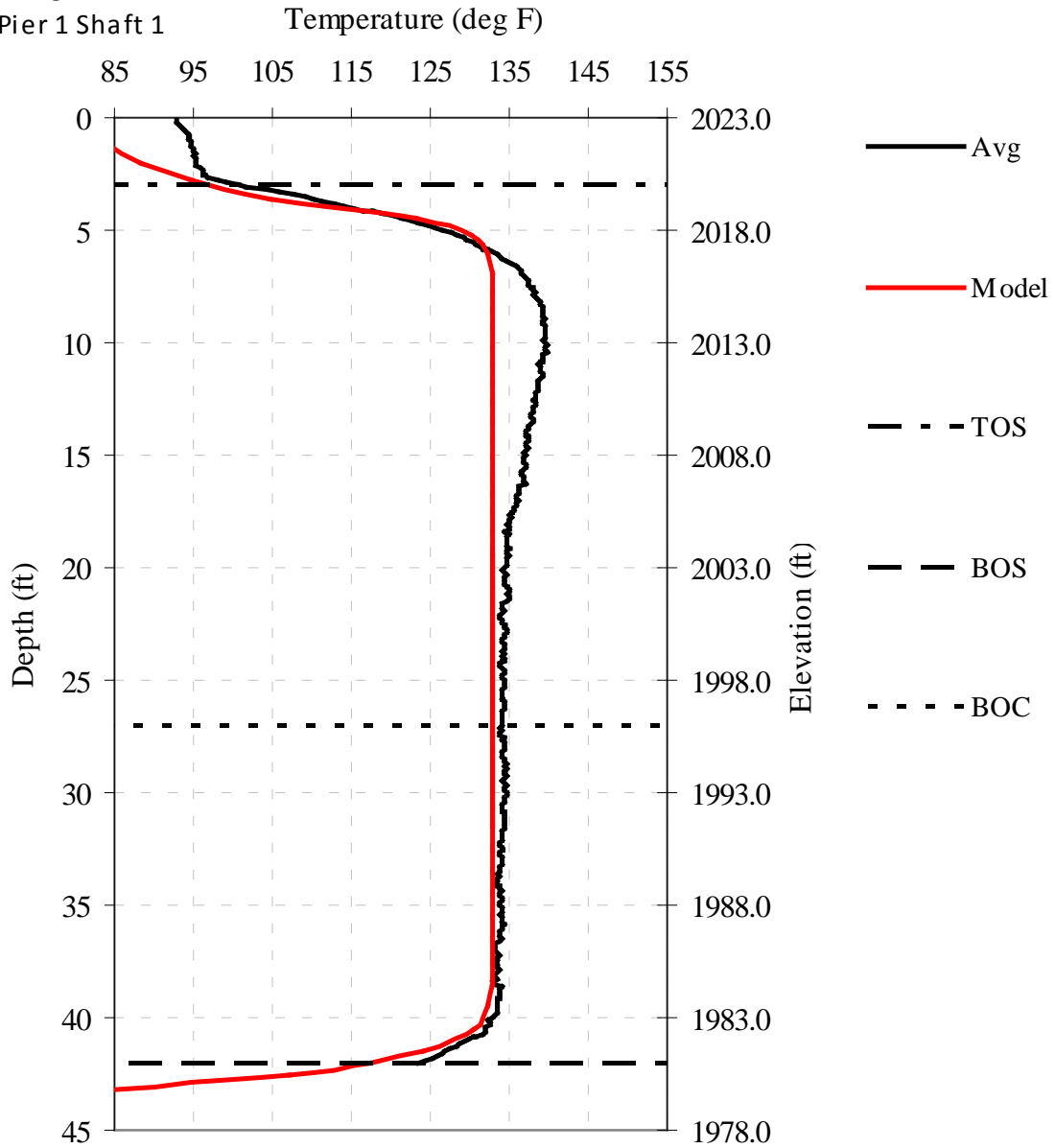


Figure 4-35 Measured and modeled temperature versus depth (Tieton River Pier 1 Shaft 1).

#### **4.4 Project 7777L: US 395 Wandermere Vicinity**

Thermal testing was conducted on a shaft at Pier 4 for the US 395 construction from US 2 to Wandermere Vicinity project. This pier is comprised of two - 10 foot diameter drilled shafts approximately 130 feet long. The shafts were equipped with 10 access tubes in general accordance with standard practice for tube plurality in State specifications. The tube identification / numbering used for this project assumed the northerly most tube to be No. 1 and increased in value in a clockwise fashion looking down on to the shaft top. Standard infrared thermal testing was conducted on the left shaft within Pier 4. Standard testing protocols were followed to verify reproducibility of each scan.

##### **4.4.1 Thermal Modeling**

Thermal modeling was conducted based on the concrete mix design (Figures 4-36 through 4-39). The mix design information was used to create the input hydration energy parameters using the **a**, **b**, and **t** method outlined by Schindler (2005). The model parameters used in the T3DModel software were 0.806, 0.552, and 21.057, respectively with an overall energy production of 72.81 kJ per kg of total concrete mass.

##### **4.4.2 Thermal Testing Pier 4 Shaft Left**

The testing was performed on January 13, 2010 approximately 383 hours after concreting Shaft L. Field measurements were taken from each of the ten tubes and are presented in Figure 4-40. The shaft was constructed to a length of 132ft; however, field measurements were only taken to a depth of approximately 90ft. The plans show the shaft to be a step shaft from 10ft diameter down to a 6ft diameter rock socket. It is likely that the reinforcement cage design limited the access of the rock socket.

A model was run based on theoretical shaft dimensions (10 ft diameter) and compared to the field measurements (Figure 4-41). The average field temperature is either in line with or greater than the model indicating an effective shaft diameter of 10ft or greater for the tested shaft length. Figure 4-42 shows the average measured temperature versus the concrete placement log. The effective radius (Figure 4-43) is predicted without axial heat dissipation corrections. Figure 4-44 shows a 3-D rendered image of the as-built shaft.

##### **4.4.3 Project 7777L Conclusions**

Based on the thermal integrity test results presented herein, the following conclusions can be drawn concerning Project 7777L, Pier 4 Shaft Left:

- Utilizing the HSC, the recommended testing times ranged from 21 to 240 hours after concreting. In this case, thermal testing was performed outside this window approximately 383 hours after concreting. Without previous knowledge of the internal shaft temperature generation, this is not

recommended. However, a better understanding of the temperature generation can be obtained through either pre-test modeling or a pilot study performed early-on in a given project. Such a study was performed for the Nalley Valley project (Figure 4-12) whereby embedded temperature sensors were installed and monitored for an extended period of time after concreting. Pilot programs provide a realistic time frame for testing shafts of similar sizes with the same mix design as well as confirm the model validity for predicting internal temperatures of all shaft sizes and various times of testing. The new extension of thermal testing capabilities using embedded thermal wires (discussed in Section 5.5) is one way of both performing a pilot program while also obtaining sufficient data to assess the shaft integrity. The criterion for acceptable testing times is established such that a sufficient gradient exists between those materials that generate heat and those that do not. In the Washington State area, average soil temperatures are near 50F. So, even at the nominal 110F observed concrete temperatures a considerable gradient still existed.

- The average field temperature is either in line with or greater than the model indicating an effective shaft diameter of 10ft or greater throughout.
- Testing was only conducted on approximately 90ft of 132ft of shaft. This likely due to cage design limits for a stepped shaft.
- The reinforcement cage alignment varies (up to approximately 2 inches) throughout the length of the shaft.

Concrete Mix Design

Contractor Graham Construction & Management / Malcolm Drilling		Submitted By Central Pre-Mix Conc. Craig I. Matteson	Date 8/11/2009
Concrete Supplier Central Pre-Mix Concrete Co.		Plant Location 1901 N. Sullivan Rd, 302 N. Park Rd, or Crestline & Magnesium	
Contract Number 7777	Contract Name US 395 - NSC US 2 to Wandermere Vicinity, MP 165.95 to 167.63		

This mix is to be used in the following Bid Item No(s): 4000P Drilled Shaft Concrete Item 56

Concrete Class: (check one only)  
 3000  4000  4000D  4000P  4000W  Concrete Overlay  Cement Concrete Pavement  
 Other

Remarks: Typical Mix - see alt. Mix 377022 for 12 hr. set delay

Mix Design No. 353110 Plant No. 1, 3, or 4

Cementitious Materials	Source	Type, Class or Grade	Sp. Gr.	Lbs/cy
Cement	Ashgrove or Lafarge	I-II	3.15	600
Fly Ash <sup>P</sup>	Wabamum or Sundance	Type F	2.01	130
GGBFS (Slag)				
Latex				
Microsilica				

Concrete Admixtures	Manufacturer	Product	Type	Est. Range (oz/cy)
Air Entrainment				0
Water Reducer	WR Grace	WRDA-64	A & D	15-30
High-Range Water Reducer				
Set Retarder	WR Grace	Recover	D	15-60
Other	<u>Craig Matteson - 42oz for 12 set delay</u>			

Water (Maximum) 321 lbs/cy Is any of the water Recycled or Reclaimed?  Yes  No

Water Cementitious Ratio (Maximum) .44 Mix Design Density 144.5 +/- lbs/cf<sup>d</sup>

Design Performance	1	2	3	4	5	Average <sup>f</sup>
28 Day Compressive Strength (cylinders) psi	6,680	7,060	6,480	6,550	6,840	6,720
14 Day Flexural <sup>g</sup> Strength (beams) psi						

**Agency Use Only** (Check appropriate Box)

This Mix Design MEETS CONTRACT SPECIFICATIONS and may be used on the bid items noted above  
 This Mix Design DOES NOT MEET CONTRACT SPECIFICATIONS and is being returned for corrections

Reviewed By: [Signature] Date: 9/16/09

PE Signature Date

Figure 4-36 US 395 Wandermere concrete mix design page 1.

Mix Design No. 353110 Plant No. 1, 3, or 4

**Aggregate Information**

Concrete Aggregates	Component 1	Component 2	Component 3	Component 4	Component 5	Combined Gradation
WSDOT Pit No.	PS C-173 or PS C-107	PS C-173 or PS C-107	PS C-297 & PS C-120			
WSDOT ASR 14-day Results (%) <sup>b</sup>	<input checked="" type="checkbox"/> Yes <input type="checkbox"/> No	<input checked="" type="checkbox"/> Yes <input type="checkbox"/> No	<input checked="" type="checkbox"/> Yes <input type="checkbox"/> No	<input type="checkbox"/> Yes <input type="checkbox"/> No	<input type="checkbox"/> Yes <input type="checkbox"/> No	
Grading <sup>c</sup>	3/8" Round Combined	Coarse Sand Combined	Blend Sand Combined			
Percent of Total Aggregate	44	20	36			100%
Specific Gravity	2.67	2.64	2.64			
Lbs/cy (ssd)	1260	560	1030			

**Percent Passing**

	Component 1	Component 2	Component 3	Component 4	Component 5	Combined
2 Inch						
1-1/2 Inch						
1 Inch						3/8" Spec
3/4 Inch						
1/2 Inch	100					100 100
3/8 Inch	99.2	100	100			99.6 86-100
No. 4	35.7	96.7	99.8			71.0
No. 8	4.4	59.6	99.1			49.5 39-73
No. 16	.9	20.2	88.9			36.4 24-54
No. 30	.6	6.3	58			22.4 13-39
No. 50	.5	2.2	24.8			9.6 06-29
No. 100	.4	1.0	6.7			2.8 0-21
No. 200	.3	.6	3.1			1.4 0-2.0

Fineness Modulus: N/A (Required for Class 2 Sand)

ASR Mitigation Method Proposed<sup>d</sup>: Using Low Alkali Cement

**Notes:**

- <sup>a</sup> Required for Class 4000D and 4000P mixes.
- <sup>b</sup> Alkali Silica Reactivity Mitigation is required for sources with expansions over 0.20% - Indicate method for ASR mitigation. For expansion of 0.21% - 0.45%, acceptable mitigation can be the use of low alkali cement or 25% type F fly ash. Any other proposed mitigation method or for pits with greater than 0.45% expansion, proof of mitigating measure, either ASTM C1280 / AASHTO T303 test results must be attached. If ASTM C 1283 testing has been submitted indicating 1-year expansion of 0.04% or less, mitigation is not required.
- <sup>c</sup> AASHTO No. 497, 57, 67, 7, 8; WSDOT Class 1, Class 2; or combined gradation. See Standard Specification 9-03.1.
- <sup>d</sup> Required for Cement Concrete Pavements.
- <sup>e</sup> Attach test results indicating conformance to Standard Specification 9-25.1.
- <sup>f</sup> Actual Average Strength as determined from testing or estimated from ACI 211

DOT Form 350-D40 EF  
Revised 6/06

Figure 4-37 US 395 Wandermere concrete mix design page 2.



# ASH GROVE CEMENT COMPANY



Durkee Plant

WESTERN REGION  
33060 SHIRTTAIL CREEK ROAD  
P.O. BOX 287  
DURKEE, OREGON 97905  
(541) 877-2411

Mill Analysis No. 09-14  
Bin No. 4,D

Cement Type I-II L.A.  
Production Period July 1 to July 31

Date 10-Aug-09

### STANDARD REQUIREMENTS ASTM C - 150

CHEMICAL				PHYSICAL			
Item	(C 114)	Spec. Limit	Test Result	Item	Spec limit	Test Result	
SiO <sub>2</sub> (%)		20.0 min	21.5	Air content of mortar (volume %)			
Al <sub>2</sub> O <sub>3</sub> (%)		6.0 max	3.4	C 185	12 max		7.9
Fe <sub>2</sub> O <sub>3</sub> (%)		6.0 max	2.7	Fineness (m <sup>2</sup> /kg)			
CaO (%)		A	64.7	C 204 (Air permeability)	280 min		394
MgO (%)		6.0 max	1.2	Autoclave expansion (%)	0.80 max		0.024
SO <sub>3</sub> (%)		3.0 max	2.6	C 151			
Loss on ignition (%)		3.0 max	2.19	Compressive strength Psi (Mpa)	Min:		
Na <sub>2</sub> O (%)		A	0.29	C 109	1 Day	A	2138 (14.7)
K <sub>2</sub> O (%)		A	0.42		3 Days		1450 (10.0) 3778 (26.0)
TiO <sub>2</sub> (%)		A	0.26		7 Days		2470 (17.0) 4894 (33.7)
P <sub>2</sub> O <sub>5</sub> (%)		A	0.11		28 Days	A	C
Mn <sub>2</sub> O <sub>3</sub> (%)		A	0.08	Time of setting (minutes)			
Insoluble Residue (%)		0.75 max	0.28	C 191 (Vicat)			
CO <sub>2</sub> (%)		A	1.66		Initial	not less than 45	112
Limestone (%)		5.0 max	3.81		Final	not more than 375	199
CaCO <sub>3</sub> in Limestone		70 min	99.35				
C <sub>3</sub> S + 4.75C <sub>3</sub> A		100 max	81				
Potential compounds (%)							
C <sub>3</sub> S		A	59				
C <sub>2</sub> S		A	17				
C <sub>3</sub> A		8.0 max	4				
C <sub>4</sub> AF		A	8				
C <sub>4</sub> AF+2(C <sub>3</sub> A)		A	16				

### OPTIONAL REQUIREMENTS ASTM C - 150, (other)

CHEMICAL				PHYSICAL			
Item		Spec. Limit	Test Result	Item	Spec. Limit	Test Result	
C <sub>3</sub> S + C <sub>3</sub> A (%)		A		False set (%) C 451	50 min		90
Equivalent alkalis (%)		0.60 max	0.57	Heat of hydration (cal/g)			
					7 days	A	78
				Compressive strength (Mpa)			
					28 Days	28.0	C

A=not applicable  
B= Limit not specified by purchaser.  
Test result provided for information only.  
C= Test results for this period not available

We certify that the above described cement, at the time of shipment, meets the chemical and physical requirement of the ASTM C 150 -08 or AASHTO M-85 -08 Type I-II specification also will meet CSA A3001-08 Type GU.

Signature: Mike Raney

Title: Chief Chemist

Figure 4-38 US 395 Wandermere Portland cement mill certificate.



**Cement**

**FLY ASH TEST REPORT**

Analysis by: Lafarge Edmonton Lab  
 Sample from : Sundance Power Plant, **Classified**  
 Average Analysis: June 01-30 2009

**Chemical Analysis**

Silicon Dioxide (SiO <sub>2</sub> )	56.2 %
Aluminum Oxide (Al <sub>2</sub> O <sub>3</sub> )	23.2 %
Iron Oxide (Fe <sub>2</sub> O <sub>3</sub> )	3.7 %
Total (SiO <sub>2</sub> ) + (Al <sub>2</sub> O <sub>3</sub> ) + (Fe <sub>2</sub> O <sub>3</sub> )	83.0 %
Sulphur Trioxide (SO <sub>3</sub> )	0.2 %
Calcium Oxide (CaO)	10.3 %
Magnesium Oxide	1.1 %
Moisture Content	0.03 %
Loss on Ignition	0.33 %
Available Alkali as Equiv. Na <sub>2</sub> O*	0.9 %

**Physical Analysis**

Fineness Retained on No. 325 Sieve (45 µm)	15.5 %
Strength Activity Index with Portland Cement	
% of Control at 7 Days	86 %
% of Control at 28 Days	86 %
Water Requirement, Percent of Control	94.8 %
Autoclave Expansion	0.07 %
Density	2.07 Mg/m <sup>3</sup>

**Uniformity Requirements**

Density, Variation from Average	0.4 %
Fineness No. 325 Sieve, Variation from Average	12.5 %

We hereby certify the fly ash represented by the above chemical and physical analysis meets the requirements of ASTM C618-04 and AASHTO M 295-07 for Class F Fly Ash.

*\*previous month's result*

Certified : 

Israel Ginez  
 Laboratory Manager - Edmonton

**CEMENT GROUP / ALBERTA SALES**  
 12420 17th St. N. E., Edmonton, AB T6S 1A8  
 Telephone: (780) 472-8933 Fax: (780) 472-6648 Toll Free: 1-800-661-1522

Figure 4-39 US 395 Wandermere fly ash mill certificate.

Project 7777L  
Pier 4 Shaft L

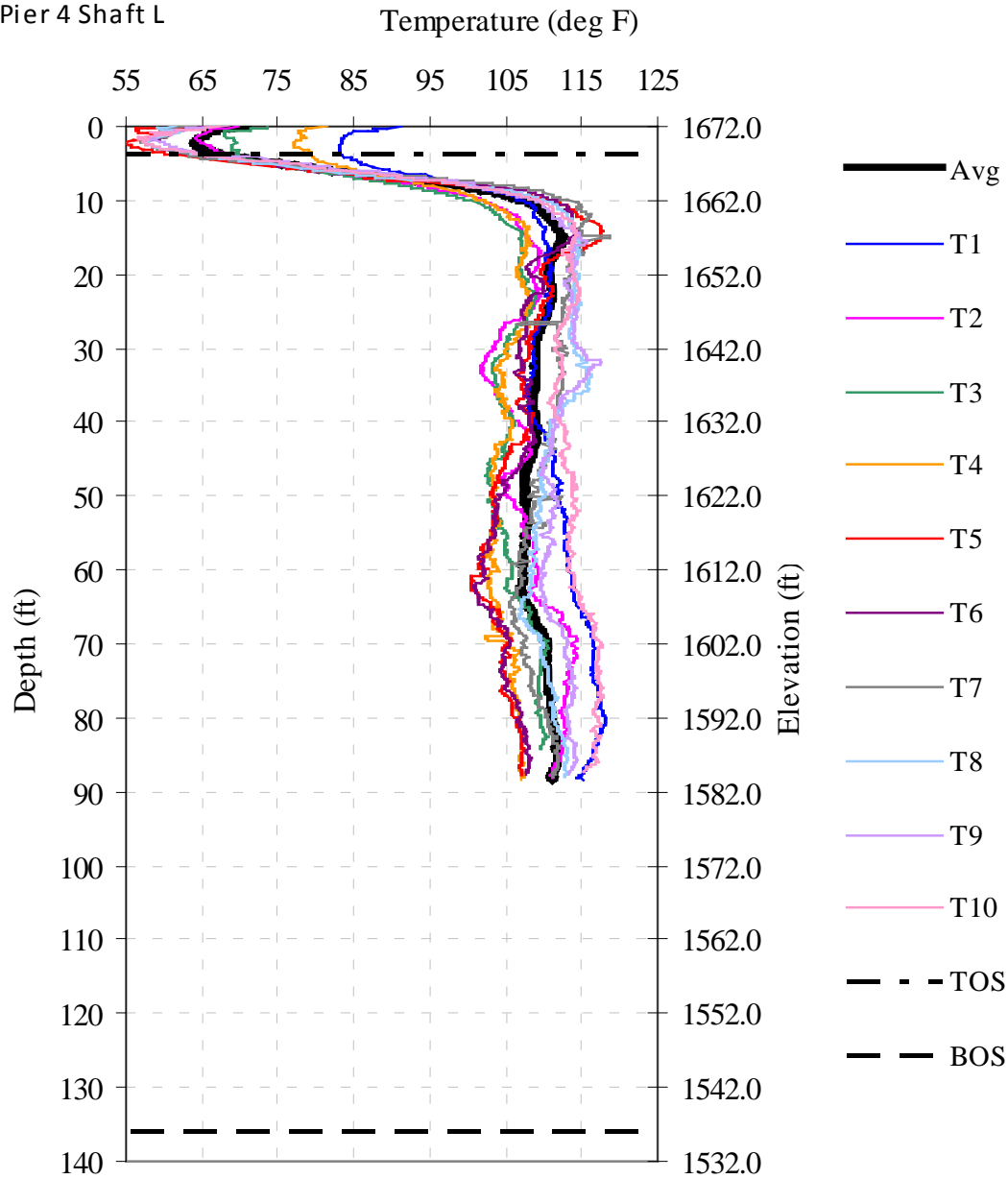


Figure 4-40 Measured tube temperatures versus depth (US 395 Wandermere Pier 4 Shaft L).

Project 7777L  
 Pier 4 Shaft L

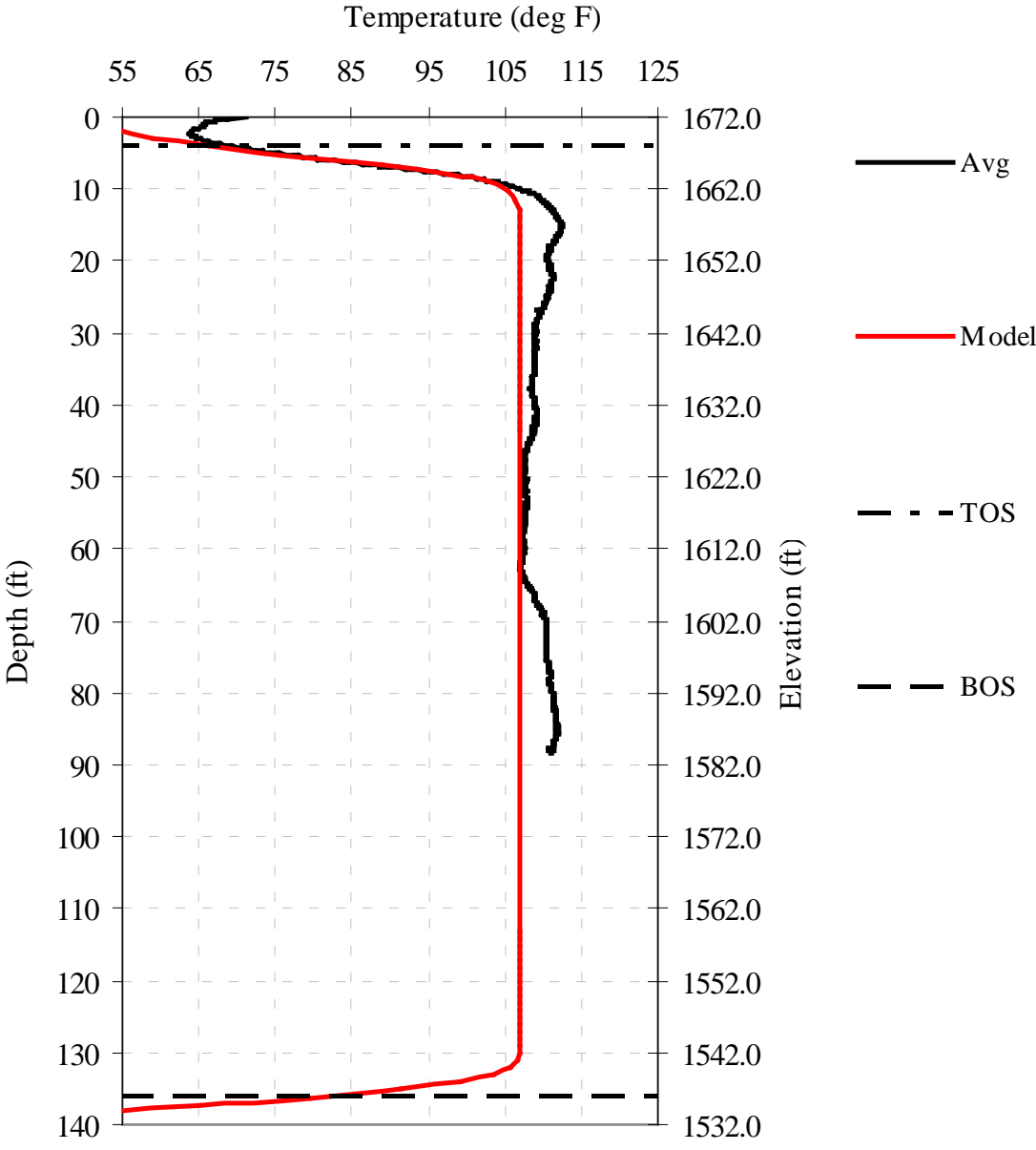


Figure 4-41 Measured and modeled temperature versus depth (US 395 Wandermere Pier 4 Shaft L).

Project 7777L  
 Pier 4 Shaft L

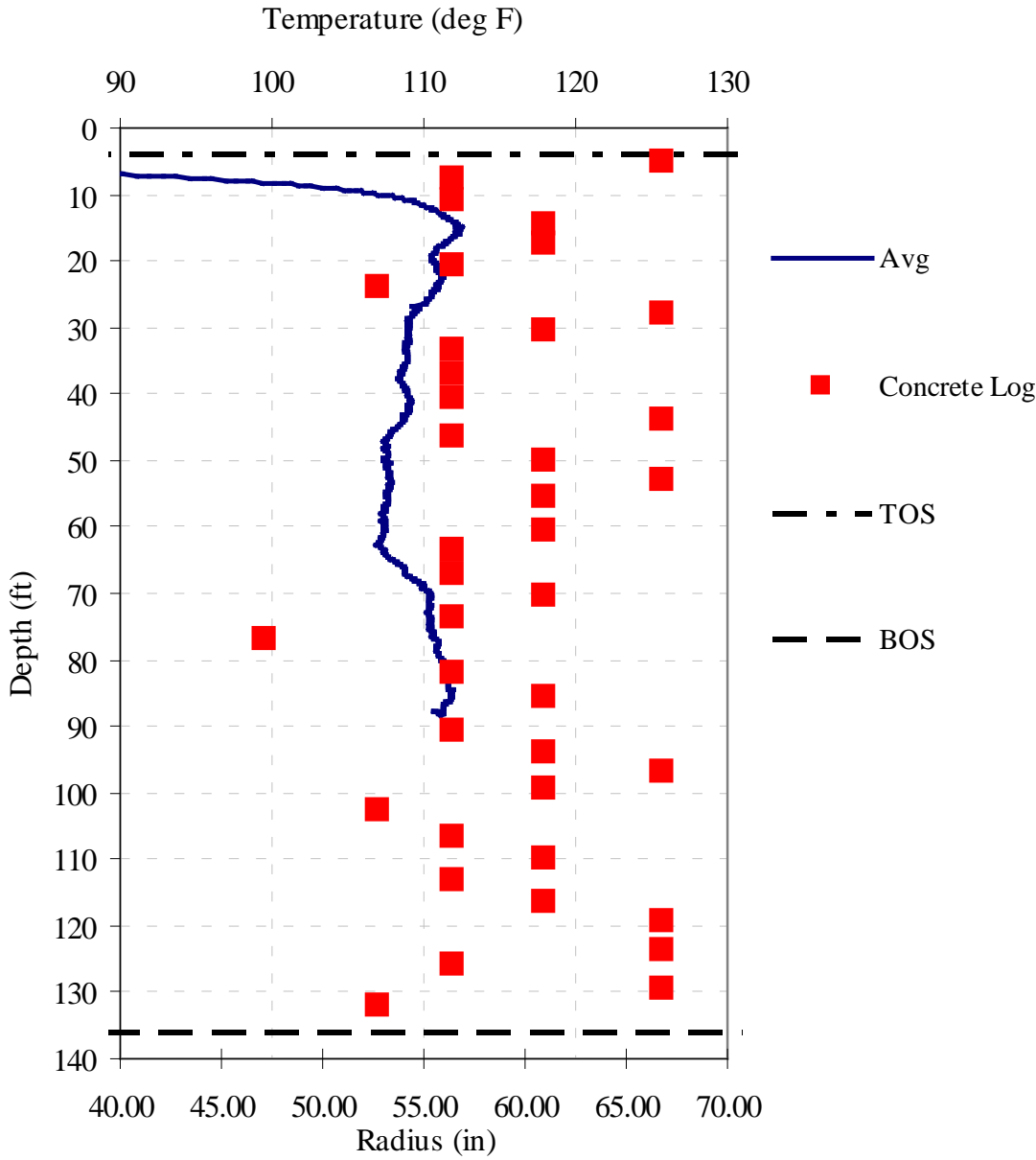


Figure 4-42 Concrete Placement Log versus average measured temperature (US 395 Wandermere Pier 4 Shaft L).

Project 7777L  
 Pier 4 Shaft L

Effective Shaft Radius (in)

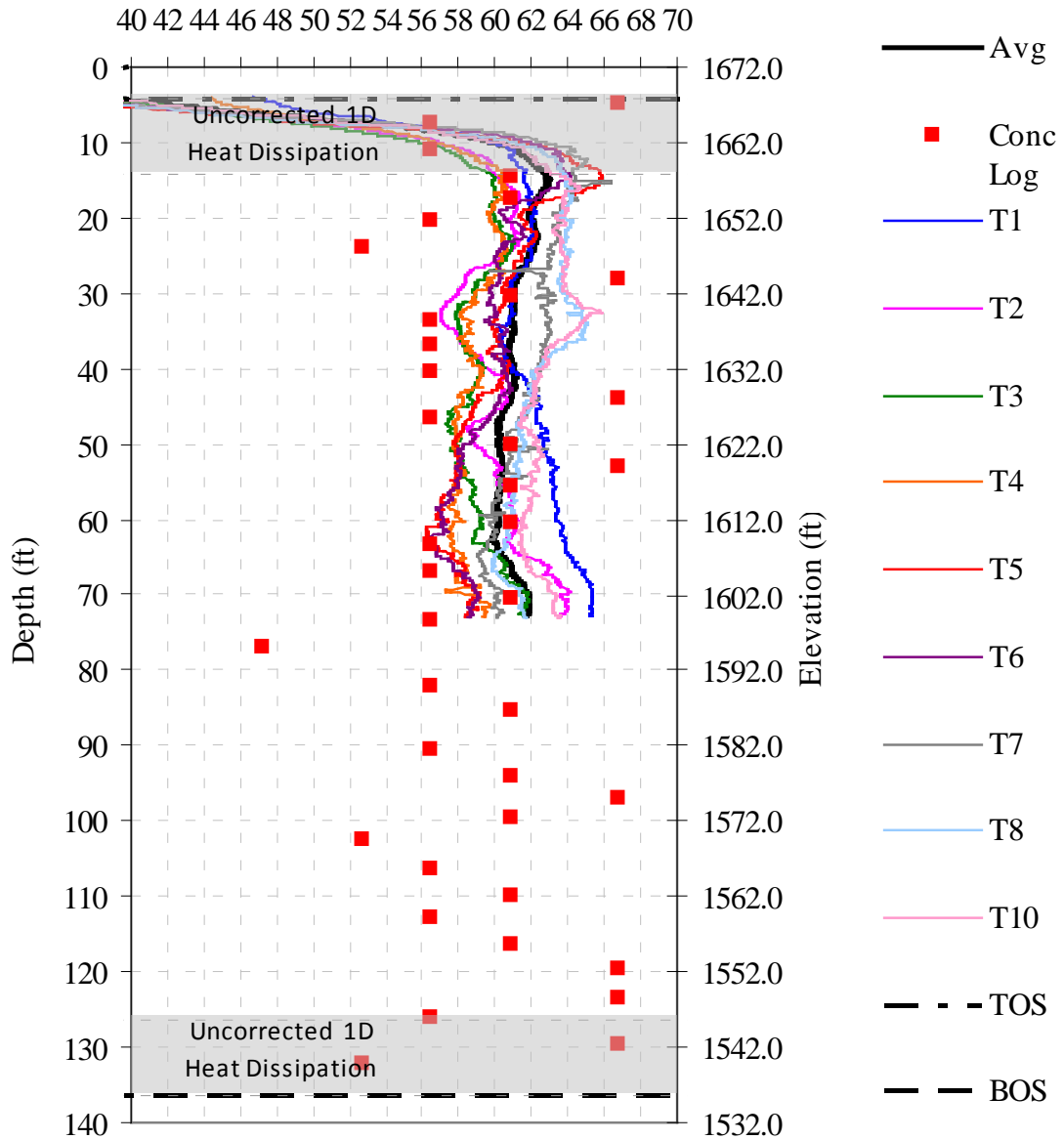


Figure 4-43 Effective shaft radius showing cage alignment uncorrected for axial heat dissipation (US 395 Wandermere Pier 4 Shaft L).

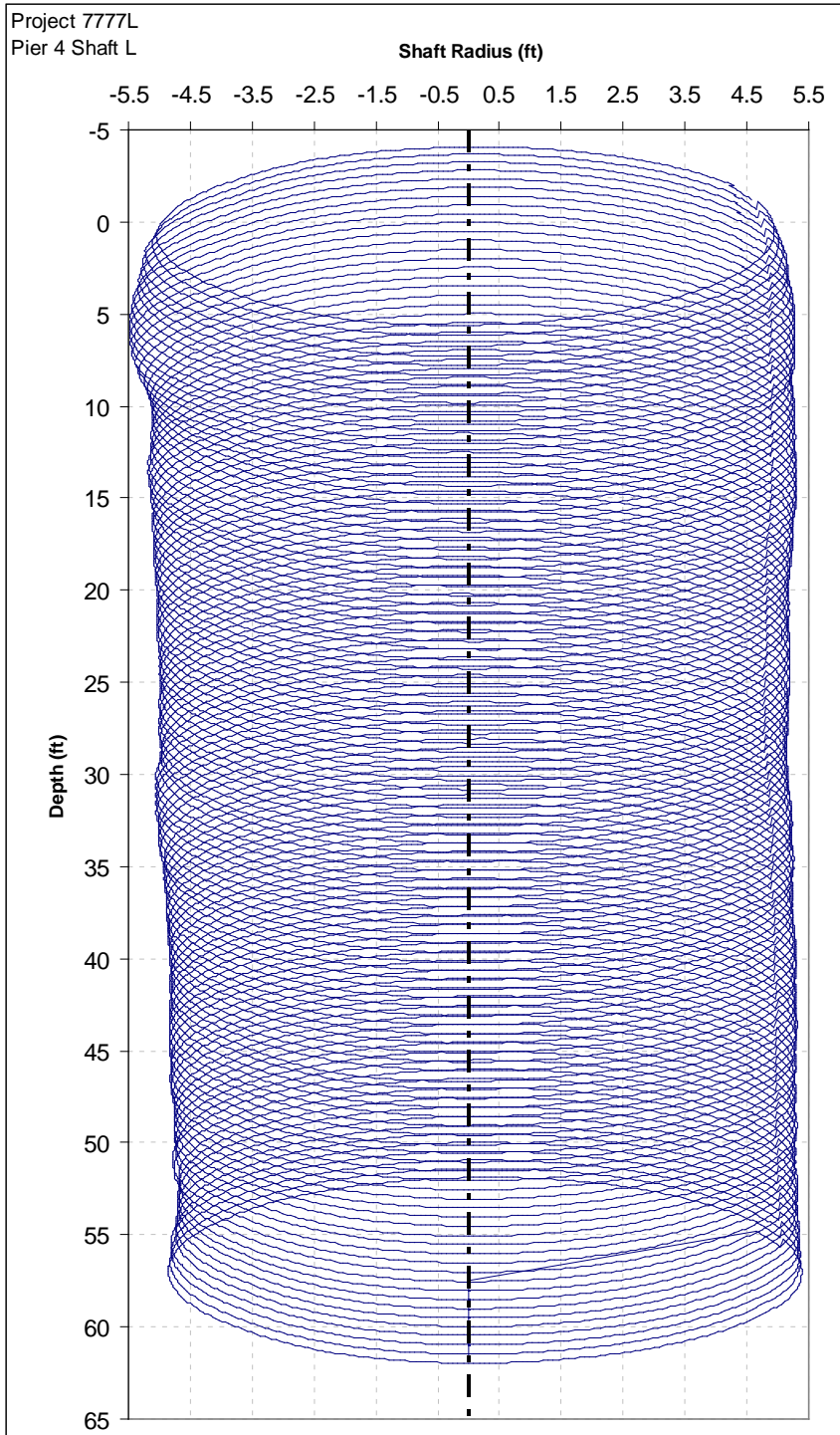


Figure 4-44 3-D rendering from tube spacings and effective radius calculations (US 395 Wandermere Pier 4 Shaft L).

## **4.5 Project 7681: Vancouver Rail**

Thermal testing was conducted on a shaft in Pier 2 for the Vancouver Rail project. This pier is comprised of three – 6.5 foot diameter drilled shafts approximately 70 feet long. The shafts were equipped with 7 access tubes in general accordance with standard practice for tube plurality in State specifications. The tube identification / numbering used for this project assumed the northerly most tube to be No. 1 and increased in value in a clockwise fashion looking down on to the shaft top. Standard infrared thermal testing was conducted on the North shaft within Pier 2. Standard testing protocols were followed to verify reproducibility of each scan.

### **4.5.1 Thermal Modeling**

Thermal modeling was conducted based on the concrete mix design (Figures 4-45 through 4-48). The mix design information was used to create the input hydration energy parameters using the **a**, **b**, and **t** method outlined by Schindler (2005). The model parameters used in the T3DModel software were 0.831, 0.578, and 35.045, respectively with an overall energy production of 91.2 kJ per kg of total concrete mass.

### **4.5.2 Thermal Testing Pier 2 Shaft North**

The testing was performed on February 24, 2010 after construction of the North shaft. Field measurements were taken from each of the seven tubes and are presented in Figure 4-49. A model was run based on theoretical shaft dimensions (6.5 ft diameter) and compared to the field measurements (Figure 4-50). The average field temperature is either in line with or greater than the model indicating an effective shaft diameter of 6.5ft or greater. However, either the tubes did not extend to the bottom of the shaft (leaking or blockages) or the shaft was excavated beyond the cage which is visible in the profiles due to no toe roll-off.

Construction logs were not received. As a result, no further analysis could be performed on the thermal data.

### **4.5.3 Project 7681 Conclusions**

Based on the thermal integrity test results presented herein, the following conclusions can be drawn concerning Project 7681, Pier 2 Shaft North:

- The average field temperature is either in line with or greater than the model indicating an effective shaft diameter of 6.5ft or greater throughout.
- Due to no toe roll-off, either the tubes did not extend to the bottom of shaft or the shaft was over excavated.
- The reinforcement cage alignment varies slightly throughout the length of the shaft.



## Concrete Mix Design

Contractor Dewitt Construction		Submitted By	Date 6/2/2009
Concrete Supplier CEMEX		Plant Location Vancouver WA	
Contract Number	Contract Name 39th ST Railway Overpass - City of Vancouver		

This mix is to be used in the following Bid Item No(s): \_\_\_\_\_

Concrete Class: *(check one only)*

- 3000  
  4000  
  4000D<sup>a</sup>  
  4000P<sup>a</sup>  
  4000W  
  Concrete Overlay  
  Cement Concrete Pavement<sup>d</sup>  
 Other \_\_\_\_\_

Remarks: Gradations Supplied for Informational Purposes Only

Mix Design No. 1317963 Plant No. \_\_\_\_\_

Cementitious Materials	Source	Type, Class or Grade	Sp. Gr.	Lbs/cy
Cement	CalPortland, Portland	ASTM C150 Type I-II	3.15	600
Fly Ash <sup>2</sup>	Boral, Boardman OR	ASTM C618 Class C	2.67	175
GGBFS (Slag)				
Latex				
Microsilica				

Concrete Admixtures	Manufacturer	Product	Type	Est. Range (oz/cy)
Air Entrainment				
Water Reducer	Grace	Daratard 17	D	10-30
High-Range Water Reducer				
Set Retarder				
Other				

Water (Maximum) 340 lbs/cy      Is any of the water Recycled or Reclaimed?    Yes<sup>e</sup>    No

Water Cementitious Ratio (Maximum) .44      Mix Design Density 143.3 lbs/cf<sup>d</sup>

Design Performance	1	2	3	4	5	Average <sup>f</sup>
28 Day Compressive Strength (cylinders) psi						
14 Day Flexural <sup>d</sup> Strength (beams) psi						

**Agency Use Only** (Check appropriate Box)

This Mix Design **MEETS CONTRACT SPECIFICATIONS** and may be used on the bid items noted above  
 This Mix Design **DOES NOT MEET CONTRACT SPECIFICATIONS** and is being returned for corrections

Reviewed By: *[Signature]*      *[Signature]*      11/23/09  
 PE Signature      Date

Figure 4-45 Vancouver Rail concrete mix design page 1.

Mix Design No. 1317963 Plant No. \_\_\_\_\_

**Aggregate Information**

Concrete Aggregates	Component 1	Component 2	Component 3	Component 4	Component 5	Combined Gradation
WSDOT Pit No.	OR73	G-106				
WSDOT ASR 14-day Results (%) <sup>b</sup>	<input type="checkbox"/> Yes <input type="checkbox"/> No	<input type="checkbox"/> Yes <input type="checkbox"/> No	<input type="checkbox"/> Yes <input type="checkbox"/> No	<input type="checkbox"/> Yes <input type="checkbox"/> No	<input type="checkbox"/> Yes <input type="checkbox"/> No	
Grading <sup>c</sup>	ASTM C33 #8	ASTM C33 / Class 2				
Percent of Total Aggregate	48% by WT	52% by WT				100%
Specific Gravity	2.63	2.6				
Lbs/cy (ssd)	1320	1433				

**Percent Passing**

2 inch	100	100				100
1-1/2 inch	100	100				100
1 inch	100	100				100
3/4 inch	100	100				100
1/2 inch	100	100				100
3/8 inch	97	100				99
No. 4	22	100				63
No. 8	.9	93				46
No. 16	.8	73				32
No. 30	0	53				23
No. 50	0	24				11
No. 100	0	3				2
No. 200	.7	.9				.8

Fineness Modulus: 2.75 (Required for Class 2 Sand)

ASR Mitigation Method Proposed <sup>b</sup> : \_\_\_\_\_

**Notes:**

- <sup>a</sup> Required for Class 4000D and 4000P mixes.
- <sup>b</sup> Alkali Silica Reactivity Mitigation is required for sources with expansions over 0.20% - Incidate method for ASR mitigation. For expansion of 0.21% - 0.45%, acceptable mitigation can be the use of low alkali cement or 25% type F fly ash. Any other proposed mitigation method or for pits with greater than 0.45% expansion, proof of mitigating measure, either ASTM C1260 / AASHTO T303 test results must be attached. If ASTM C 1293 testing has been submitted indicating 1-year expansion of 0.04% or less, mitigation is not required.
- <sup>c</sup> AASHTO No. 467, 57, 67, 7, 8; WSDOT Class 1, Class 2; or combined gradation. See Standard Specification 9-03.1.
- <sup>d</sup> Required for Cement Concrete Pavements.
- <sup>e</sup> Attach test results indicating conformance to Standard Specification 9-25.1.
- <sup>f</sup> Actual Average Strength as determined from testing or estimated from ACI 211.

DOT Form 350-040 EF  
Revised 6/06

Figure 4-46 Vancouver Rail concrete mix design page 2.



1050 N River St  
 Portland, OR 97227  
 Ph# 503 335-2600  
 F# 503 331-3700

**Certificate of Analysis**

Source : Nanjing, China

We hereby certify that CalPortland (Lot #10-017) Type I/II Low Alkali cement meets the standard requirements of ASTM C 150-07 for Type I and Type II low alkali cement. Additionally CalPortland Type I/II Low Alkali cement meets the requirements of AASHTO M-85 for Type I cement. Following are the chemical and physical testing results of this cement.

**Astm C150 Chemical Requirements**

Lot# 10-017 Cape York	Type II Requirements	Test Results Type II Cement
Silicon dioxide (SiO <sub>2</sub> ), min. %		20.9
Aluminum oxide (Al <sub>2</sub> O <sub>3</sub> ), max. %	6.0	3.9
Ferric oxide (Fe <sub>2</sub> O <sub>3</sub> ), max. %	6.0	3.8
Magnesium oxide (MgO), max. %	6.0	1.0
Sulfur trioxide (SO <sub>3</sub> ), max. %	3.0	2.31
Loss on ignition, max. %	3.0	1.6
Insoluble residue, max. %	0.75	0.64
Alkalies (Na <sub>2</sub> O+0.658 K <sub>2</sub> O), max. %	0.60	0.50
Tricalcium aluminate (C <sub>3</sub> A), max. %	8.0	3.9
%CO <sub>2</sub>	-----	1.08
%CaCO <sub>3</sub> in limestone min.	70	91.8
%Limestone	5	2.7
C <sub>3</sub> S + 4.75 x C <sub>3</sub> A *		79

**Astm C150 Physical Requirements**

Air content of mortar, max. %	12	8.1
Fineness, specific surface, min. *	280	392
Autoclave expansion, max. %	0.8	-0.02
Compressive strength psi, Mpa, min.		
1 Day psi (MPa)	-----	2145 14.8
3 Day psi (MPa)	1450 (10.0)	3940 27.2
7 Day psi (MPa)	2470 (17.0)	4830 33.3
28 Day psi (MPa)	-----	
Vicat time of setting, min. not less than, min.	45	127
Vicat time of setting, min. not greater than, min.	375	
L value	-----	48.73

\* If C<sub>3</sub>S +(4.75xC<sub>3</sub>A) > 90 then the maximum Blaine fineness shall be 420

Date January 21, 2010

*Hein Wolf*  
 Technical Services Manager

Figure 4-47 Vancouver Rail Portland cement mill certificate.



### ASTM C 618 TEST REPORT

Sample Number: S-091208004  
Sample Date: November 2009

Report Date: 2/15/2010  
Sample Source: Boardman  
Tested By: jx

TESTS	RESULTS	ASTM C 618 CLASS F/C	AASHTO M 295 CLASS F/C
<b>CHEMICAL TESTS</b>			
Silicon Dioxide (SiO <sub>2</sub> ), %	31.91		
Aluminum Oxide (Al <sub>2</sub> O <sub>3</sub> ), %	18.58		
Iron Oxide (Fe <sub>2</sub> O <sub>3</sub> ), %	6.05		
Sum of SiO <sub>2</sub> , Al <sub>2</sub> O <sub>3</sub> , Fe <sub>2</sub> O <sub>3</sub> , %	56.54	70.0/50.0 min.	70.0/50.0 min.
Calcium Oxide (CaO), %	27.41		
Magnesium Oxide (MgO), %	6.96		
Sulfur Trioxide (SO <sub>3</sub> ), %	2.77	5.0 max.	5.0 max.
Sodium Oxide (Na <sub>2</sub> O), %	2.48		
Potassium (K <sub>2</sub> O), %	0.35		
Total Alkalies (as Na <sub>2</sub> O), %	2.71		
Available Alkalies (as Na <sub>2</sub> O), %	1.19		
<b>PHYSICAL TESTS</b>			
Moisture Content, %	0.05	3.0 max.	3.0 max.
Loss on Ignition, %	0.12	6.0 max.	5.0 max.
Amount Retained on No. 325 Sieve, %	17.00	34 max.	34 max.
Specific Gravity	2.74		
Autoclave Soundness, %	0.07	0.8 max.	0.8 max.
SAI, with Portland Cement at 7 Days, % of Control	89.8	75 min.*	75 min.*
SAI, with Portland Cement at 28 Days, % of Control	88.5	75 min.*	75 min.*
Water Required, % of Control	93.4	105 max.	105 max.
Loose, Dry Bulk Density, lb/cu. ft.	75.00		

Meets ASTM C 618 and AASHTO M 295, Class C

The Class (C) Fly Ash from this plant meets the requirements of the MDOT and SCDHPT specifications.

\* Meeting the 7 day or 28 day Strength Activity Index will indicate specification compliance.

Approved By:

*Diana Benfield*  
Diana Benfield  
QC Specialist

Approved By:

*Brian Shaw*  
Brian Shaw  
Materials Testing Manager

Figure 4-48 Vancouver Rail fly ash mill certificate.



Project 7681  
 Pier 2 Shaft N

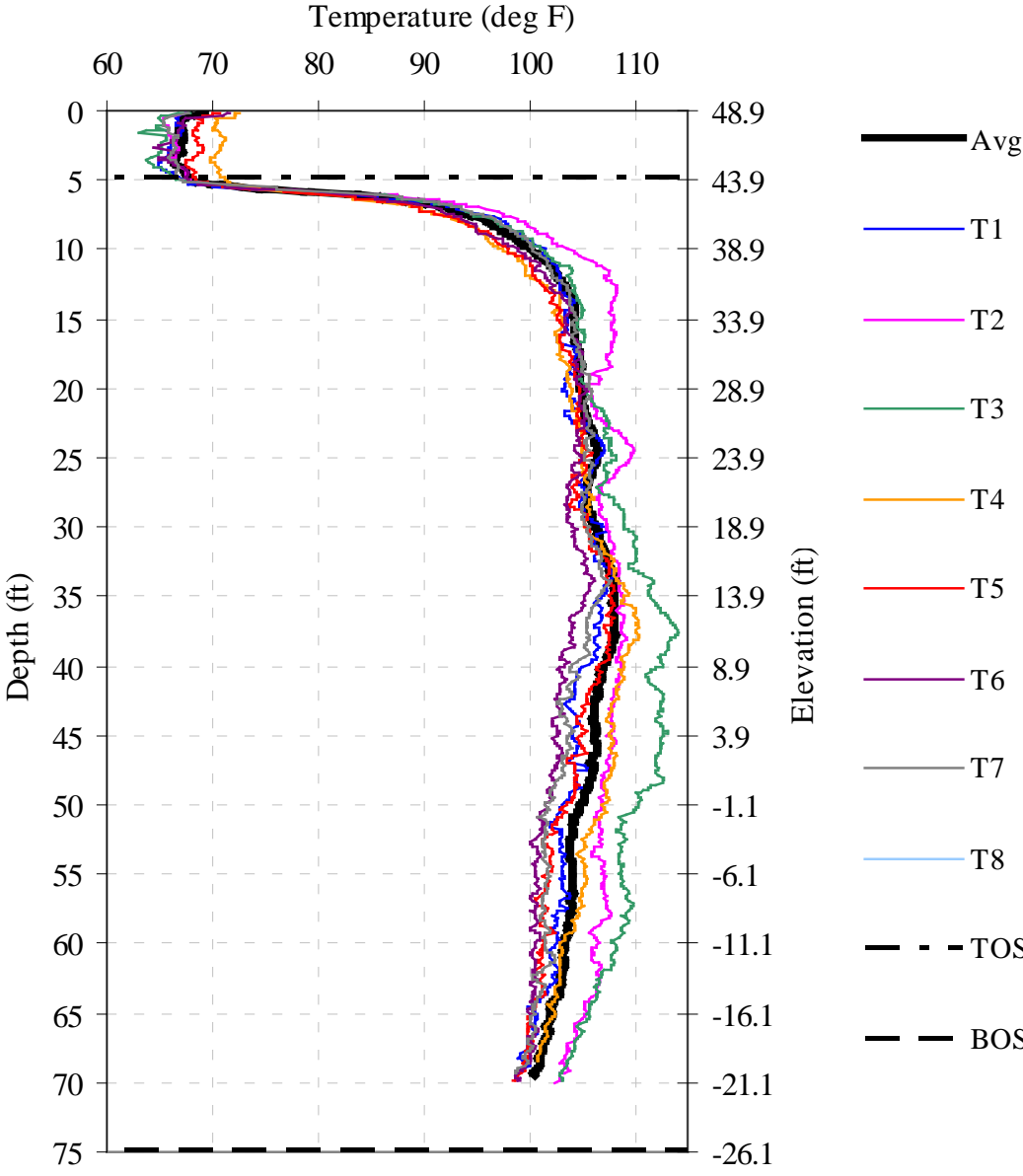


Figure 4-49 Measured tube temperatures versus depth (Vancouver Rail Pier 2 Shaft N).

Project 7681  
 Pier 2 Shaft N

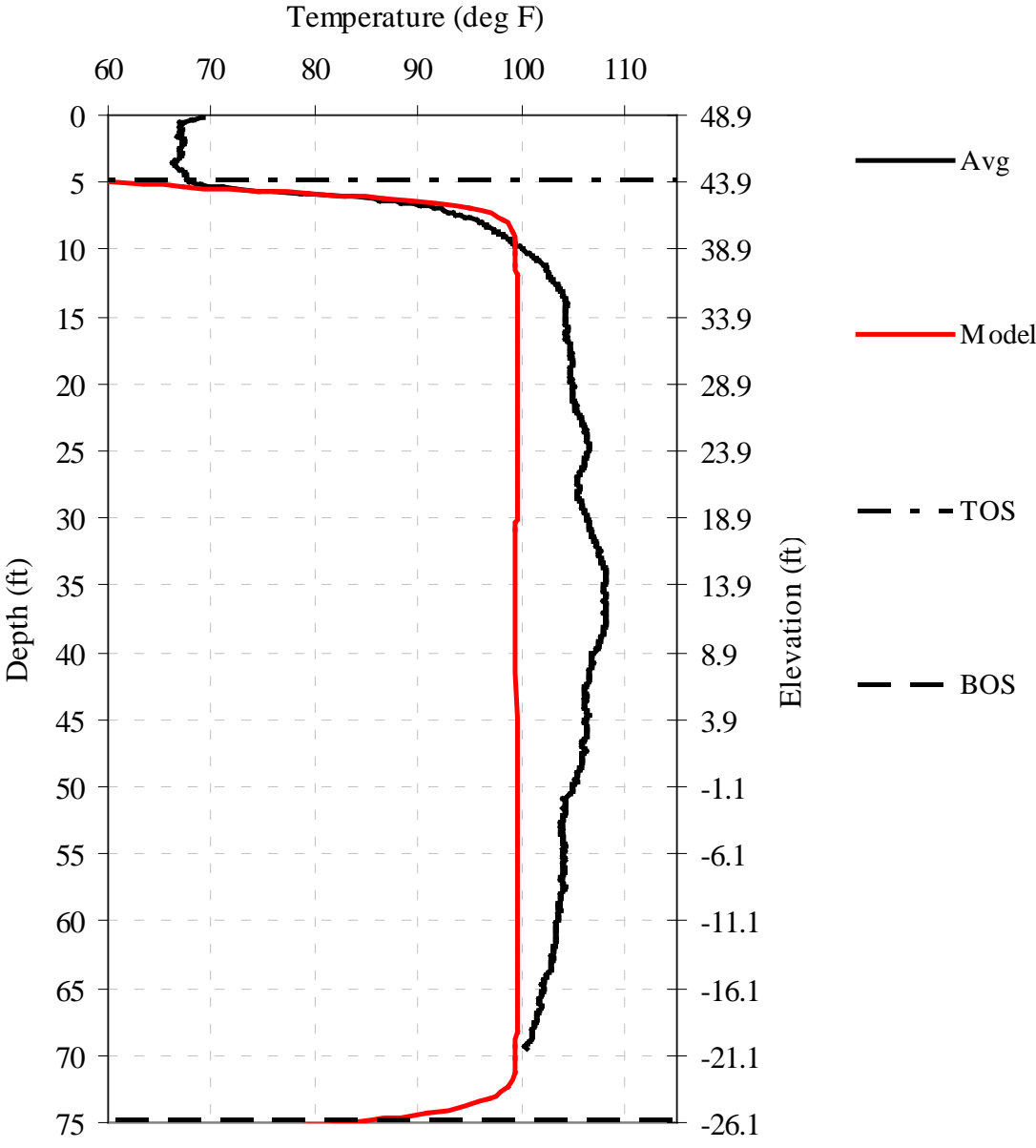


Figure 4-50 Measured and modeled temperature versus depth (Vancouver Rail Pier 2 Shaft N).

## 4.6 Project 7911: Gallup Creek

Thermal testing was conducted on a shaft at Pier 1 for the Gallup Creek bridge replacement project. The test shaft 7 foot in diameter and equipped with 7 access tubes in general accordance with standard practice for tube plurality in State specifications. The tube identification / numbering used for this project assumed the northerly most tube to be No. 1 and increased in value in a clockwise fashion looking down on to the shaft top. Standard infrared thermal testing was conducted on the South shaft within Pier 1. Standard testing protocols were followed to verify reproducibility of each scan.

### 4.6.1 Thermal Modeling

Thermal modeling was conducted based on the concrete mix design (Figures 4-51 through 4-53). The fly ash mill certificate was not provided, as such, typical values ( $\text{SO}_3 = 0.7\%$  and  $\text{CaO} = 13.3\%$ ) for the area was used to generate the hydration energy parameters. The mix design information was used to create the input hydration energy parameters using the **a**, **b**, and **t** method outlined by Schindler (2005). The model parameters used in the T3DModel software were 0.775, 0.596, and 18.905, respectively with an overall energy production of 74.85 kJ per kg of total concrete mass.

### 4.6.2 Thermal Testing Pier 1 Shaft South

The testing was performed on August 1, 2010 approximately 40 hours after concreting the South shaft. Field measurements were taken from each of the seven tubes and are presented in Figure 4-54. Field measurements indicate a uniform shaft within the cased region with the reinforcement cage alignment varying. Below the casing, there is a large bulge in the direction of tubes 6 and 7. A model was run based on theoretical shaft dimensions (7 ft diameter) and compared to the field measurements (Figure 4-55). The average field temperature is either in line with or greater than the model indicating an effective shaft diameter of 7ft or greater from an approximate elevation of +898 to +839. From an approximate elevation of +839 to +830, the average temperature is lower than the model prediction indicating an effective shaft diameter less than 7ft. Figure 4-56 shows the average measured temperature versus the concrete placement log. The effective radius (Figure 4-57) is predicted without axial heat dissipation corrections. This shaft has a large range of radii (and average temperatures) due to the bulge from which a temperature-to-radius correlation developed (Multi-Truck Method). Figure 4-58 shows a 3-D rendered image of the as-built shaft based on temperature-to-radius correlations.

Tubes appear to have not extended to the bottom of the excavation due to the lack of toe roll-off. Inspection of the toe roll-off relative to the reported bottom elevation indicates the shaft was over-excavated and not reported correctly.

### 4.6.3 Project 7911 Conclusions

Based on the thermal integrity test results presented herein, the following conclusions can be drawn concerning Project 7911, Pier 1 Shaft South:

- The average field temperature indicates a uniform shaft to an approximate elevation of 868ft.
- From an approximate elevation of 868ft to 846ft, a large bulge in the direction of tubes 6 and 7 is detected.
- The fly ash mill certificate was not received. Typical values for calculating the hydration energy parameters were used for  $\text{SO}_3$  and CaO (0.7% and 13.3%, respectively). Slight variation in the fly ash chemistry will cause small changes in the hydration energy curve.
- From an approximate elevation of +839 to +830, the average temperature is lower than the model prediction indicating an effective shaft diameter less than 7ft.
- Field elevations are likely reported incorrectly for the bottom of the shaft.
- The reinforcement cage alignment varies (up to approximately 2 inches) throughout the length of the shaft.



Contractor <b>DPM CONTRACTORS</b>	Submitted By	Date <b>6/2/10</b>
Concrete Supplier <b>Concrete Ready Mix and Gravel Inc.</b>	Plant Location <b>209 201, 202</b>	
Contract Number <b>PA024 1911</b>	Contract Name <b>SR592 GALLUP CREEK BRIDGE REPLACEMENT</b>	

This mix is to be used in the following Bid Item No(s): \_\_\_\_\_

Concrete Class: (check one only)

8000  4000  4000B  4000P  4000W  Concrete Overlay  Cement Concrete Pavement

Other \_\_\_\_\_

Remarks: \_\_\_\_\_

Mix Design No. **8023** Plant No. **209, 201, 202**

Constituent Materials	Source	Type, Class or Grady	Sp. Gr.	Usage
Cement	<b>Lehigh 1/4</b>	<b>1/4</b>	<b>3.15</b>	<b>64</b>
Fly Ash <sup>a</sup>	<b>LAGARCE</b>	<b>F</b>	<b>2.17</b>	<b>100</b>
COARSE (slag)				
Latex				
Miscellion				

Concrete Additives	Manufacturer	Product	Type	Est. Range (vol %)
Air Entrainment				
Water Reducer	<b>Grace</b>	<b>Ezyl 610</b>	<b>A</b>	<b>2-5</b>
High-Range Water Reducer	<b>Grace</b>	<b>Admix 195</b>	<b>F</b>	<b>0-6</b>
Set Retarder	<b>Grace</b>	<b>Retarder</b>	<b>D</b>	<b>0-3</b>
Other				

Water (Maximum) **300** lbs/cy. Is any of the water Recycled or Reclaimed?  Yes  No

Water Cement Ratio (Maximum) **.42** Mix Design Density **146.25** lbs/cy

Design Performance	1	2	3	4	5	Average
28 Day Compressive Strength (cylinders) psi	<b>7060</b>	<b>7170</b>	<b>8000</b>	<b>7740</b>	<b>7590</b>	<b>7512</b>
14 Day Flexural Strength (beams) psi						

**Agency Use Only (Check appropriate Box)**

This Mix Design **MEETS CONTRACT SPECIFICATIONS** and may be used on the bid items noted above.

This Mix Design **DOES NOT MEET CONTRACT SPECIFICATIONS** and is being returned for corrections.

Reviewed By: *[Signature]* Date: **6/14/10**

PE Signature Date

Figure 4-51 Gallup Creek concrete mix design page 1.

Mix Design No. 8023

Plant No. 200, 201, 202

**Aggregate Information**

General Aggregate	Component 1	Component 2	Component 3	Component 4	Component 5	Combined Gradation
WSDOT M.C.S. No.	F-175	F-175				
WSDOT ASR Mitigation Rate (in %) <sup>1</sup>	<input type="checkbox"/> Yes <input type="checkbox"/> No	<input type="checkbox"/> Yes <input type="checkbox"/> No	<input type="checkbox"/> Yes <input type="checkbox"/> No	<input type="checkbox"/> Yes <input type="checkbox"/> No	<input type="checkbox"/> Yes <input type="checkbox"/> No	
Grading <sup>2</sup>	#8	Class 2				
Percent of Total Aggregate	61%	39%				100%
Specific Gravity	2.69	2.65				
Unit Weight (pcf)	1800	1450				

**Percent Passing**

Sieve Size	Component 1	Component 2	Component 3	Component 4	Component 5	Combined
2-inch						
1 1/2-inch						
1-inch						
3/4-inch						
3/8-inch						
#40	100					100
#60	99.4					99.6
No. 4	18.7	100				50.4
No. 8	.5	86.3				37.86
No. 16	.3	59.5				23.38
No. 30		36.1				18.26
No. 60		15.2				6.7
No. 100		2.4				1.18
No. 200	.04	1.85				1.76

Fineness Modulus: 3.69 (Required for Class 2 Sand)

ASR Mitigation Method Proposed:

**Notes:**

- <sup>1</sup> Required for Class 4000 and 4000P mixes.
- <sup>2</sup> Alkali-Silica Reactivity Mitigation is required for sources with expansions over 0.20%. Include method for ASR mitigation. For expansion of 0.21% - 0.25%, acceptable mitigation can be the use of low alkali cement or 20% replacement with pozzolan. Any other mitigation method or for mix with greater than 0.40% expansion, proof of mitigating measure, such as ASTM C1289 (ASTM C1289 test results must be attached).
- <sup>3</sup> ASTM C1289 testing has been submitted indicating 1-year expansion of 0.04% or less, mitigation is not required.
- <sup>4</sup> AASHTO No. 42, 57, 67, 7, 8; WSDOT Class 1, Class 2; or combined gradation. See Standard Specification P-00.1.
- <sup>5</sup> Required for Cement Concrete Pavements.
- <sup>6</sup> ASTM test results indicating performance to Standard Specification P-28.1.
- <sup>7</sup> Actual Average Strength is determined from testing or estimated from ACI 211.

DOT Form 950-040 EP  
Revised 9/00

Figure 4-52 Gallup Creek concrete mix design page 2.

**MILL TEST REPORT**

Cement Type: **ASTM Type I/II, AASHTO Type I  
Low Alkali Portland Cement**

Plant: **Delta, BC**

**Certificate #: D2-387**

Production Period:	Jul 01 2010 Jul 31 2010	Test Result	ASTM C150-07 Specification	AASHTO M 85-07 Specification
SiO <sub>2</sub> (%)	ASTM C114	20.0	-	-
Al <sub>2</sub> O <sub>3</sub> (%)	ASTM C114	4.78	max. 6.0	-
Fe <sub>2</sub> O <sub>3</sub> (%)	ASTM C114	3.69	max. 6.0	-
CaO (%)	ASTM C114	64.4	-	-
MgO (%)	ASTM C114	0.84	max. 6.0	max. 6.0
SO <sub>3</sub> (%)	ASTM C114	2.77	max. 3.0	max. 3.0
Na <sub>2</sub> O (%)	ASTM C114	0.32	-	-
K <sub>2</sub> O (%)	ASTM C114	0.38	-	-
TiO <sub>2</sub> (%)	ASTM C114	0.24	-	-
C <sub>3</sub> S (%)	ASTM C150	56	-	-
C <sub>2</sub> S (%)	ASTM C150	15	-	-
C <sub>3</sub> A (%)	ASTM C150	6.4	max. 8	max. 8
C <sub>4</sub> AF (%)	ASTM C150	11.2	-	-
Equivalent Alkalies (%)	ASTM C150	0.57	max. 0.60	max. 0.60
C <sub>4</sub> AF + 2(C <sub>3</sub> A) (%)	ASTM C150	24.1	-	-
C <sub>3</sub> S + 4.75(C <sub>3</sub> A) (%)	ASTM C150	86.6	max. 100	-
Loss on Ignition (%)	ASTM C114	2.8	max. 3.0	max. 3.0
Insoluble Residue (%)	ASTM C114	0.20	max. 0.75	max. 0.75
Free Calcium Oxide (%)	ASTM C114	0.38	-	-
CO <sub>2</sub> in Cement (%)	ASTM C114	1.68	-	-
CaCO <sub>3</sub> in Limestone (%)	ASTM C114	96	min. 70	min. 70
Limestone in Cement (%)	ASTM C150	4.0	max. 5.0	max. 5.0
Vicat Setting Time				
Initial (minutes)	ASTM C191	98	min. 45 max. 375	min. 45 max. 375
Final (minutes)	ASTM C191	201	-	-
Blaine Fineness (m <sup>2</sup> /kg)	ASTM C304	398	min. 280	min. 280
+325 mesh	ASTM C430	1.5	-	-
Air Content (%)	ASTM C185	7.05	max. 12	max. 12
Autoclave Expansion (%)	ASTM C151	-0.01	max. 0.80	max. 0.80
Compressive Strength		MPa / psi		
3 Day	ASTM C109/109M	30.3 / 4387	min. 12.0	min. 12.0
7 Day	ASTM C109/109M	35.9 / 5208	min. 19.0	min. 19.0
28 Day (previous month)	ASTM C109/109M	42.5 / 6169	-	-

This will certify that the above described cement meets the standard chemical and physical requirements of ASTM Specification C-150-07 for Type I and Type II Low Alkali Portland Cements and AASHTO Specification M-85-07 for Type I Low Alkali Portland Cement.

Bileen M. Jang  
Quality Control Manager/Mill Engineer



August 13, 2010

Figure 4-53 Gallup Creek Portland cement mill certificate.

Project 7911  
 Pier 1 Shaft S

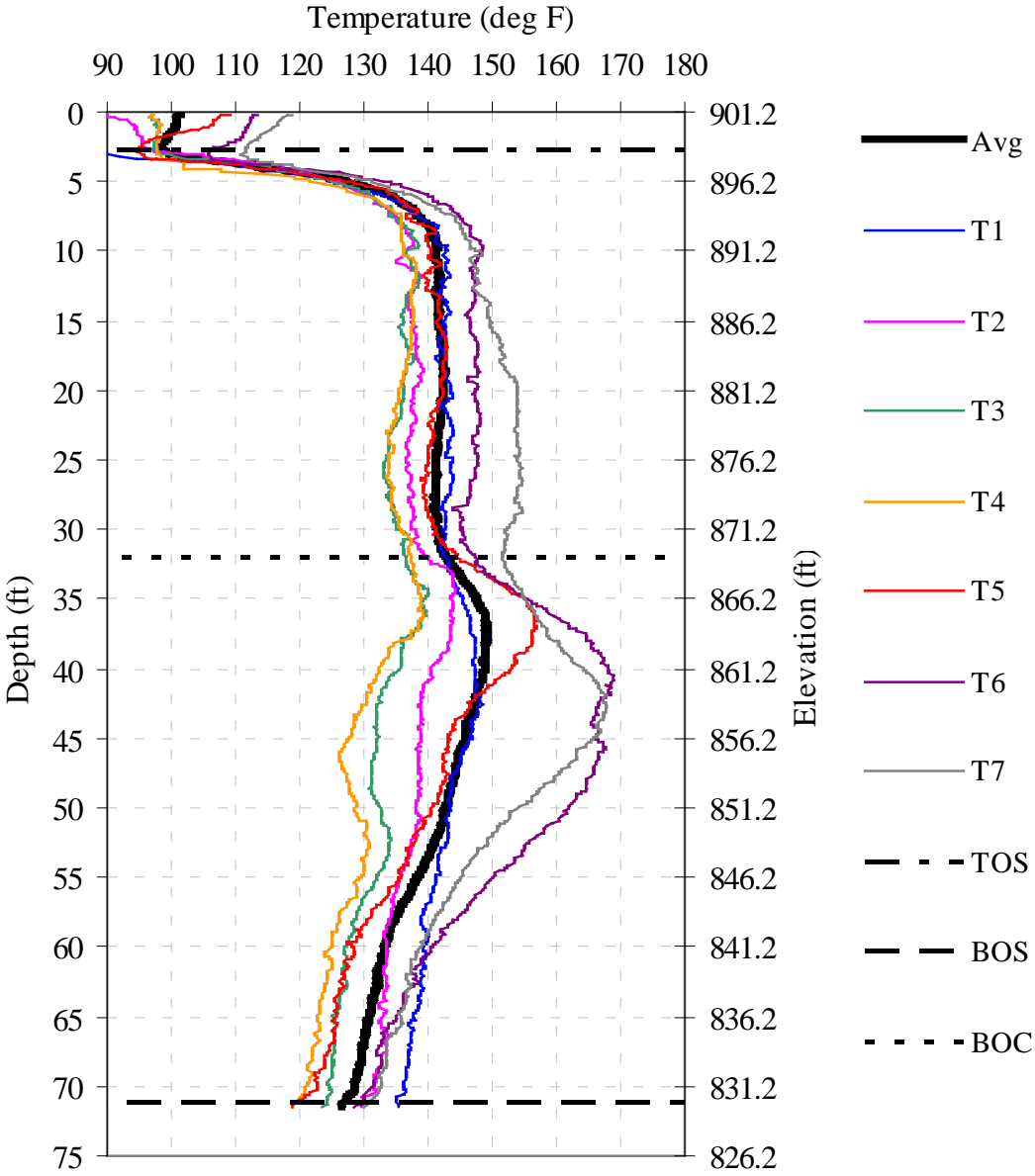


Figure 4-54 Measured tube temperatures versus depth (Gallup River Pier 1 Shaft S).

Project 7911  
 Pier 1 Shaft S

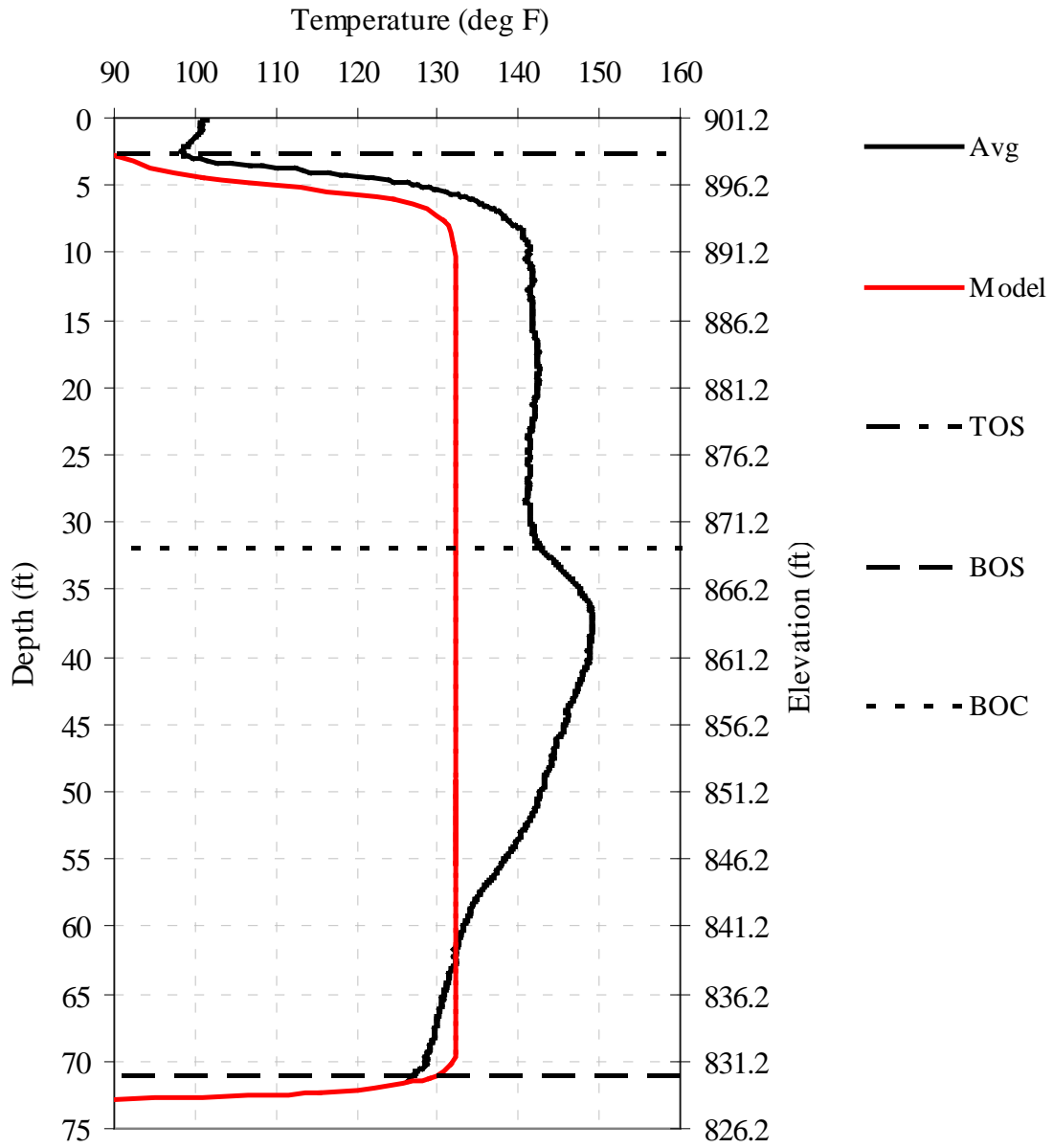


Figure 4-55 Measured and modeled temperature versus depth (Gallup Creek Pier 1 Shaft S).

Project 7911  
 Pier 1 Shaft S

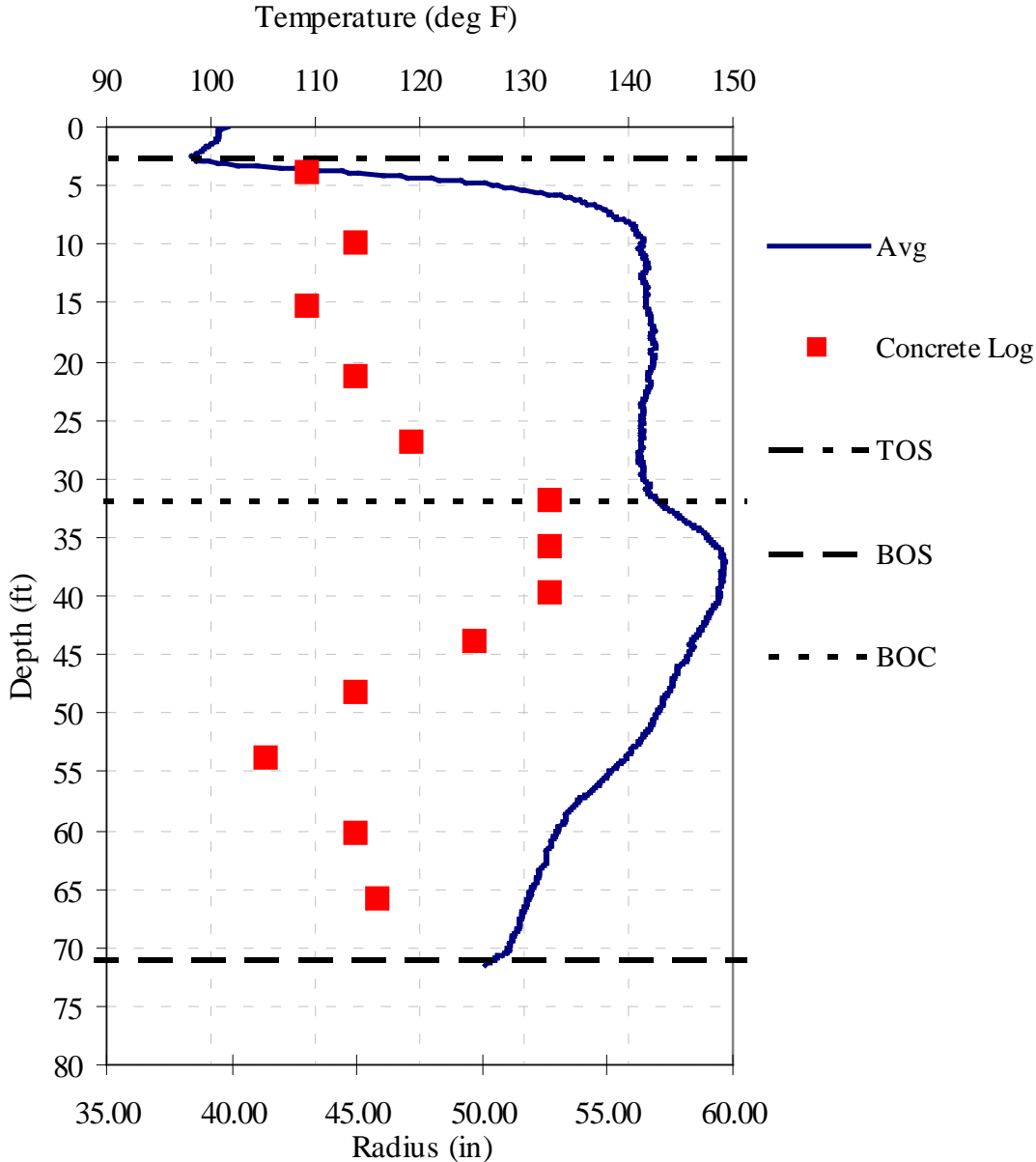


Figure 4-56 Concrete Placement Log versus average measured temperature (Gallup River Pier 1 Shaft S).

Project 7911  
 Pier 1 Shaft S

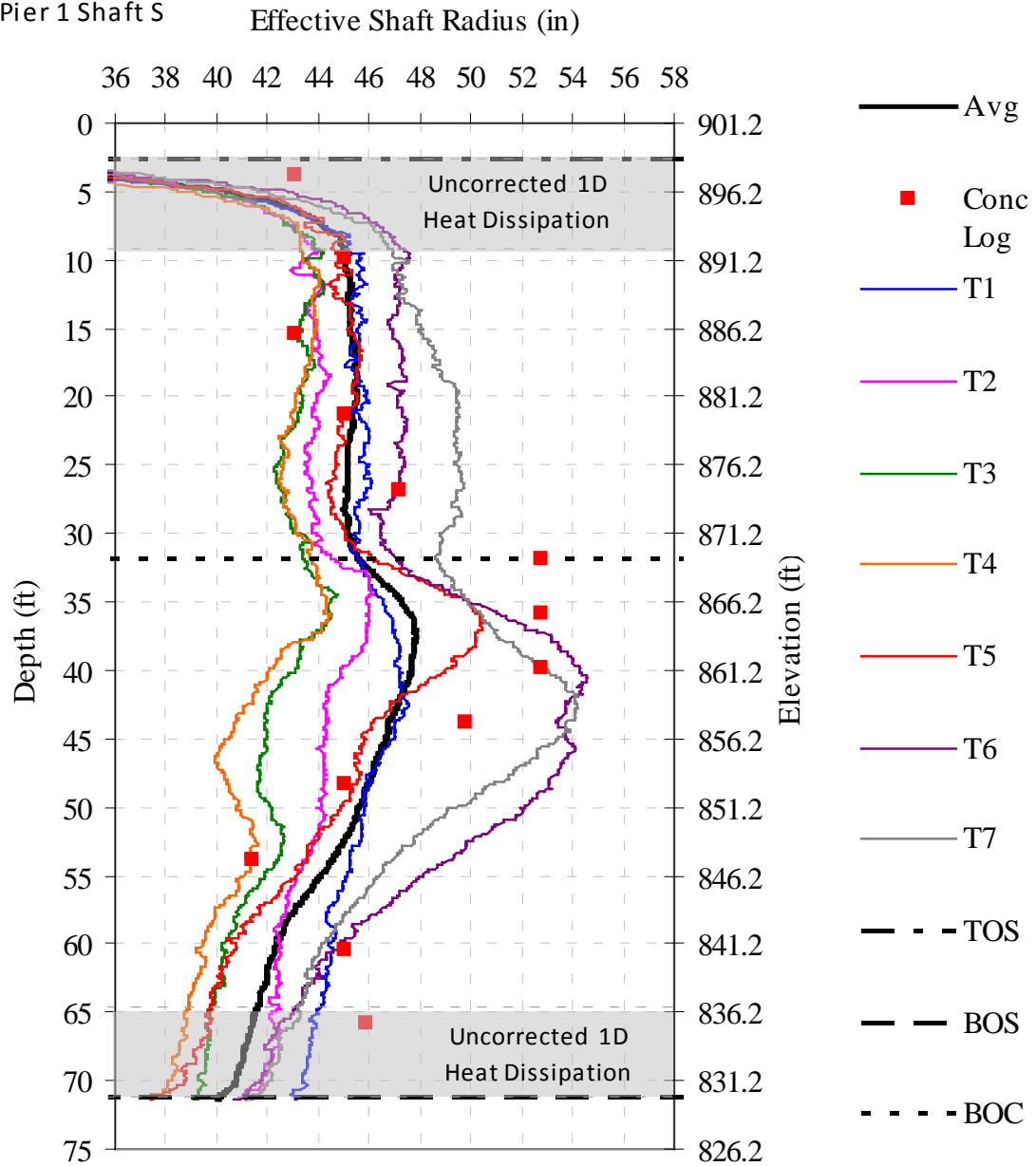


Figure 4-57 Effective shaft radius showing cage alignment uncorrected for axial heat dissipation (Gallup River Pier 1 Shaft S).

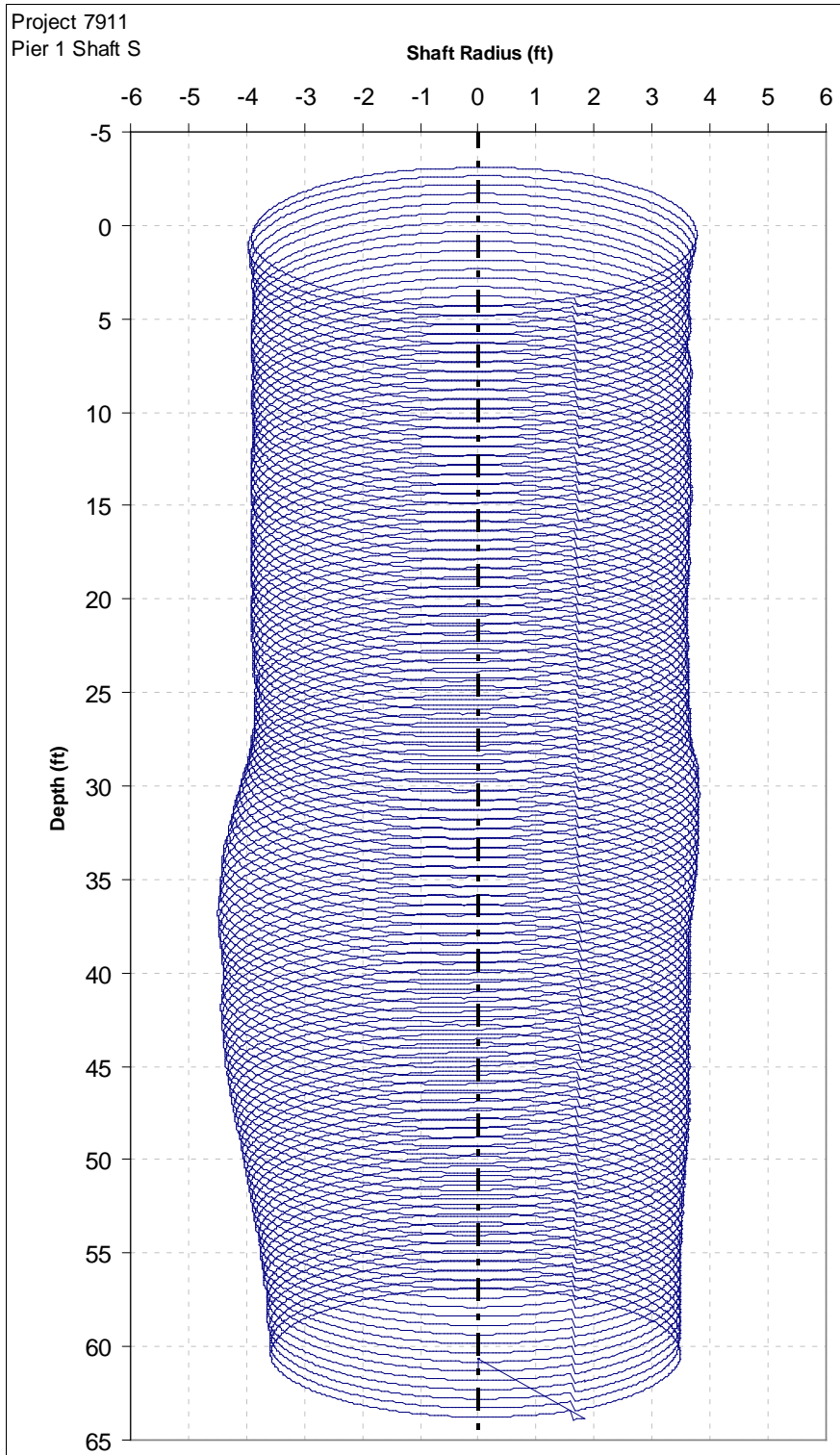


Figure 4-58 3-D rendering from tube spacings and effective radius calculations (Gallup River Pier 1 Shaft S).



## **4.7 Project 7852: Hyak to Snowshed**

Thermal testing was conducted on a shaft at Pier 4 for the I-90 Hyak to Snowshed bridge replacement project. The test shaft was 9 foot in diameter and equipped with 9 access tubes in general accordance with standard practice for tube plurality in State specifications. The tube identification / numbering used for this project assumed the northerly most tube to be No. 1 and increased in value in a clockwise fashion looking down on to the shaft top. Standard infrared thermal testing was conducted on Shaft B within Pier 4. Standard testing protocols were followed to verify reproducibility of each scan.

### **4.7.1 Thermal Modeling**

Thermal modeling was conducted based on the concrete mix design (Figures 4-59 through 4-62). The mix design information was used to create the input hydration energy parameters using the **a**, **b**, and **t** method outlined by Schindler (2005). The model parameters used in the T3DModel software were 0.769, 0.479, and 26.298, respectively with an overall energy production of 87.66 kJ per kg of total concrete mass.

### **4.7.2 Thermal Testing Pier 4 Shaft B**

The testing was performed on August 20, 2010 approximately 48 hours after concreting Shaft B. Field measurements were taken from each of the nine tubes and are presented in Figure 4-63. A model was run based on theoretical shaft dimensions (9 ft diameter) and compared to the field measurements (Figure 4-64). The average field temperature is either in line with or greater than the model indicating an effective shaft diameter of 9ft or greater from an approximate elevation of +2496 to +2387. From an approximate elevation of +2387 to +2382, the average temperature is lower than the model prediction indicating an effective shaft diameter less than 9ft. The reinforcement cage varies throughout the length of the shaft, as well. Figure 4-65 shows the average measured temperature versus the concrete placement log. The effective radius (Figure 4-66) is predicted without axial heat dissipation corrections. Figure 4-67 shows a 3-D rendered image of the as-built shaft.

### **4.7.3 Project 7852 Conclusions**

Based on the thermal integrity test results presented herein, the following conclusions can be drawn concerning Project 7852, Pier 4 Shaft B:

- The average field temperature is either in line with or greater than the model indicating an effective shaft diameter of 9ft or greater from an approximate elevation of +2496 to +2387.
- From an approximate elevation of +2387 to +2382, the average temperature is lower than the model prediction indicating an effective shaft diameter less than 9ft.

- The reinforcement cage alignment varies (up to approximately 2 inches) throughout the length of the shaft.



### Concrete Mix Design

Contractor Malcolm Drilling		Submitted By Tait McCutchan		Date 3/22/2010
Concrete Supplier Stoneway Concrete			Plant Location Cle Elum, WA or Easton, WA	
Contract Number 7852		Contract Name Hyak to Snowshed Vicinity Phase 1B		

This mix is to be used in the following Bid Item No(s): 108.01

Concrete Class: (check one only)  
 3000  4000  4000D  4000P  4000W  Concrete Overlay  Cement Concrete Pavement<sup>d</sup>  
 Other \_\_\_\_\_

Remarks: Sign Structure/Shaft Foundation. Target Slump 8in - 9in (Underground only as there's no air entrainment)  
Revision 1

Mix Design No. CL4KP Plant No. 818436 or C.S. Johnson

Cementitious Materials	Source	Type, Class or Grade	Sp. Gr.	Lbs/cy
Cement	Ashgrove, Seattle WA	I-II ✓	3.15	600 ✓
Fly Ash <sup>a</sup>				
GGBFS (Slag)	LAFARGE	Lafarge GGBFS 120 C989	2.87	181 ✓
Latex				
Microsilica				

Concrete Admixtures	Manufacturer	Product	Type	Est. Range (oz/cy)
Air Entrainment				
Water Reducer	WR Grace, Kent WA	WRDA 64	Type A ✓	1.0 - 50.0
High-Range Water Reducer				
Set Retarder	WR Grace, Kent WA	Recover	Type D ✓	15-115
Other				

Water (Maximum) 315 lbs/cy Is any of the water Recycled or Reclaimed?  Yes<sup>e</sup>  No

Water Cementitious Ratio (Maximum) 0.40 ✓ Mix Design Density 147.3 lbs/cf<sup>d</sup>

Design Performance	1	2	3	4	5	Average <sup>f</sup>
28 Day Compressive Strength (cylinders) psi	5,480	5,515	4,965	5,410	5,340	5,342 ✓
14 Day Flexural <sup>d</sup> Strength (beams) psi						

**Agency Use Only** (Check appropriate Box)

This Mix Design MEETS CONTRACT SPECIFICATIONS and may be used on the bid items noted above  
 This Mix Design DOES NOT MEET CONTRACT SPECIFICATIONS and is being returned for corrections

Reviewed By: Wain Sun PE Signature Date 4/3/10

DOT Form 350-949 EF  
Revised 8/08

Distribution: Original - Contractor (e-mail)  
 Copies To - State Materials Lab-Structural Materials Eng.; Regional Materials Lab; Project Inspector (e-mail)  
 Leonard Harris

Figure 4-59 Hyak concrete mix design page 1.

Mix Design No. CLAKP Plant No. 2

**Aggregate Information**

Concrete Aggregates	Component 1	Component 2	Component 3	Component 4	Component 5	Combined Gradation
WSDOT Pit No.	S304	S304				
WSDOT ASR 14-day Results (%) <sup>b</sup>	<input type="checkbox"/> Yes <input checked="" type="checkbox"/> No	<input type="checkbox"/> Yes <input checked="" type="checkbox"/> No	<input type="checkbox"/> Yes <input type="checkbox"/> No	<input type="checkbox"/> Yes <input type="checkbox"/> No	<input type="checkbox"/> Yes <input type="checkbox"/> No	
Grading <sup>c</sup>	AASHTO 8	Class 1				
Percent of Total Aggregate	52.5	47.5				100%
Specific Gravity	2.73	2.60				
Lbs/cy (ssd)	1519	1375				

**Percent Passing**

	Component 1	Component 2	Component 3	Component 4	Component 5	Combined
2 inch	100	100				100
1-1/2 inch	100	100				100
1 inch	100	100				100
3/4 inch	100	100				100 ✓
1/2 inch	100	100				100 ✓
3/8 inch	84.05	100				91.63 ✓ 100
No. 4	26.80	100				61.57 ✓ 86-100
No. 8	3.80	86.30				42.99 ✓ 39-73
No. 16	1.20	61.20				29.70 ✓ 24-54
No. 30	0	34.20				16.25 ✓ 13-39
No. 50	0	14.40				6.84 ✓ 6-29
No. 100	0	4.50				2.14 ✓ 0-21
No. 200	0.40	1.70				1.02 ✓ 0-2

Fineness Modulus: \_\_\_\_\_ (Required for Class 2 Sand)

ASR Mitigation Method Proposed<sup>d</sup>: Petrographic Analysis pass, Not Required; refer to ASA

**Notes:**

- a Required for Class 4000D and 4000P mixes.
- b Alkali Silica Reactivity Mitigation is required for sources with expansions over 0.20% - Indicate method for ASR mitigation. For expansion of 0.21% - 0.46%, acceptable mitigation can be the use of low alkali cement or 25% type F fly ash. Any other proposed mitigation method or for pits with greater than 0.45% expansion, proof of mitigating measure, either ASTM C1260 / AASHTO T303 test results must be attached. If ASTM C 1203 testing has been submitted indicating 1-year expansion of 0.04% or less, mitigation is not required.
- c AASHTO No. 467, 67, 67, 7, 8; WSDOT Class 1, Class 2; or combined gradation. See Standard Specification 9-03.1.
- d Required for Cement Concrete Pavements.
- e Attach test results indicating conformance to Standard Specification 9-25.1.
- f Actual Average Strength as determined from testing or estimated from ACI 211.

DOT Form 350-040 EF  
Revised 6/08

Figure 4-60 Hyak concrete mix design page 2.



Plant Seattle Cement Type I-II Low Alkali Date 19-Jan-10  
 Production Period December 1, 2009 - January 1, 2010 Certification No. 2009-19

**STANDARD REQUIREMENTS  
ASTM C - 150**

CHEMICAL			PHYSICAL		
Item	Spec. Limit	Test Result	Item	Spec. Limit	Test Result
SiO <sub>2</sub> (%)	A	20.9	Air content of mortar (volume %)	12 max	7.3
Al <sub>2</sub> O <sub>3</sub> (%)	6.0 max	3.9	Blaine fineness (m <sup>2</sup> /kg)	280 min	411
Fe <sub>2</sub> O <sub>3</sub> (%)	6.0 max	3.4		420 max	
CaO (%)	A	64.6	% Passing 325 mesh	A	95.9
MgO (%)	6.0 max	1.0	Autoclave expansion (%)	0.80 max	0.02
SO <sub>3</sub> (%)	3.0 max	2.7	Compressive strength MPa (PSI)	min:	
Ignition loss (%)	3.0 max	1.5	1 Day	A	14.8 (2142)
Na <sub>2</sub> O (%)	A	0.35	3 Days	12.0	25.0 (3627)
K <sub>2</sub> O (%)	A	0.28	7 Days	19.0	31.6 (4588)
Insoluble residue (%)	0.75 max	0.18	Time of setting (minutes)		
CO <sub>2</sub> (%)	A	1.1	Vicat Initial not less than	45	95
Limestone (%)	5.0 max	2.5	Final not more than	375	194
CaCO <sub>3</sub> in limestone (%)	70 min	98	Heat of hydration (kJ/kg)		
Potential (%)			7 Days	B	89
C3S	A	80			
C2S	A	14			
C3A	8 max	5			
C4AF	A	10			
C4AF+ 2(C3A)	A	19			
C3S + 4.75(C3A)	100 max	82			

**OPTIONAL REQUIREMENTS  
ASTM C - 150**

CHEMICAL			PHYSICAL		
Item	Spec. Limit	Test Result	Item	Spec. Limit	Test Result
Equivalent alkalies (%)	0.60 max	0.93	False set (%)	50 min	87

<sup>A</sup>Not applicable

<sup>B</sup>Test result represents most recent value and is provided for information only.

We certify that the above described cement, at the time of shipment, meets the chemical and physical requirements of the ASTM C 150-07 specification.

Signature:   
 Edward C. Rafacz

Title: Chief Chemist

3801 E Marginal Way S, Seattle, WA 98134; Ph: (206) 623-5596; Fax: (206) 623-5355

Figure 4-61 Hyak cement mill certificate.

**LAFARGE** Cement Test Report  
CEMENT

Mill Test Report Number: SEA\_NEWCEM\_FEB10  
 YEAR: 2010  
 MONTH: February  
 PLANT: Seattle  
 CEMENT TYPE: Grade 100 NewCom

Reference Cement		Slag			
Fineness by Air Permeability (m <sup>2</sup> /kg; ASTM C204)	389	Fineness by Air Permeability (m <sup>2</sup> /kg; ASTM C204)	433		
Fineness by 45 µm (No. 325) Sieve (% retain; ASTM C430)	4.1	Fineness by 45 µm (No. 325) Sieve (% retain; ASTM C430)	2.7		
Compressive Strength (ASTM C109/C109 M)	psi	Compressive Strength (ASTM C109/C109 M)	psi	SAI	Min
7-day	4,840	7-day	4,045	84	75
28-day (previous month's data)	5,860	28-day	6,050	107	95
	<u>Actual</u>		<u>Actual</u>	<u>Max Limit</u>	
Total Alkalies (Na <sub>2</sub> O + 0.658 K <sub>2</sub> O) (%, ASTM C114)	0.88				
	<u>Max Limit</u>				
	0.9	Specific Gravity (Mg/m <sup>3</sup> ; ASTM C188)	2.89		
		Air Content of Mortar (%, ASTM C185)	<u>Actual</u>	<u>Max Limit</u>	
			8.9	12	
		Sulfated Sulfur (% S, ASTM C114)	0.7	2.5	
		Sulfate Ion (% as SO <sub>3</sub> , ASTM C114)	3.2	4	

Slag	
<b>CHEMICAL ANALYSIS</b>	<b>Percent</b>
Silica Dioxide (SiO <sub>2</sub> ; ASTM C114)	34
Ferric Oxide (Fe <sub>2</sub> O <sub>3</sub> ; ASTM C114)	0.59
Aluminum Oxide (Al <sub>2</sub> O <sub>3</sub> ; ASTM C114)	13
Calcium Oxide (CaO; ASTM C114)	43.5
Sulfur Trioxide (SO <sub>3</sub> ; ASTM C114)	4.9
Magnesium Oxide (MgO; ASTM C114)	5.5
Potassium Oxide (K <sub>2</sub> O; ASTM C114)	0.49
Titanium Oxide (TiO <sub>2</sub> ; ASTM C114)	0.59
Loss on Ignition (L.O.I.; ASTM C114)	2.0

The ground granulated blast furnace slag complies with the current specification of the chemical physical requirement of ASTM C-989, AASHTO M-302 for grade 100 Ground Granulated Blast Furnace Slag (GGBFS).


Certified by:  
  
 Daniel Waldron  
 Quality Control Laboratory Supervisor

Figure 4-62 Hyak slag mill certificate

Project 7852  
 Pier 4 Shaft B

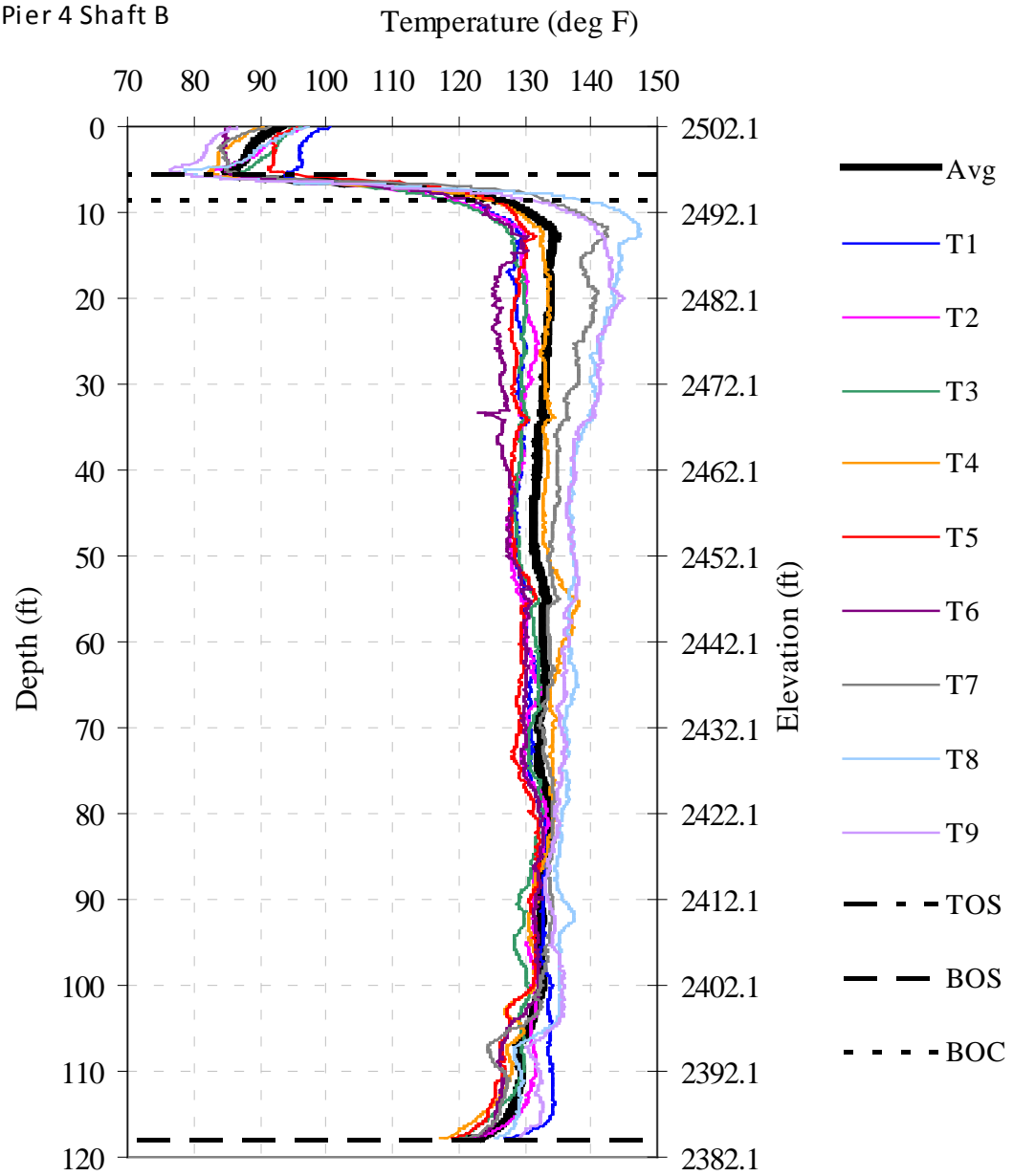


Figure 4-63 Measured tube temperatures versus depth (Hyak Pier 4 Shaft B).

Project 7852  
 Pier 4 Shaft B

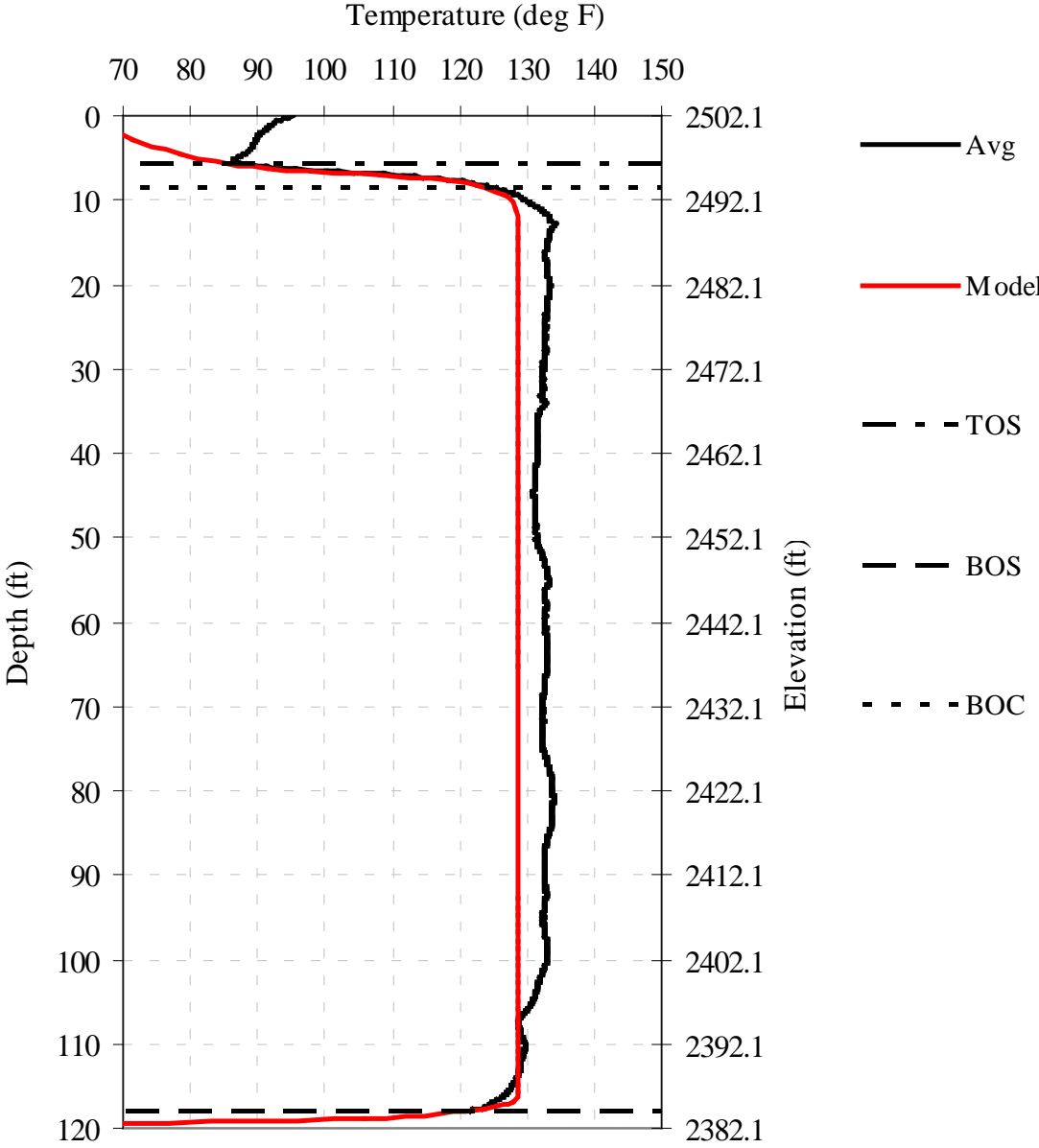


Figure 4-64 Measured and modeled temperature versus depth (Hyak Pier 4 Shaft B).

Project 7852  
 Pier 4 Shaft B

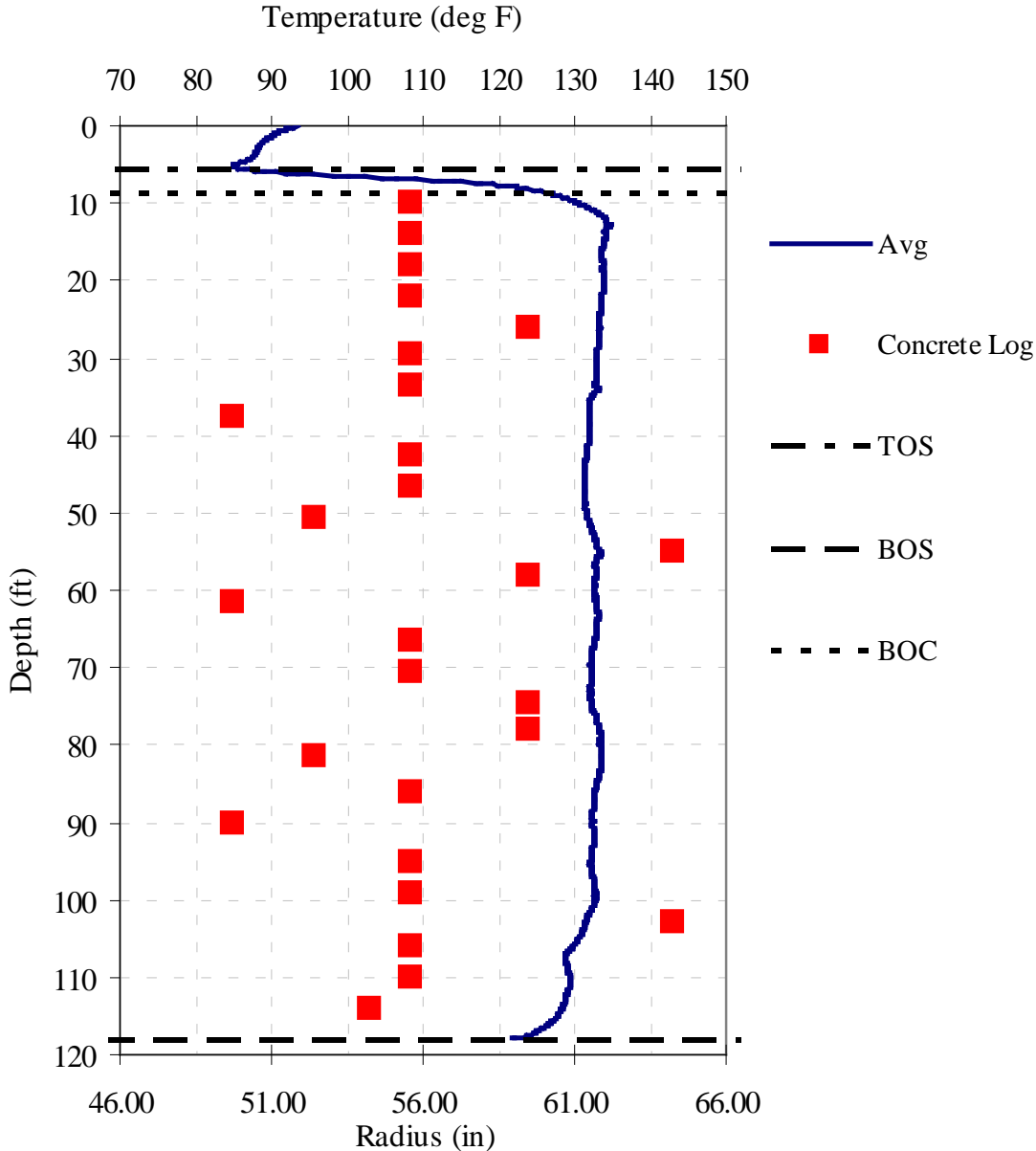


Figure 4-65 Concrete Placement Log versus average measured temperature (Hyak Pier 4 Shaft B).



Project 7852  
 Pier 4 Shaft B

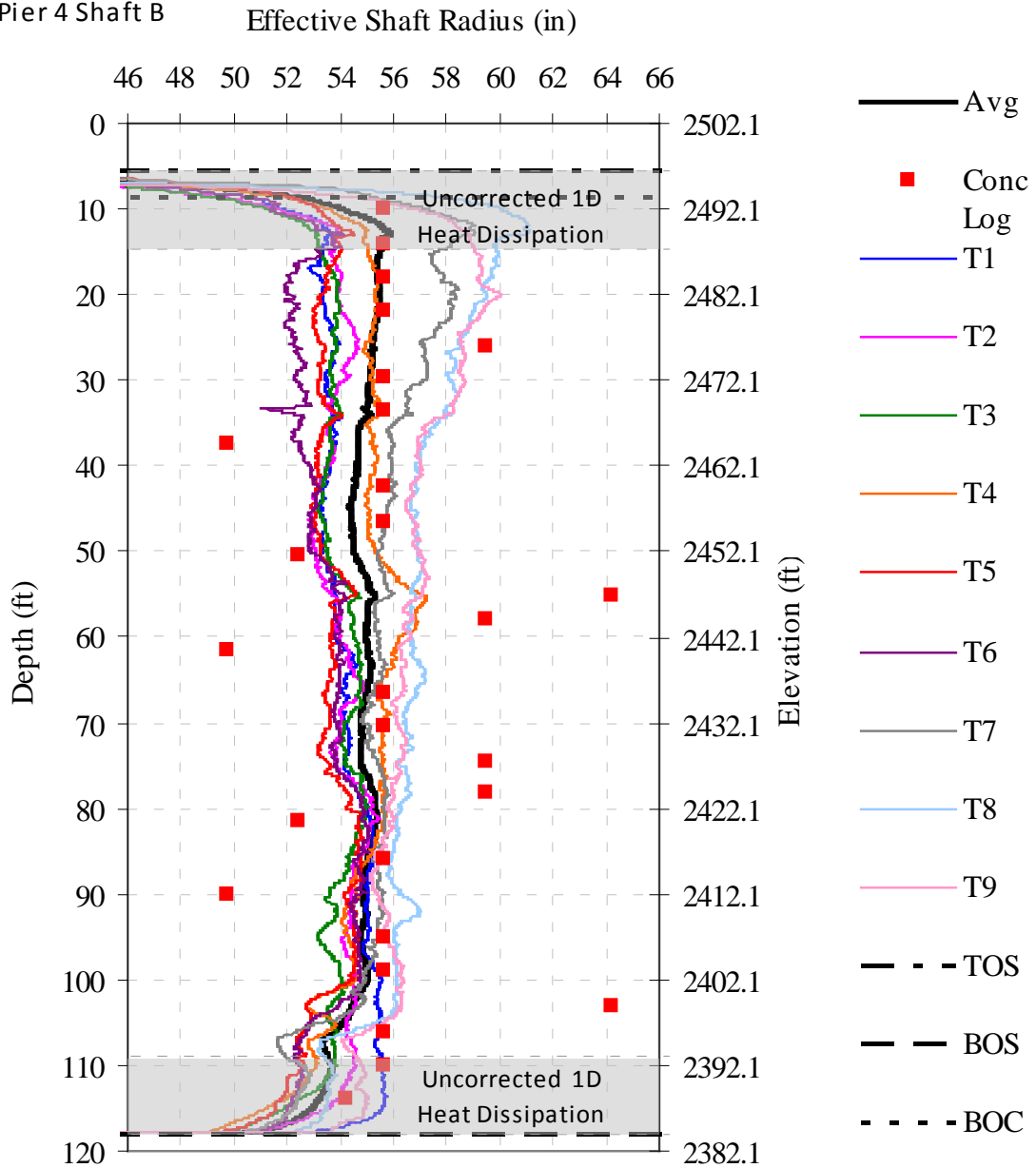


Figure 4-66 Effective shaft radius showing cage alignment uncorrected for axial heat dissipation (Hyak Pier 4 Shaft B).

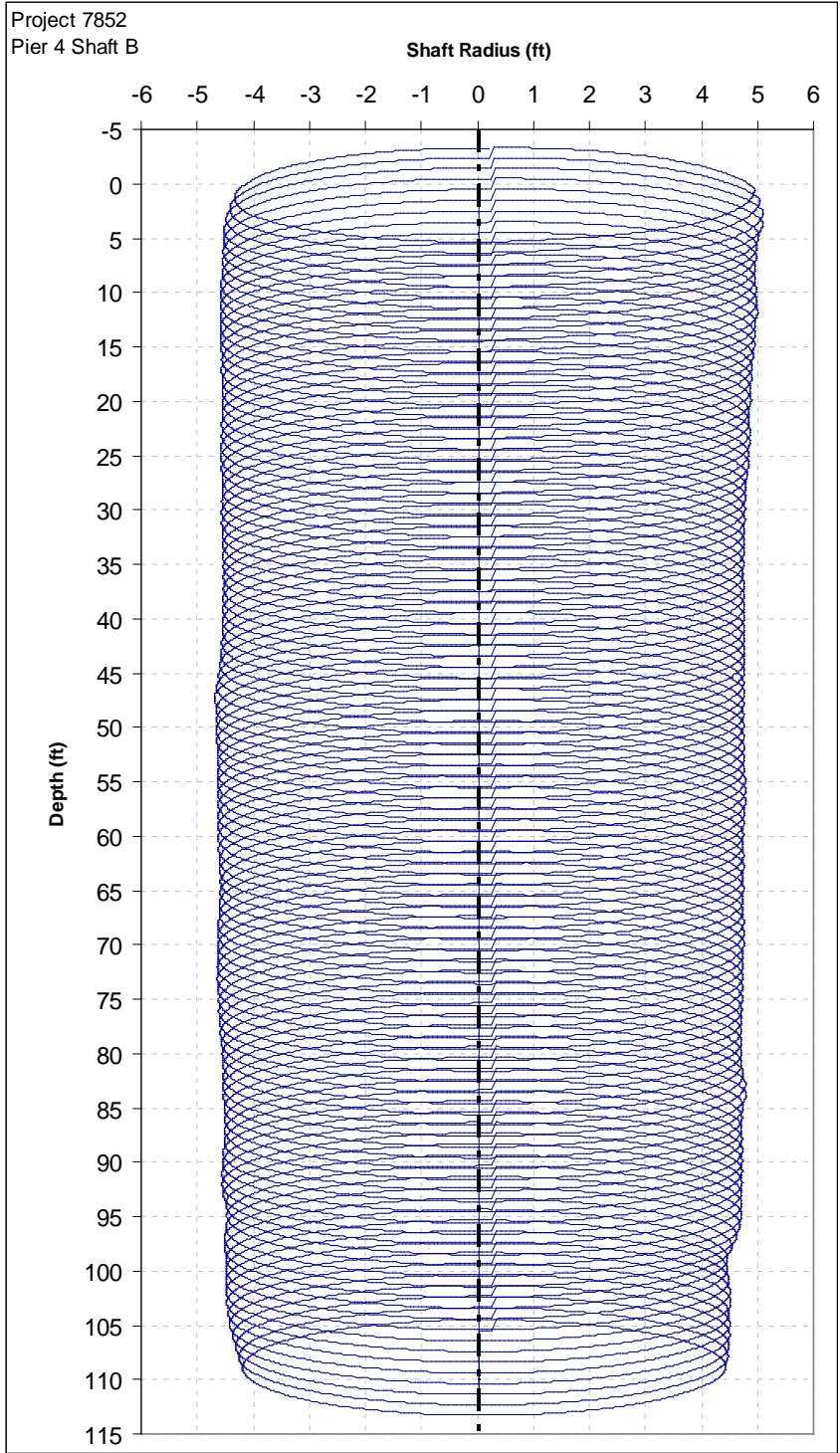


Figure 4-67 3-D rendering from tube spacings and effective radius calculations (Hyak Pier 4 Shaft B).

## **4.8 Project 7926: Manette Bridge**

Thermal testing was conducted on a shaft at Pier 2 for the Manette bridge replacement project. Thermal testing was directed due to soil cave-in from poor sidewall stability during excavation. The test shaft was 12 foot in diameter and equipped with 12 access tubes in general accordance with standard practice for tube plurality in State specifications. The tube identification / numbering used for this project assumed the northerly most tube to be No. 1 and increased in value in a clockwise fashion looking down on to the shaft top. Standard infrared thermal testing was conducted on the South shaft within Pier 2. Standard testing protocols were followed to verify reproducibility of each scan.

### **4.8.1 Thermal Modeling**

Thermal modeling was conducted based on the concrete mix design (Figures 4-68 through 4-70). The mix design information was used to create the input hydration energy parameters using the **a**, **b**, and **t** method outlined by Schindler (2005). The model parameters used in the T3DModel software were 0.753, 0.602, and 19.102, respectively with an overall energy production of 71.69 kJ per kg of total concrete mass (current parameters).

### **4.8.2 Thermal Testing Pier 2 Shaft South**

The testing was performed on September 13, 2010 approximately 81 hours after concreting the South shaft. Field measurements were taken from each of the twelve tubes and are presented in Figure 4-71. Field measurements indicate a large bulge near tubes 11 and 12 from an approximate elevation of -36ft to -66ft. A model was run based on theoretical shaft dimensions (12 ft diameter) and compared to the field measurements (Figure 4-72). The average field temperature is either in line with or greater than the model indicating an effective shaft diameter of 12ft or greater.

Figure 4-73 shows the average measured temperature versus the concrete placement log. The effective radius (Figure 4-74) is predicted without axial heat dissipation corrections. Figure 4-75 shows a 3-D rendered image of the as-built shaft.

### **4.8.3 Project 7926 Conclusions**

Based on the thermal integrity test results presented herein, the following conclusions can be drawn concerning Project 7926, Pier 2 Shaft South:

- Thermal testing was directed after sidewall soil stability problems were encountered during excavation of the shaft.
- The average field temperatures exceed the model prediction (12ft diameter model) indicating an effective shaft diameter 12ft or greater throughout the length of the shaft.

- Field measurements indicate a large bulge near tubes 11 and 12 from an approximate elevation of -36ft to -66ft, which confirms the field inspector's observations during excavation.
- The reinforcement cage alignment varies (up to approximately 3 inches) throughout the length of the shaft.



P.O. BOX 698 · POULSBORO, WA 98370

Design Mix No: **CL4000P**

Design Strength: **4000 PSI**  
@ **28 Days**

Material	Weight per Cubic Yard	Volume
<b>Cementitious:</b>	<b>700 lbs</b>	<b>3.76</b>
Cement:	600 lbs	
Fly Ash:	100 lbs	
Silica Fume:	0 lbs	
<b>Coarse Aggregate:</b>	<b>1830 lbs</b>	<b>10.86</b>
#467	0 lbs	
#67	0 lbs	
#8	1830 lbs	
<b>Fine Aggregate:</b>	<b>1290 lbs</b>	<b>7.72</b>
<b>Water:</b>	<b>32.0 gal</b>	<b>4.27</b>
<b>Air:</b>	<b>1.5 percent</b>	<b>0.41</b>
<b>Air Entrainment:</b>	<b>0.00 oz/cwt</b>	
Polyheed:	8.0 oz/cwt	
VMA 358:	0.0 oz/cwt	
Delvo:	3.0 oz/cwt	
FC- 7500	0.0 oz/cwt	
Other:	0.0 oz/cwt	
Yield:		<b>27.02 cu ft</b>
W/C:		<b>0.38</b>
Unit Weight:		<b>151.26</b>
Slump :		<b>8"</b>

Note: This mix is per WSDOT standard specifications  
Rheomac UW450 may be added to this mix per manufactures recommendation

Bremerton (360) 674-3154 · Toll Free 1-800-480-3286 · Fax (360) 674-3276

Figure 4-68 Manette concrete mix design.

061.01, 148.22.03



Lehigh Cement, a division of Lehigh Hanson Materials Limited  
 7777 Ross Road  
 Delta, British Columbia, V4G 1B3  
 P.O. Box 950, V4K 3S9  
 ph: 604.946.0411

**MILL TEST REPORT**

Cement Type: ASTM Type III, AASHTO Type I  
 Low Alkali Portland Cement

Plant: Delta, BC

Certificate #: D2-384

Production Period:	Apr 01 2010 Apr 30 2010	Test Result	ASTM C150-07 Specification	AASHTO M 85-07 Specification
SiO <sub>2</sub> (%)	ASTM C114	20.0	-	-
Al <sub>2</sub> O <sub>3</sub> (%)	ASTM C114	4.91	max. 6.0	-
Fe <sub>2</sub> O <sub>3</sub> (%)	ASTM C114	3.75	max. 6.0	-
Cr <sub>2</sub> O <sub>3</sub> (%)	ASTM C114	64.4	-	-
MgO (%)	ASTM C114	0.78	max. 5.0	max. 6.0
SO <sub>3</sub> (%)	ASTM C114	2.77	max. 3.0	max. 3.0
Na <sub>2</sub> O (%)	ASTM C114	0.28	-	-
K <sub>2</sub> O (%)	ASTM C114	0.30	-	-
TiO <sub>2</sub> (%)	ASTM C114	0.26	-	-
C <sub>3</sub> S (%)	ASTM C150	55	-	-
C <sub>2</sub> S (%)	ASTM C150	16	-	-
C <sub>3</sub> A (%)	ASTM C150	6.7	max. 8	max. 8
C <sub>4</sub> A <sub>F</sub> (%)	ASTM C150	11.4	-	-
Equivalent Alkalies (%)	ASTM C150	0.46	max. 0.60	max. 0.60
C <sub>4</sub> A <sub>F</sub> + 2(C <sub>3</sub> A) (%)	ASTM C150	24.7	-	-
C <sub>3</sub> S + 4.75(C <sub>3</sub> A) (%)	ASTM C150	66.3	max. 70.0	-
Loss on Ignition (%)	ASTM C114	2.9	max. 3.0	max. 3.0
Insoluble Residue (%)	ASTM C114	0.18	max. 0.75	max. 0.75
Free Calcium Oxide (%)	ASTM C114	0.44	-	-
CO <sub>2</sub> in Cement (%)	ASTM C114	1.83	-	-
CaCO <sub>3</sub> in Limestone (%)	ASTM C114	96	min. 70	min. 70
Limestone in Cement (%)	ASTM C150	4.3	max. 5.0	max. 5.0
Vicat Setting Time				
Initial (minutes)	ASTM C191	99	min. 45 max. 375	min. 45 max. 375
Final (minutes)	ASTM C191	203	-	-
Blaine Fineness (m <sup>2</sup> /kg)	ASTM C304	393	min. 280	min. 280
+325 mesh	ASTM C304	1.4	-	-
Air Content (%)	ASTM C188	6.96	max. 12	max. 12
Autoclave Expansion (%)	ASTM C151	-0.01	max. 0.80	max. 0.80
Compressive Strength		MPa / psi		
3 Day	ASTM C109/T09M	20.5 / 4137	min. 13.0	min. 13.0
7 Day	ASTM C109/T09M	34.9 / 5060	min. 19.0	min. 19.0
28 Day (previous month)	ASTM C109/T09M	41.6 / 6026	-	-

This will certify that the above described cement meets the standard chemical and physical requirements of ASTM Specification C-150-07 for Type I and Type II Low Alkali Portland Cements and AASHTO Specification M-85-07 for Type I Low Alkali Portland Cement.

Eileen M. Jang  
 Quality Control Manager/Mill Engineer

May 12, 2010

**QPL-0015**  
**RJM**

Figure 4-69 Manette Portlant cement mill cert.



Cement

FLY ASH TEST REPORT

Analysis by: Lafarge Seattle Concrete Lab
Sample from : Centralia Power Plant
Average Analysis: May 1st - May 31st 2010
Test Report Number 6-10

Chemical Analysis

Table with 2 columns: Component Name and Percentage. Components include Silicon Dioxide (SiO2), Aluminum Oxide (Al2O3), Iron Oxide (Fe2O3), Total (SiO2) + (Al2O3) + (Fe2O3), Sulphur Trioxide (SO3), Calcium Oxide (CaO), Magnesium Oxide, Moisture Content, Loss on Ignition, Available Alkali as Equiv. Na2O, and Total Alkalies as Equivalent Na2O.

Physical Analysis

Table with 2 columns: Component Name and Percentage. Components include Fineness Retained on 45 um (No. 325 Sieve), Strength Activity Index with Portland Cement, % of Control at 7 Days, % of Control at 28 Days, Water Requirement, Percent of Control, Autoclave Expansion, and Density.

Uniformity Requirements

Table with 2 columns: Component Name and Percentage. Components include Density, Variation from Average and Fineness 45um Sieve, Variation from Average.

We hereby certify that the composite fly ash sample above meets the chemical and physical requirements of ASTM C618-08 and AASHTO M295-07 for class F and C fly ash.

Certified: Robert S. Shapiro

WESTERN REGION
5400 West Marginal Way SW, Seattle, Washington 98106-1517
Office: 206.923.0098 or 800.477.0100 Fax: 206.923.0388

Figure 4-70 Manette fly ash mill cert.

Project 7926  
Pier 2 Shaft S

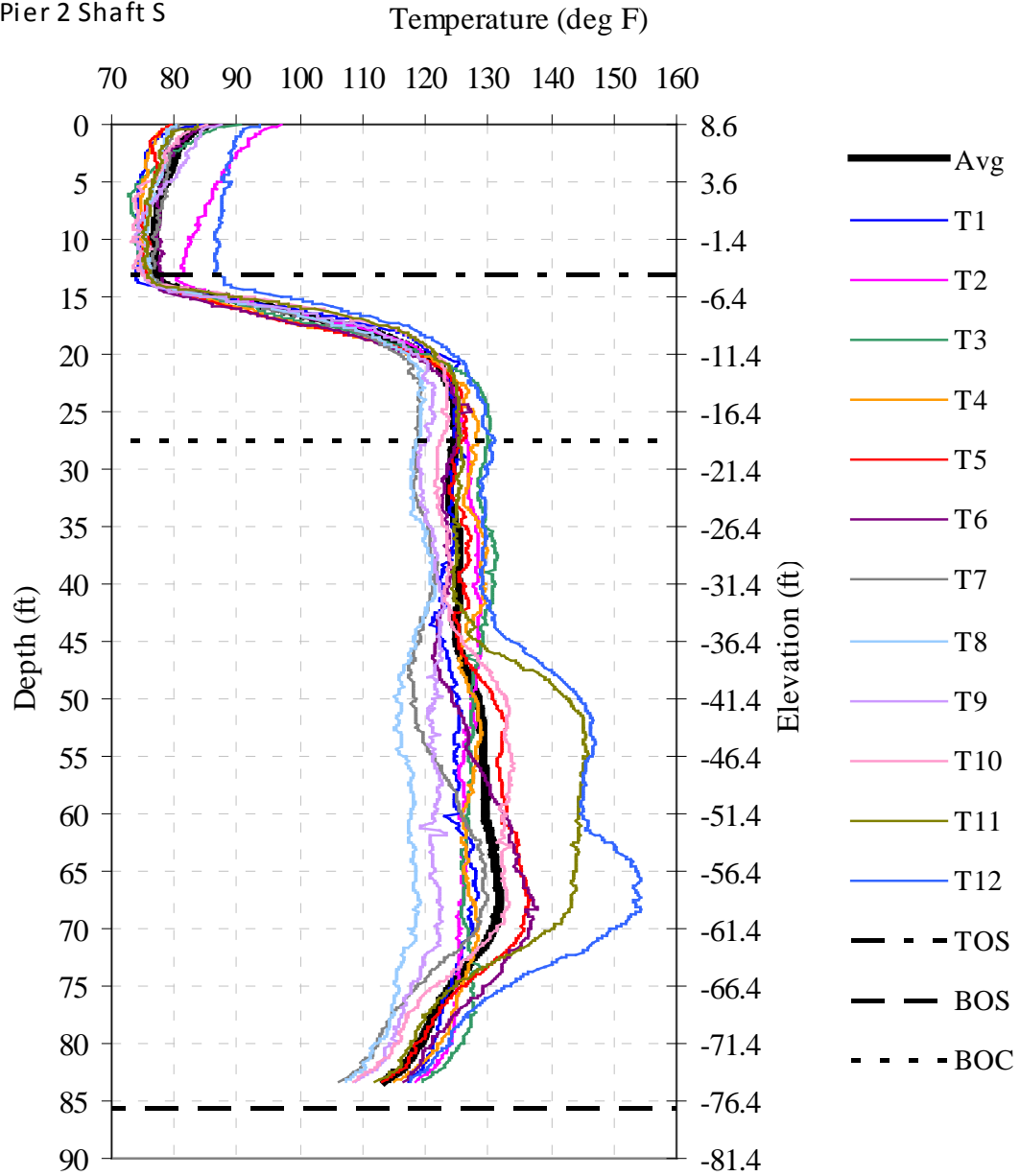


Figure 4-71 Measured tube temperatures versus depth (Manette Pier 2 Shaft S).



Project 7926  
 Pier 2 Shaft S

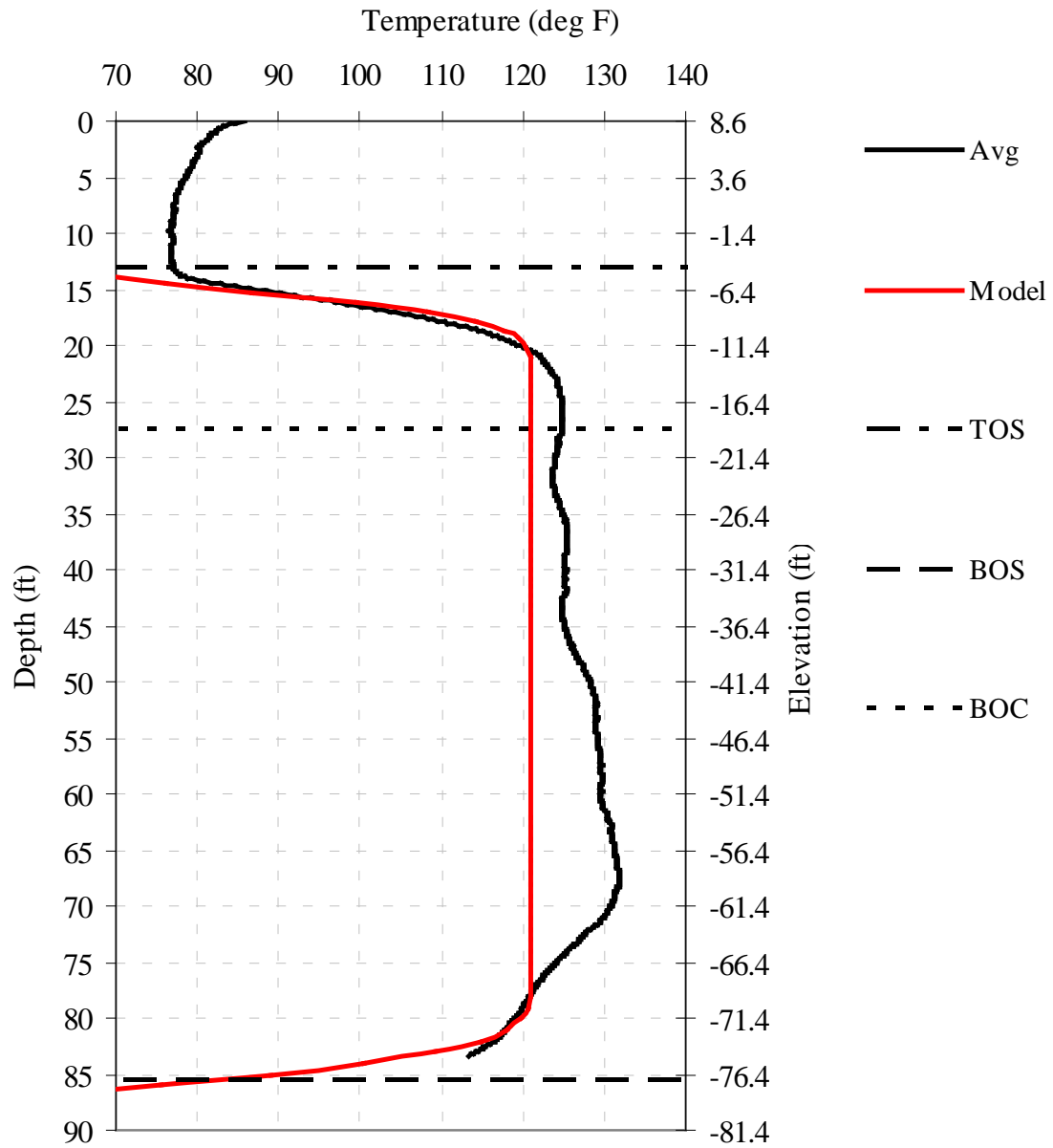


Figure 4-72 Measured and modeled temperature versus depth (Manette Pier 2 Shaft S).

Project 7926  
 Pier 2 Shaft S

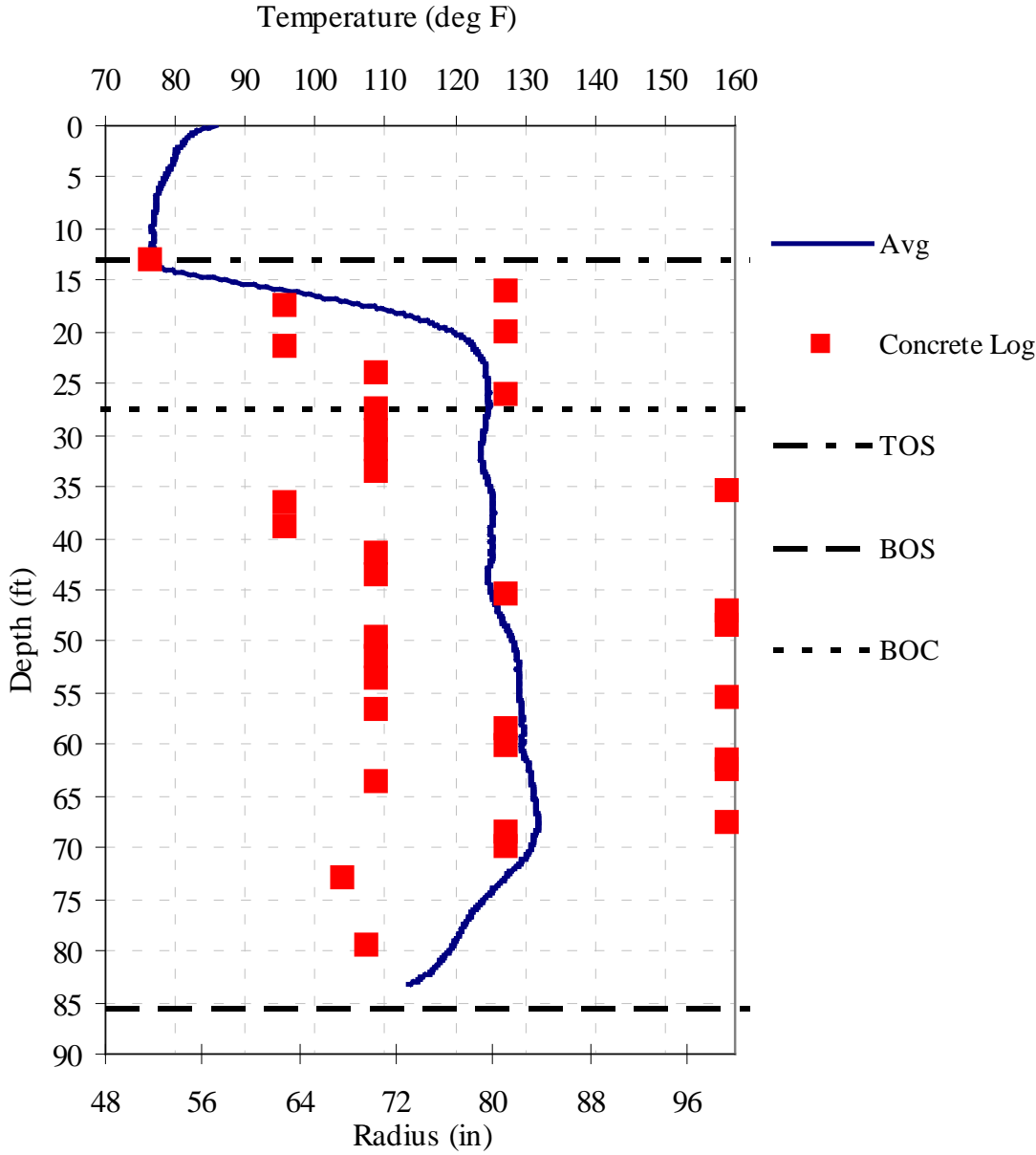


Figure 4-73 Concrete Placement Log versus average measured temperature (Manette Pier 2 Shaft S).

Project 7926  
 Pier 2 Shaft S

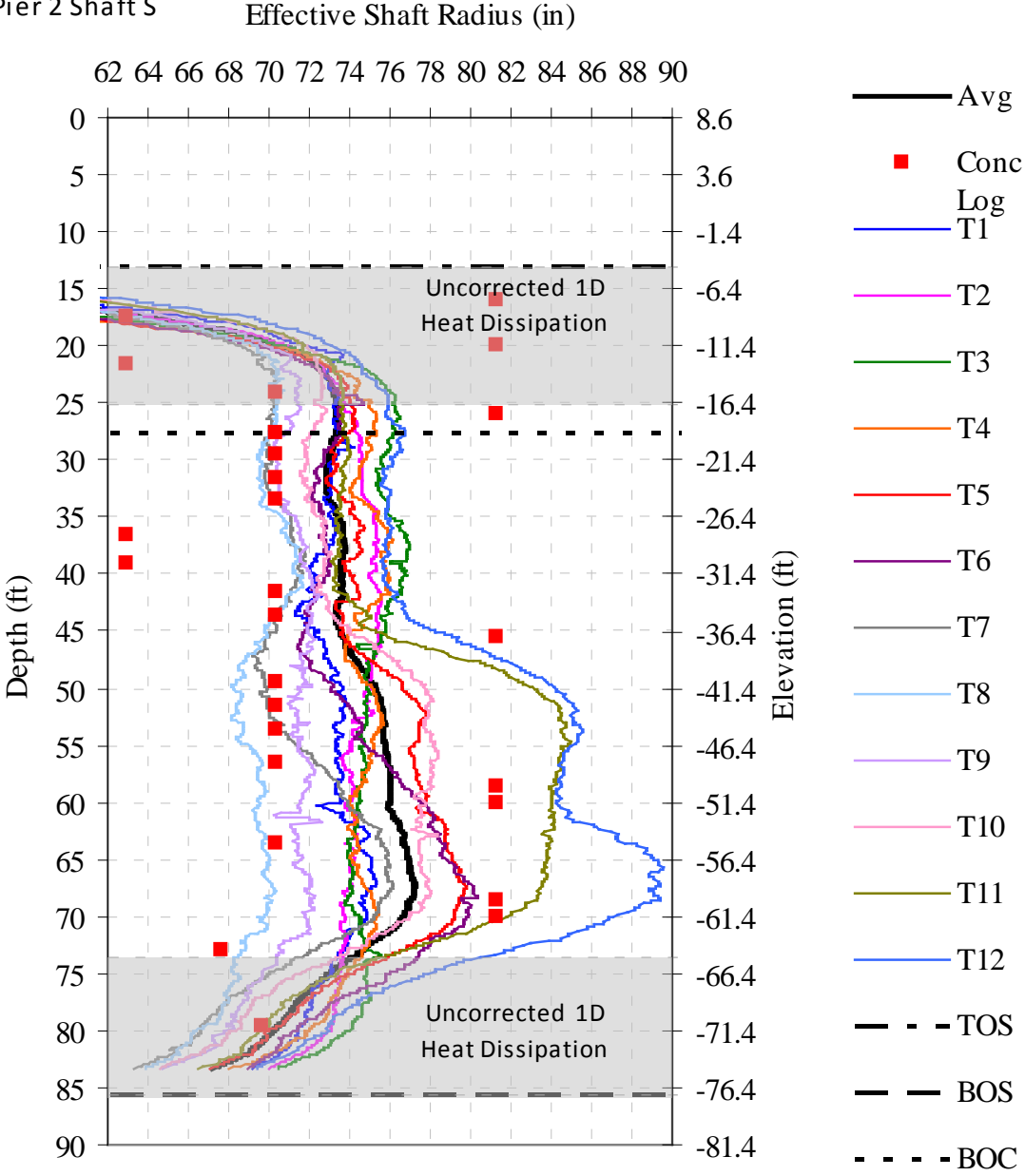


Figure 4-74 Effective shaft radius showing cage alignment uncorrected for axial heat dissipation (Manette Pier 2 Shaft S).

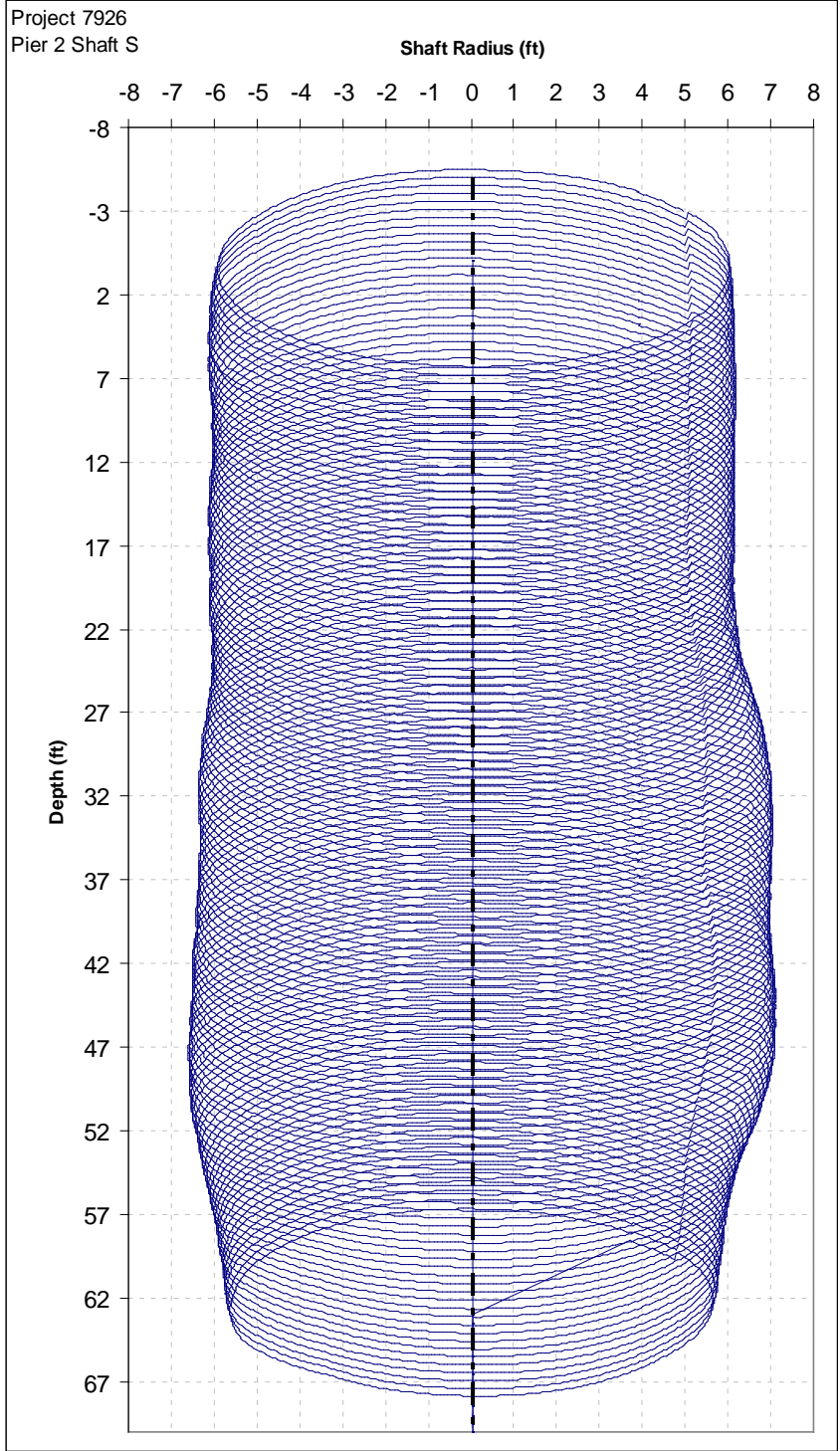


Figure 4-75 3-D rendering from tube spacings and effective radius calculations (Manette Pier 2 Shaft S).

## *Chapter Five: Recommendations and Conclusions*

### **5.1 Overview**

Over the past 3 decades, a trend toward higher quality assurance in constructed drilled shafts has moved from monitoring only concrete quantities to refined slurry properties and post-construction, non-destructive testing. Although not always practical, the use of multiple test methods can provide more information and better assessment of shaft acceptability. These methods vary in the types of information obtained as well as the regions of the shaft that can be tested. Recognizing the limitations of state-of-the-art quality assurance methods to inspect these subsurface concrete columns, the Washington State Department of Transportation opted to entertain other technologies for their assessment. As a result, a relatively new testing method that uses the energy expended from hydrating concrete (and the associated temperature signature) was selected for this study. This thermal integrity approach provides an overall perspective of the shaft based on the presence or absence of intact heat producing concrete. The shaft shape, cage placement, cover and concrete health can all be addressed.

As with other test methods thermal integrity profiles identify a normal baseline temperature; GGL and CSL identify a normal baseline gamma count or arrival time, respectively. From these measurements physical parameters are estimated (density, GGL; compression wave velocity, CSL). TIP measurements verify the presence of curing cementitious materials from which a volume of intact concrete is estimated. Consequently, predictions of normal density, velocity, or temperature can be made prior to or after testing as a measuring stick of normalcy but in reality local variations from the shaft norm are more reasonable and practical. This is often the mode of evaluation for thermal testing.

Several levels of analysis can be performed. *Level 1* begins with a qualitative review of the temperature measurements which can identify top and bottom of shaft elevations, cage alignment, and gross section changes. *Level 2* makes use of construction and concreting logs to produce correlations between diameter and temperature which identify the final location of the poured concrete volume. *Level 3* involves numerical modeling of the shaft dimensions, the concrete properties, and the surrounding environment. The majority of TIP results do not require modeling for interpretation; rather, an understanding of the normal temperature profiles and features is necessary. However, results of numerical modeling can be directly compared to field measurements using the recent advancements in hydration energy predictions for modern concrete constituents. Finally, *Level 4* applies signal matching modeling techniques to dovetail all levels of analysis to determine the extent and magnitude of anomalous regions. Such comparisons additionally serve to verify the proper hydration process.

## 5.2 Thermal Testing Sites

Over the duration of the study, eleven shafts were tested at 8 sites throughout the state of Washington. Various shaft sizes and geology were encountered. Shafts sizes included: 4, 6.5, 7, 8, 9, 10, and 12 ft diameters. Time of testing (TOT) ranged from 1 to 16 days after casting. Recommended testing time ranges from  $t$  to D days where  $t$  is computed from the concrete mix design (Section 3.1) and D is the diameter of the shaft in feet. Table 5.1 lists all the mix designs, cement constituents, testing times from each site where thermal integrity profiling was conducted.

Table 5-1 Summary of shaft mix, model parameters, and testing information.

Concrete Constituents	Nalley Valley	Scatter Creek	Tieton River	Wandermere	Vancouver Rail	Gallup Creek	Hyak	Manette
Cement, lbs (%)	610 (85%)	610 (85%)	600 (85%)	600 (82%)	600 (77%)	611 (86%)	600 (77%)	600 (86%)
MgO, %	0.83	1.3	1.1	1.4	1.0	0.84	1	0.78
C <sub>2</sub> S, %	13	15	15	18	18	15	14	16
C <sub>3</sub> A, %	7.1	7	7	4	3.9	6.4	5	6.7
C <sub>3</sub> S, %	58	60	59	57	60.5	56	60	55
SO <sub>3</sub> , %	2.8	2.8	2.8	2.7	2.31	2.77	2.7	2.77
C <sub>4</sub> AF, %	11.2	10	10	9	9	11.2	10	11.4
Blaine, m <sup>2</sup> /kg	387	402	401	388	392	398	411	393
Flyash, lbs (%)	110 (15%)	110 (15%)	110 (15%)	130 (18%)	175 (23%)	100 (14%)	-	100 (14%)
SO <sub>3</sub> , %	1	0.5	0.2	0.2	2.77	N/A	-	0.7
CaO, %	15.1	9.8	10.5	10.5	27.41	N/A	-	13.3
Slag, lbs (%)	-	-	-	-	-	-	181 (23%)	-
w/c	0.40	0.37	0.45	0.44	0.44	0.42	0.41	0.38
Energy (kJ/kg)	76.2	76.42	76.02	72.81	91.2	74.85	87.7	71.69
<b>a</b>	0.769	0.751	0.795	0.806	0.831	0.775	0.769	0.753
<b>b</b>	0.629	0.611	0.605	0.552	0.578	0.596	0.479	0.602
<b>t</b> , hrs	19.3	17.2	17.5	21.1	35.1	18.9	26.3	19.1
Diam, ft	10	4	8	10	6.5	7	9	12
TOT (hrs)	52-141*	50	25	383	N/A	40	48	81
Temp (F)	120-145*	105	135	110	105	140	135	125

\*Three shafts were tested at this site ranging between 52 and 141 hours and 120 and 145F average shaft temperature.

With the exception of the Wandermere site, all shafts were tested in the recommended testing window between  $\tau$  and D. This range is a rule-of-thumb used to provide reasonable flexibility to the contractor and the testing agency while still providing a temperature gradient with the surrounding environment sufficient to identify cementitious from non-cementitious materials. For larger sized shafts the rule is conservative (longer elevated temperature) and for smaller shafts it tends to be less conservative (e.g. 3 days maximum window for a 3 ft shaft). As a point of interest the peak core temperature of the 10 ft diameter shaft at Wandermere was predicted to have been on the order of 190F occurring at 65hrs; the peak access tube temperature was predicted to be 160F at 35 hrs.

### 5.3 Field Testing and Equipment

Recommended testing times can also be identified using level 3 modeling techniques where a predicted tube temperature and a function of time can be plotted for various shaft sizes. Figure 5-1 shows an example of this planning approach prepared early on in the study. The shaded regions cut off the testing window when it falls below 120F. This study and simultaneous work elsewhere have successfully demonstrated that time can be extended to the  $\tau$  through D window. The Heat Source Calculator (Section 3.1) provides much of the needed information more quickly. Extended testing times can be also reasonable in lower temperature soils typical of Washington state down to cut-off thresholds as low as 100F. Further, these detailed tube temperature predictions help estimate when shafts are under or oversized.

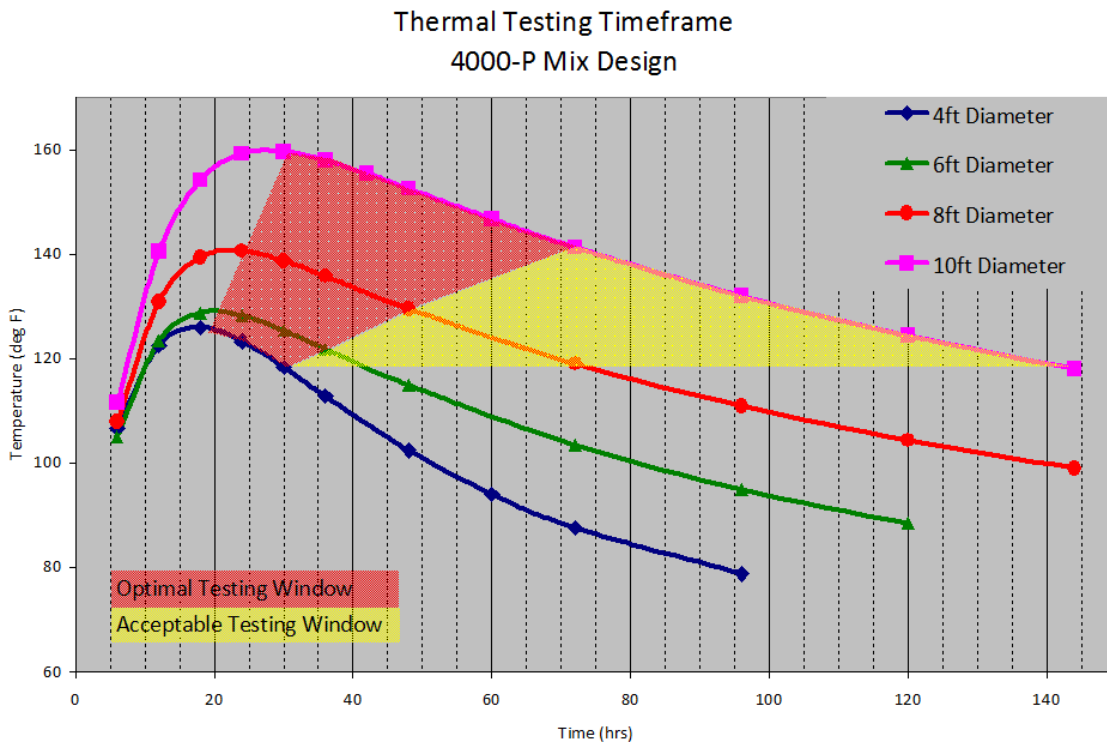


Figure 5-1 Predicted tube temperature for various sizes of shafts (Nalley Valley mix).

Several iterations of equipment modification have transpired since the onset of this study. These included: development of task-specific data collection software tailored to walk the user through the test and automate file handling, ruggedized sunlight readable data collection computer with extended battery life, increase digital filtration to remove aberrant or stray signals, and improved de-watering procedures to both expedite testing and increase data quality.

Concurrent to this study, commercial thermal integrity profiling systems have been developed that promise to even further improve the quality of the equipment (e.g. increased portability, even longer battery life, etc). These systems include the option for both embedded strings of temperature sensors and probe type systems (like used in this study) and are scheduled for release virtually the same time as this report is finalized.

#### **5.4 Significant Features**

Thermal testing provides various details of shaft integrity which include effective shaft size (diameter and length), anomaly detection inside and outside reinforcement cage, cage alignment, and proper hydration of the concrete. The ability to detect concrete volumes outside the reinforcing cage is perhaps its strongest feature.

Conceptually, as an access tube moves closer the shaft center (or center of heat) an increase in temperature is realized. This in turn implies that for a fixed cage location relative to the heat center, the temperature will increase as the excavation wall expands away from the cage and vice versa. The linear relationship that is formed by this phenomenon (within limits) is demonstrated in Figure 5-2. This example is based on the predicted temperature measurements from a 3 ft diameter cage placed in a variable diameter step shaft (Figure 5-3).



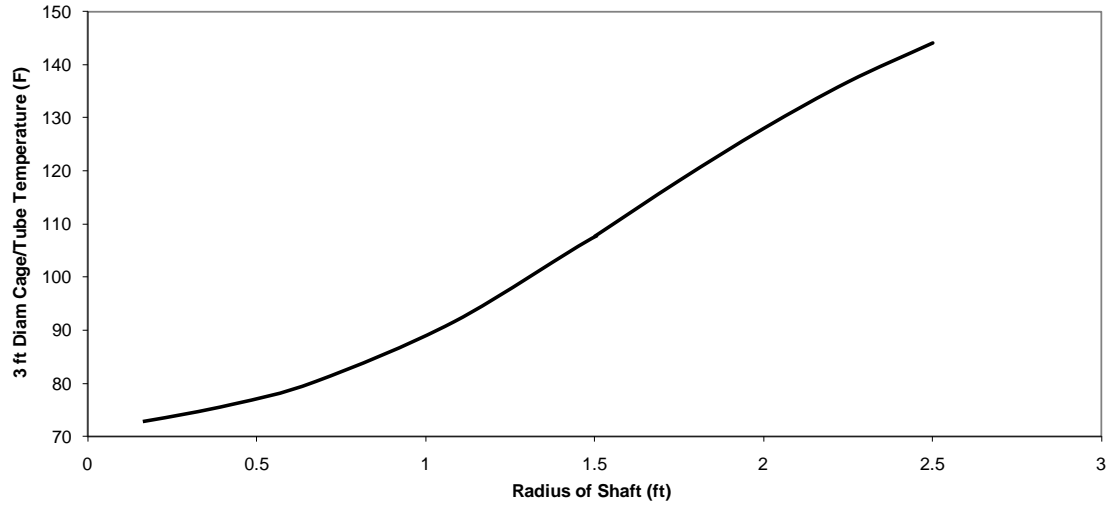


Figure 5-2 Effective radius from increases or decreases in cover around 3 ft cage.

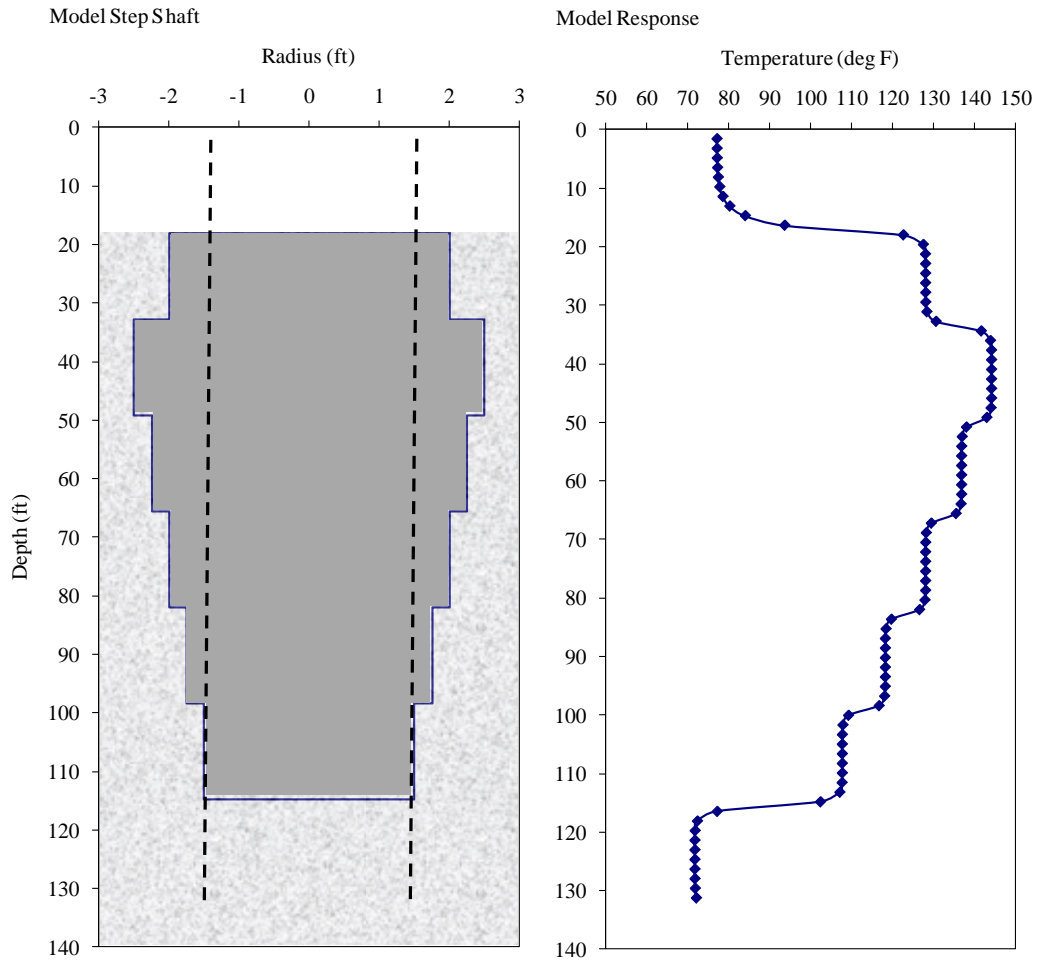


Figure 5-3 Modeled step shaft and resultant temperature from a fixed radius from shaft center.

## **5.5 New Developments**

Two new developments are foreseen for the near future that deal with hardware and analysis. With regards to hardware, disposal strings of temperature sensors are being developed that would be tied to the cage at the same plurality as access tubes that have individual miniature data loggers for each string. The data from this type of system provides time – temperature relationships as well as the profiles for each string like that discussed in the report. The top of string data loggers might be accessed through wired or wireless communications that in concept could be retrieved remotely. Further, data of this type could be collected from every shaft on a project without scheduling a test and only analyzed if needed.

Software improvements are envisioned to incorporate gradient calculators to aid in further isolating anomalous regions. Therein, the measurements from all four infrared sensors will be converted into gradients and directionality to essentially point toward the coldest sections (e.g. inclusions, necks, or to the outside / normal gradient).

## **5.6 Limitations**

Thermal integrity profiling requires temperature generation from hydrating materials to provide distinction between cementitious and non-cementitious materials. Testing should be performed while these materials are warm enough to establish a usable temperature gradient which ranges from 2 to 10 days depending on shaft diameter (roughly proportional to shaft diameter in feet, respectively). Consequently, planning for thermal testing should be incorporated into the time required to review construction logs to assure a timely response.

Thermal integrity profiling can be performed in both PVC and steel access tubes. However, if tubes are filled with water during construction, the water must be expelled prior to testing, stored, and returned after testing if CSL tests are to be conducted. If CSL tests are not planned, water is not necessary during construction as TIP results are not sensitive to debonding and the water is not required to take temperature measurements.

When thermal modeling is used as the comparative basis for shaft acceptance, verification of mill certifications from the concrete supplier (constituent fractions) may be necessary as the most common method used by industry to establish constituent percentages are not exact tests. As a result, field validation of model predicted time versus temperature relationships can be performed by simple shaft temperature monitoring using small inexpensive thermocouple data collectors. Thermal integrity profiling using multiple embedded can provide data for both purposes.

Finally, as with all integrity assessment methods, thermal integrity profiling provides comparison of localized shaft conditions to the average or shaft norm. A reduced temperature implies an alteration of the concrete quality in that region which may or may

not result in a concrete strength less than needed. For example, a shaft with a compressive strength of 8000 psi as the norm with a section of 5000 psi (due to concrete-soil contamination) will result in a reduced temperature in the 5000 psi section. Even though 5000 psi may meet minimum specifications, the thermal integrity results will flag this region as anomalous. Correlations between temperature and compressive strength (or maturity) can be performed but are not an intrinsic component.

## **5.7 Thermal Testing Checklist**

### From Field Testing Engineer

- Access Tube Spacing
- Access Tube Lengths
- Access Tube Stickup (above top of shaft)
- Thermal Test Data
- Time of Testing

### From Contractor or Shaft Inspector

- Top of Shaft Elevation
- Bottom of Shaft Elevation
- Top of Tube Elevations
- Top of Casing Elevation (if applicable)
- Bottom of Casing Elevation (if applicable)
- Ground Surface Elevation
- Water Table Elevation
- Concrete Mix Design
- Cement Mill Certifications
- Fly Ash Mill Certifications (if applicable)
- Shaft Construction Log
- Reinforcement Cage Design
- Concrete Placement Log
- Concrete Batch Date and Time
- Concrete Placement Temperature

This page is intentionally left blank.

## *References*

- AASHTO (2010). "AASHTO LRFD Bridge Design Specifications Customary U.S. Units, Fourth Edition," ISBN: 1-56051-250-4 Publication Code: LRFDUS-4.
- Caltrans (2005). Method of ascertaining the homogeneity of concrete in cast-in-drilled-hole (CIDH) piles using the gamma-gamma test method. California Department of Transportation Specifications, California Test 233.
- Caltrans (2010). Gamma-gamma logging (GGL).  
<http://www.dot.ca.gov/hq/esc/geotech/ft/gamma.htm>
- Duarte, A., Campos, T., Araruna, J., and Filho, P. (2006). Thermal properties of unsaturated soils. *Unsaturated Soils*, GSP, ASCE, pp. 1707-1718.
- Farouki, O. (1966). Physical properties of granular materials with reference to thermal resistivity. Highway Research Record 128, National Research Council, Washington, DC, pp 25-44.
- FDOT (2010). Standard specifications for road and bridge construction. Florida Department of Transportation, <ftp://ftp.dot.state.fl.us/LTS/CO/Specifications>.
- Harris, M. (1999). *Sams Teach Yourself Microsoft Excel 2000 Programming in 21 Days*. Sams Publishing, Indianapolis, Indiana.
- Hertlein, B. (2001). Are our client's expectations realistic? Geo-Strata, Geo-Institute of the American Society of Civil Engineers, January, p.11.
- Johansen, O. (1975). Thermal conductivity of soils and rocks. Proceedings of the Sixth International Congress of the Foundation Francaise d'Etudes Nordiques, Vol. 2, pp.407-420.
- Johnson, K. and Mullins, G. (2007). Concrete temperature control via voiding drilled shafts. *Contemporary Issues in Deep Foundations*, ASCE Geo Institute, GSP No.158, Vol. I, pp. 1-12.
- Kranc, S.C. and Mullins, G. (2007). Inverse method for the detection of voids in drilled shaft concrete piles from longitudinal temperature scans. Inverse Problems Design and Optimization Symposium, Miami, FL, April 16-18, 2007.
- Mullins, G. (2010). Thermal integrity profiling of drilled shafts. *DFI Journal*, Deep Foundations Institute, Vol. 4, No. 2, pp. 54-64.

Mullins, G. and Ashmawy, A. (2005). Factors affecting anomaly formation in drilled shafts. Final Report, FDOT Project BC353-19, March.

Mullins, A.G. and Kranc, S.C. (2004), "Method for Testing Integrity of Concrete Shafts," US Patent No.: US6,783,273 B1, filed April 22, 2002.

Mullins, G. and Kranc, S. (2007). "Thermal Integrity Testing of Drilled Shafts - Final Report." FDOT Grant #BD544-20, May.

Mullins, G., Winters, D., and Johnson, K. (2009). "Attenuating Mass Concrete Effects in Drilled Shafts." FDOT Grant #BD-544-39, September.

O'Neill, M.W. and Reese, L. C. (1999). Drilled shafts: construction procedures and design methods. U.S. Department of Transportation, Publication No. FHWA-IFF-99-025, ADSC-TL 4, Volume II.

Pauly, N. (2010). Thermal conductivity of soils from the analysis of boring logs. Master's Thesis, University of South Florida Department of Civil and Environmental Engineering, December.

Schindler, A. and Folliard, K. (2005). Heat of hydrations models for cementitious materials. ACI Materials Journal, Vol. 102, No.1, pp. 24-33.

Schneider, D.I. (1999). An Introduction to Programming Using Visual Basic 6.0 Fourth Edition. Prentice Hall, Upper Saddle River, New Jersey.

U.S. Department of the Interior (2004). Story of Hoover dam; concrete. Bureau of Reclamation, <http://www.usbr.gov/lc/hooverdam/History/essays/concrete.html>.

Whitfield, T. (2006). "Effect of C<sub>3</sub>S content on expansion due to ettringite formation. Master's Thesis, University of South Florida Department of Civil and Environmental Engineering, June.

WSDOT (2009). "Report of CSL Testing, Pier 6 Shaft A & Shaft C," Nalley Valley I-16 Bridge Project, Tacoma, WA, Washington State Department of Transportation, Olympia, WA.